

DTIC FILE COPY

AFWAL-TR-89-3019

AD-A205 160



STABILITY AND CONTROL OF HYPERVELOCITY VEHICLES

Rudrapatna V. Ramnath

Sparta, Inc.  
21 Worthen Road  
Lexington, MA 02173

February 1989

Final Report for Period April 1986 - December 1987

DTIC  
ELECTE  
MAR 08 1989  
S D  
D &

Approved for Public Release; Distribution is Unlimited

89 3 07 068

FLIGHT DYNAMICS LABORATORY  
AIR FORCE WRIGHT AERONAUTICAL LABORATORIES  
AIR FORCE SYSTEMS COMMAND  
WRIGHT-PATTERSON AIR FORCE BASE, OHIO 45433-6553

NOTICE

When Government drawings, specifications, or other data are used for any purpose other than in connection with a definitely Government-related procurement, the United States Government incurs no responsibility or any obligation whatsoever. The fact that the government may have formulated or in any way supplied the said drawings, specifications, or other data, is not to be regarded by implication, or otherwise in any manner construed, as licensing the holder, or any other person or corporation; or as conveying any rights or permission to manufacture, use, or sell any patented invention that may in any way be related thereto.

This report is releasable to the National Technical Information Service (NTIS). At NTIS, it will be available to the general public, including foreign nations.

This technical report has been reviewed and is approved for publication.

  
MARY K MANNING, 1st Lt, USAF  
Project Engineer  
Control Dynamics Branch  
Flight Control Division

  
DAVID K. BOWSER, Chief  
Control Dynamics Branch  
Flight Control Division

FOR THE COMMANDER

  
H. MAX DAVIS, Assistant for  
Research and Technology  
Flight Control Division  
Flight Dynamics Laboratory

If your address has changed, if you wish to be removed from our mailing list, or if the addressee is no longer employed by your organization please notify AFWAL/FIGCA, WPAFB, OH 45433-6553 to help us maintain a current mailing list.

Copies of this report should not be returned unless return is required by security considerations, contractual obligations, or notice on a specific document.

## REPORT DOCUMENTATION PAGE

Form Approved  
OMB No. 0704-0188

1a. REPORT SECURITY CLASSIFICATION UNCLASSIFIED		1b. RESTRICTIVE MARKINGS N/A	
2a. SECURITY CLASSIFICATION AUTHORITY N/A		3. DISTRIBUTION / AVAILABILITY OF REPORT Approved for public release; distribution is unlimited.	
2b. DECLASSIFICATION / DOWNGRADING SCHEDULE N/A			
4. PERFORMING ORGANIZATION REPORT NUMBER(S)		5. MONITORING ORGANIZATION REPORT NUMBER(S) AFWAL-TR-89-3019	
6a. NAME OF PERFORMING ORGANIZATION Sparta, Inc	6b. OFFICE SYMBOL (If applicable)	7a. NAME OF MONITORING ORGANIZATION Flight Dynamics Laboratory (AFWAL/FIGCA) Air Force Wright Aeronautical Laboratories	
6c. ADDRESS (City, State, and ZIP Code) 21 Worthen Road Lexington, MA 02173		7b. ADDRESS (City, State, and ZIP Code) Wright-Patterson AFB, Ohio 45433-6553	
8a. NAME OF FUNDING / SPONSORING ORGANIZATION AF Wright Aeronautical Labs	8b. OFFICE SYMBOL (If applicable) AFWAL/FIGCA	9. PROCUREMENT INSTRUMENT IDENTIFICATION NUMBER F33615-86-C-3616	
8c. ADDRESS (City, State, and ZIP Code) Wright-Patterson AFB, Ohio 45433-6553		10. SOURCE OF FUNDING NUMBERS	
		PROGRAM ELEMENT NO. 65502F	PROJECT NO. 3005
11. TITLE (Include Security Classification) Stability and Control of Hypervelocity Vehicles			
12. PERSONAL AUTHOR(S) Rudrapatna V. Ramnath			
13a. TYPE OF REPORT Final	13b. TIME COVERED FROM Apr 86 TO Dec 87	14. DATE OF REPORT (Year, Month, Day) 1989 February	15. PAGE COUNT 154
16. SUPPLEMENTARY NOTATION → This report investigates			
17. COSATI CODES			18. SUBJECT TERMS (Continue on reverse if necessary and identify by block number) Hypervelocity Vehicles Stability and Control Generalized Multiple Time Scales. (code) A
FIELD	GROUP	SUB-GROUP	
17	07		
19. ABSTRACT (Continue on reverse if necessary and identify by block number) In this research effort, the general class of problems associated with the flight dynamics of hypervelocity vehicles and their control. <del>is</del> investigated. After an examination of typical vehicles, flight environment, operating conditions and trajectories, a general analytical theory is developed to solve the significant problems. Based on typical flight scenarios, the dynamics are appropriately formulated to fit the situation in question. Thus the flight dynamics are investigated on a variety of trajectories, including re-entry and flight on constant-latitude minor circles at constant altitude. Re-entry dynamics are analyzed along steep, shallow, and arbitrary trajectories. Asymptotic analytical solutions are developed by the Generalized Multiple Scales method, in which the clock functions are necessarily nonlinear and complex quantities in order to solve the nonlinear and time varying dynamics.			
20. DISTRIBUTION / AVAILABILITY OF ABSTRACT <input checked="" type="checkbox"/> UNCLASSIFIED/UNLIMITED <input type="checkbox"/> SAME AS RPT. <input type="checkbox"/> DTIC USERS		21. ABSTRACT SECURITY CLASSIFICATION UNCLASSIFIED	
22a. NAME OF RESPONSIBLE INDIVIDUAL Mary K. Manning		22b. TELEPHONE (Include Area Code) (513)255-8678	22c. OFFICE SYMBOL AFWAL/FIGCA

## ABSTRACT

This constitutes the final report on the Phase I SBIR Contract, "Stability and Control of Hypervelocity Vehicles". In this research effort the general class of problems associated with the flight dynamics of hypervelocity vehicles and their control is investigated. After an examination of typical vehicles, flight environment, operating conditions and trajectories, a general analytical theory is developed to solve the significant problems. Based on typical flight scenarios, the dynamics are appropriately formulated to fit the situation in question. Thus the flight dynamics are investigated on a variety of trajectories, including re-entry and flight on constant-latitude minor circles at constant altitude. Re-entry dynamics are analyzed along steep, shallow and arbitrary trajectories. Asymptotic analytical solutions are developed by the Generalized Multiple Scales (GMS) method, in which the clock functions are necessarily nonlinear and complex quantities in order to solve the nonlinear and time varying dynamics. Re-entry dynamics along arbitrary trajectories are solved simply and accurately by the GMS method.

Another class of trajectories along which the dynamics are analyzed concerns flight at constant altitude along minor circles of different radii. The GMS method enables us to solve for the dynamics in the longitudinal and lateral-directional motions, for flight with acceleration and deceleration. For accelerating flight the usual short period, phugoid, Dutch Roll and roll/spiral modes show nonlinear phase changes. The frequencies are variable and additional damping results from the changing flight conditions. Fast and slow aspects of the dynamics are systematically separated by the GMS method. The accuracy of the GMS solutions is extremely good. Indeed, the GMS solutions are indistinguishable from the numerical solutions. The GMS theory is applied to a generic hypersonic vehicle in typical situations. The re-entry case is validated by application to the Space Shuttle. Minor circle flight is illustrated by application to a generic delta-winged hypersonic vehicle. Stability criteria including the critical altitude during re-entry are developed by the GMS method, followed by solutions to the problem of sensitivity of the dynamics to parameter variations. Sensitivities of the Space Shuttle to typical parameter variations are calculated. An error analysis follows, and strict, sharp error bounds are given. Finally a control analysis and design methodology and framework are developed by means of the GMS method.



Accession For	
NTIS CRA&I	<input checked="" type="checkbox"/>
DTIC TAB	<input type="checkbox"/>
Unannounced	<input type="checkbox"/>
Justification	
By _____	
Distribution _____	
Availability _____	
Dist _____	
A-1	

## TABLE OF CONTENTS

SECTION	PAGE
ABSTRACT	iii
LIST OF FIGURES	iv
1. INTRODUCTION AND OVERVIEW	1
2. PROBLEM FORMULATION	4
2.1 Features of Hypervelocity Vehicles	4
2.2 Re-Entry Paths	5
2.3 Flight Along Minor Circles	9
2.3.1 Dynamics of a Vehicle Flying on a Minor Circle	11
2.3.2 Accelerating Flight on a Minor Circle	14
3. ANALYSIS APPROACH	3
3.1 General Remarks	17
3.2 Generalized Multiple Scales (GMS) Method	18
4. APPLICATION TO RE-ENTRY DYNAMICS	23
4.1 GMS Solutions	24
4.2 Application	26
5. HYPERVELOCITY FLIGHT DYNAMICS ON A MINOR CIRCLE	28
5.1 General Remarks	28
5.2 Development of Solution	28
5.3 Application to a Generic Vehicle	31
5.4 Discussion of the GMS Solutions	33
5.5 Turning Point Phenomenon	34
6. STABILITY ANALYSIS	36
6.1 Peculiarities of Dynamics through Variable Flight Conditions	36
6.2 Stability and Response During Re-Entry	37
7. PARAMETER SENSITIVITY	41
7.1 General Remarks	41
7.2 Application to Re-Entry	42
8. ERROR ANALYSIS	44
8.1 General Remarks	44
8.2 Strict Bounds	45

## TABLE OF CONTENTS

SECTION	PAGE
9. CONTROL CONSIDERATIONS	46
9.1 General Remarks	46
9.2 Control System Design	49
10. FURTHER WORK	53
11. SUMMARY AND CONCLUSIONS	55
12. REFERENCES	57
APPENDIX A - REPRESENTATIVE VEHICLE	60
APPENDIX B	142
FIGURES	65

## LIST OF FIGURES

- Fig. 1. Axis System and Nomenclature (Re-entry).
- Fig. 2. Geometry of Minor Circle Flight.
- Fig. 3. Forces and Axis System (Minor Circle).
- Fig. 4. Concept of Extension.
- Fig. 5. Extension to Multiple Time Scales.
- Fig. 6. Hypervelocity Vehicles.
- Fig. 7. Hypervelocity Vehicles (cont.).
- Fig. 8. Typical Environmental Properties.
- Fig. 9. Space Shuttle Re-entry.
- Fig. 10. Space Shuttle Re-entry.
- Fig. 11. Space Shuttle Re-entry.
- Fig. 12. Space Shuttle Re-entry.
- Fig. 13. Space Shuttle Re-entry.
- Fig. 14. Space Shuttle Re-entry.
- Fig. 15. Space Shuttle Re-entry.
- Fig. 16. Space Shuttle Re-entry.
- Fig. 17. Space Shuttle Re-entry.
- Fig. 18. Space Shuttle Re-entry.
- Fig. 19. Space Shuttle Re-entry.
- Fig. 20. Space Shuttle Re-entry.
- Fig. 21. Space Shuttle Re-entry.
- Fig. 22. Space Shuttle Re-entry.
- Fig. 23. Space Shuttle Re-entry.
- Fig. 24. Space Shuttle Re-entry.
- Fig. 25. Space Shuttle Re-entry.
- Fig. 26. Space Shuttle Re-entry.
- Fig. 27. Space Shuttle Re-entry.
- Fig. 28. Acceleration on Minor Circles.
- Fig. 29. Flight on Minor Circles.
- Fig. 30. Flight on Minor Circles.
- Fig. 31. Flight on Minor Circles.
- Fig. 32. Flight on Minor Circles.
- Fig. 33. Flight on Minor Circles.
- Fig. 34. Flight on Minor Circles.
- Fig. 35. Flight on Minor Circles.
- Fig. 36. Flight on Minor Circles.

- Fig. 37. Flight on Minor Circles.
- Fig. 38. Flight on Minor Circles.
- Fig. 39. Numerical Instability: Dutch Roll Case (Minor Circle).
- Fig. 40. Flight on Minor Circles.
- Fig. 41. Flight on Minor Circles.
- Fig. 42. Flight on Minor Circles.
- Fig. 43. Flight on Minor Circles.
- Fig. 44. Flight on Minor Circles.
- Fig. 45. Flight on Minor Circles.
- Fig. 46. Flight on Minor Circles.
- Fig. 47. Flight on Minor Circles.
- Fig. 48. Flight on Minor Circles.
- Fig. 49. Flight on Minor Circles.
- Fig. 50. Flight on Minor Circles.
- Fig. 51. Flight on Minor Circles.
- Fig. 52. Flight on Minor Circles.
- Fig. 53. Flight on Minor Circles.
- Fig. 54. Flight on Minor Circles.
- Fig. 55. Flight on Minor Circles.
- Fig. 56. Flight on Minor Circles.
- Fig. 57. Flight on Minor Circles.
- Fig. 58. Flight on Minor Circles.
- Fig. 59. Flight on Minor Circles.
- Fig. 61. Flight on Minor Circles.
- Fig. 62. Flight on Minor Circles.
- Fig. 63. Flight on Minor Circles.
- Fig. 64. Flight on Minor Circles.
- Fig. 65. Flight on Minor Circles: Turning Point Problem.
- Fig. 66. Flight on Minor Circles: Turning Point Problem.
- Fig. 67. Flight on Minor Circles: Turning Point Problem.
- Fig. 68. Flight on Minor Circles: Turning Point Problem.
- Fig. 69. Flight on Minor Circles: Turning Point Problem.
- Fig. 70. Flight on Minor Circles: Turning Point Problem.
- Fig. 71. Flight on Minor Circles: Turning Point Problem.
- Fig. 72. Flight on Minor Circles: Turning Point Problem.
- Fig. 73. Parameter Sensitivity (Re-entry).
- Fig. 74. Parameter Sensitivity (Re-entry).
- Fig. 75. Parameter Sensitivity (Re-entry).

- Fig. 76. Parameter Sensitivity (Re-entry).
- Fig. 77. Parameter Sensitivity (Re-entry).
- Fig. 78. Parameter Sensitivity (Re-entry).
- Fig. 79. Parameter Sensitivity (Re-entry).
- Fig. 80. Parameter Sensitivity (Re-entry).
- Fig. 81. Parameter Sensitivity (Re-entry).
- Fig. 82. Standard Control Design Procedure for Time Varying Systems.
- Fig. 83. Time Varying Control Design for GMS Approach.
- Fig. A. Generic Hypersonic Vehicle (Drummond's Model).

## 1 INTRODUCTION AND OVERVIEW

The advent of the Space Shuttle vehicle (or the space transportation system) has sparked great interest in an entirely new class of vehicles capable of being operated in a conventional way in the atmosphere but also of achieving orbital motion. This necessitates the ability of the vehicle to operate at hypersonic speeds, in addition to flight at low speeds. The dynamics of a flight vehicle at low speeds is understood quite well. However, the dynamics of flight at hypersonic velocities are not fully understood and present a number of qualitative and quantitative difficulties. The trajectories flown by the vehicle can be quite varied. For example, the re-entry motion might be along a steep trajectory or a shallow one. On the other hand, the vehicle could also be required to perform steady turns. Thus the actual trajectories could be several different great circle paths. It would appear that the new hypersonic flight vehicles would normally fly along great circles, but would change the trajectory, perhaps to a new great circle. This might be the case if a different landing site became necessary during the flight. The new transition trajectory might be along a minor circle or a series of minor circles. Steady hypersonic flight might be for, say 5,000 miles, the total range being up to 10,000 miles. Both military and meteorological surveillance missions would require flight along such trajectories, where a restricted region of the earth must be flown over.

The organization and overall problem formulation are as follows. The first class of problems considered is that of re-entry at hypersonic speeds. The conventional approach involves entry along steep, ballistic trajectories. Earlier theoretical results are available for basically two types of entry trajectories - (1) steep ballistic entry, and (2) shallow entry. The dynamic equations are developed after making appropriate assumptions for a particular flight scenario. The early approach by Friedrich and Dore [1] and Allen [2] neglected gravity compared to aerodynamic drag along the trajectories, i.e., where deceleration is high. In this case, at hypersonic speeds, the longitudinal dynamic response is described by zeroth order Bessel functions [2]. Stability criteria can be developed based on these solutions. When the flight path is approximately parallel to the earth's surface, the dynamics can be described in terms of damped Mathieu functions from an inhomogeneous equation [8].

However, in considering the operational scenarios of a shuttle type vehicle and more general hypersonic flight vehicles, it is clear that the actual trajectory is likely to be neither the steep ballistic one, nor the shallow (or flat) trajectory, but one which is between these two extreme cases. Therefore, a unified approach is highly desirable, in order to investigate a variety of re-entry situations and for a general type of hypersonic vehicle. The difficulty in developing such a unified formulation rests on the fact that different transformations are called for in converting real time to another suitable variable, for different trajectories. Thus, for the case of ballistic entry, altitude, instead of time is the appropriate independent variable [2]. On the other hand, mean anomaly along the average flight path has been used instead of time, for the case of shallow gliding entry [8]. Combining these two approaches, use of the distance along the trajectory as the independent variable leads to a unified equation in angle of attack variations along the trajectory [8]. However, solution

of this equation was attempted only along steep and shallow entry trajectories. For these two limiting cases the solutions approach the earlier descriptions in terms of Bessel functions and damped Mathieu functions. The general problem of motion along arbitrary trajectories was solved by Ramnath [15], using the technique of Generalized Multiple Scales (GMS). By using a nesting of transformations - first transforming time to distance along the trajectory and then by means of multiple scaling of the distance variable, he derived highly accurate asymptotic general solutions to the unified equation.

Another important class of dynamic problems is that dealing with flight at hypervelocities along the minor circle. Although one can point to a relatively smaller number of earlier studies on this class of problems, it is growing in interest because of mission requirements. Early work by Loh [18], Arthur and Baxter [19], involves minor circle trajectories including descent of gliding and maneuvering re-entry vehicles. Work on the stability and dynamics at steady flight on minor circles is quite sparse. Etkin [20], Rangi [21] considered the longitudinal dynamics of vehicle in a circular orbit. Laitone [5] and his associates considered short period and phugoid oscillations at hypersonic speeds. However, the study of lateral-directional dynamics at hypervelocities is, for the most part, not reported in the literature. The main exceptions are the qualitative analysis of Nonweiler [22] and the detailed work of Drummond [23]. However it is important to note that most of these deal with the analysis of the dynamics at steady flight. The case of variable flight conditions, as in transition trajectories of minor circles, especially dealing with lateral-directional dynamics, is almost totally lacking.

In this report an approach is developed extending the earlier work of Ramnath [15], for the analysis of the general motion and control of a class of hypervelocity flight vehicles. With particular emphasis on the dynamics of a hypervelocity vehicle during *variable flight conditions*, two broad categories of flight are analyzed:

- (1) Re-entry dynamics on steep, shallow, or intermediate entry trajectories
- (2) Flight dynamics on minor circle trajectories at constant altitude and constant (or variable) latitudes.

Reflecting this view, the report is organized as follows. In Section 2, the problem formulation is developed for both re-entry and minor circle flight. It includes such considerations as the flight scenario, physical aerodynamic and vehicle properties in each situation, and development of the appropriate equations of motion. In Section 2.1 the re-entry dynamics are formulated and examined by means of a unified mathematical model valid for general re-entry trajectories. Section 2.2 consists of the formulation of the mathematical and physical model reflecting the flight dynamics on minor circles, at constant and variable flight conditions, the latter being descriptive of accelerating flight. Section 3 consists of an outline of the general analysis method, namely the Generalized Multiple Scales (GMS) method. In Section 4, the GMS method is applied to the re-entry dynamics. Asymptotic solutions are developed by the GMS method exhibiting the separation of the fast and slow motions during the re-entry deceleration. For general re-entry trajectories and a vehicle represented by the Space Shuttle, the GMS solutions are compared with the numerical solutions of the equations of motions, showing excellent accuracy.

Next, Section 5 presents an application to the flight dynamics on minor circles. Again, asymptotic solutions are developed by the GMS method for the case of *accelerating* flight on minor circles, showing excellent agreement with numerical solutions. New phenomena of *turning points* and *bifurcations* are discovered for this class of flight. In Section 6, some major peculiarities of time varying systems are presented, and simple and useful stability criteria for re-entry dynamics are developed, including an estimate of the critical altitude below which the dynamics could become unstable. Next, Section 7 presents an outline of an analytical asymptotic theory of parameter sensitivity by the GMS method. The sensitivity of the flight dynamics to parameter variations is developed in a separable form reflecting the fast and slow dynamics, and applied to the re-entry case. In Section 8, a brief error analysis is presented, relating to the errors caused by the GMS approach. Of particular interest is the powerful error theorem showing the strict and sharp bounds on the errors. Section 9 consists of the development of a new general framework for control analysis and design for time varying systems by the GMS methodology. Transfer functions are systematically developed in a separable form showing the fast and slow contributions. This representation, which is valid and accurate for time varying systems, includes the time-invariant case as a special case. Main limitations of linear time-invariant(LTI) control theory are presented.

A top level control design procedure using the GMS approach is also presented. This will obviate the usual limitations of the LTI approach resulting in a more satisfactory control design procedure. Further work is outlined in Section 10, followed by summary and conclusions in Section 11.

## 2 PROBLEM FORMULATION

### 2.1 Features of Hypervelocity Vehicles

The use of transatmospheric vehicles travelling at hypersonic velocities has been studied by the Air Force and other organizations with increasing interest, being motivated by a need for a more economical access to space. Such vehicles are eventually envisioned to be similar to aircraft with enormously enhanced flight envelopes. Ability to take-off and land from airfields and having short turnaround times are some important considerations. The large flight envelope imposes severe requirements on the hypervelocity vehicle. The need to operate at low speeds during take-off and landing and also at hypersonic speeds at some other times leads to complications in the stability and control characteristics of the vehicle. For example, at subsonic speeds the aerodynamic center is near the quarter-chord point whereas it moves to half-chord at supersonic speeds. Thus the vehicle may have weak static stability (or even instability) at subsonic speeds, but may be statically too stable at supersonic speeds. As the subsonic speed increases the overall trend is one of forward movement of the aerodynamic center as Mach number  $M$  approaches unity, and then rearward movement at supersonic speeds. The extent of this shift depends greatly on aspect ratio, planform, etc. The largest change occurs for (i) high aspect ratio and (ii) rectangular planform. The hypersonic vehicle is likely to have low aspect ratio and triangular wing planform and so probably has the least shift in aerodynamic center. Even a small shift could conceivably have a noticeable effect on the static stability of the vehicle.

The effects of power on the stability and control characteristics of the vehicle depend on the vehicle configuration, power plant type and flight condition. The effects of power can be categorized as follows:

- (i) Balance of forces along the flight path. Usually these belong to performance studies and not to the discipline of stability and control.
- (ii) Effect on lift. These effects are small even for propeller aircraft and are definitely negligible for jet aircraft.
- (iii) Effect on pitching moments. They influence the way in which the vehicle is trimmed and for determining allowable range of movement of the center of gravity.

The effects of power which depend on the change in angle-of-attack for jet engine driven vehicles are contained in the parameter  $dC_m/dC_L$  for both steady flight conditions and for pull-ups. Thus both the neutral point  $N_0$  and the maneuver point  $N_m$  are influenced by the power effects. Trim changes due to power are also worthy of consideration but these are important mainly at low speeds where the power effects are large. The power-on power-off effects would include (i) static stability, and (ii) initiation of transients. These effects would be relatively small and tractable at steady flight conditions. However, their effect during accelerated flight would be tractable by the asymptotic eigenfunction expansions developed by the GMS theory later.

An important consideration of flight at hypersonic speeds is that of aerodynamic heating of the vehicle. Transatmospheric vehicles using air breathing propulsion systems for long periods at hypersonic speeds are exposed to severe aerodynamic heat fluxes. The thermal protection of these vehicles is an important consideration in the design of the vehicle. The heat load depends on the vehicle shape, attitude, speed, density etc. (largely trajectory-dependent). The problem of determining optimal trajectories leading to minimum thermal protection system weight has been studied by some investigators. However, we do not consider this problem in this study.

Density variations with altitude are considered, using an exponential decay with altitude, with the standard adiabatic or isothermal lapse rate. This model is used to develop analytical solutions to angle-of-attack variations along a steep entry trajectory (Chapter 4). However, in generating GMS solutions to the Space Shuttle dynamics, density variations using the Space Shuttle data base were used (Fig 8). Flowfield characteristics were considered. The principal effects are captured in the movement of the aerodynamic center with Mach number change. In any case, the changes caused by this effect are within the applicability of the GMS theory.

The dynamics of the hypervelocity vehicle are formulated along basically two different classes of trajectories. Each scenario is the consequence of different mission requirements, as discussed earlier. First we will consider the re-entry class of trajectories and later, flight on minor circle paths. During the course of these investigations, we will consider longitudinal motions and lateral-directional dynamics as well.

## 2.2 Re-Entry Paths

In this section we will consider the longitudinal stability of hypervelocity flight vehicles. Only motion in the plane of symmetry is considered, under the action of aerodynamic forces and moments. We assume a spherical earth and that the vehicle experiences lift but does not roll. The axis system is chosen so that it rotates about the center of mass of the vehicle and that the x-axis is always tangential to the instantaneous flight path (Figure 1). The equations of motion for arbitrary flight paths and no thrust, involve inertia, gravity and aerodynamic forces and moments. Drag and lift along the tangent and normal to the flight paths are considered in the force equations. The pitching moment equation considers the balance of aerodynamic, inertial and gravity torques.

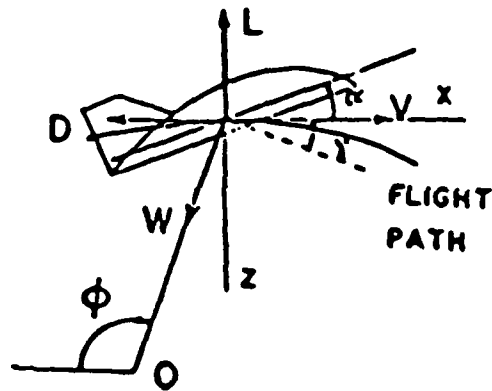


Fig. 1. Axis System and Nomenclature (Re-Entry).

In order to develop the equation describing the motion in the plane of symmetry, we assume that the center of mass of the vehicle travels along a known trajectory. In general it may be prescribed from other considerations, being optimal according to some criterion. For example, the trajectory resulting in the minimal thermal protection system weight was considered in an earlier work [15]. Any particular trajectory may be considered. In the present case a typical trajectory flown by the Space Shuttle as obtained from NASA-JSC is considered. It is neither the steep ballistic trajectory nor a very shallow one. Indeed, the theory and approach developed in this work are applicable to any trajectory. Now as the vehicle center of mass travels along this trajectory, we address the problem of analyzing the vehicle dynamics *about* the trajectory. We assume that the perturbed motion about the trajectory does not affect the trajectory. As a consequence, the perturbation equations are nonautonomous and have time varying coefficients.

The equations of motion for symmetric motions are [3-6, 42]:

$$\dot{V} = -\rho S C_D V^2 / (2m) - g \sin \gamma \quad (2.1)$$

$$V \dot{\gamma} = \frac{\rho S C_L V^2}{2m} - \left( g - \frac{V^2}{r} \right) \cos \gamma \quad (2.2)$$

$$\dot{q} = \frac{\rho S L C_m V^2}{2I_y} - \frac{3g}{2r} \left( \frac{I_x - I_z}{I_y} \right) \sin 2\theta \quad (2.3)$$

and by the kinematic relations

$$\dot{\theta} = q + (V/r) \cos \gamma \quad (2.4)$$

$$\dot{r} = V \sin \gamma \quad (2.5)$$

$$\theta = \gamma + \bar{\alpha} \quad (2.6)$$

where the dot denotes differentiation with respect to time. We assume that the slope of the lift curve is approximately independent of the flight speed and Mach number in high supersonic flight and linearize the aerodynamic coefficients about the nominal trajectory.

From the above relations, we can derive the following nonlinear differential equation for  $\bar{\alpha}$  by eliminating the  $V$  and  $\theta$  variables [8]. That is,

$$\begin{aligned} \frac{d^2 \bar{\alpha}}{dt^2} + \frac{SC_L V}{2m} \frac{d\rho}{dt} + \frac{\rho S V}{2m} \frac{dC_L}{dt} - \frac{\rho S L C_m V^2}{2I_y} \\ + \frac{3g}{2r} \left( \frac{I_x - I_z}{I_y} \right) \sin 2(\gamma + \bar{\alpha}) \\ + \left( \frac{3}{r} - \frac{2g}{V^2} \right) \frac{g}{2} \sin 2\gamma - \frac{\rho S C_D}{2m} g \cos \gamma - \frac{\rho^2 S^2}{4m^2} C_D C_L V^2 = 0 \end{aligned} \quad (2.7)$$

We now change the independent variable from  $t$  to a distance variable  $\xi$  (i.e. distance along the reference trajectory) according to

$$L \dot{\xi}(t) = V(t) \quad (2.8)$$

where  $L$  is the reference length for the vehicle. Thus the new independent variable  $\xi$  is interpreted as the number of reference lengths traversed along the reference trajectory by the hypervelocity vehicle. By virtue of (2.8) we can write

$$\frac{d}{dt}(\ ) = \frac{d}{d\xi}(\ ) \cdot \frac{d\xi}{dt} = \frac{V}{L} \frac{d}{d\xi}(\ ) \quad (2.9)$$

and

$$\frac{d^2}{dt^2}(\ ) = \left( \frac{V}{L} \right)^2 \frac{d^2}{d\xi^2}(\ ) + \frac{V}{L^2} (dV/d\xi) \cdot d/d\xi(\ ) \quad (2.10)$$

Further, let

$$\delta = \frac{\rho SL}{2m}, \quad v = \frac{I_x - I_z}{I_y}, \quad \sigma = \frac{mL^2}{I_y} \quad (2.11)$$

Following [8,42], we assume, for small variations in  $\alpha$

$$C_D = C_{D_0} + C_{D_\alpha} \alpha$$

$$C_L = C_{L_0} + C_{L_\alpha} \alpha \quad (2.12)$$

where  $\alpha = \bar{\alpha} - \alpha_0 =$  perturbation angle of attack and that

$$C_m = C_{m_\alpha} \alpha + C_{m_{\dot{\alpha}}} \dot{\alpha} + C_{m_q} \left(\frac{L}{V}\right) \dot{\theta} \quad (2.13)$$

Combining (2.7) - (2.13), the angle of attack oscillations can be seen to satisfy the equation

$$\frac{d^2 \alpha}{d\xi^2} + \omega_1(\xi) \frac{d\alpha}{d\xi} + \omega_0(\xi) \alpha = f(\xi) \quad (2.14)$$

where

$$\omega_1(\xi) = \delta [C_{L_\alpha} - \sigma (C_{m_{\bar{\alpha}}} + C_{m_q})] + \frac{V'}{V}$$

$$\omega_0(\xi) = -\delta \left( \sigma C_{m_\alpha} + \frac{gL}{V^2} C_{D_\alpha} \cos \gamma \right) + \delta' C_{L_\alpha} + \delta \frac{V'}{V} C_{L_\alpha}$$

$$- \delta^2 [C_{L_\alpha} (\sigma C_{m_q} + C_{D_0}) + (C_{L_0} C_{D_\alpha})]$$

$$+ \frac{3L}{r} \left( \frac{gL}{V^2} \right) v \cos 2(\gamma + \alpha_0) \quad (2.15)$$

$$f(\xi) = \delta \left( \frac{gL}{V^2} \right) [C_{D_0} - \sigma C_{m_q} \left( 1 - \frac{V^2}{gr} \right)] \cos \gamma - \delta' C_{L_0}$$

$$+ \delta^2 C_{L_0} (C_{D_0} + \sigma C_{m_q}) - \left( \frac{gL}{V^2} \right) \left[ \left( \frac{3L}{r} - \frac{gL}{V^2} \right) \sin 2\gamma \right.$$

$$\left. + \frac{3L}{2r} v \sin 2(\gamma + \alpha_0) \right]$$

Equation (2.14) is time-varying and inhomogeneous. The coefficients of this equation are known in terms of the trajectory at the center of mass. In general, it cannot be solved in closed form. It is important to note that the time-to-distance transformation of eq.(2.8) enables us to preserve the aerodynamic nonlinearity in the equations of motion. As consistent with standard theory, only linear dependence of the aerodynamic parameters  $C_D$ ,  $C_L$  and  $C_m$  on variables such as angle of attack are assumed.

For special cases of trajectories, the coefficients have particular known forms. In these cases the motion can be approximated by well-known functions of mathematical physics. They include, for example, Bessel functions, confluent hypergeometric functions and Mathieu functions [15,37].

### 2.3 Flight Along Minor Circles

In this section we will consider the dynamics of a generic hypervelocity vehicle on minor circles. As discussed earlier, this class of trajectories may be dictated by certain mission requirements. Flight at a constant altitude and latitude (minor circle) might be required because of military or meteorological reasons. A new landing site might become necessary midway in the hypersonic flight. Steady turns from a great circle and the trajectories for the other situations in the general class discussed above are all likely to be on minor circles.

The formulation of the problem of dynamic analysis of a hypervelocity flight vehicle traveling along a minor circle is based on [23]. Following Drummond [23], we consider the vehicle on a minor circle of radius  $r$  (Figure. 2) about an axis passing through the center of the earth. The axis system is given in Figure 3. We consider a spherical, nonrotating earth and flight at constant altitude  $h$  above the earth surface. The velocity of the center of mass of the vehicle is  $V_0$  directed along the  $x$  axis. The thrust vector  $T$  is in the  $xz$  plane and at an angle  $\gamma_T$  to the  $x$  axis. With the usual definitions of  $x, y, z$ , the angle of attack  $\alpha$ , bank angle  $\phi$  at zero side slip, and with this notation and specification of the problem, the equations for force balance in the  $x, y$ , and  $z$  directions are:

$$\begin{aligned}
 T \cos \gamma_T - D &= 0 \\
 mg \sin \phi - \frac{mV^2}{r} (\sin \beta_c \cos \phi - \cos \beta_c \sin \phi) &= 0 \\
 -L - T \sin \gamma_T - mg \cos \phi - \frac{mV^2}{r} (\sin \beta_c \sin \phi - \cos \beta_c \cos \phi) &= 0
 \end{aligned}
 \tag{2.16}$$

Using the local circular velocity  $\sqrt{gr}$ , and the earth's radius  $R_e$ , the speed  $V$  and the radius  $r$  of the minor circle are nondimensionalized by

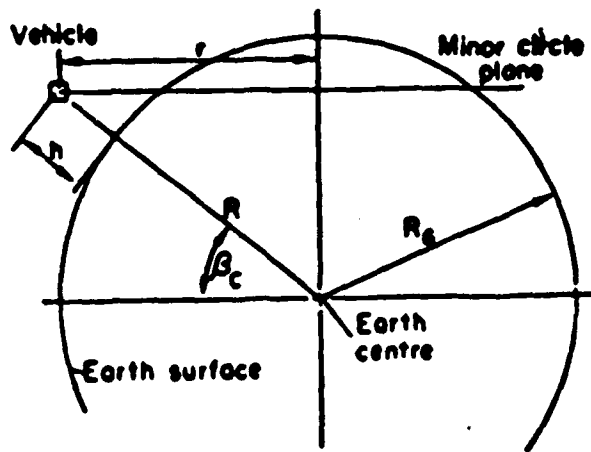


Fig. 2. Geometry of Minor Circle Flight.

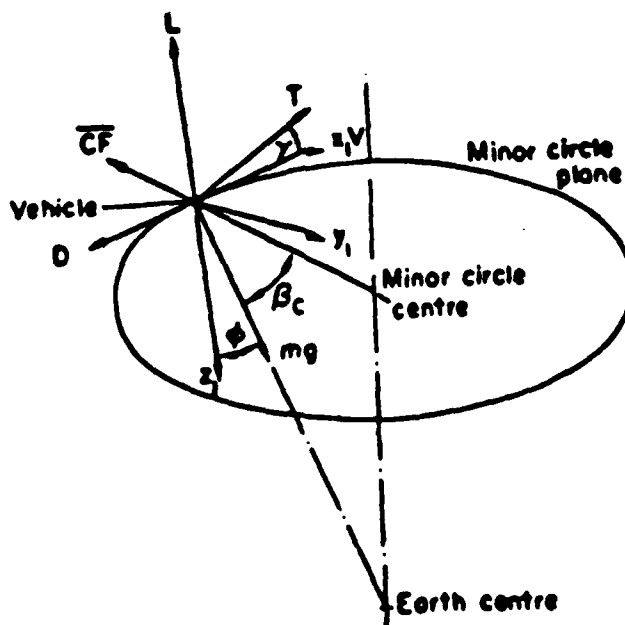


Fig. 3. Forces and Axis System (Minor Circle).

$$s = V/\sqrt{gR_e} \quad (2.17)$$

and

$$\bar{r} = r/R_e \quad (2.18)$$

Physically, if  $\beta_c = 0$ , the flight is on a great circle (a special minor circle), leading to

$$mg = m\frac{V^2}{r} \quad (2.19)$$

the weight being exactly counterbalanced by the centrifugal force. Now the vehicle is in a circular orbit, with the bank angle  $\phi$  being indeterminate. If  $\beta_c = 90^\circ$ , the radius of the minor circle  $\bar{r} = 0$ , and  $\phi = 90^\circ$ . This situation is physically not meaningful and is unrealizable. But large lift is required for small radius turns.

Flight on a minor circle is possible at different speeds. These are parameterized by the speed ratio  $s$ , whose value lies in the range  $s = 0.2$  to  $s = 1.4$ . The value of  $s = 1$  corresponds to orbital velocity. At this flight condition the centrifugal force counteracts the weight and aerodynamic lift is not required to maintain flight. In general, flight on a minor circle is possible at different altitudes. For a small radius circle, large aerodynamic lift is required. For small values of the speed ratio, the centrifugal force is small and aerodynamic lift is needed to balance the weight. For supercircular flight on a minor circle it is necessary to add a downward component of lift, thus countering the additional centrifugal force. This leads to bank angles greater than  $90^\circ$ . For tight turns (i.e. small radius) the bank angle  $\phi \approx 90^\circ$ . For flight on minor circles of large radius,  $\phi$  is near  $0^\circ$  for subcircular speeds and  $\phi$  is near  $180^\circ$  for  $s > 1$ . It has been suggested [23] that a candidate hypersonic vehicle might have a delta-wing configuration with a sweep angle of about  $75^\circ$  leading to temperatures in flight of about  $3500-4000^\circ\text{F}$ . It is felt that the highest temperatures will be attained for the minor circle of the smallest radius ( $\bar{r} = 0.1$ ) and lowest altitude. Just as we may consider a nominal re-entry trajectory as the one for the minimal thermal protection system weight, we may consider, as the nominal case, the minor circle of the smallest meaningful radius which is likely to produce the highest temperatures.

### 2.3.1 Dynamics of a Vehicle Flying on a Minor Circle

We now consider the dynamics of the hypervelocity flight vehicle as its center of mass travels along a minor circle. This problem formulation closely follows the development by Drummond [23]. Using a spherical nonrotating earth model and body-fixed stability axes, the exact nonlinear equations are developed by balancing terms arising from inertia, gravity and aerodynamics. We note that in the model used we neglect the small contributions due to Coriolis and centripetal accelerations

as well as earth's oblateness effects and gravity gradient effects at the operating altitude. The nonlinear equations of motion are then linearized in the usual way about the reference flight condition.

As usual the aerodynamic forces and moments are expanded in a Taylor's series representation in  $u, v, w, p, q, r$ , and  $z$  and only first order terms are retained. As shown in [23], the linearized equations of motion in this case have additional terms due to flight on a minor circle, in comparison with the standard linear equations of motion at steady flight for a conventional aircraft. Therefore, a strict separation of the longitudinal and lateral-directional motion on a minor circle may not be achievable because of coupling terms. However, such a coupling may be weak enough to warrant neglecting it in many cases of interest.

In an effort to retain connection with the dynamics of conventional aircraft at steady flights, we will treat the dynamics as symmetric motions and antisymmetric motions. Therefore the symmetric motions will consist of Short period and Phugoid modes. The lateral-directional dynamics of Dutch Roll and the usual roll and spiral modes will constitute the remaining modes of motion. In addition to these, Drummond discusses a new symmetric mode which he calls the  $u, x_1, z_1$  mode. This involves  $x_1$  the coordinate of mass center of the vehicle relative to the minor circle in the flight direction. The frequency of this oscillatory mode is independent of the new minor circle radius but varies inversely with the speed ratio  $s$ . This mode is relatively of lesser importance than the others and so it will not be discussed further.

The development of the equations of motion of a hypersonic vehicle flying on a minor circle at constant velocity and other flight conditions is given by Drummond [23]. He then develops solutions to these equations in terms of the basic modes of motion such as Dutch Roll, Short Period, etc. This solution process is valid only when the flight conditions are steady. In this case the differential equations have constant coefficients. The system eigenvalues are then constant. The linearized equations of motion given by Drummond [23] are of the vector-matrix form

$$\dot{\vec{x}} = F\vec{x}$$

where  $\vec{x}$  is the vector of state variables and  $F$  is the matrix of system coefficients. Drummond then considers a separation of the longitudinal (i.e., symmetric) motions and the lateral-directional dynamics. As usual each of these modes leads to a constant-coefficient linear differential equation. In the longitudinal mode, the familiar phugoid and short period motions combine with a new symmetric oscillatory " $u, x_1, z_1$ " mode. The lateral-directional motions involve the usual roll, Dutch Roll, and spiral modes. Following Drummond, the decoupled homogenous equation describing the symmetric motions in the variables  $(u, \alpha, q, \theta, x_1, z_1)$  can be written in the scalar form

$$\sum_{i=0}^6 A_i x^{(i)} = 0 \quad (2.20)$$

where  $A_6 = 1$  and  $x^{(i)} \equiv d^i x / dt^i$

The coefficients  $A_i$  are determined by the radius of the minor circle and the flight condition. In the case of flight on a particular minor circle at a specified flight condition, the coefficients  $A_i$  are constant. In this simple case the general symmetric motion is described by the familiar short period and phugoid modes, and the new symmetric  $u, x_1, z_1$  mode. The characteristic equation

$$\sum_{i=0}^6 A_i \lambda^i = 0 \quad (2.21)$$

can be factored into

$$(\lambda^2 + a_{sp}\lambda + b_{sp})(\lambda^2 + a_{ph}\lambda + b_{ph})(\lambda^2 + w_{u,x_1,z_1}^2) = 0 \quad (2.22)$$

where the short period roots are given by

$$\lambda^2 + a_{sp}\lambda + b_{sp} = 0 \quad (2.23)$$

and the phugoid roots by

$$\lambda^2 + a_{ph}\lambda + b_{ph} = 0 \quad (2.24)$$

The roots given by

$$\lambda^2 + w_{u,x_1,z_1}^2 = 0 \quad (2.25)$$

constitute the new symmetric  $u, x_1, z_1$  mode.

Similarly in the lateral-directional dynamics, we identify the classical Dutch Roll oscillations and the roll-spiral nonoscillatory mode. The Dutch Roll mode is a damped oscillation involving all the lateral variables.

The decoupled differential equation is of the form

$$\sum_{i=0}^4 B_i x^{(i)} = 0 \quad (2.26)$$

where  $B_4 = 1$  and  $x^{(i)} \equiv \frac{d^i x}{dt^i}$ .

Again, the characteristic equation can be written as

$$(\lambda^2 + a_{dr}\lambda + b_{dr})(\lambda^2 + a_{rs}\lambda + b_{rs}) = 0 \quad (2.27)$$

In this case the Dutch Roll oscillations are represented by the complex roots

$$\lambda^2 + a_{dr}\lambda + b_{dr} = 0 \quad (2.28)$$

The roll-spiral roots, both being real, are given by

$$\lambda^2 + a_{rs}\lambda + b_{rs} = 0 \quad (2.29)$$

Using this basic approach, we will now go on to consider the linearized equations of motion of the hypervelocity vehicle flying on a minor circle, while its velocity changes continuously.

### 2.3.2 Accelerating Flight on a Minor Circle

With the usual notation [39], the linearized equations of motion are as follows. The longitudinal equations are,

$$\begin{aligned} \dot{u} - X_u u - (X_\alpha + g)\alpha + g_\theta &= 0 & (i) \\ -\frac{Z_u}{V_o} u + \dot{\alpha} - \frac{Z_\alpha}{V_o} \alpha - \dot{\theta} &= 0 & (ii) \\ -M_u u - M_\alpha \alpha - M_{\dot{\alpha}} \dot{\alpha} + \ddot{\theta} - M_{\dot{\theta}} &= M_\delta \delta_e & (iii) \end{aligned} \quad \left. \vphantom{\begin{aligned} \dot{u} - X_u u - (X_\alpha + g)\alpha + g_\theta &= 0 \\ -\frac{Z_u}{V_o} u + \dot{\alpha} - \frac{Z_\alpha}{V_o} \alpha - \dot{\theta} &= 0 \\ -M_u u - M_\alpha \alpha - M_{\dot{\alpha}} \dot{\alpha} + \ddot{\theta} - M_{\dot{\theta}} &= M_\delta \delta_e \end{aligned}} \right\} (2.30)$$

Similarly the linearized lateral-directional equations are

$$\begin{aligned} \dot{v} - Y_v v + V r - g \phi &= 0 & (i) \\ -L_v v - L_r r + \ddot{\phi} - L_p \dot{\phi} &= L_{\delta_a} \delta_a & (ii) \\ -N_v v + \dot{r} - N_r r - N_p \dot{\phi} &= N_{\delta_a} \delta_a + N_{\delta_r} \delta_r & (iii) \end{aligned} \quad \left. \vphantom{\begin{aligned} \dot{v} - Y_v v + V r - g \phi &= 0 \\ -L_v v - L_r r + \ddot{\phi} - L_p \dot{\phi} &= L_{\delta_a} \delta_a \\ -N_v v + \dot{r} - N_r r - N_p \dot{\phi} &= N_{\delta_a} \delta_a + N_{\delta_r} \delta_r \end{aligned}} \right\} (2.31)$$

These are the basic linearized equations of motion of the flight vehicle over a flat earth. However, slight modifications due to minor circle trajectories are made, in accordance with Drummond's [23] analysis. For instance, for minor circle flight,  $\phi$  depends not only on  $\dot{p}$  but also on  $\theta$  and  $\psi$ . Further,  $\psi$  depends on  $\dot{q}$  and  $\phi$  as well as  $\dot{r}$ . These points are discussed in detail by Drummond [23]. Modifications to the stability derivatives and to the equations of motion are given in [23]. We use Drummond's model, after further introducing the variable velocity. In this case all stability derivatives such as  $X_u$ ,  $M_\alpha$ , etc. are dependent on flight velocity - i.e.,  $X_u(V)$ ,  $M_\alpha(V)$ ... With a particular acceleration profile, these parameters vary with time, thereby leading to time varying differential equations.

The mathematical model of the vehicle dynamics for the accelerating case is developed starting from Drummond's model for the case of steady flight [23] on minor circles. In this case we consider the vehicle to fly on a minor circle

with a slowly increasing velocity, i.e., the velocity increases slowly from  $s = 0.2$  to  $s = 1.4$ . We consider a linearization of the equations of motion about this slowly varying velocity. Thus the linearization is about a nominal or prescribed variation or time history in velocity, instead of a constant velocity. Drummond's model is still valid, but his solution based on constant coefficient model is no longer valid. In our approach, we use Drummond's model involving a generic hypersonic vehicle, linearization of the equations and the nominal velocity profile. However, we introduce an acceleration profile to correspond to the velocities in Drummond's model [23]. This results in a time varying model. We solve this set of nonautonomous differential equations by the GMS method. It is useful to note that this constitutes a time varying model as an extension and developed from Drummond's constant coefficient model which is only valid at steady flight.

The dynamic equations describing the motion on a minor circle are written separately in terms of the symmetric and the antisymmetric parts. We note that eq.(2.30) is written in a coupled form, coupling the variables  $u, \alpha$  and  $\theta$ . If this equation is decoupled by cross-differentiation and elimination, a *single* equation of fourth order would represent the dynamics of *each* of the variables. Similarly the decoupling the lateral-directional equations (2.31) by the same process, another equation of fourth order is obtained for *each* of the variables  $v, r$  and  $\phi$ . Each of these decoupled equations in the longitudinal or lateral-directional motions can be written in the general form

$$\sum_{i=0}^4 \omega_i x^{(i)} = 0 \quad (2.32)$$

The coefficients  $\omega_i$  depend on the minor circle radius and the flight condition. We will now consider that the vehicle is accelerating (or decelerating) while continuing to fly on the minor circle. This is best treated by parameterizing the coefficients  $\omega_i$  by the speed ratio  $s$ , which is the ratio of the actual vehicle speed to the orbital speed. Physical constraints on the type of power plant and acceleration capability indicate that the velocity of the vehicle changes *slowly* compared to the important time constants of the motion. Thus the coefficients  $\omega_i$  vary on a slow time scale  $\tilde{t} = \epsilon t$ , while the aircraft dynamics vary on the normal time scale  $t$ . The physical problem is, therefore, to describe the dynamics of the vehicle as its center of mass accelerates (or decelerates) on the  $\tilde{t}$  time scale. The differential equation can, therefore, be written as

$$\sum_{i=0}^4 \omega_i(\tilde{t}) x^{(i)} = 0 \quad (2.33)$$

The formulation assumes that only short period and phugoid modes are treated in the longitudinal case and the Dutch roll and roll-spiral motions in the lateral case, each leading to an equation of the above form, the highest order being four. The

additional symmetric modes and the resulting two characteristic roots can easily be included in this general formulation.

These equations are now time varying and cannot be solved exactly. We develop asymptotic solutions by the GMS method.

### 3 ANALYSIS APPROACH

#### 3.1 General Remarks

The dynamics of hypervelocity flight vehicles are characterized by the high speeds at which they operate. Taking this fact into consideration the dynamics can be analyzed in two situations - (1) at steady flight conditions and (2) variable flight conditions. The case of steady flight presents no great problems in regard to the analysis of small perturbation motion about a prescribed flight condition. However special situations such as steady flight on minor circles introduce special considerations and are treated in the literature [23]. However, the case of variable flight conditions is interesting but is difficult to analyze. We will investigate this class of problems by the GMS method.

The steady flight case arises as a special case of the more general result, as will be clear later. However, in both cases, i.e., steady and variable flight conditions, it is convenient to treat the flight dynamics from the point of symmetric and antisymmetric motions. These are the familiar longitudinal and lateral-directional motions of conventional aircraft at steady flight. In our approach an effort is made to keep these notions in analyzing the dynamics of hypervelocity vehicles. For instance, when the flight conditions are steady, the oscillatory motions are typically described by mathematical functions of the form

$$\theta(t) = C_1 \exp(-at) \sin(\omega t) + C_2 \exp(-at) \cos(\omega t) \quad (3.1)$$

where  $\exp(-at)$  represents the damping (or decay) of the oscillation and  $\omega$  is the frequency of the oscillation. The arbitrary constants  $C_1$  and  $C_2$  are fixed by the initial or boundary conditions on the motion. The important point is that when the flight conditions are constant, the exponent  $(-at)$  of the damping term  $\exp(-at)$  is linear in the variable  $t$ . Similarly the phase of the oscillatory motion which is given by  $\omega t$  is also linear in  $t$  and the frequency  $\omega$  is constant. Because of these simple relations the characteristic motions of the flight vehicles are well understood. However these notions are no longer valid if the flight conditions change continuously. In this case, the damping and phase of the oscillatory motion are no longer linear in  $t$ . The frequency is not constant and varies nonlinearly with  $t$ . Further the damping is not even an exponential of the form  $\exp(-at)$  which occurs in the steady flight case. All these complications are introduced by the changing flight conditions. Further, the prediction of system stability also becomes extremely difficult due to the inadequacy of the conventional steady flight analysis.

In this case of variable flight conditions, the linearized equations of motion are time-varying. The behavior of such systems can be extremely complex and counter-intuitive. However, in the dynamics of flight vehicles, it is possible, under certain conditions, to represent the motions in terms of simple characteristic functions such as elementary transcendental functions and algebraic functions however, with nonlinear arguments, by means of asymptotic theory. For instance, the short period motion can be represented by mathematical functions of the form

$$\theta(t) = C_1 \exp(a(t)) \sin(\omega(t)) + C_2 \exp(a(t)) \cos(\omega(t)) \quad (3.2)$$

Unlike the steady flight case, the terms  $a(t)$  and  $\omega(t)$  are now *nonlinear* functions of  $t$ . This complexity is essential in time-varying and nonlinear systems. This means that the frequency is not constant and varies nonlinearly. These representations for the amplitude and phase (or frequency) are developed by the GMS theory.

In developing the asymptotic analytical representations of the complex dynamics, two important properties must be kept in mind, - (1) variable flight conditions leading to time varying systems, and (2) separation of fast and slow motions. The nature of variable flight conditions has been discussed above. The mixture of rapid and slow motions present in most dynamic systems, renders the analysis very difficult in a manner quite different from the complexities due to the variable flight conditions. The properties (1) and (2) stated above are independent properties and co-exist in a particular dynamic system. We note, for example, that the hypervelocity flight dynamics are characterized by a mixture of rapid and slow motions. The simplest such examples are found even in the steady flight case. The short period oscillations with high frequency and large damping are fast compared to the slower phugoid oscillations with low frequency and small or zero damping. Sometimes the phugoid can even be unstable. Similarly in the lateral-directional case, the Dutch Roll oscillations lie between the fast roll mode and the slow spiral mode, the later two being nonoscillatory. When considering changes in flight conditions (speed in particular), the frequencies are no longer constant. The behavior is nonautonomous and complex. Nonetheless, there is an inherent separation implicit in the fast and slow variations in the dynamics of the vehicle. For instance the nonlinear phase changes in one "mode" occur more rapidly than similar changes in other "modes". A systematic separation of such motions is highly desirable, as it leads to great simplification in the dynamic analysis. This, in turn leads to greater insight, improved constructive procedures for computation, analysis and design. Such a systematic separation is the *raison d'etre* of the Generalized Multiple Scales (GMS) method. By means of this method, asymptotic solutions are developed systematically, for several classes of flight dynamic problems. In particular, the GMS method leads to accurate asymptotic representation of the vehicle dynamics for re-entry trajectories as well as constant altitude minor circle trajectories at hypersonic speeds. The GMS method is briefly outlined as follows. It has been developed relatively recently and has led to a large number of applications.

### 3.2 Generalized Multiple Scales (GMS) Method

This technique is particularly useful in the study of phenomena which exhibit a mixture of rapid and slow motions. The inherent time constants present in the dynamics of such systems are systematically separated leading to simpler representations. Such a separation of the fast and slow motions is achieved by employing a number of independent "observers", each using a "clock" which counts time at

a different rate. Each observer perceives a different aspect of the phenomenon. A combination of the different aspects yields a composite description of the dynamics. The method is fairly recent in its development but has already been applied to study a great variety of phenomena, with considerable success.

The technique consists of enlarging the domain of the independent variable time, into a space of higher dimension by means of "clocks" or scale functions. The differential equations describing a dynamic phenomenon are extended into a set of partial differential equations. A small parameter  $\epsilon$  ( $\ll 1$ ) is identified as the ratio of the fast and slow time constants. By means of this parameter the extended equations are solved order by order and lead to asymptotic solutions. Thus the concept of transformations forms a particular case of this general process of extension.

There are many dynamic phenomena where the choice of linear scales is inadequate. Examples are those which are described by time varying and nonlinear differential equations. In such cases, the solution process by the GMS method requires greater freedom in the choice of scale functions. The method was generalized by Ramnath and Sandri [13,44] to include nonlinear and complex scales.

This generalization is tantamount to the use of "accelerating" or "decelerating" clocks, i.e., time is counted at an increasingly faster or slower rate, depending on the phenomenon. By this means, simple and uniform representations of the dynamics are obtained. These ideas have been developed and elaborated by Ramnath through theoretical developments and applications to a variety of aerospace applications [9-17]. Therefore, the GMS technique will not be treated in depth in this report. Rather, we will invoke the principal results of the GMS technique to the problem of hypervelocity flight dynamics.

The main idea of the GMS method is to extend the independent variable into a new space. The dependent variable is also suitably extended. The problem is solved in the new space and the solutions are expressed in the original problem variables. The general concept can be usefully described in an abstract framework as follows.

Consider a class of single-valued mapping functions  $\Phi$  with a domain  $\delta$  and a range  $\rho$  (Figure 4). This may be the differential equation of motion

$$\Phi : L\{x(t), t, \epsilon\} = 0 \quad (3.3)$$

Here  $t$  and  $x$  are defined on the sets  $\delta$  and  $\rho$  respectively and  $L$  is a differential operator. The small parameter  $\epsilon$  ( $0 < \epsilon \ll 1$ ) is the ratio of the fast and slow time constants. We now consider new mappings  $E_\delta$  of  $\delta$  onto the set  $I_\delta$  which is included in a larger set of  $\underline{\delta}$ . Thus  $I_\delta$  is the image of  $\delta$ . The dimension of  $\underline{\delta} >$  dimension of  $\delta$  and  $\underline{\delta}$  is defined as the extension of  $\delta$ . Now we consider the mapping  $\underline{\Phi}$  of  $\underline{\delta}$  onto a set  $\underline{\rho}$  which includes  $\rho$ . We define the mapping  $\underline{\Phi}$  as the extension of  $\Phi$  if and only if

$$\underline{\Phi} \circ E_\delta = \Phi \quad (3.4)$$

That is, we seek the extensions of the domain and the mapping such that their composition yields the original mapping  $\Phi$ . In other words, the solution of a differential equation is sought by first extending it into a new space and then solving it in the new space. The solution to the original problem is directly obtained by restricting the extended solution to the original problem variables.

In a practical sense we can also define extension as:

### EXTENSION

Given a function  $f(t, \epsilon)$  and another function  $F(\underline{\tau}, \epsilon)$  of the  $n$  independent variables  $\tau \equiv \tau_0, \tau_1, \dots, \tau_n$  (each of which can be an  $n$ -dimensional vector), we say that  $F(\underline{\tau})$  is an extension of  $f(t)$  if and only if there exists a set of relations

$$\tau_i = \tau_i(t, \epsilon) \quad (3.5)$$

i.e.,

$$\tau_i = \{ \tau_1(t, \epsilon), \tau_2(t, \epsilon), \dots, \tau_n(t, \epsilon) \} \quad (3.6)$$

such that, when inserted into  $F(\underline{\tau}, \epsilon)$  yield  $F(\underline{\tau}(t, \epsilon), \epsilon) = f(t, \epsilon)$ .

In applications we extend

$$t \rightarrow \{ \tau_0, \tau_1, \dots \} \quad (3.7)$$

$$x(t, \epsilon) \rightarrow x(\tau_0, \tau_1, \dots, \epsilon) \quad (3.8)$$

where  $\tau_i = \tau_i(t, \epsilon)$  are the time scales and are chosen to yield accurate asymptotic solutions.

The development of solutions using the GMS method depends on the presence of a small parameter  $\epsilon$ , where and how it appears in the mathematical model of a system. Indeed these factors determine whether a problem is singular or secular in regard to perturbations and approximate solutions. The "clock" functions are appropriately chosen to render the asymptotic solutions uniformly valid. In general, we extend the variables as shown above. A fairly general class of these extensions is given by

$$\tau_0 = t, \tau_1 = \epsilon^m \int k(t) dt \quad (3.9)$$

where  $k(t)$  is the "clock" function and the exponent  $m$  determines whether the technique solves *singular* or *secular* perturbation problems. The precise value of  $m$  is determined from the *Principle of Minimal Simplification* and its extensions [16,41]. For a given problem, Ramnath has shown [16] that there is a correct choice of  $m$  for a proper asymptotic analysis, based on the Kruskal diagram. Having determined  $m$ , then the clock  $k(t)$  can be determined from the governing

differential equation of motion. This again, will change, according to whether the perturbation is *singular* or *secular*.

### **Singular and Secular Perturbation:**

These terms are used in asymptotic analysis to describe the nature of nonuniformity in the perturbation solution. In developing an approximate representation of a complicated function (for example, the solution of a nonautonomous differential equation)  $x(t, \epsilon)$ , one writes,

$$x(t, \epsilon) \sim x_0(t) + \epsilon x_1(t) + \epsilon^2 x_2(t) + \dots \quad (3.10)$$

In this asymptotic expansion, the successive terms decrease rapidly in magnitude. In this case, the accuracy of the approximation increases dramatically by considering terms of higher order. Thus, most of the contribution to the solution is contained in the first term, and the second term is a small correction. The third term is an even smaller correction, and so on. Often however, in real problems, this may happen in one part of the domain of interest and break down in another part. This is termed a nonuniformity in the perturbation expansion. If this nonuniformity occurs for small or finite values of the independent variable (for example, for  $t = 0$ ), then it is termed a *singular* perturbation. If it occurs for large values of the argument (for example,  $t \rightarrow \infty$ ), then it is a *secular* perturbation. These and related points are discussed in detail in [9,13,44] and other works on asymptotic analysis and perturbation theory. The interested reader may refer to these works for further details.

In the present class of problems dealing with hypervelocity flight dynamics, Ramnath [9-17] shows that, in general the clock functions are not only nonlinear, but complex quantities.

### **Application of GMS Technique**

The GMS theory has been developed in a very general context on a large variety of mathematical models, including ordinary and partial differential equations. It has been particularly useful in analyzing systems described by ordinary differential equations occurring in dynamic systems analysis and control. Hypervelocity flight vehicle dynamics belong to this area. In order to facilitate an understanding of the mechanics of applying the GMS theory, application of the GMS technique to simple problems is illustrated in Appendix B. The presentation is based on Ramnath's [9,13] work on the GMS theory. The theory and applications thus illustrated can be extended to higher order systems. The reader interested in the GMS analysis of distributed parameter systems and partial differential equations may consult [10,11] by Ramnath and Jenie.

### **Higher Order Equations**

The simple examples in Appendix B illustrate the mechanics of applying the multiple scales theory on differential equations of first order. A similar approach is taken even with higher order equations. For time-varying equations of second

and higher order, even when they are linear, it is impossible in general to derive exact analytical solutions. Therefore, for general classes of systems, asymptotic solutions are obtained by the GMS method as shown by Ramnath [9-17].

The precise form and nature of the GMS solutions would depend on whether the problem is of the singular or secular perturbation type, and the nature of the extension chosen. These are matters of detail which are discussed in [9-17] on various types of systems. For example, in second order linear systems, the GMS theory recovers the WKBJ solutions under certain conditions [13]. The equations of motion of hypervelocity flight vehicles are of fourth order. The GMS technique is employed on this class of systems to generate asymptotic solutions following the approach developed in [13].

Thus the equations corresponding to say, the Dutch Roll, short period, or phugoid mode are suitably extended into multiple time scales and solved in the new space. Application to the re-entry problem, however, involves a nesting of transformations in terms of a distance variable. In this case the GMS technique leads to multiple space scales (instead of time scales). This approach is now presented in the next section.

#### 4 APPLICATION TO RE-ENTRY DYNAMICS

In Section 2.2 a unified equation describing the angle of attack variations was derived. This involves a transformation from  $t$  to a distance variable  $\xi$ , defined as the number of reference lengths traversed by the vehicle. We will now consider variations in angle of attack as described in this unified Equation (2.14), and applied to the space shuttle vehicle.

In the early stages of re-entry the Space Shuttle may have high angles-of-attack. However, in order to develop some degree of insight, we may choose to study some special trajectories. A well-studied class of re-entry problems are those along ballistic trajectories. For a ballistic entry the gravity terms are much smaller than the aerodynamic drag and are therefore neglected. Only the drag force is retained. Further, considering straight line ballistic trajectories in accordance with standard practice [8,15], the terms  $C_{L_0}$  and  $C_{D_0}$  are neglected. This is based on the rationale that when the flight path angle is high enough such that the descent is ballistic, the lift can be neglected and the drag is independent of  $\alpha$ . Under these conditions, as the vehicle center of mass travels along a ballistic trajectory at hypersonic speeds, the angle of attack variations are described by the equation

$$\alpha'' + \delta(C_{L_\alpha} - C_{D_0} - \sigma C_{m_q})\alpha' - \delta[C_{m_\alpha} + \delta C_{L_\alpha}(\sigma C_{m_q} + C_{D_0}) + \delta' C_{L_\alpha}]\alpha = 0 \quad (4.1)$$

where the prime denotes differentiation with respect to  $\xi$ . Considering the atmospheric density variation to be represented by

$$\rho = \rho_s \exp(-\beta h) \quad (4.2)$$

where  $\rho_s$ ,  $h$  are the density at sea level and altitude of vehicle respectively and  $\beta$  a constant, the coefficients of (4.1) can be determined as a function of the trajectory. Employing several transformations and algebraic manipulations [2,8], it can be shown that Equation (4.1) is expressible as Kummer's equation. Solutions can then be developed in terms of confluent hypergeometric functions. The actual vehicle parameters and the trajectory determine the values of the coefficients in Equation (4.2). Let us define new parameters

$$\begin{aligned} K_1 &= \frac{\delta_s}{2\beta L \sin \gamma_0} [C_{L_\alpha} - C_{D_0} - \sigma C_{m_q}] & (i) \\ K_2 &= -\frac{\delta_0}{(\beta L \sin \gamma_0)^2} (\sigma C_{m_\alpha} + \beta L C_{L_\alpha} \sin \gamma_0) & (ii) \\ K_3 &= -\frac{\delta_s^2 C_{L_\alpha} (\sigma C_{m_q} + C_{D_0})}{\beta^2 L^2 \sin \gamma_0} & (iii) \end{aligned} \quad \left. \vphantom{\begin{aligned} K_1 \\ K_2 \\ K_3 \end{aligned}} \right\} (4.3)$$

These are now defined by the vehicle parameters and the trajectory. When the nondimensional density  $\bar{\rho} = \frac{\rho}{\rho_s}$  is much less than the ratio

$$K_R = \frac{K_1 + K_2^2}{K_3 - K_1}$$

that is,

$$\bar{\rho} \ll K_R \quad (4.4)$$

it can be shown that the angle of attack variations can be described by Bessel functions [2,8].

$$\alpha(h) \approx \exp(K_1 \rho(h)) \left\{ C_1 J_0(\eta(h)) + C_2 Y_0(\eta(h)) \right\} \quad (4.5)$$

where  $C_1, C_2$  are constants and

$$\eta(h) \equiv 2\sqrt{K_1 + K_2} \rho(h) \quad (4.6)$$

and  $J_0, Y_0$  are the zeroth order Bessel functions of the first and second kind respectively. This agrees with the results of Allen [2] and Vinh and Laitone [8].

However, when the condition stated in (4.4) is not satisfied, and the parameters  $K_1, K_2, K_3$  are not constant and vary rather rapidly with the trajectory, then the solution (4.5), is not valid. In this case, the more general solution in terms of confluent hypergeometric functions [8] must be used. Indeed, Vinh and Laitone state that small changes in the constants  $K_i$  can produce a profound change in the character of the solutions. When  $K_i$  are not constants, as in our problem, the Vinh-Laitone approach through Kummer's equation cannot be used. Against this rather complicated background, we will develop solutions by means of the GMS method.

#### 4.1 GMS Solutions

The complex nature of the angle of attack variations in re-entry demand, even in specialized cases, a representation in terms of higher transcendental functions such as Bessel functions and confluent hypergeometric functions. Even then, a simple description of the dynamics in terms of stability, frequency, damping and control analysis is difficult. Recognizing that the motion of the vehicle exists on different scales – i.e., fast and slow, we appeal to the GMS method and develop the solutions as follows.

The basic solution of the re-entry dynamics by the GMS method was developed by Ramnath [15], and illustrated by using the space shuttle 049 vehicle. In the present context, a different vehicle and trajectory are used. Instead of addressing the re-entry equations in specialized cases, we consider the general Equation (2.14) for angle of attack. The GMS solution is derived as follows. The coefficients of

equation (2.14) vary "slowly" in that the characteristic time constant of the solution is much smaller than the time constants of the variation of the coefficients. Thus the coefficients  $\omega_1$  and  $\omega_0$  are parameterized by a small parameter  $\epsilon (\ll 1)$  as  $\omega_1(\epsilon\xi)$  and  $\omega_0(\epsilon\xi)$  and if necessary,  $f(\epsilon\xi)$ . Invoking GMS theory, we extend

$$\bar{\xi} \rightarrow \{\xi_0, \xi_1\}; \xi = \bar{\xi}, \xi_1 = \int \frac{k(\bar{\xi})}{\epsilon} d\bar{\xi} \quad (4.7)$$

where

$$\bar{\xi} = \epsilon\xi \text{ and } \alpha(\xi, \epsilon) \rightarrow \alpha(\xi_0, \xi_1)$$

According to the GMS theory, the fast or dominant solution is given by [15]:

$$\begin{aligned} \alpha_f(\xi) = \exp\left[-\frac{1}{2} \int \omega_1(\xi) d\xi\right] \left\{ C_1 \sin\left(\int \left(\omega_0 - \frac{\omega_1^2}{4}\right)^{\frac{1}{2}} d\xi\right) \right. \\ \left. + C_2 \cos\left(\int \left(\omega_0 - \frac{\omega_1^2}{4}\right)^{\frac{1}{2}} d\xi\right) \right\} \end{aligned} \quad (4.8)$$

The slow solution is given by:

$$\alpha_s(\xi) = \left| \omega_0 - \frac{\omega_1^2}{4} \right|^{-1/4} \quad (4.9)$$

The complete GMS solution is given by:

$$\hat{\alpha}(\xi) = \alpha_s(\xi)\alpha_f(\xi) \quad (4.10)$$

The principal results of the GMS theory and its application are developed in [9-17]. However, the current application involves a different vehicle, environment and parameters. Therefore, additional analysis is required to ensure the applicability of the GMS theory as presented in references [9-17] and its accuracy on the new class of systems. This involves such technical considerations as magnitudes and rates of variation of the coefficients, etc. These factors have been fully taken into consideration in our investigation of the hypervelocity flight dynamics and the necessary technical conditions have been satisfied. The theoretical and application results as embodied in this report represent a useful and satisfactory validity of the technical conditions.

## 4.2 Application

The theory discussed above is applied to a recent Space Shuttle vehicle and its trajectories. (Figures 9-27). The data for the vehicle, the trajectories and the environment are all obtained from NASA-JSC. For one class of vehicles, the ratio  $K_R$  is computed along the trajectory (Figure 27). The GMS theory is not limited to a specific trajectory (e.g., steep, ballistic entry) or to a specific vehicle. The trajectory parameters are shown in Figures 8-18. The coefficients and the complex scale functions are also shown (Figures 19-22). Based on these, the fast and slow GMS solutions are computed and compared with numerical solutions for the same set of initial conditions (Figures 23-26). In these figures displaying the solutions, it must be noted that the numerical solutions are shown by solid lines and the corresponding GMS solutions by broken lines. Further, the ordinate represents a scaled value of the dependent variable (ie, angle of attack). As the governing equations are linear and time-varying, the solutions scale directly with the size of the input or the initial conditions. Therefore, the plots show mainly the eigenfunctions.

It is seen that the GMS-fast solution represents the frequency extremely well, but shows a small error in the amplitude peaks. However, this error is corrected by introducing the slow variation of  $\alpha(\xi)$ . The GMS-total solution is extremely accurate and is, in fact, indistinguishable from the numerical solution. This excellent agreement is seen for other initial or boundary conditions as well.

Figure 23 shows the angle-of attack oscillations against distance along the re-entry trajectory. Two solutions, - (1) numerical and (2) GMS-fast solutions are displayed superimposed, for the initial condition of  $\alpha(0) = 0$  and  $\dot{\alpha}(0) = 1$ . The phase change and frequency are nonlinear and this point is reflected in the figure. Indeed the frequency increases monotonically as shown by the increasing proximity of the zero-crossings. This is due to the fact that as the vehicle penetrates into the atmosphere, the aerodynamic spring becomes tighter, - i.e., the spring constant increases, thereby increasing the frequency. However, this frequency change has a subtle effect on the damping of the oscillation as well, - i.e., the damping increases. This elusive effect cannot be predicted by overly simplistic approximations such as the frozen solution. The GMS-fast solution, on the other hand, picks up the frequency variations extremely well as seen by the zero-crossings which coincide with those of the numerical solutions. In addition, it also picks up the subtle variation in damping, but has a slight error in the amplitude representation. This is not surprising, as the fast solution is designed to describe mainly the fast variations of the solution, and this is done with great accuracy. The slow part of the GMS solution is designed to (and does indeed) represent the slow variations of the solution accurately. By combining the fast and slow parts of the GMS solution, a highly accurate analytical description of the *fast* and *slow* aspects of the solution are obtained by the GMS-total solution. The great advantage is that the GMS solutions are *analytical*. Therefore, they can be used for a variety of purposes such as parameter trade-off studies. Figure 24 shows a comparison of the numerical and the GMS-total solutions for the same initial conditions. It is

clear that the GMS-total solution represents the true behavior extremely accurately in that it is indistinguishable from the numerical solution. The effect of changing initial conditions on the accuracy of the solution is examined by generating the solutions, (1) numerical, (2) GMS-fast and (3) GMS-total, for a different set of initial conditions,  $\alpha(0) = 1$ ,  $\dot{\alpha}(0) = 0$ . Even in this case, the GMS-fast solution represents the frequency extremely well, but has a slight error in amplitude. Again, the GMS-total represents both the frequency and amplitude of the true solution extremely accurately, as evidenced by the comparisons with the numerical solutions. The result of the increasing spring constant due to the increasing aerodynamic density is shown very clearly by the solutions. It is important to note that the high accuracy and ease of applicability of the solutions are preserved even when initial conditions are changed.

Typical trajectories may be steep, ballistic ones along a straight line, spirals at shallow angles, or those between these extremes. Allen derived approximate solutions using Bessel functions, Vinh and Laitone considered the above two extreme trajectories. An arbitrary trajectory between these extremes cannot be treated by either approach. Our GMS solutions are derived for an arbitrary trajectory and are extremely accurate. In the case of limiting trajectories, the GMS solutions recover the Bessel or confluent hypergeometric behavior for steep trajectories and that of the damped Mathieu functions for shallow spiral trajectories.

In the next section, we develop the GMS solutions to the dynamics of hypervelocity vehicles flying on minor circles. In particular, the effect of acceleration on the vehicle dynamics is investigated. Analytical solutions by the GMS theory are developed. This presentation then leads to an analysis of the stability of motion of the hypersonic vehicles in Section 6.

## 5 HYPERVELOCITY FLIGHT DYNAMICS ON A MINOR CIRCLE

### 5.1 General Remarks

In this section we will analyze the dynamics of the vehicle traveling at hypersonic speeds at constant altitudes on minor circle trajectories. The steady flight case leads to a conventional interpretation in terms of the usual modes of motion of an aircraft, such as Dutch Roll, Short Period, phugoid, roll and spiral modes. This case, including deviations from the standard modes because of the minor circle geometry and related issues are discussed in [23]. The more complicated case of accelerated flight on minor circles has not been treated in the literature. In this section we will first develop asymptotic solutions by the GMS method. The approach is then applied to a generic vehicle flying on extreme minor circle radii as are realistic and meaningful. The GMS solutions are compared with direct numerical solutions for the different geometries and are seen to be highly accurate. The fast and slow solutions of the GMS approach show a clear separation. These solutions are discussed in detail. The peculiarities and counter-intuitive behavior of the vehicle on some trajectories are recognized as due to the turning point phenomenon and are discussed later..

### 5.2 Development of the Solution

It is clear that the dynamic equations for the longitudinal and lateral-directional modes of the hypervelocity vehicle on a minor circle can be written in the form

$$\sum_{i=0}^4 \omega_i(\tilde{t}) x^i = 0 \quad (5.1)$$

Depending on the acceleration (or deceleration) profile of the vehicle, the coefficients  $\omega_i$  vary on a slow  $\tilde{t}$  time scale, where  $\tilde{t} = \epsilon t$ ,  $\epsilon$  being a small parameter ( $0 < \epsilon \ll 1$ ). Indeed  $\epsilon$  is the order of the ratio of the time constant of the dynamics to that of the acceleration change. That is, we assume that the dynamics change much faster than the acceleration change. In this case we can re-write the differential equations of motion as

$$\sum_{i=0}^4 \epsilon^i \omega_i(\tilde{t}) \frac{d^i x}{d\tilde{t}^i} = 0 \quad (5.2)$$

We have now expressed the dynamics by a singularly perturbed time varying equation. In order to solve it we invoke the theory and technique of Generalized Multiple Scales [9-17].

In accordance with the concept of multiple scales, we extend the domain of the independent variable, time, as follows:

$$\tilde{t} \rightarrow \{\underline{\tau}\} \text{ with } \underline{\tau} = (\tau_0, \tau_1, \dots, \tau_n) \quad (5.3)$$

The variables  $\tau_0, \tau_1, \dots, \tau_n$  are functions of  $\tilde{t}$  and  $\epsilon$ . The space of  $\{\tau_0, \tau_1, \dots, \tau_n\}$  constitutes the extended domain. The solution  $x(\tilde{t}, \epsilon)$  is also extended as

$$x(\tilde{t}, \epsilon) \rightarrow x(\underline{\tau}, \epsilon).$$

We also have the freedom to expand  $x(\underline{\tau}, \epsilon)$  i.e.,

$$x(\underline{\tau}, \epsilon) = x_0(\underline{\tau}) + \epsilon x_1(\underline{\tau}) + \dots$$

In general the asymptotic behavior with respect to  $\epsilon$  is represented as some power  $m$  of  $\epsilon$ . We have two degrees of freedom in developing approximations – (1) expansion of the dependent variable and (2) use of more scale functions. This freedom is utilized in getting a simpler and smoother description with respect to  $\epsilon$ . The correct behavior in  $\epsilon$  is obtained by choosing a proper exponent  $m$  of  $\epsilon$ . This choice is facilitated by the application of the Principle of Minimal Simplification. According to this principle, a compromise must be made between completeness and simplicity in developing a correct and useful asymptotic approximation. Because an approximation is made basically by neglecting some terms in a mathematical model, it is of utmost importance to

- (1) neglect only the proper terms in a certain asymptotic limit
- (2) retain as many terms as possible and not neglect too many terms.

This is because, each term contains information and neglecting terms results in a loss of information. However, unless some terms are neglected, the system cannot be simplified. Therefore, in view of these conflicting requirements, the Principle of Minimal Simplification enables us to neglect the proper terms consistent with completeness and simplicity. It was first enunciated by Kruskal [41] and was refined and extended by Ramnath[16], who then applied it to a variety of aerospace dynamic systems. A detailed discussion of this technique is beyond the scope of the current effort and relevance. The interested reader may consult [16]. In the context of the GMS approach this principle can be applied as follows. Using two time scales  $\tau_0$  and  $\tau_1$  defined as

$$\tilde{t} \rightarrow \{\tau_0, \tau_1\}; \tau_0 = \tilde{t}, \tau_1 = \epsilon^m \int k(\tilde{t}) d\tilde{t} \quad (5.4)$$

The time derivative operator  $d/d\tilde{t}$  be extended as

$$\frac{d}{d\tilde{t}} \rightarrow \frac{\partial}{\partial \tau_0} + \epsilon^m k \frac{\partial}{\partial \tau_1} \quad (5.5a)$$

Higher order derivatives can be similarly extended. The extension of the  $n$ th order derivative operator was given by Ramnath[44]. The proof is by induction. The problem now is to find the asymptotically correct value for  $m$ .

In the case of the longitudinal and lateral directional equations of the hypervelocity vehicle, we have considered the mathematical model to be of order four. In this case the extension of the fourth order derivative operator is obtained as follows:

$$d^4/d\tilde{t}^4 \rightarrow \left( \frac{\partial}{\partial \tau_0} + \epsilon^m k \frac{\partial}{\partial \tau_1} \right)^4 \quad (5.5b)$$

By means of the binomial theorem the operator can be expanded in powers of  $\epsilon^m$  as:

$$d^4/d\tilde{t}^4 \rightarrow \left( \frac{\partial^4}{\partial \tau_0^4} \right) + \epsilon^m ( ) + \epsilon^{2m} ( ) + \dots \quad (5.6)$$

By using arguments of the Principle of Minimal Simplification [16], the best value of  $m$  is found to be

$$m = -1 \quad (5.7)$$

It should be noted that in general, several choices can be made for  $m$ . Indeed, the value of  $m$  leading to the proper ordering depends on the kind of asymptotic problem. However, for the class of problems involving slowly varying coefficients,  $m = -1$  is the optimal choice. This is particularly true for the dynamics of hypervelocity flight vehicles along different trajectories studied in this report.

Other choices for  $m$  will lead to asymptotically inappropriate forms as shown by Ramnath [16]. Using the correct value for  $m$ , we can develop the asymptotic solutions for the vehicle dynamics in a multiplicatively separable form on the time scales  $\tau_0$  and  $\tau_1$ . Thus the solution is given by

$$x(\tilde{t}, \epsilon) \sim x_{fast}(\tilde{t}) \cdot x_{slow}(\tilde{t}) \dots \quad (5.8)$$

where

$$x_{fast} = x_{fast}(\tau_1) \quad (5.9)$$

and

$$x_{slow} = x_{slow}(\tau_0) \quad (5.10)$$

The development of the specific solutions is illustrated in the actual application to the dynamics of a representative vehicle.

### 5.3 Application to a Generic Vehicle

The theory of Generalized Multiple Scales is now applied to the dynamic analysis of a representative vehicle [23] as it flies at hypersonic speeds on minor circles. The generic vehicle used to illustrate the GMS approach is the vehicle configuration of Drummond [23] given in Appendix A. In our model, we consider this vehicle configuration and parameters. However, the velocity of the vehicle flying on minor circles is allowed to change continuously, corresponding to an acceleration profile. Following [23] we consider flight along three minor circles, defined by the normalized radius  $\bar{r} = \frac{r}{R_E}$

$$(i) \bar{r} = 1.0 \quad (ii) \bar{r} = 0.5 \quad \text{and} \quad (iii) \bar{r} = 0.1 \quad (5.11)$$

In particular, the two extreme radii  $\bar{r} = 1.$  and  $\bar{r} = 0.1$  are considered, with  $\bar{r} = 0.5$  being an intermediate case. However, the nature of the dynamics for the intermediate case is bounded by the two extreme cases, both qualitatively and quantitatively and offered no special insight. Therefore, data and discussions are presented only for the two extreme cases. On each minor circle, we consider accelerated flight, with the speed ratio  $s = V/\sqrt{gR}$  ranging from  $s = 0.2$  to  $s = 1.4$  in a linear fashion. The independent variable,  $t$  (time), is first transformed to aerodynamic time,  $t^*$  given by

$$t^* = (2V/L)t \quad (5.12)$$

where  $t^*$  is in airseconds,  $t$  in real seconds  $L$  is the scale length of the vehicle (= 150 ft) and  $V$  is the vehicle velocity. Therefore, when the speed ratio is  $s = 0.2$ , the vehicle velocity is about 5000 ft/sec, being about  $0.2 \times$  orbital speed. In this low speed range, the relation between real time and aerodynamic time is given by

$$1 \text{ real second} \approx 70 \text{ airseconds} \quad (5.13)$$

The acceleration capability of the power plant of the vehicle will determine the rate of change of the speed ratio  $s$ . This would depend on the ability to burn hydrogen at supersonic speeds and the related technology. For example, assuming the vehicle to have an average acceleration capability of  $2g$  over the speed range of  $s = 0.2$  to  $s = 1.4$ , the time over which this speed change takes place can be calculated to be about 500 real seconds. At the low speed this would correspond to about 35000 airseconds, as the lower limit. From these considerations, the variation of speed ratio with aerodynamic time is determined as

$$s = s(\epsilon t^*) = a_0 + a_1 \epsilon t^* \quad (5.13)$$

where  $10^{-4} < \epsilon < 10^{-3}$ . This is an example of a suitable value of  $\epsilon$ . Indeed, the theory is valid for any  $\epsilon \ll 1$ . The smaller  $\epsilon$  is, the more accurate is the theory, as consistent with asymptotic analysis. The actual variation of  $s(t^*)$  is shown in Fig.

28. Therefore this is now a situation where the hypervelocity vehicle accelerates from an initial velocity of  $s = 0.2$  to a final velocity of  $s = 1.4$ , while flying on a particular minor circle. In this case the equations of motion are parameterized by the small parameter  $\epsilon$ . The GMS theory is now invoked to yield asymptotic solutions.

Starting from an initial *constant* velocity of  $s = 0.2$  the dynamics of the vehicle are characterized by the usual modes of motion - i.e., Dutch Roll, short period, phugoid, roll-spiral modes. Of these the modulus of the Dutch Roll mode is dominant, followed by the short period mode and then the others. As the vehicle accelerates (or decelerates) slowly, these modes will change continuously and the conventional time-invariant theory is no longer applicable, both with respect to stability analysis and response prediction. We appeal to GMS theory to develop asymptotic solutions.

In accordance with the GMS approach, the "clock" functions  $k(\tilde{t}) = k(\epsilon t^*)$  are not only nonlinear functions of  $t^*$ , but are also complex quantities. In the limit of constant velocity (say  $s = 0.2$ ) the clocks yield the Dutch Roll (and other) characteristic roots. However, as the speed ratio changes continuously, the clocks also change continuously and nonlinearly with  $t^*$ . The solution is then obtained in a separable form with respect to fast and slow variations.

We consider the dimensions of the representative vehicle, the operating minor circle geometry ( $\bar{r} = 1.0, 0.5$  and  $0.1$ ) and the acceleration profile as discussed above. Asymptotic solutions are developed by the GMS method, for each mode starting with the Dutch Roll. In each case two sets of linearly independent boundary conditions are chosen. Three kinds of solutions were computed:

- (1) Direct numerical solution
- (2) GMS - fast solution
- (3) GMS - total (fast and slow) solutions.

All these are computed for the same initial and boundary conditions. They are plotted together on the same plot to show a comparison of the relative accuracy. Then the entire set of computations and plots are repeated for other minor circle radii. All the relevant plots for the minor circle case are shown in Figures 28-72. In all the figures displaying a comparison of the numerical and the GMS solutions, it should be noted that the numerical solutions are depicted by solid lines and the GMS solutions by the broken lines.

Again, it is important to note that the scales of the ordinates in the responses are not specified. The model investigated is a linear time-varying system and the plots represent the characteristic solutions (i.e., eigenfunctions). The exact scales are not important to study the system properties such as stability, frequency and damping. The shapes of the solutions would be directly scaled according to the scale factor.

## 5.4 Discussion of the GMS Solutions

As the velocity of the hypersonic vehicle increases linearly, an examination of the stability derivatives and the characteristic roots shows that they vary highly nonlinearly with respect to the speed ratio, and aerodynamic time. At the flight condition represented by the initial constant velocity, the Dutch Roll frequency is higher than that of the short period mode. However, as the vehicle accelerates, one cannot even speak of the "frequency" of a mode, but only of nonlinear phase changes. Even in this situation, the nonautonomous "Dutch Roll" phase changes faster than that of the time varying short period. Further, within a particular mode the phase change gets less rapid as the vehicle accelerates. These points can be noted from the responses. The GMS solutions exhibit the following features. The GMS-fast solution,  $\tilde{x}$ , represents the fast part of the behavior - i.e., the oscillatory aspect very well. This is evidenced by the fact that the zero-crossings of the GMS-fast ( $\tilde{x}(t^*)$ ) and the numerical solution are the same (to within the resolution of the plots). However, the amplitude representation is initially very accurate, but a small error in amplitude can be noticed (see figures) as  $t^*$  increases. By combining the fast and slow behaviors, we obtain the "GMS-total" solution,  $\hat{x}(t^*)$ . From the figures we see that this solution is highly accurate with regard to both phase and amplitude. Indeed, the GMS-total solution  $\hat{x}(t^*)$  is indistinguishable from the numerical solution. The slow behavior introduces corrections to the amplitudes precisely at the right times and by the right amounts. The amplitude and phase variations are quite unlike the dynamics at steady flight. This general pattern can be seen for the many cases of solutions for both the "Dutch Roll" and the "short period" modes, - at different initial conditions, different minor circles. In fact, when attempting a numerical integration using a step size which is not small, it is found that there is a numerical instability leading to a spurious "damping" and a complete misrepresentation of the dynamics (Figure 39). Further, it is seen that, starting from a given initial velocity, the same acceleration leads to more rapid oscillations and faster damping for flight on minor circles of smaller radii. These remarks are true for both the "Dutch Roll" and the "short period" modes. The effect of changing the radius of the minor circle trajectory is shown in Figures 48, 49, 56 and 59. The Dutch Roll mode is shown in Figures 48 and 49 and the Short Period oscillations are shown in Figures 56 and 59. The increase in the nonlinear phase changes and the amplitude decay due to the smaller radius of the minor circle are clearly seen in these figures.

## “Phugoid”and “Roll-Spiral” Modes

Continuing the analogy with the standard modes of motion of conventional aircraft, we note that the phugoid and the roll-spiral motions are quite different from the Dutch Roll and short period modes. Taking the “phugoid” mode first, we see that there is a qualitative difference between the minor circles defined by  $\bar{r} = 1.0$  and  $\bar{r} = 0.1$  as seen from the root variations. For  $\bar{r} = 0.1$ , the nonlinear phase change of the “phugoid” oscillation is monotonic and real. However, for the case  $r = 1.0$  the “phase” becomes imaginary after some time into the acceleration and the dynamics are nonoscillatory. That is, at some point in the flight envelope, there is a *turning point*. At this point the asymptotic solutions must be continued into the complex plane to account for the dominant and subdominant contributions as they interchange their roles. This phenomenon will be discussed later.

However, for flight on the minor circle  $\bar{r} = 0.1$ , the phugoid oscillations show a continuously decreasing “frequency”. In this case, even with no explicit damping, the oscillations are implicitly damped, engendered by the nonlinear phase change. This damping is different from the familiar dynamics of a constant linear system where the damping is an exponential of linear phase. These points are clearly displayed in the phugoid oscillations. Again, the GMS solutions are highly accurate. The GMS-fast solution represents the zero-crossings very well and the GMS-total solutions are accurate in both phase and amplitude.

### 5.5 Turning Point Phenomenon

The dynamics of the hypervelocity vehicle for flight on the minor circle  $\bar{r} = 1.0$  are far more complicated. In particular, the phugoid mode and the roll, spiral modes lead to very complex behavior. Considering the phugoid mode first, the dynamics at low speed are characterized by oscillatory behavior. As the vehicle accelerates, to high speeds near or exceeding supercircular speeds, the oscillations disappear and the motion becomes completely nonoscillatory. This change in the essential qualitative behavior in the dynamics is termed a *turning point* or *transition point* phenomenon. The point which separates the two kinds of behavior is the turning point or the transition point. This kind of complex behavior cannot be represented by a simple function. In particular, accurate asymptotic solutions can be developed on either side of the turning point, but they cannot be easily continued to the other side. Indeed such a continuation requires the use of higher transcendental functions such as hypergeometric functions. Solution of this problem is facilitated by a study of the related Stokes’ phenomenon and analytic continuation of the solution into the complex plane. Solutions can be effected by developing the specifiable but intricate *connection formulae* analogous to the well known technique of Jeffries in physics. These sophisticated approaches are beyond the scope of the current effort and are not treated in this report. However, a comparison of the numerical and GMS solutions shows excellent accuracy in phase and amplitude from the start up to a neighborhood of the turning point (which is about  $6.6 \times 10^4$  airseconds). The solutions become unstable as the vehicle continues accelerating beyond this point..

The amplitude would still be correct beyond the turning point, although, in general, there would be a phase error, unless this problem is addressed and corrected. The plots (Fig. 68) are valid only in the range 0 to  $4 \times 10^4$  airseconds.

### **“Roll-Spiral” Mode**

The dynamic behavior of the phugoid is complex because of a turning point in the domain of interest. The roll-spiral dynamics are even more complex because, in this case, there are two turning points in the flight envelope, one between  $2 \times 10^4$  and  $3 \times 10^4$  airseconds, and the other between  $7 \times 10^4$  and  $8 \times 10^4$  airseconds. The problem in this case is much more difficult. Although in principle, such a multiple turning problem can be solved, such a solution is not attempted in this effort. Without considering such a sophistication, the numerical and GMS solutions are displayed as before, and clearly shows the turning point phenomenon.

## 6 STABILITY ANALYSIS

The stability of a hypervelocity vehicle as it moves along a prescribed trajectory is a complex matter to analyze. The difficulty stems mainly from the fact that the system is nonautonomous. The usual approach in stability and control analysis of such flight vehicles is first to "freeze" the system at a particular operating point. This is based on the assumption that the system is "slowly" varying. The resulting constant linear system is analyzed from the point of stability and control, using the standard methods. Although this approach is not rigorous, it works reasonably well sometimes. The results are eventually validated by computer simulation. However, sometimes, such a simplistic approach can lead to a total misrepresentation of the temporal behavior, both in regard to stability and control. It is, therefore, of primary importance that a proper and rigorous stability analysis be carried out.

Nonautonomous systems often exhibit behaviors that can be totally counter-intuitive. Some of these peculiarities can be enumerated as follows [34,35].

### 6.1 Peculiarities of Dynamics through Variable Flight Conditions

- (a) System stability is not necessarily given completely by the location of the eigenvalues. For instance, a system may have its eigenvalues with negative real parts and have an unstable response. However, a system may be stable even when its eigenvalues have positive real parts.
- (b) Eigenvalues on the imaginary axis do not necessarily imply neutral stability.
- (c) Eigenvalues on the imaginary axis do not necessarily imply oscillatory response.
- (d) In a coupled system, the different variables may have different stability characteristics.
- (e) Response of a periodic system may not be periodic.

Because of these and other properties, the methods of constant linear systems cannot be applied directly. A careful analysis is required to interpret the dynamics properly.

Recognition of these peculiarities is not easy as they lie buried in the abstruse recesses of mathematical systems theory. Identification and prediction of these effects is even more esoteric as they demand a fundamental understanding of such complex nonautonomous behaviors. Often such an insight into system behavior is possible only through exact mathematical solutions which constitute a rare event. As a consequence, the applied engineers as a class are generally unaware of these important but counter-intuitive (and certainly not obvious) nonautonomous effects. Ordinarily, references are relatively obscure or incomplete in regard to a clear exposition of these peculiarities. Ramnath [34] has distilled a comprehensive enumeration of these effects from the standpoint of systems theory.

## 6.2 Stability and Response During Re-Entry

It is known that [44] that an equation of the form

$$\alpha'' + \omega_1 \alpha' + \omega_0 \alpha = 0 \quad (6.1)$$

can be written in the form

$$z'' + \Omega z = 0 \quad (6.2)$$

where

$$\alpha = z \exp\left(-\int \omega_1 dt/2\right) \quad (6.3a)$$

and

$$\Omega = \omega_0 - \frac{\omega_1^2}{4} - \frac{\dot{\omega}_1}{2} \quad (6.3b)$$

From the GMS solutions for  $\alpha$  and  $z$  it can be shown that the angle of attack oscillations would decay in amplitude if

$$\dot{\Omega}/\Omega > -2\omega_1 \quad (\text{and } \Omega > 0) \quad (6.4)$$

A more detailed mathematical analysis of the stability and response of such systems would involve a separation of the nonoscillatory and oscillatory cases. Such questions have been pursued at great length in the mathematical literature [40,44].

For the present, we are mainly interested in deriving simple criteria for stability and critical altitude for the hypervelocity vehicle descending into the atmosphere. The nature of the criteria become particularly simple in the case of ballistic trajectories, analyzed as follows.

The equation for the angle-of-attack oscillations of a Shuttle type vehicle has been shown to be of the form eq.(2.14). Assuming that the atmosphere is isothermal (typical at re-entry into earth's atmosphere), the density  $\rho$  is modeled as an exponential decay with altitude. A stability criterion for arbitrary trajectories can now be developed. However, for purpose of illustration, we will present an outline of the development of the stability criterion for steep trajectories, as it leads to a simple result in terms of aerodynamic parameters. Also it must be noted that a rigorous theory of stability would require an examination of the nonoscillatory and oscillatory cases separately. We will treat the oscillatory case as it is of greater interest. The density is taken to vary exponentially with  $\xi$ , and

$$\rho = \rho_0 \exp(A\xi) \quad (6.5)$$

where

$$\rho_0 = C e^{-\beta h_0} \quad (6.6)$$

$h_0$  is the altitude above sea level and

$$A = -\beta L \sin \gamma_0 \quad (6.7)$$

and  $\gamma_0$  is the initial descent angle ( $< 0$ ). Also let

$$\delta = \delta_0 \exp(A\xi) \quad (6.8)$$

where

$$\delta_0 = \rho_0 S L / (2m) \quad (6.9)$$

Typical values for the above constants, as per the International Standard Atmosphere (ISA) are given as:  $C \sim 2 \text{ kg/m}^3$ ,  $\beta \sim 1.6 \times 10^{-4}$ . The asymptotic solutions developed by the GMS theory enable us to develop a stability analysis of the shuttle vehicle during re-entry. The fast and slow solutions are asymptotically ordered as the dominant parts of the actual dynamics.

The GMS solution for the angle of attack variations during re-entry is given by:

$$\begin{aligned} \alpha(\xi) = & |\omega_1^2 - 4\omega_0|^{-1/4} \left\{ \exp\left(-\frac{1}{2} \int \omega_1 d\xi\right) \left[ C_1 \cos\left(\frac{1}{2} \int_0^\xi (4\omega_0 - \omega_1^2)^{1/2} d\xi \right. \right. \right. \\ & \left. \left. \left. + C_2 \sin\left(\frac{1}{2} \int_0^\xi (4\omega_0 - \omega_1^2)^{1/2} d\xi\right) \right] \right\} \quad (6.10) \end{aligned}$$

The  $\alpha$ -equation can now be written as:

$$\frac{d^2 \alpha}{d\xi^2} + (g_1 \delta_0 e^{A\xi}) \frac{d\alpha}{d\xi} + (g_2 \delta_0 e^{A\xi} + g_3 \delta_0^2 e^{2A\xi}) \alpha = 0 \quad (6.11)$$

where

$$g_1 = C_{L_\alpha} - C_{D_T} - \sigma(C_{m_{\dot{\alpha}}} + C_{m_q}) \quad (6.12)$$

$$g_2 = -(\beta L \sin \gamma_0 C_{L_\alpha} + \sigma C_{m_\alpha}) \quad (6.13)$$

$$g_3 = -C_{L_\alpha} (C_{D_T} + \sigma C_{m_q}) \quad (6.14)$$

and  $C_{D_T}$  is the drag coefficient at trim.

The stability condition (6.4) leads to

$$\delta_0 \exp(A\xi) \left( g_3 - \frac{g_1^2}{4} \right) > \left( g_2 - \frac{A}{2} g_1 \right) \quad (6.15)$$

Now for a conventional hypervelocity vehicle configuration (e.g., Space Shuttle)

$$g_2 > \frac{A}{2}g_1 \quad (6.16)$$

and

$$g_2 = O(1) \quad (6.17)$$

Now (6.15) leads to

$$\left(\frac{g_1^2}{4} - g_3\right) < \frac{1}{\delta_o} \exp(A\xi) \quad (6.18)$$

This condition is satisfied for a conventional vehicle. Therefore  $\alpha(\xi)$  response is stable if (6.4) holds.

Now

$$\Omega = \delta_o^2 \exp(2A\xi) \left(g_3 - \frac{g_1^2}{4}\right) + \delta_o \exp(A\xi) \left(g_2 - \frac{Ag_1}{2}\right) \quad (6.19)$$

It can be shown that

$$\Omega' / \Omega \approx 2A \quad (6.20)$$

Therefore the condition (6.4) leads to

$$A > -\delta_o g_1 \exp(A\xi) \quad (6.21)$$

Now  $A = -\beta L \sin \gamma_o > 0$  for descent (i.e.,  $\gamma_o < 0$ ). The condition (6.21) is satisfied if

$$g_1 > 0 \quad (6.22)$$

Therefore, for stability,

$$g_1 = C_{L\alpha} - C_{DT} - \sigma(C_{m\dot{\alpha}} + C_{m\alpha}) > 0 \quad (6.23)$$

Such conditions have been discussed in [8]. However, the present approach, interpretation and conclusions stem from the GMS theory.

### Critical Altitude

From the solutions obtained by the GMS theory and the stability criterion discussed above, an estimate can be of the critical altitude,  $h_c$ . This is the altitude at which the angle of attack oscillations could potentially become unstable, leading to amplitude divergence. We note that the condition for stability is that

$$\Omega'/\Omega > -2\omega_0$$

This leads to the relation

$$A(\xi) > -\delta_0 g_1 \exp(A\xi) \quad (6.24)$$

Defining  $\xi_c$  as the critical distance at which the strict inequality of the stability condition is violated, i.e.,  $\xi = \xi_c$  where  $A(\xi_c) = -\delta_0 g_1 \exp(A\xi_c)$ , the critical distance  $\xi_c$  may be estimated as

$$\xi_c = \frac{1}{A} \ln(-A/(\delta_0 g_1)) \quad (6.25)$$

For a ballistic straight line trajectory in which the altitude  $h$  varies linearly with distance, i.e.,  $h \sim \xi$ , the critical altitude  $h_c$  is estimated as

$$h_c = \frac{1}{\beta} \ln\left(\frac{SLC}{2\beta L \sin \gamma_0}\right) \quad (6.26)$$

For altitudes less than  $h_c$  the oscillations may be unstable.

These criteria are to be used mainly as guidelines. As we have considered asymptotic approximations by the GMS theory, only dominant contributions have been taken into account and the results can be used as indicators of the potential problems such as instability, when the criteria are violated. The results are qualitatively similar to those in [8], but are derived by the GMS theory. Further, although the simple criteria have been demonstrated for ballistic trajectories, the GMS theory is itself valid for other general trajectories, and lead to variations on the form of the stability criteria and critical altitudes.

## 7 PARAMETER SENSITIVITY

### 7.1 General Remarks

An important problem in system dynamics is the effect of parameter uncertainties or variations. The exact values of the parameters are never known and there is always a certain degree of uncertainty. When the parameters are constant the effect of changes in the parameters can be described by means of conventional sensitivity theory. We can illustrate the difficulty as follows. Consider a linear time-invariant (LTI) system

$$\dot{x} = A(p)x \quad (7.1)$$

where  $p$  is a particular parameter which assumes constant values. The sensitivity of the solution  $x$  with respect to small changes in the parameter  $p$  can be described in terms of the first order sensitivity  $S$  defined as

$$S \equiv \frac{\partial x}{\partial p} \quad (7.2)$$

The sensitivity can also be defined as the fractional change in the solution due to a fractional change in the parameter.

Assuming some technical conditions to be satisfied, the sensitivity function is given by the equation

$$\dot{S} = AS + A_p x \quad (7.3)$$

where  $A_p \equiv \frac{\partial A}{\partial p}$ . Consider a mathematical model of flight vehicles at hypersonic speeds given by:

$$\dot{x} = A(t, p(t))x \quad (7.4)$$

where  $x$  is an  $n$ -vector,  $A$  is an  $n \times n$  matrix of elements which are functions of  $t$  and a variable parameter  $p(t)$ , the sensitivity of the solution  $x$  with respect to a variable parameter  $p(t)$  is rigorously treated as the variation  $\delta x$  of  $x$  due to a variation  $\delta p$  of  $p$ . In the context of GMS theory, we develop asymptotic solutions  $\tilde{x}$  such that

$$\tilde{x}(t) \sim x(t) \quad (7.5)$$

Here the symbol  $\sim$  denotes that " $\tilde{x}(t)$  is asymptotic to  $x(t)$ "; i.e.,  $\tilde{x}(t)$  approaches  $x(t)$  more and more closely and the error  $E = x(t) - \tilde{x}(t)$  is of the order of the highest power of the small parameter  $\epsilon$  to which the asymptotic expansion is carried out. In other words,  $\tilde{x}(t)$  is the best approximation to the exact solution  $x(t)$ .

Similarly, if  $S$  is the exact sensitivity of the dynamics to variations in a particular parameter, we will generate an asymptotic approximation to the sensitivity,  $\tilde{S}$  by the GMS method. This is because, the exact or true sensitivity function  $S$  cannot be determined, in general, because of the nonautonomous nature of the system. This problem can be addressed in the context of asymptotic theory. Indeed, a highly accurate asymptotic approximation for the sensitivity function can be developed by means of GMS theory. we define the asymptotic sensitivity function  $\tilde{S}$  as the first variation of the asymptotic solution  $\tilde{x}$  with respect to a parameter  $p$ . When the coefficients are constants, we can write,

$$\tilde{S} = \frac{\partial \tilde{x}}{\partial p} \quad (7.6)$$

The exact sensitivity of the solution is represented by an asymptotic expansion  $\tilde{S}$  such that

$$\tilde{S} \sim S \quad (7.7)$$

The asymptotic sensitivity  $\tilde{S}$  is developed by the GMS method [36]. In general, special care is needed in rendering (7.5) and (7.7) compatible. In most cases of practical interest, including our problem of flight dynamics, such a procedure is justified, as there are no pathologies in the system dynamics. The asymptotic sensitivities are developed by the GMS approach by means of variations in  $x(t, p(t))$  due to variations in  $p(t)$ . In particular the GMS theory enables us to express the sensitivity  $\tilde{S}$  systematically separated on the fast and slow scales  $\tau_1$  and  $\tau_0$ .

Asymptotic sensitivity is determined as follows:

- (1) Identify state variable  $x$  and parameter  $p(t)$
- (2) Develop equations of motion
- (3) Develop GMS solution  $\tilde{x}$
- (4) Develop first variation of  $\tilde{x}$  with respect to  $p(t)$ . This is the asymptotic first order sensitivity  $\tilde{S}$ .

## 7.2 Application to Re-Entry

This approach is now illustrated in the case of the angle-of-attack variations in re-entry. The response is developed by GMS method in the form

$$\alpha(\xi) \sim \tilde{\alpha}\{\xi_0(\xi), \xi_1(\xi)\} \quad (7.8)$$

and

$$\tilde{\alpha}(\xi_0, \xi_1) = \tilde{\alpha}_s(\xi_0) \cdot \tilde{\alpha}_f(\xi_1) \quad (7.9)$$

where the subscripts  $s$  and  $f$  denote the slow and fast parts of the solution respectively.

Defining the first order sensitivity  $\tilde{S}$  as a variation in the *fractional change* in  $\alpha(\xi, p(\xi))$  due to a variation in the parameter  $p(\xi)$ , it can be shown that the sensitivity  $S$  can be written as

$$S \sim \tilde{S}_f + \tilde{S}_s \quad (7.10)$$

where, again, the subscripts  $f$  and  $s$  denote the fast and slow parts of the *fractional* changes in the asymptotic sensitivity function. That is,  $\tilde{S}_f$  is the fractional change of the fast part of the asymptotic solution  $\tilde{\alpha}_f$  with respect to the parameter and  $\tilde{S}_s$  is the fractional change in the slow part of the asymptotic solution,  $\tilde{\alpha}_s$ .

Rigorously, the sensitivities vary with the argument  $\xi$ , and are complex quantities, with the amplitude and phase varying with  $\xi$ . This theory is now applied to the Space Shuttle entry for purposes of illustration. The parameters chosen are  $C_L, C_D$  and  $C_m$  along the re-entry trajectory. The sensitivity of the magnitude of  $\alpha$  with respect to each of these parameters as they are all changing along the trajectory is analytically derived as shown above. The results are plotted as seen in Figures 73-81.

The sensitivity function is a complex quantity, indicating the real and imaginary components typical of oscillatory dynamic systems. The absolute value of the sensitivity represents the total magnitude, without following the real and imaginary contributions. Using the GMS solutions, the sensitivity has been computed with the GMS-fast solution only or combining the fast and slow solutions in the GMS-total solutions. The sensitivity computed from both of these indicates that the fast solution yields most of the contribution to the sensitivity. It is therefore quite simple to incorporate the GMS- fast solution only, in the sensitivity analysis, being the dominant contribution. It is clear that this approach provides the means by which parametric studies of parameter uncertainties can be systematically carried out, using analytical methods. We note that a simple and direct approach is possible by the GMS theory on a class of difficult nonautonomous problems such as hypervelocity vehicle dynamics through variable flight conditions.

## 8 ERROR ANALYSIS

### 8.1 General Remarks

In any system of approximations, it is of great interest and importance to carry out a proper analysis of the errors. This subject is itself very deep and has occupied many mathematicians for a long time because of the inherent difficulties in this process. The greatest difficulty is due to the fact that the knowledge of the approximation and the exact error at every point, implies knowledge of the mathematically exact solution. This is impossible in general, and therefore, it is impossible to evaluate the error exactly at every point. However, because we are dealing with asymptotic solutions the errors may be estimated.

It is useful to recall the standard definitions of the Landau order symbols [38], using the given functions  $f(t)$  and  $g(t)$ .

#### O Symbol

A function  $f(t)$  is said to be  $O(g(t))$  in the limit  $t \rightarrow t_0$ , if

$$\lim_{t \rightarrow t_0} \frac{f(t)}{g(t)} = M = \text{Constant} < \infty$$

#### o Symbol

A function  $f(t)$  is said to be  $o(g(t))$  in the limit  $t \rightarrow t_0$ , if

$$\lim_{t \rightarrow t_0} \frac{f(t)}{g(t)} = 0$$

Thus, consistent with Poincaré's definition of asymptotic expansions, the error magnitude is of the order of the first term that is neglected in the expansion. If

$$\sum_{i=0}^n \epsilon^i \phi_i(t)$$

is an asymptotic expansion of  $n^{\text{th}}$  order for a function  $f(t, \epsilon)$ , then the error is estimated as

$$\left| f(t, \epsilon) - \sum_{i=0}^n \epsilon^i \phi_i(t) \right| = O(\epsilon^{n+1}) \quad (8.1)$$

where  $\phi_i, i = 1, 2, \dots$  is an asymptotic sequence.

Indeed, this is how Poincaré defined an asymptotic expansion. It is one of the most attractive reasons for using asymptotic methods such as the GMS method.

The magnitude of the error at any order is estimated as that of the first term that is neglected. Because the successive terms decrease rapidly, the error becomes very small after only the first few terms.

## 8.2 Strict Bounds

While the asymptotic error estimates are useful, it is possible to develop strict and sharp error bounds in some cases. Ramnath [15] has derived such bounds on the GMS solutions for several general classes of nonautonomous differential equations. These are similar to Olver's bounds. See [15] for details. These bounds are similar to those of Olver. See [15,44] for details. These are applicable to several problems in flight dynamics, including the re-entry and minor circle flight. For the re-entry problem, Ramnath's error theorem yields:

$$| E | \equiv | a(\xi) - \tilde{a}_{GMS}(\xi) |$$

$$| E | \leq D^{-\frac{1}{4}}(\xi) \exp\left(-\int \frac{\omega_1}{2} d\xi\right) \exp\left(\left|\int^{\xi} | m(\xi) | d\xi\right|\right) - 1 \quad (8.2)$$

where

$$D(\xi) = | 4\omega_0 - \omega_1^2 |$$

and

$$m(\xi) = D^{-\frac{1}{4}}(\xi) \frac{d^2}{d\xi^2} (D^{-\frac{1}{4}}(\xi))$$

From this powerful theorem we can see that as the re-entry trajectory changes, the terms in (8.2) also change. But their effect is easily analytically tractable. The case of constant flight arises as a natural limit. In this case the error completely vanishes and the GMS solutions recover the known exact solutions. However, the real advantages and usefulness of this theorem are in studying different vehicles, trajectories and variable flight conditions. In these cases, the GMS solutions are asymptotic to the exact solutions, with the errors as bounded by (8.2).

## 9 CONTROL CONSIDERATIONS

### 9.1 General Remarks

The complex dynamics of a hypervelocity vehicle have been investigated in a variety of significant situations. They include re-entry trajectories at steep angles and at shallow angles involving rapid deceleration. Another class of trajectories analyzed include minor circles as the vehicle flies at constant altitude. In particular the dynamics are investigated as the vehicle accelerates from subcircular to supercircular velocities on the minor circles of different radii. Highly accurate asymptotic solutions are developed by the GMS method. Stability of the motion has also been analyzed by this method leading to simple, rigorous and useful criteria. We now consider control implications in connection with this class of problems. In particular we consider control analysis and design techniques by the GMS approach.

In carrying out this phase of research our philosophy was to identify and treat most of the important aspects of the dynamics of a generic hypervelocity vehicle. Such an approach would uncover the areas needing modification of the system response, i.e., control. The effort to follow would consist of the actual development of the control system analysis and synthesis.

Concurrently however, we have continued to develop the theoretical framework for such control-theoretic investigations. The time varying nature of the hypervelocity flight mechanics precludes even the availability of some basic relationships such as the transfer function. However, these questions are answered by invoking the GMS method.

Both the classical control methods and the modern approach are amenable to the GMS technique. Considering the classical approach the procedure for control design is usually practiced as shown in Figure 82. The flight vehicle system is linearized about an operating flight condition, and a control system is designed using an approximate transfer function at the "frozen" point, and standard methods such as root loci and Bode plots. The same procedure is followed at a different flight condition, and another one yet, and so on until the whole range of variation is covered. The procedure is tedious, not accurate, and can potentially lead to a complete misrepresentation of the system stability and response. While there is a useful role for this approach (backed by computer simulation), there is clearly a need for a better analysis and design method. The GMS method fills this need.

The GMS theory of variable systems is developed by Ramnath [9-17]. The elements of this theory can be illustrated by considering a class of general linear time varying systems in the scalar form

$$\sum_{i=0}^n a_i(\tau)x^{(i)} = Ku(t) \quad (9.1)$$

where  $x^{(i)} \equiv (d^i x/dt^i)$  and  $a_i$  are *slowly varying coefficients*. At this point a brief discussion of what is *slowly varying* might be useful. This is a concept that is used often by practising dynamics and control engineers rather unrigorously. Conceptually, a system varies *slowly* if the variation of the coefficients is much smaller than the variation of the dynamics, - i.e., the solutions. However, this calls for knowledge not yet available, - i.e., the nature of the solutions. Therefore, a rigorous approach to the definition of a slowly varying system involves parameterizing the coefficients in terms of a small parameter,  $\epsilon \ll 1$ . In this way, one can conclude that if the  $\epsilon$  parameter is very small, the system is slowly varying: the smaller  $\epsilon$ , the more slowly varying system.

By appealing to the GMS method the variables can be extended as

$$\begin{aligned} \tilde{t} &\rightarrow \{\tau_0, \tau_1\}; \tau_0 = t \\ \tau_1 &= \int \frac{k}{\epsilon}(\tilde{t}) d\tilde{t} \end{aligned} \quad (9.2)$$

and  $x(t) \rightarrow x(\tau_0, \tau_1)$ . The dominant contribution to the system response can be described by [9].

$$\sum_{i=0}^n a_i(\tau_0) k^i \frac{d^i x}{d\tau_1^i} = K u(\tau_1) \quad (9.3)$$

Now considering a Laplace transform with respect to  $\tau_1$ ,

$$X(\tau_0, s) \equiv \int_0^\infty x(\tau_0, \tau_1) \exp(-s\tau_1) d\tau_1 \quad (9.4)$$

we can write the dominant transfer function of the system in the form

$$\tilde{G}(s, \tau_0) = \frac{X(s, \tau_0)}{U(s)} = \frac{K}{\sum_{i=0}^n a_i(\tau_0) s^i k^i} \quad (9.5)$$

where the coefficients  $a_i$  vary on a slow scale  $\tau_0$ . When the input-output relation is of the more general form.

$$\sum_{i=0}^n a_i(\tilde{t}) x^{(i)} = K \sum_{j=0}^m b_j u^{(j)} \quad (9.6)$$

The GMS method leads to the dominant transfer function

$$\tilde{G}(s, \tau_0) = \frac{K \sum_{j=0}^m b_j(\tau_0)(sk)^j}{\sum_{j=0}^n a_j(\tau_0)(sk)^j} \quad (9.7)$$

The response to an input  $U(s)$  is given by

$$\tilde{X}(s, \tau_0) = \tilde{G}(s, \tau_0)U(s) \quad (9.8)$$

where  $U(s)$  is the Laplace transform of  $U(\tau_0, \tau_1)$  with respect to  $\tau_1$ .

The dominant response in time is given by the inverse Laplace transform of  $\tilde{X}(s, \tau_0)$  by evaluating the complex line integral

$$x(\tau_0, \tau_1) = \frac{1}{2\pi i} \int_{Br} \tilde{G}(s, \tau_0)U(s) \exp(s, \tau_1) ds \quad (9.9)$$

where  $Br$  is the Bromwich contour given by the line  $c - i\infty$  to  $c + i\infty$  on the complex  $s$ -plane, where  $c$  is a suitable positive real number. This line integral may be evaluated by means of the poles and zeros in the  $s$ -plane and Cauchy's theorem. Stability can be analyzed by inverse Laplace transformation and restriction along the trajectories  $\tau_i(t, \epsilon)$ .

We have thus achieved a rigorous system representation in the form of the dominant contribution to the transfer function. This is a true extension of standard classical control theory (Figure 83).

In a similar manner several important problems in modern control theory can also be solved by the GMS method. For example, the time varying linear quadratic optimal control problem was solved by Ramnath by the GMS method [43]. Analytical asymptotic solutions yield highly accurate representations of the optimal control.

Research is continuing on the development of the GMS method to the control analysis and design techniques in both the classical and modern approaches. Actual implementation and refinement of the techniques to the problems of hypervelocity flight is to be performed.

It should be noted that this methodology is very general and presents a novel approach. By this means the asymptotic transfer functions for a general class of time varying systems can be systematically developed. **The approach is new and includes the case of constant coefficients as a special case.** In particular the transfer functions thus derived, readily recover the transfer functions for the time-invariant case. Thus it represents a true and natural extension of the standard control design methodology. Having developed this general framework, we are about to further develop the control design procedures for the hypervelocity vehicle through the variable flight conditions.

## 9.2 Control System Design

The implications of the peculiarities of linear time varying (LTV) systems on control systems analysis and design can be quite subtle. The standard performance measures of a linear time-invariant (LTI) system such as bandwidth, rise time, gain margin, phase margin cannot be directly carried over to the LTV systems. Even in the relatively simple case of *slowly* varying systems, such notions have to be dealt with carefully. An overly permissive prescription for extending these ideas to LTV systems could lead to serious misrepresentations. At the very least, the LTI performance measures are necessarily parameterized by time, i.e., the instant at which such a simple representation is made.

For *slowly* varying systems, the standard practice is to “freeze” the LTV systems at an operating point  $t_1$  and consider the LTI system at  $t_1$  to approximate the LTV system at  $t = t_1$ . A control system is designed based on LTI control theory. The system is then allowed to vary and frozen at a different time  $t = t_2$ . Analysis and control design are carried out at this time again, by LTI methods. This procedure is repeated at a number of frozen points and a sequence of parameter values and gains are incorporated within a prescribed control structure and a “gain scheduling” is implemented accordingly.

Some limitations of such a simplistic approach are:

- (1) System stability and response can be seriously misrepresented, as outlined in Section 6.
- (2) The “frozen” model should be used only in a very small neighborhood of the operating point.
- (3) A uniformly valid continuous solution cannot be obtained, as the “frozen” solutions need to be patched.
- (4) The larger the number of frozen instants, the better is the approximation. However, stability predictions, in general, are beyond the scope of the frozen model, however closely spaced the frozen instants.

The control design approaches derived from GMS theory, help obviate most of the above difficulties. We will now present an outline of control design procedures based on the GMS methodology.

### Control Design Procedure

The great generality and accuracy of the GMS theory enables us to develop a systematic control design procedure for a general class of time-varying systems exemplified by the hypervelocity flight vehicles. It should be noted that the GMS theory offers us at least three approaches to control systems design. These can be stated as:

1. Extended Classical Approach
2. GMS Control in Extended Space
3. Vector-Matrix (or Multivariable) GMS Approach

In what follows, we will mainly consider the first approach listed above. The

other two will only be briefly touched upon. We will present an enumeration of the various steps in a top level control design procedure based on the GMS approach.

At the outset a recognition must be made of the differences in a heuristic or quasi-heuristic approach and a "mechanical" approach. The heuristic approach is mostly by trial-and-error and is intuitive, with a considerable degree of "art" in the process. The "mechanical" approach, such as the use of functional optimization techniques, allow the designer little freedom other than choosing the specifications or the cost functional. A compromise is therefore desirable, consisting of a combination of largely heuristic design steps and largely "mechanical" analysis steps. Such a combination allows for the injection of insight while not making it mandatory. The designer is allowed to use the simplifying but incorrect assumption that the system function (i.e., transfer function) of a cascaded system is the product of the system functions of its subsystems. The subsequent procedure is so chosen as to enable the designer to identify the errors and compensate for them in successive analysis and design stages until the residual error is negligible. With this in mind we may consider the design sequence as follows:

1. System Description. The differential equations accurately representing the hypervelocity vehicle dynamics are found. These are assumed to be linearized and usually have time-varying coefficients.
2. Introduction of an Expansion Parameter. The slowness of coefficient variation is examined to ensure the accuracy of the GMS solutions. The system is then parameterized in terms of a small parameter,  $\epsilon$ , as the expansion parameter.
3. Open-Loop Specifications. Specifications are examined in the time domain and frequency domain and correlated. Also, specifications in the closed loop and the open loop are similarly treated, using relations between the two forms of system functions. One approach to multi-loop systems is to treat them one feedback loop at a time. A suggested guideline is to treat the specifications at the level of the outermost loops first, while compensation is designed for the innermost loops first. As a consequence the design involves finding a forward-loop or feedback loop cascade compensators which result in an acceptable open-loop function.
4. Zeroth-Order Analysis. The transfer function of the plant to  $O(1)$  is calculated by the GMS theory.
5. A compensator is designed such that the composition of its transfer function and the zeroth order GMS transfer function of the plant (calculated in step four) is acceptable. This would call for a judicious use of standard design techniques for the performance measures and the methods are parameterized by time.
6. System Performance Analysis. The performance of the system is examined to see whether the specifications are met. If they are, the design process is completed. It remains only to verify that the closed loop system satisfies the closed loop specifications. If not, then one would proceed as follows.
7. First Order Analysis. In this step the first order correction to the GMS

transfer function of the plant is developed leading to a more accurate representation. Using this transfer function a more accurate compensator is designed.

8. Performance Verification. Again, this step would ensure that the system performs as required. If it does, the design process is complete. If not, then higher order compensation would be resorted to.
9. Higher Order Compensation. This step would involve the development of a more accurate GMS transfer function by including higher order corrections. A compensator is designed at this stage. For instance, a  $k$ th order compensator would ensure that the errors are of the order  $\epsilon^{(k+1)}$ , leading to a very accurate representation. In principle, this would be followed by performance verification, and if necessary, a  $(k + 1)$ th order compensator. This whole design process is shown in Figure 84.

In regard to the structure or configuration of the control system, compensators can be designed either as cascade or feedback compensators. In time-varying systems, transposition of the transfer functions is not commutative. In other words, if  $G_1$  and  $G_2$  are the time-varying transfer functions, then

$$G_1G_2 \neq G_2G_1 \quad (9.10)$$

Similarly, the closed loop transfer functions cannot be derived directly as in the time-invariant case. In spite of these difficulties, the GMS theory enables us to develop useful relations for both cascade and feedback compensators from open loop transfer functions.

An important point to note is that because the GMS procedure is asymptotic, the errors decrease very rapidly as the order of the design increases. Therefore, for most purposes, it is envisioned that a satisfactory design could be developed with only one or two (rarely three) levels of control design.

The approach entitled "GMS Control in Extended Space" is an alternative approach. Instead of extending the classical methods of control design, it is a variation on the theme and exploits the special forms and relationships that are derived from the GMS theory. For example, it deals with such issues as multiple Laplace transforms with respect to the multiple, nonlinear scale functions  $\tau_0, \tau_1$ , etc., the Laplace variables being  $s_0, s_1$ , etc. In this formalism, determination of a proper control gain profile would be governed by solution of appropriate differential inequalities. Thus, new insights into system representation, transfer functions and control design are obtained by this approach. Details of this approach is beyond the present scope.

Finally, the "modern" approach to control design can be considered. This deals with the system mathematical model in the vector-matrix formulation. Ramnath [43] has extended the GMS theory to this class of time-varying systems as well. Therefore, systems of linear time-varying differential equations can be solved asymptotically by this method. Related control problems such as the linear-quadratic optimal control problems can be solved by the GMS method.

Three control design approaches have been outlined in the above discussion. What is needed, however, is an in-depth analysis of the relative merits of the methods in regard to design and implementation. Such questions are beyond the scope of the current effort and will be discussed in future work.

## 10 FURTHER WORK

A general theory has been developed to investigate the stability, flight dynamics and control of hypervelocity flight vehicles. A variety of trajectories including re-entry at different angles and hypersonic flight at constant altitude and constant latitudes on different minor circles has been analyzed. Analytical solutions have been developed for symmetric and antisymmetric motions by the GMS method. Fast and slow aspects of the motion are systematically separated by means of the fast and slow scales. It is essential that the clock functions are nonlinear and complex quantities in order to describe the dynamics. This corresponds to accelerating and decelerating clocks, counting time at different rates. This generalized approach is necessary in order to study the effects of acceleration and deceleration on the vehicle dynamics. The theory has been successfully applied to scenarios involving accelerations from subcircular to supercircular velocities. Asymptotic sensitivities to parameter variations have been developed. System stability during accelerating or decelerating flight profiles has been analyzed. A sharp estimate of the critical altitude marking the stability boundary has been developed for arbitrary re-entry trajectories, derived from the GMS solutions.. A general error analysis has also been presented for the GMS solutions. A general GMS methodology for the analysis and design of time varying control systems has been developed. This includes the systematic development of transfer functions by the GMS theory. A top level control design procedure has also been presented. Based on these developments the stage is set for a more detailed and complete development of dynamics and control analysis and design for hypervelocity vehicles. In particular the following areas are identified as being useful and important in a continuation of the research effort.

- o Detailed analysis of candidate hypersonic vehicles
  - Mission/Scenario
  - Vehicle shape
  - Parameters
  - Environment
  - Trajectories
  - Constraints
- o Analysis of flight dynamics during transitions on different minor circles
  - at constant velocity
  - during accelerations
  - during decelerations
- o Turning point analysis of phugoid oscillations
- o Double turning point analysis of roll-spiral mode
- o Complete longitudinal-lateral coupled dynamics during accelerations
- o Lateral-directional motion during re-entry
- o Complete longitudinal-lateral coupled motion during re-entry

- o Effect of parameter variations of complete set of longitudinal-lateral stability derivatives
- o Unusual flight situations, bifurcations in minor circle flight
  - relaxed static stability.
- o Detailed stability analysis during
  - (a) Re-entry – lateral directional motion  
full longitudinal motion
  - (b) Accelerated flight on minor circles
  - (c) Transition trajectories on minor circles
- o Classical control system development
  - Fast and slow transfer functions, control law development
  - time domain analysis
  - frequency domain analysis
- o Control design by multiple scales; Comparison with conventional control design
- o Control design in extended Laplace space
- o Optimal control
  - Trajectory optimization
  - Linear quadratic optimal control
  - Robust control - insensitive to parameter variations
- o Computational considerations
  - Variable sampling
  - Algorithmic development
  - Implementation issues
  - Requirements of computer time and memory
- o Simulation
  - Complete model of hypersonic vehicle
  - Development of 6 DOF simulation of complete model
  - Efficient simulation
  - Variable sampling
- o Control implementation
  - Transformation to measurable flight parameters
  - Control implementation with respect to flight parameters
  - Compensational constraints
  - Component performance constraints
- o Hardware in the Loop (HIL) simulation
- o Pilot in the Loop (PIL) simulation

## 11 SUMMARY AND CONCLUSIONS

In this investigation a general approach was developed to analyze the flight dynamics and control of a hypervelocity vehicle. This approach, consisting of the Generalized Multiple Scales technique, enables us to develop asymptotic approximations to the complex flight dynamics. These solutions display a natural and systematic separation of the fast and slow aspects of the dynamics.

The theory is illustrated by application to a generic hypervelocity vehicle flying on typical trajectories. These include re-entry along steep and shallow spiraling paths. Other trajectories involve flight on minor circles at constant altitudes. Several minor circles of different radii are considered. Flight dynamics as the vehicle accelerates from subcircular to supercircular speeds are analyzed by the GMS method. In these situations the standard modes of motion of the vehicle in the plane of symmetry and out of the plane of symmetry are systematically analyzed, for flight on different minor circles. Two different solutions - (1) GMS fast solution and (2) GMS slow and fast solutions are computed and compared with numerical solutions, for each case. The comparisons show that the GMS fast solution represents the true frequency extremely well, with a very small error in amplitude. This error is corrected by including the slow scale correction. Thus the total GMS solution is extremely accurate in both amplitude and phase. Indeed the GMS solutions are indistinguishable from the numerical solutions. We note that the dynamics during acceleration or deceleration lead to nonlinear phase variation and variable frequency, which are not tractable by standard methods.

In the case of flight on minor circles, our analysis has shown that the phugoid mode (for some radii) and the roll-spiral mode exhibits a *turning point* problem. This is a situation where, for some particular velocity, the dynamics undergo a significant topological change, from oscillatory to nonoscillatory behavior (or vice versa). Even in these cases, the GMS fast solution leads to useful and accurate description of the dynamics. However, a simple analysis is not sufficient to deal with turning point situations and careful analysis is necessary. This is beyond the scope of this effort.

For motion along re-entry trajectories, we have derived from the GMS solutions, a stability criterion in terms of the aerodynamic parameters. This leads to an analytical estimate of the critical altitude below which the angle of attack oscillations might be unstable. Our approach towards such questions and the derivation are novel as they stem from the GMS theory.

By means of the GMS solutions we also derive analytical expressions for the sensitivities of the dynamics to parameter variations. This theory is illustrated for the angle of attack variations along re-entry by computing the sensitivities to the parameters  $C_L$ ,  $C_m$  and  $C_{m'}$ . This approach would be very useful in preliminary design and to perform parametric studies. An error analysis is presented, including not only asymptotic error estimates, but also strict and sharp bounds on the errors in the general case. Finally a control methodology is developed by the GMS approach, leading to a framework for analyzing control system performance and design, for a class of time-varying systems. Hypervelocity flight vehicles belong

to this class. Transfer functions are developed for the time-varying systems by the GMS theory. This representation is rigorous and systematic, showing a separation of the fast and slow aspects of the control dynamics. Further, a top level control design procedure is presented, using the GMS methodology. This is a systematic procedure ensuring that the design specifications are satisfied, order by order. It should be noted that this addresses a problem in which even the basic notions of what is desirable in regard to system response, are lacking. For example, time-varying specifications such as rise time, bandwidth, etc are not available. Indeed, three different approaches to the design of time-varying control systems are outlined.

The methodology and technique are to be applied to develop an actual control system design for a hypersonic vehicle.

Finally, we note that with the GMS methodology, a large spectrum of problems connected with hypervelocity flight mechanics and control can be investigated. In general, the effects of acceleration (or deceleration) on the vehicle dynamics can be quite complex and non-intuitive. Many such effects cannot be predicted by extrapolating conventional theory, – either in flight dynamics analysis or control analysis and design. The trends shown in our study indicate that when the frequency of the motion increases, there is an increase in the apparent damping, which reinforces the damping due to other effects. This happens to be true for both the Space Shuttle during re-entry and a generic hypervelocity vehicle flying on minor circles. In the re-entry case, the critical altitude estimate is useful in studying different entry trajectories and the rate of penetration into the atmosphere. In the case of minor circle flight, the Dutch Roll mode is the most important, followed by the Short Period and then the phugoid and roll-spiral modes. In the Dutch Roll and Short Period modes, the effect of acceleration is to decrease the frequency and damping of the motion. The phugoid and roll-spiral modes are more complicated. Essentially new phenomena such as *turning points* and *bifurcations* are predicted for these modes, depending on the rate of acceleration, radius of the minor circle, and such considerations. Such a prediction is essentially due to the GMS methodology which also offers us an approach to investigate and solve problems related to these effects.

The basic thrust of the GMS methodology being analytical (or quasi-analytical), the important areas of system dynamics analysis and control design such as response predictions, stability analysis, performance and sensitivity analysis, error bounds and control analysis and design, are all subsumed by the GMS approach. Study of unusual dynamic phenomena is readily brought into the scope of the GMS theory. In view of this consistent, cogent and unified theory, the dynamics and control of hypervelocity vehicles constitute an ideal candidate for further investigation by the GMS approach.

## 12 REFERENCES

1. Friedrich, H.R., and Dore, F.J., "The Dynamic Motion of a Missile Descending through the Atmosphere," *J. Aero. Sci.*, 22, No. 9, pp 628-632, 638, Sept. 1955.
2. Allen, H.J., "Motion of a Ballistic Missile Angularly Misaligned with the Flight Path Upon Entering the Atmosphere and Its Effect Upon Aerodynamic Heating, Aerodynamic Loads and Miss Distance," NACA TN 4048, Oct. 1957.
3. Laitone, E.V., "Dynamic Longitudinal Stability Equations for the Re-entry Ballistic Missile," *J. Aerospace Sci.*, 26, pp 94-98, Feb. 1959.
4. Etkin, B., "Longitudinal Dynamics of a Lifting Vehicle in Orbital Flight," *J. Aerospace Sci.*, 28, pp 779-788, Oct. 1961.
5. Laitone, E.V., and Chou, Y.S., "Phugoid Oscillations at Hypersonic Speeds," *AIAA Journal*, 3, pp 732-735, April 1965.
6. Vinh, N.X., and Dobrzelecki, A.J., "Non-Linear Longitudinal Dynamics of an Orbital Lifting Vehicle," NASA CR-1449, Oct. 1969.
7. Laitone, E.V., "On the Damped Oscillations Equation with Variable Coefficients," *Quart. Appl. Math.*, 16, No. 1, pp 90-93, April 1958.
8. Vinh, N.X., and Laitone, E.V., "Longitudinal Dynamics Stability of a Shuttle Vehicle," *J.A.S.*, Vol. XIX, No. 5, March 1972.
9. Ramnath, R.V., Hedrick, J.K., Paynter, H.M.; Editors, Vol. II *Nonlinear Systems Analysis and Synthesis* ASME 1981.
10. Ramnath, R.V. and Jenie, S.D., "Vibrational Dynamics of the Helio-gyro Spacecraft," Proceedings of 35th IAF Congress, Lausanne, Switzerland, October 1984.
11. Ramnath, R.V. and Jenie, S.D., "Analysis of a Class Distributed Parameter Systems by the Multiple Scales Method," Proceedings of 1985 Conference on Information Sciences and Systems, Baltimore, MD, March 1985.
12. Bogoliubov and Mitropolsky, *Asymptotic Methods in Nonlinear Oscillations*, Gordon and Breach, New York.
13. Ramnath, R.V. and Sandri, G., "A Generalized Multiple Scales Approach to a Class of Linear Differential Equations, *Journal of Mathematical Analysis and Applications*," Vol. 28, No. 2, Nov. 1969. Also in *Zentralblatt für Mathematik*, Berlin, W.Germany, 1968
14. Ramnath, R.V. and Bowles, W.M., "Asymptotic Analysis of a Class of Time Varying Linear Filters," Proceedings Allerton Conference, U. of Illinois, Urbana, IL, 1977.
15. Ramnath, R.V. and Sinha, P., "Dynamics of the Space Shuttle During Entry into the Earth's Atmosphere," *AIAA Journal*, Vol. 13, No. 3, 1975.
16. Ramnath, R.V., "Minimal and Subminimal Simplification," *AIAA Journal of Guidance and Control*, Jan.-Feb., 1979.

17. Ramnath, R.V., "Transition Dynamics of VTOL Aircraft," AIAA Journal, Vol. 8, No. 7, 1970.
18. Loh, W.H.T., *Dynamics and Thermodynamics of Planetary Entry*, Prentice-Hall, 1963.
19. Arthur, P.d., and Baxter, B.E., "Observations on Minor Circle Turns," AIAA Journal, 1910), 2408, Oct. 1963.
20. Etkin, H.B., "Longitudinal Dynamics of a Lifting Vehicle in Orbital Flight," J. Aero Sci., Oct. 1961.
21. Rangi, R.S., "Non-linear Effects in the Longitudinal Dynamics of a Lifting Vehicle in a Circular Orbit," UTIA TN-40, OCT. 1960.
22. Nonweiler, T., "The Control and Stability of Glider Aircraft at Hypersonic Speeds," ARC 21, 301, S&C 3391, Oct. 1959.
23. Drummond, A.M., "Performance and Stability of Hypervelocity Aircraft Flying on a Minor Circle," Progress in Aerospace Sci., Vol. 13.
24. Kuchemann, D., "Hypersonic Aircraft and Their Aerodynamic Problems," R.A.E. TN Aero. 849, May 1964.
25. Ferri, A., "Goals of Hypersonic Aerodynamics," Astronautics and Aeronautics," p. 34, Oct. 1966.
26. Plank, P.P., Sakata, I.F., Davis, G.W., and Richie, C.C., "Hypersonic Cruise Vehicle Wing Structure Evaluation," NASA CR 1568, May 1970.
27. Petersen, R.H., Gregory, T.J., and Smith, S.L., "Some Comparisons of Turbo-ramjet Powered Hypersonic Aircraft for Cruise and Boost Mission," Journal of Aircraft, 3, No. 5, Sept./Oct. 1966.
28. Simpson, R.W., and Hursh, J.W., "Guiding the Hypersonic Transport," Astronautics and Aeronautics, Oct. 1966.
29. Clark, E.L., and Trimmer, L.L., "Equations and Charts for the Evaluation of Hypersonic Aerodynamic Characteristics of Lifting Configuration by the Newtonian Theory," AEDC-TDR-64-25, March 1964.
30. Intrieri, P.F., "Experimetal Stability and Drag of a Pointed and Blunted 30 Half Angle Cone at Mach Numbers from 11.5 to 34 in Air," NASA TN D-3183, Jan. 1966.
31. Tobak, M., and Wehrend, W.R., "Stability Derivatives of Cones at Supersonic Speeds," NACA TN 3788, Sept. 1956.
32. Hayes, W.D., and Probstein, R.F., *Hypersonic Flow Theory*, Academic Press, New York, 1959.
33. Popinski, A., and Ehrlich, C.F., "Development Design Methods for Predicting Hypersonic Aerodynamic Control Characteristics," AFFDL-TR-66-85, Sept. 1966.
34. Ramnath, R.V., Course Notes, "Advanced Flight Dynamics and Control," Massachusetts Institute of Technology, Cambridge, MA, 1980-1987.
35. Hsu, J.C.V. and Meyer, A.U., *Modern Control Theory*, McGraw-Hill, New York.

36. Ramnath, R.V. and Radovsky, S., "Parameter Sensitivity in Variable Linear Systems with an Application to VTOL Transition." Proc. JACC, Denver, CO.
37. Abramowitz, M. and Stegun, I., *Handbook of Mathematical Functions*, N.B.S., June 1964.
38. Erdelyi, A., *Asymptotic Expansions*, Dover, New York.
39. Etkin, B., *Dynamics of Atmospheric Flight*, Wiley, New York, 1972.
40. Bellman, R., *Stability Theory of Differential Equations*, McGraw-Hill, New York.
41. Kruskal, M., "Asymptotology," *Plasma Physics*, Int. Atomic En. Ag., Vienna, 1965.
42. Vinh, N.X., Busemann, A., and Culp, R., *Hypersonic and Planetary Entry Flight Mechanics*, U. of Michigan Press.
43. Ramnath, R.V., "The Time Varying Linear Quadratic Problem: A Multiple Scales Approach," Proc. CCAC-SIAM Conf. "Optimization Days," Concordia University, 1979.
44. Ramnath, R.V., "A Multiple Scales Approach to the Analysis of Linear Systems", Ph.D. Dissertation, Princeton University, 1968. Also Rept. AFFDL-TR-68-60, Wright-Patterson AFB, Ohio, Oct.1968.

## A APPENDIX - REPRESENTATIVE VEHICLE

The generic hypervelocity vehicle flying on a minor circle is chosen following Drummond [23]. The Generalized Multiple Scales (GMS) theory is applied to the analysis of the dynamics of this vehicle for purposes of illustration. Based on considerations of (a) the right shape for hypersonic flight, (b) the right mission-dictated size, (c) facilitating analysis but including important effects, and (d) available experimental data, the following model [23] is used.

The general shape is a highly swept delta wing of diamond cross section with a spherical nose and cylindrical leading edges (Fig. A). The parameters are as follows:

$$\text{Sweep Angle} = 75^\circ$$

$$\text{Reference Length} = 150 \text{ ft}$$

$$\frac{\text{Span}}{2} = \frac{b}{2} = 37 \text{ ft}$$

$$\text{Reference Area} = S = 5550 \text{ ft}^2$$

$$x_{CG} = 1.375$$

$$\text{Maximum Wing Loading} = \frac{W}{S} = 58.5 \text{ lb ft}^2$$

$$\text{Minimum Wing Loading} = 24.5 \text{ lb ft}^2$$

$$\text{Cruise Mach Number} = M = 5 \text{ to } 8$$

$$\text{Range} = 5000 \text{ to } 6000 \text{ miles}$$

The data for the stability derivatives and related parameters are given by Drummond [23] by separately considering the various contributions due to wing, flap, fin, etc. Our model includes the same parameters and trajectories. However, the speed of the vehicle is allowed to change as it flies along a particular minor circle.

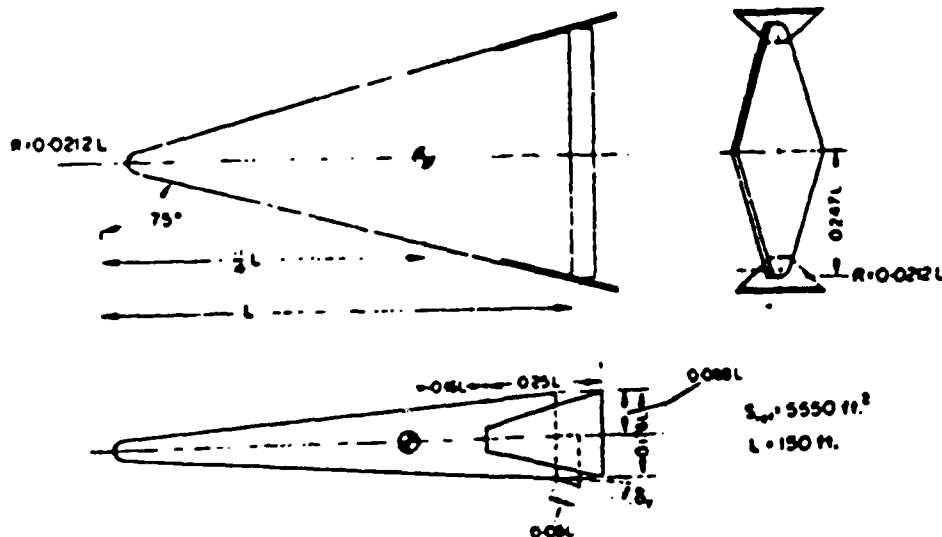


Fig. A. Generic Vehicle Configuration (Drummond's Model).

## APPENDIX B

### Example 1

Consider a first order equation

$$\dot{x} + \epsilon x = 0; \quad x(0) = 1 \quad (B1)$$

where  $0 < \epsilon \ll 1$ . A direct perturbation expansion

$$x(t, \epsilon) = x_0(t) + \epsilon x_1(t) + \dots$$

leads to the perturbation equations

$$\dot{x}_0 = 0 \quad (B2)$$

$$\dot{x}_1 = -x_0 \quad (B3)$$

$$\vdots \quad (B4)$$

Solving these order by order, we have,

$$x_0 = 1 \quad (B5)$$

$$x_1 = -t \quad (B6)$$

$$x_2 = t^2/2 \quad (B7)$$

Substituting these into the perturbation expansion we have,

$$x(t, \epsilon) \approx 1 - \epsilon t + \epsilon^2 t^2/2 + \dots \quad (B8)$$

This expansion is seen to be secularly nonuniform (i.e., for  $t > 1/\epsilon$ ) as the correction term ceases to be small.

### Multiple Time Scales (MTS)

The above problem can be solved by the MTS approach as follows. Let us extend

$$t \rightarrow \{\tau_0, \tau_1\}; \quad \tau_0 = t, \quad \tau_1 = \epsilon t \quad (B9)$$

The time derivative operator is now extended as

$$\frac{d}{dt} \rightarrow \frac{\partial}{\partial \tau_0} + \epsilon \frac{\partial}{\partial \tau_1} \quad (B10)$$

and

$$x(t, \epsilon) \rightarrow x(\tau_0, \tau_1) \quad (B11)$$

The differential equation becomes

$$\frac{\partial x}{\partial \tau_0} + \epsilon \frac{\partial x}{\partial \tau_1} + \epsilon x = 0 \quad (B12)$$

Equating like powers of  $\epsilon$ , we have

$$\frac{\partial x}{\partial \tau_0} = 0 \quad (B13)$$

$$\frac{\partial x}{\partial \tau_1} + x = 0 \quad (B14)$$

Solving these, we obtain

$$x(\tau_0, \tau_1) = A(\tau_1) = c \exp(-\tau_1) \quad (B15)$$

where  $c$  is a constant.

Upon restriction of this extended solutions along the "trajectories"  $\tau_0 = t, \tau_1 = \epsilon t$ , the solution is obtained as

$$x(t, \epsilon) = c \exp(-\tau_1)|_{\tau_1=\epsilon t} = c \exp(-\epsilon t) \quad (B16)$$

which is not only uniformly valid, but is indeed the *exact* solution.

## Example 2

Consider the time varying problem

$$\dot{x} + \epsilon t x = 0 \quad (B17)$$

This is also a secular perturbation problem as the direct perturbation expansion is secularly nonuniform (i.e., for  $t > 1/\epsilon$ ). An attempt to uniformize this by the MTS approach as in Example 1 will not be successful as (B17) is a time-varying equation. This can be illustrated as follows. As before, the extension

$$t \rightarrow \{\tau_0, \tau_1\}; \quad \tau_0 = t, \tau_1 = \epsilon t \quad (B18)$$

leads to

$$\frac{\partial x}{\partial \tau_0} = 0 \quad (B19)$$

$$\frac{\partial x}{\partial \tau_1} + \tau_0 = 0 \quad (B20)$$

Thus the solution is obtained as

$$x(\tau_0, \tau_1) = A(\tau_1) = c \exp(-\tau_0 \tau_1) \quad (B21)$$

Upon restriction

$$x(t, \epsilon) = c \exp(-\tau_0 \tau_1) \Big|_{\substack{\tau_0=t \\ \tau_1=\epsilon t}} = c \exp(-\epsilon t^2) \quad (B22)$$

While this is not a bad approximation an inconsistency can be seen in (B21).

### Solution by GMS Theory

The reason for the lack of complete success with the MTS approach is that only *linear* scales are employed in the MTS theory. In time-varying (and, in general nonlinear) problems, it is essential that *nonlinear* scales are used. This was demonstrated by Ramnath [9-17] who generalized the multiple scales technique and called it the GMS theory. According to this generalization, we extend

$$t \rightarrow \{\tau_0, \tau_1\}; \quad \tau_0 = t, \tau_1 = \epsilon \int k(t) dt \quad (B23)$$

and

$$x(t, \epsilon) \rightarrow x(\tau_0, \tau_1) \quad (B24)$$

where  $k(t)$  is an undetermined "clock" function. The derivative operator now becomes

$$\frac{d}{dt} \rightarrow \frac{\partial}{\partial \tau_0} + \epsilon k \frac{\partial}{\partial \tau_1} \quad (B25)$$

and the extended perturbation equations are

$$\frac{\partial x}{\partial \tau_0} = 0 \quad (B26)$$

$$k \frac{\partial x}{\partial \tau_1} + \tau_0 x = 0 \quad (B27)$$

The clock function  $k$  is chosen to be equal to the time-varying coefficient  $\tau_0$  and this leads to the solution

$$x(\tau_0, \tau_1) = c \exp(-\tau_1) \quad (B28)$$

and

$$k(t) = t \quad (B29)$$

$$\tau_1(t, \epsilon) = \frac{\epsilon t^2}{2} \quad (B30)$$

Therefore, upon restriction along the "trajectories"  $\tau_0 = t$ , and  $\tau_1 = \epsilon t^2/2$  the solution is obtained as

$$x(t, \epsilon) = c \exp(-\tau_1) \Big|_{\tau_1 = \frac{\epsilon t^2}{2}} = c \exp\left(-\frac{\epsilon t^2}{2}\right) \quad (B31)$$

This is not only uniformly valid, but is indeed the *exact* solution. This is possible only by making the scale functions *nonlinear* in  $t$ .

# CONCEPT OF EXTENSION

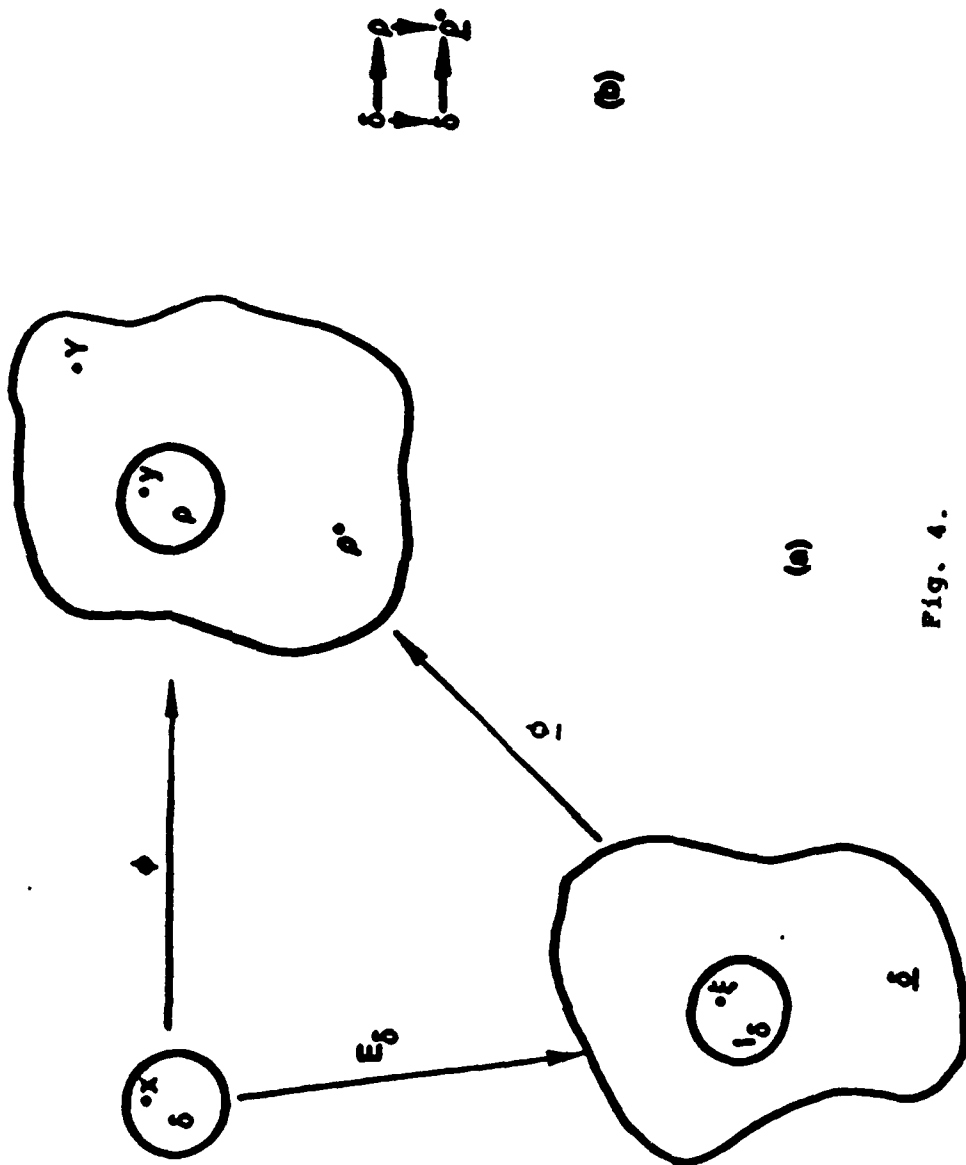


Fig. 4.

# EXTENSION TO MULTIPLE TIME SCALES

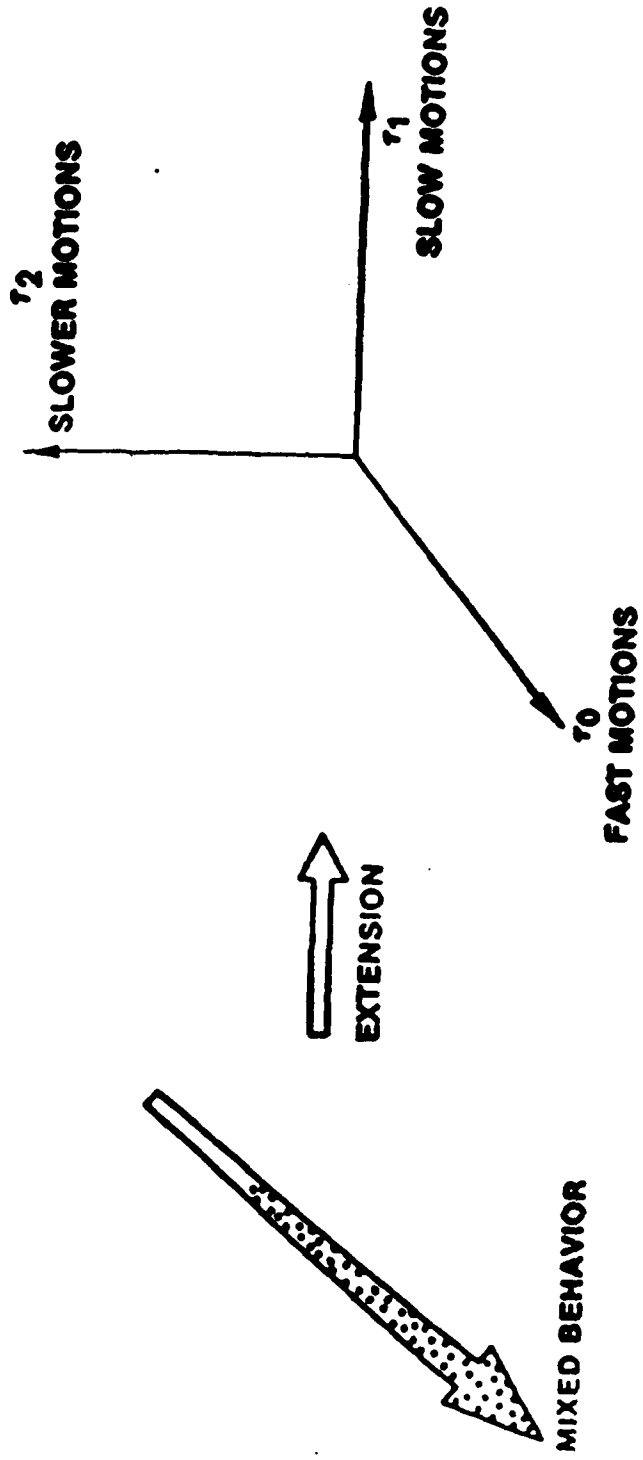
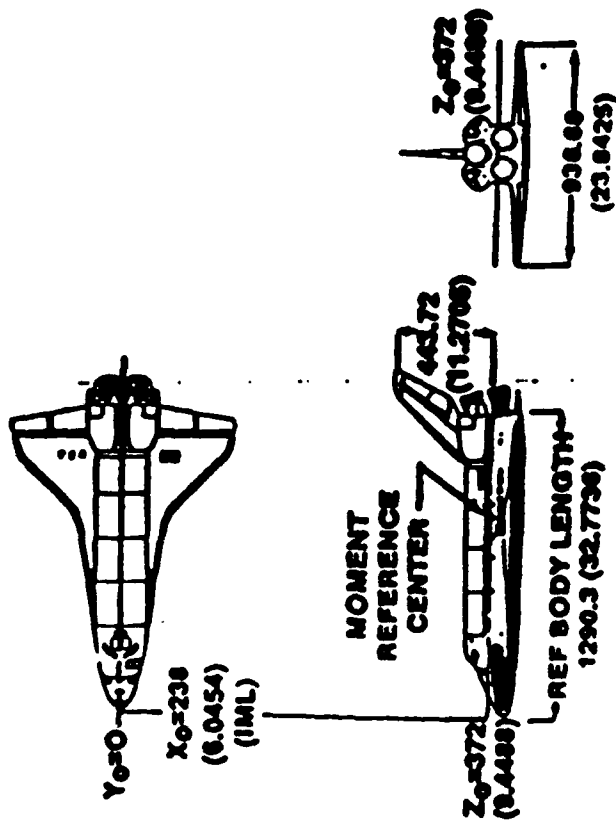


Fig. 5

# HYPERVELOCITY VEHICLES

• Existing

- Space Shuttle



67

GEOMETRY	COMPONENT	
	WING	VERTICAL TAIL
AREA	2000 FT <sup>2</sup> (240.9002 m <sup>2</sup> )	413.26 FT <sup>2</sup> (38.3022 m <sup>2</sup> )
SPAN	938.66 (23.8425)	318.72 (8.0169)
ASPECT RATIO	2.286	1.675
TAPER RATIO	0.2	0.404
SWEEP (LE)	81/45 DEG	45 DEG
DHEDRAL	3.5	--
INCIDENCE	0.5 DEG	--
MAC	474.81 (12.0002)	199.81 (5.0782)

NOTE: UNLESS OTHERWISE NOTED, ALL DIMENSIONS ARE IN INCHES (METERS)

Fig. 6.

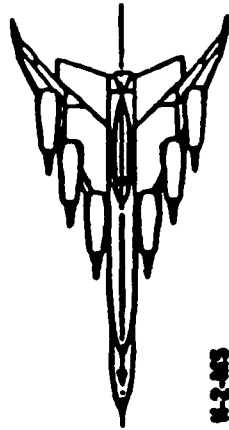
HYPERVELOCITY VEHICLES (CONT'D)

• Proposed

- Aerospace Plane



- Orbit-on-Demand Vehicle



#2-883



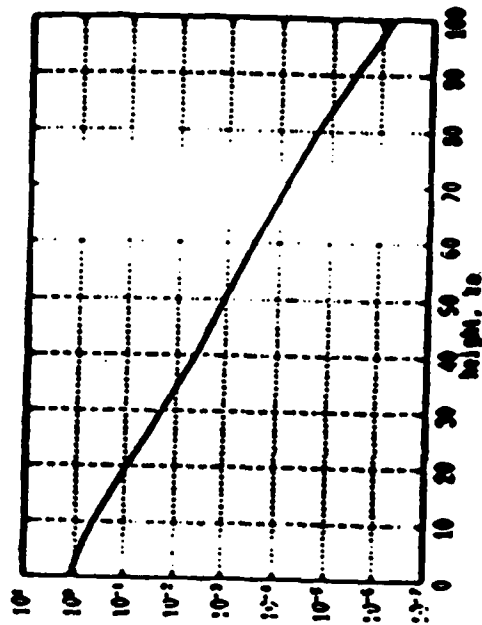
Horizontal-takeoff two-stage  $\Delta$  concept with hypersonic staging.

Orbiter Ref. Length	152 ft.
Orbiter Wing	1,655 ft.
System Length	239 ft.
Wing Loading	52.3 lb/ft <sup>2</sup>
Entry L/D	1.31
Average $\alpha$	36.1°

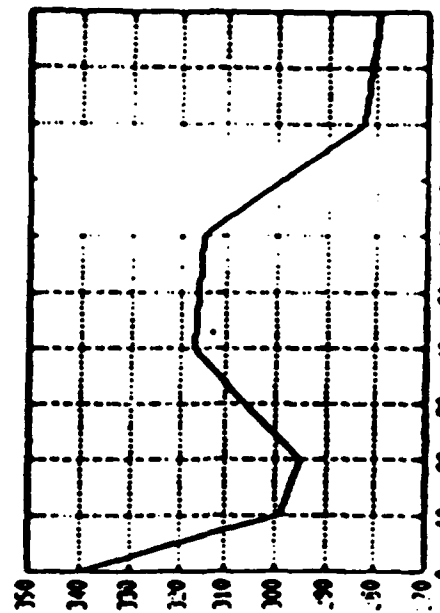
Fig. 7.

## TYPICAL ENVIRONMENTAL PROPERTIES

- Atmospheric Density Variations
- Velocity of Sound =  $\sqrt{\gamma R T}$



Density  
Kg/m<sup>3</sup>



Velocity of  
Sound  
a  
m/sec

Fig. 8.

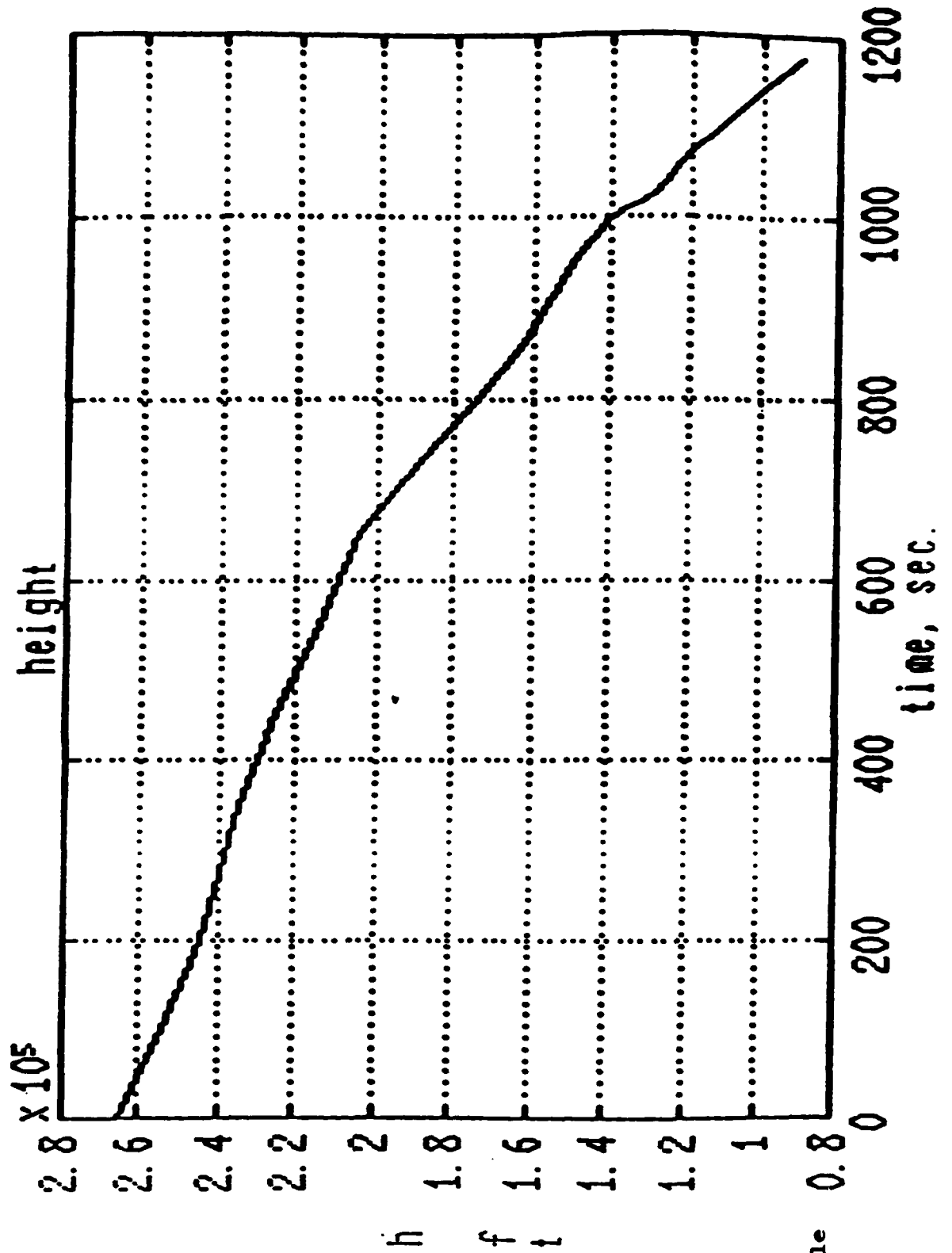


Fig. 9.

Space Shuttle  
Re-entry.

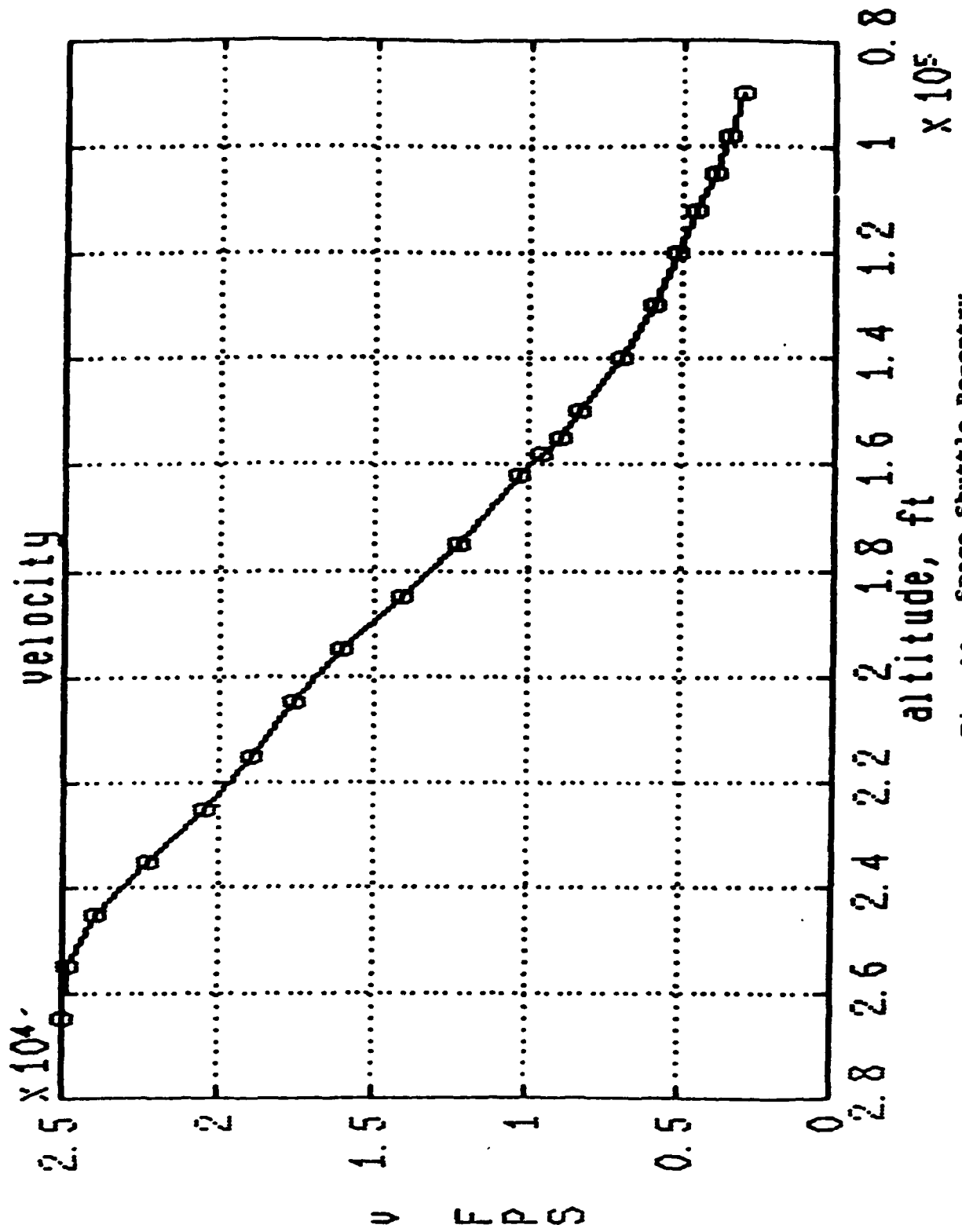


Fig. 10. Space Shuttle Re-entry.

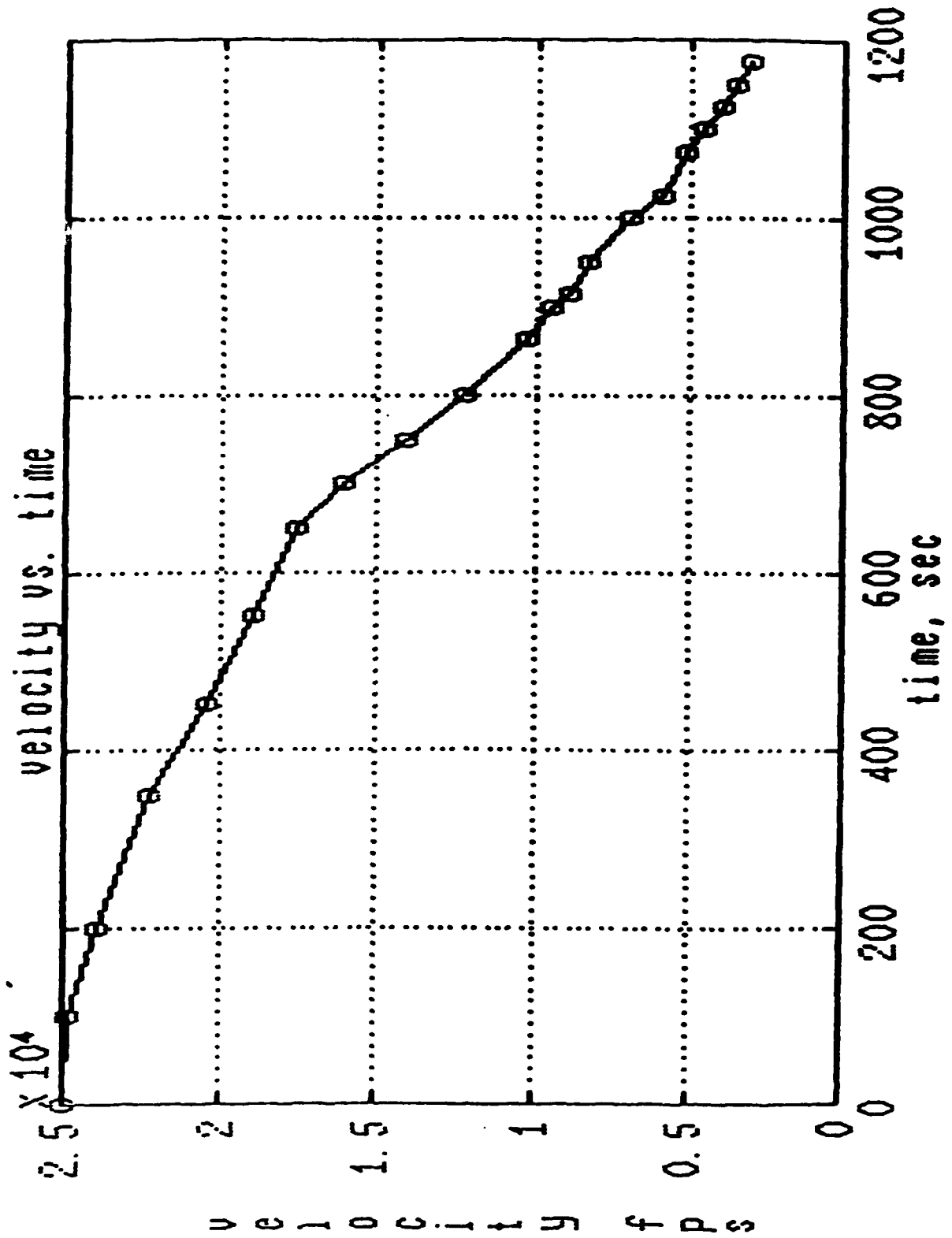


Fig. 11. Space Shuttle Re-entry.

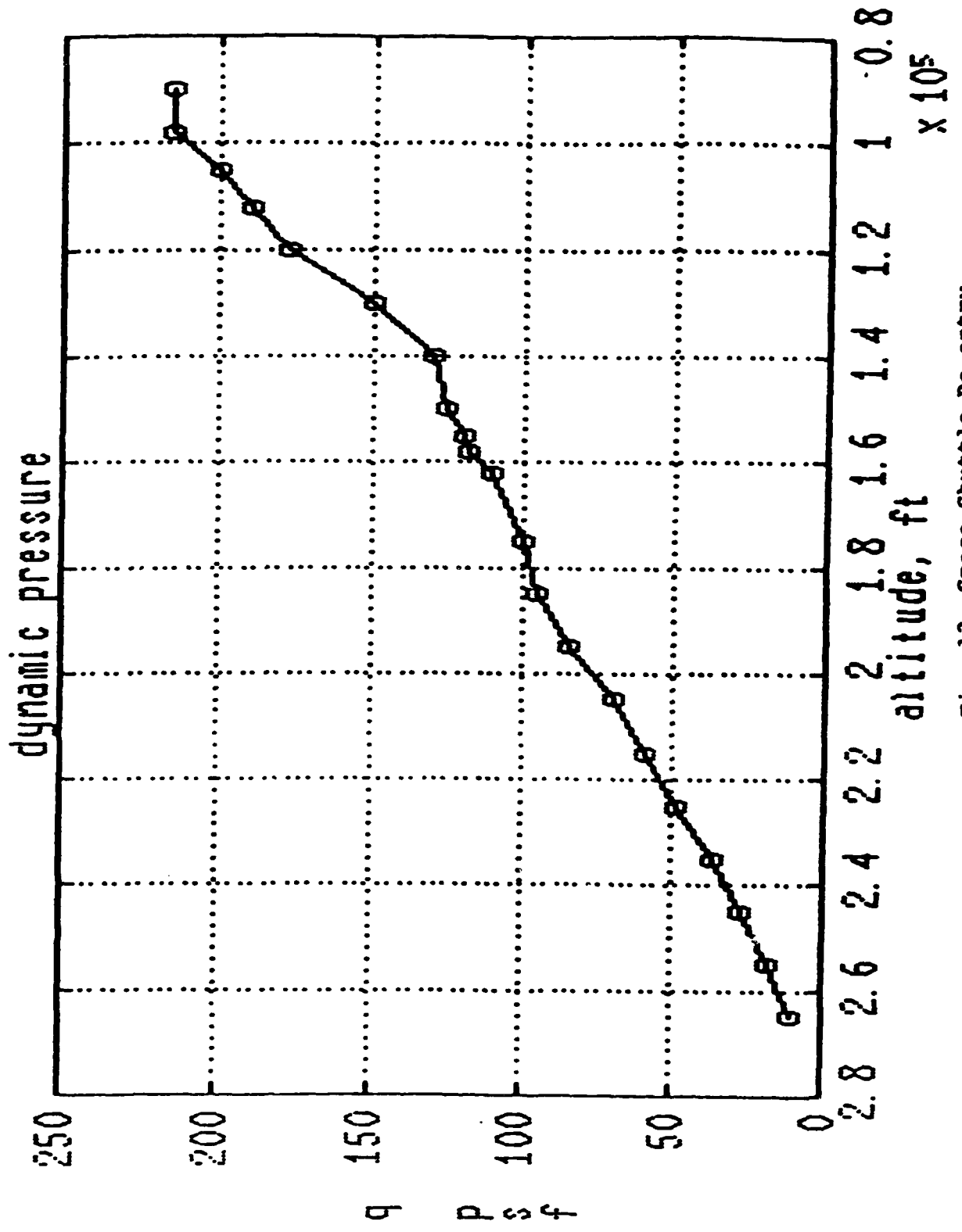


Fig. 12. Space Shuttle Re-entry.

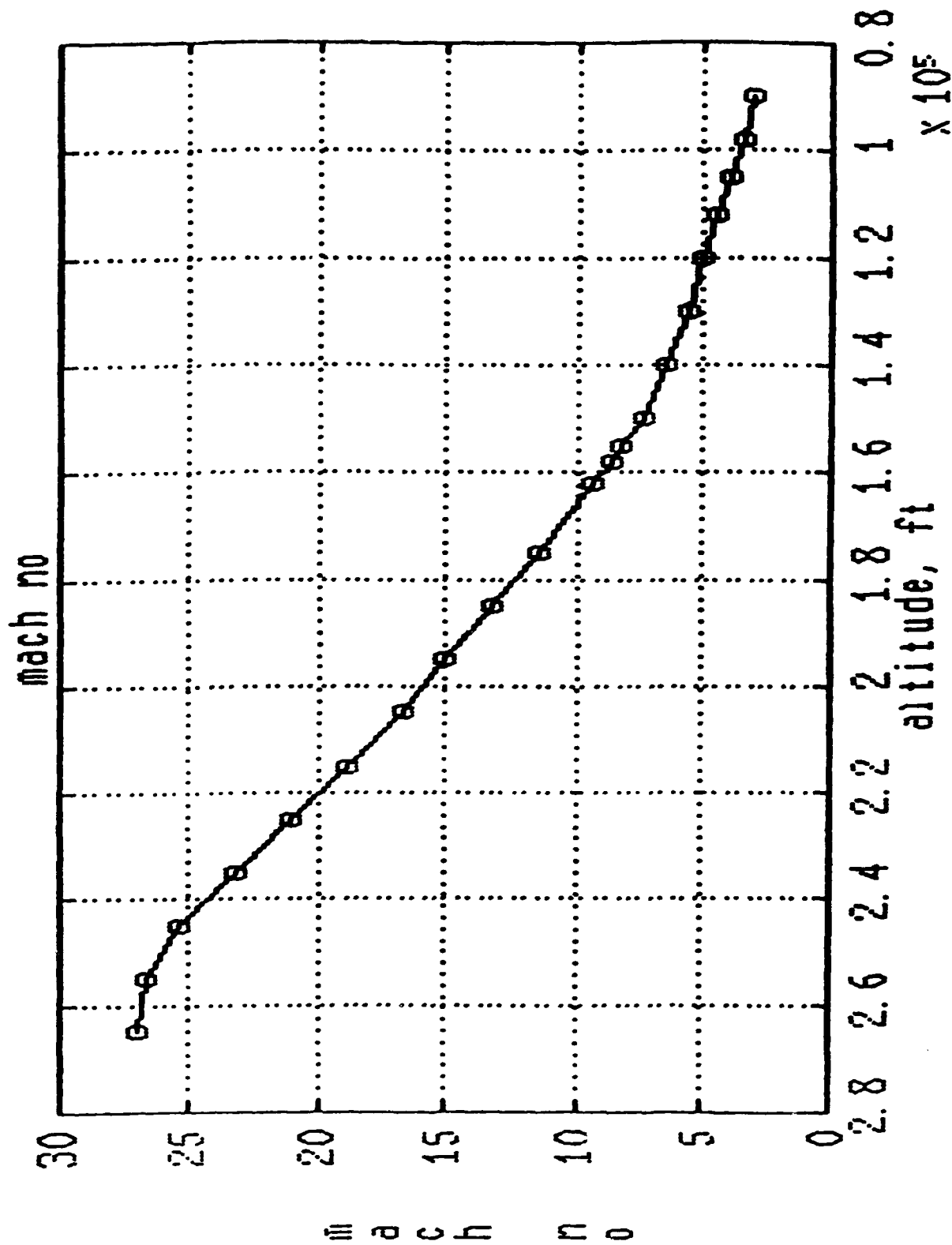


Fig. 13. Space Shuttle Re-entry.

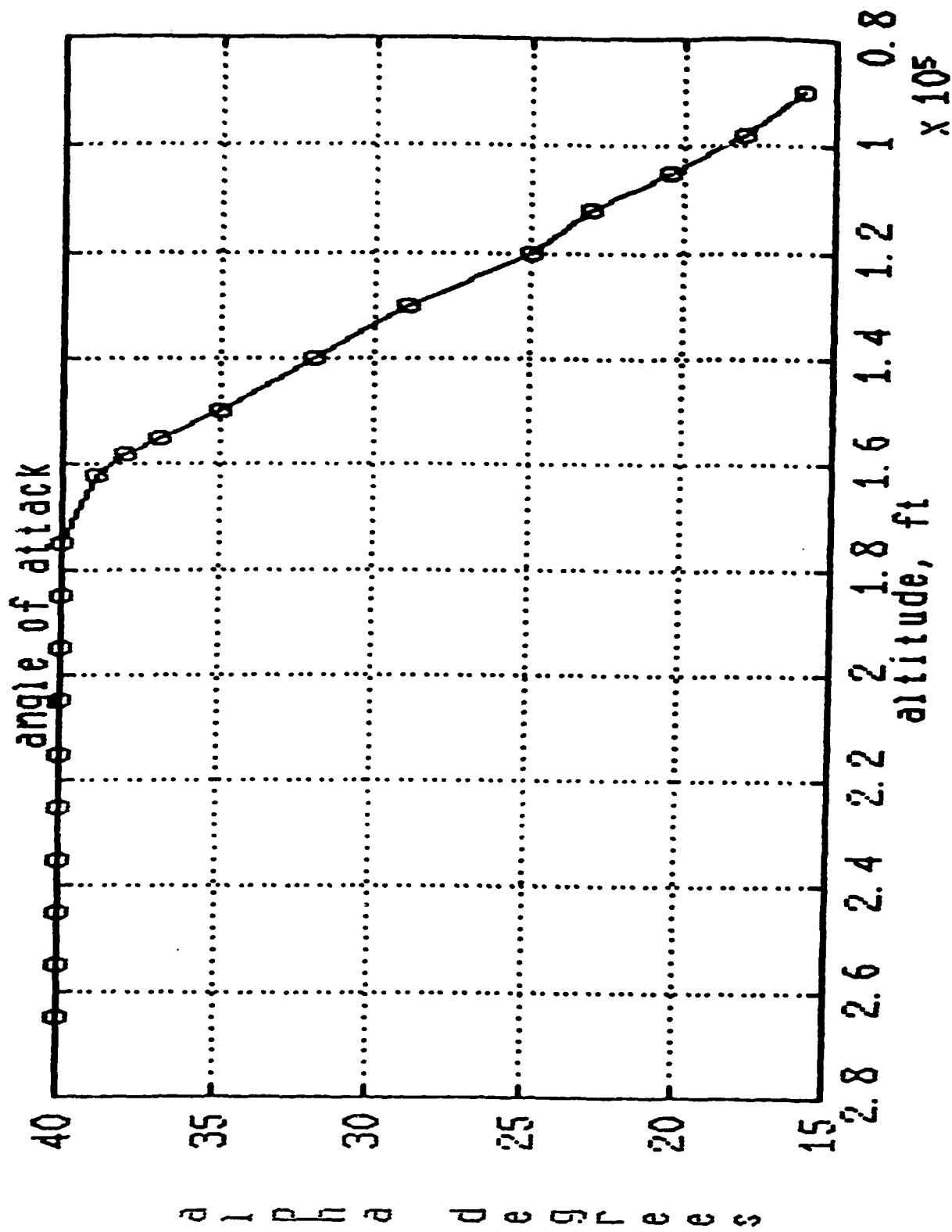


Fig. 14. Space Shuttle Re-entry.

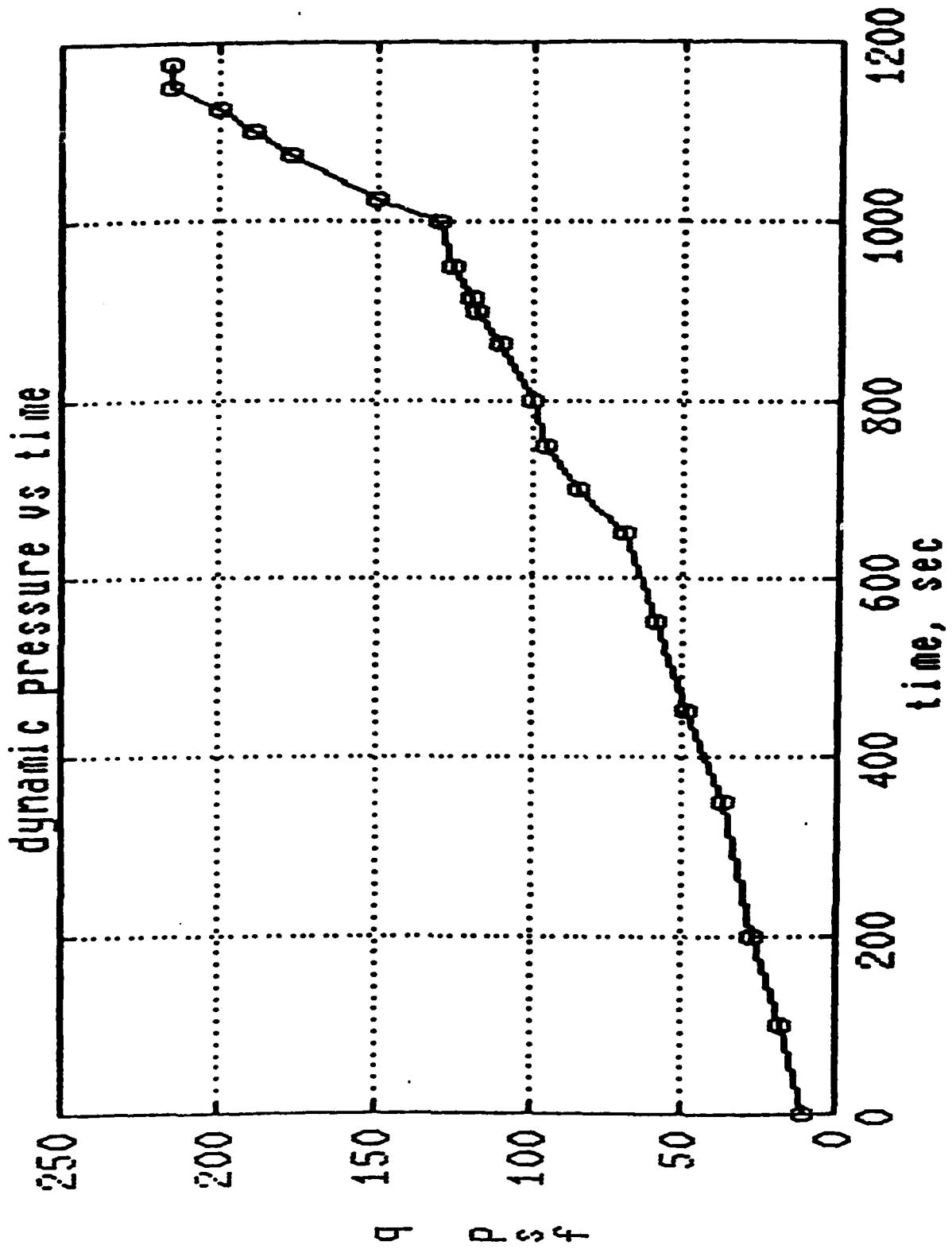


Fig. 15. Space Shuttle Re-entry.

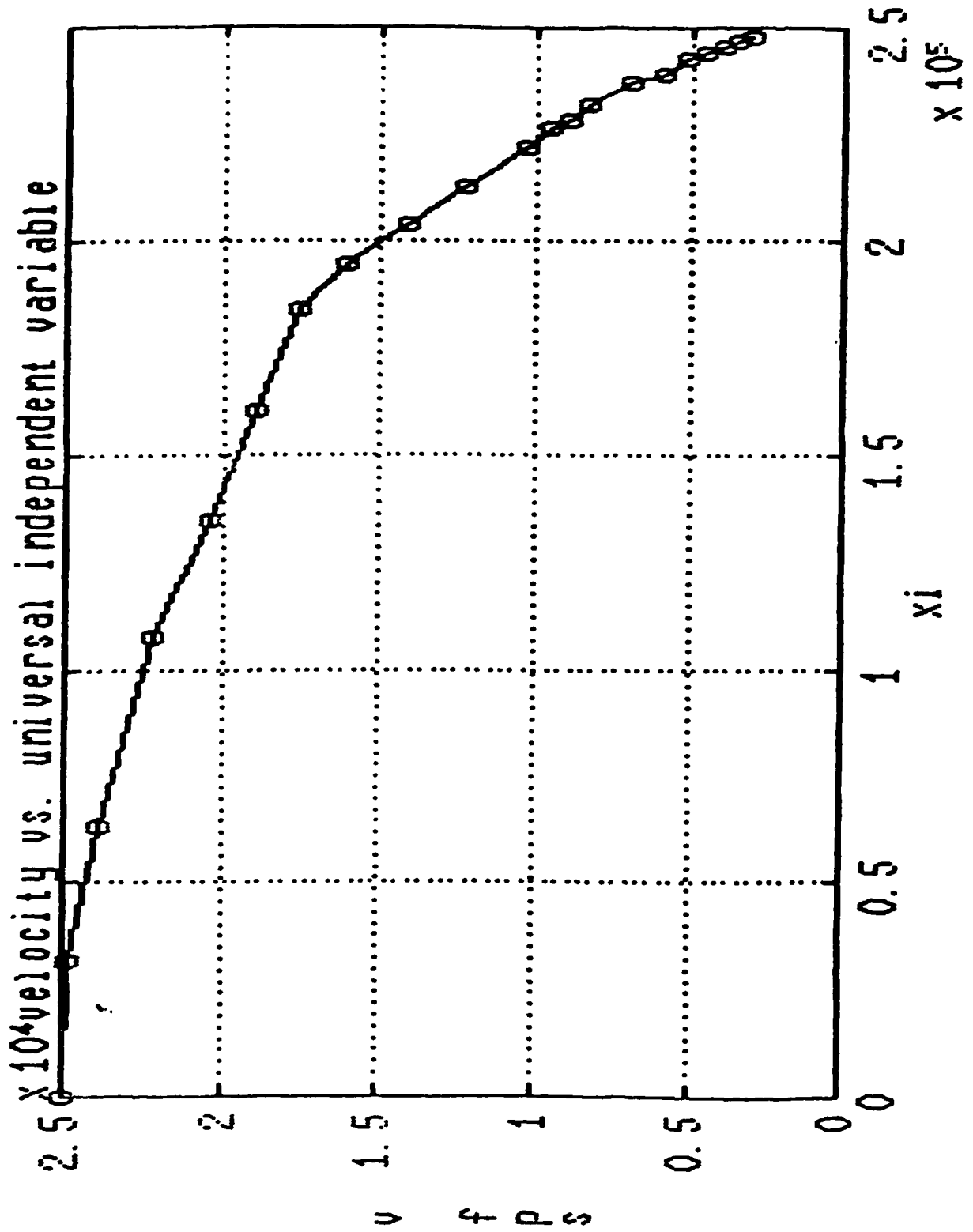


Fig. 16. Space Shuttle Re-entry.

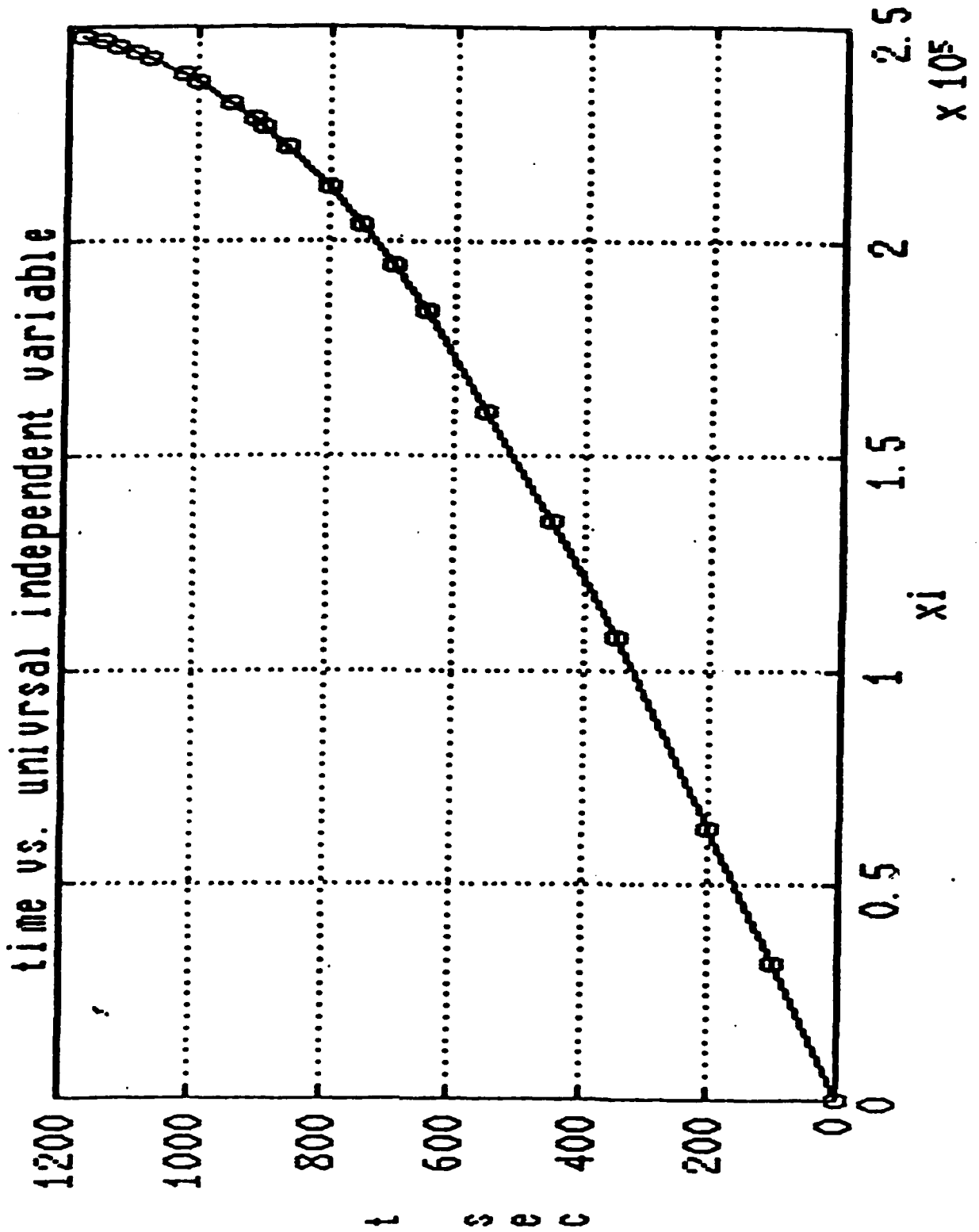


Fig. 17. Space Shuttle Re-entry.

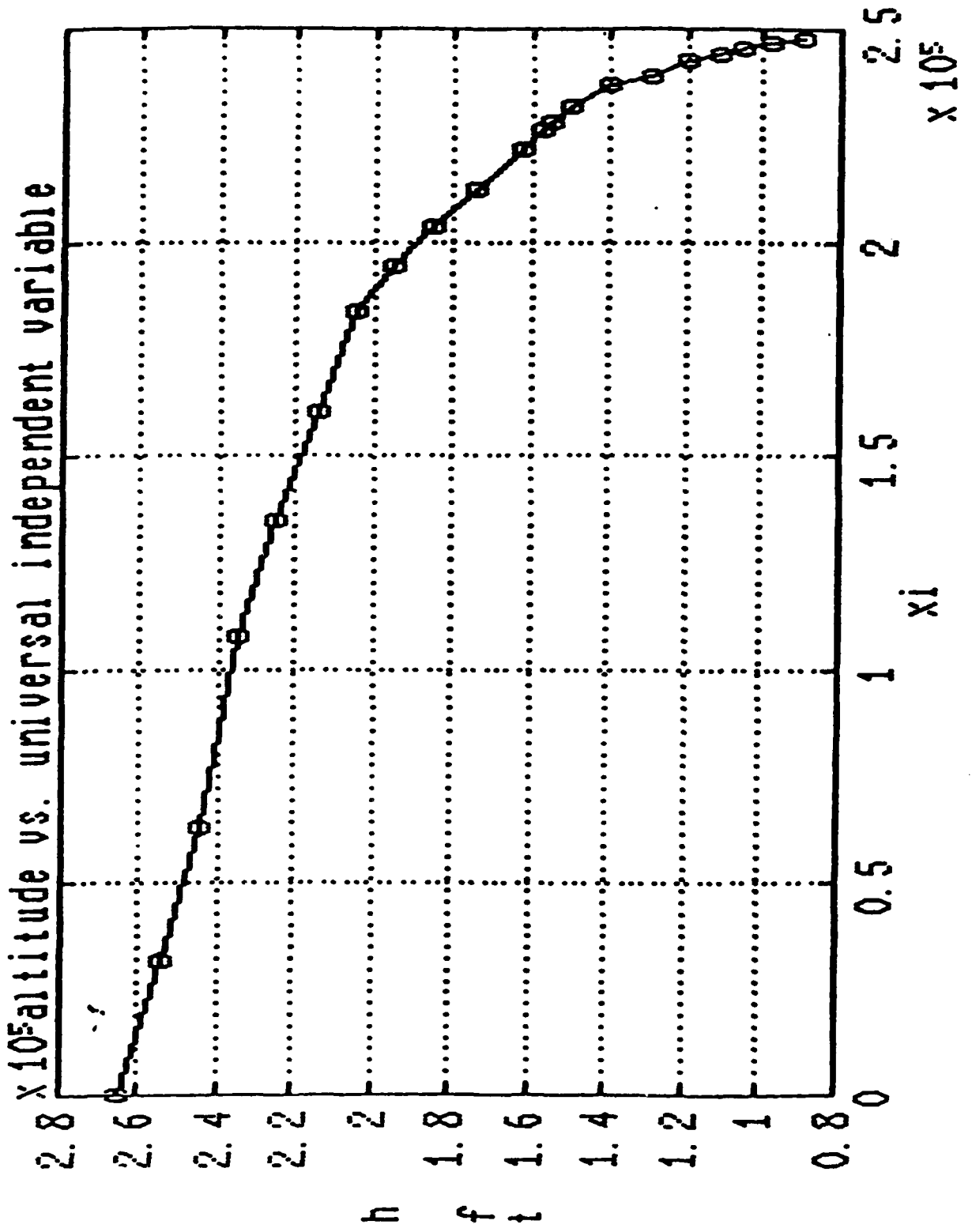


Fig. 18. Space Shuttle Data

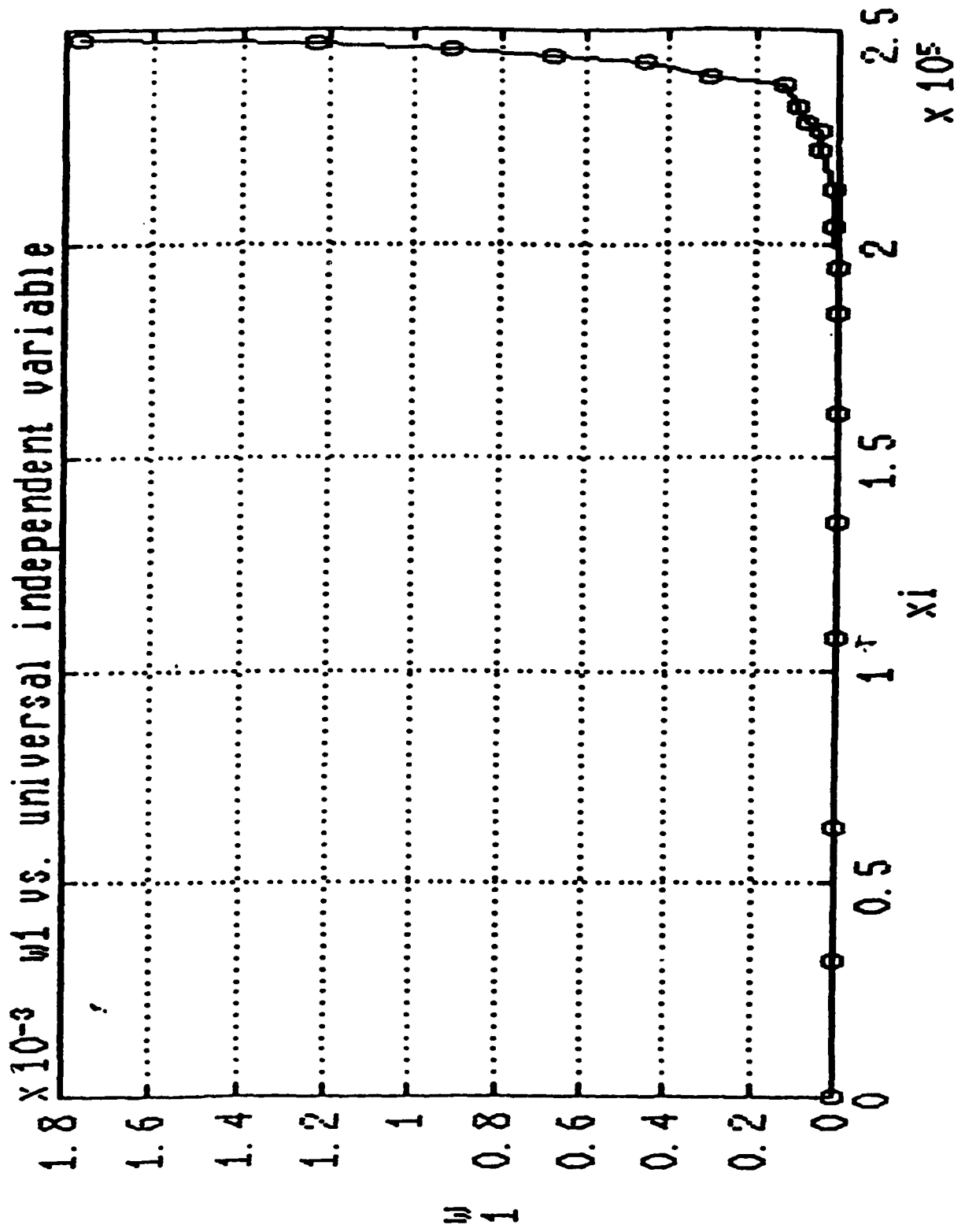


Fig. 19. Space Shuttle Re-entry.

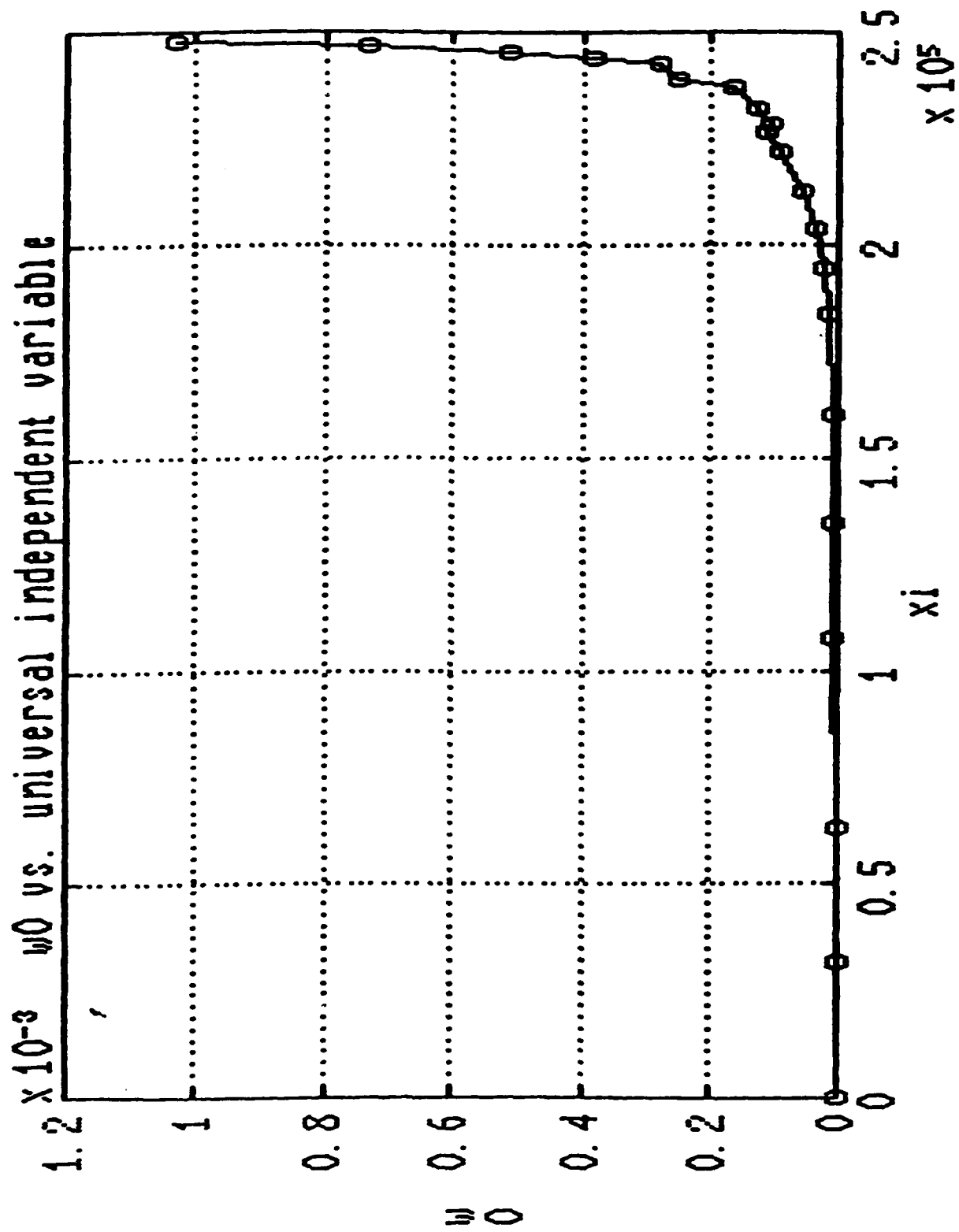


Fig. 20. Space Shuttle Re-entry.

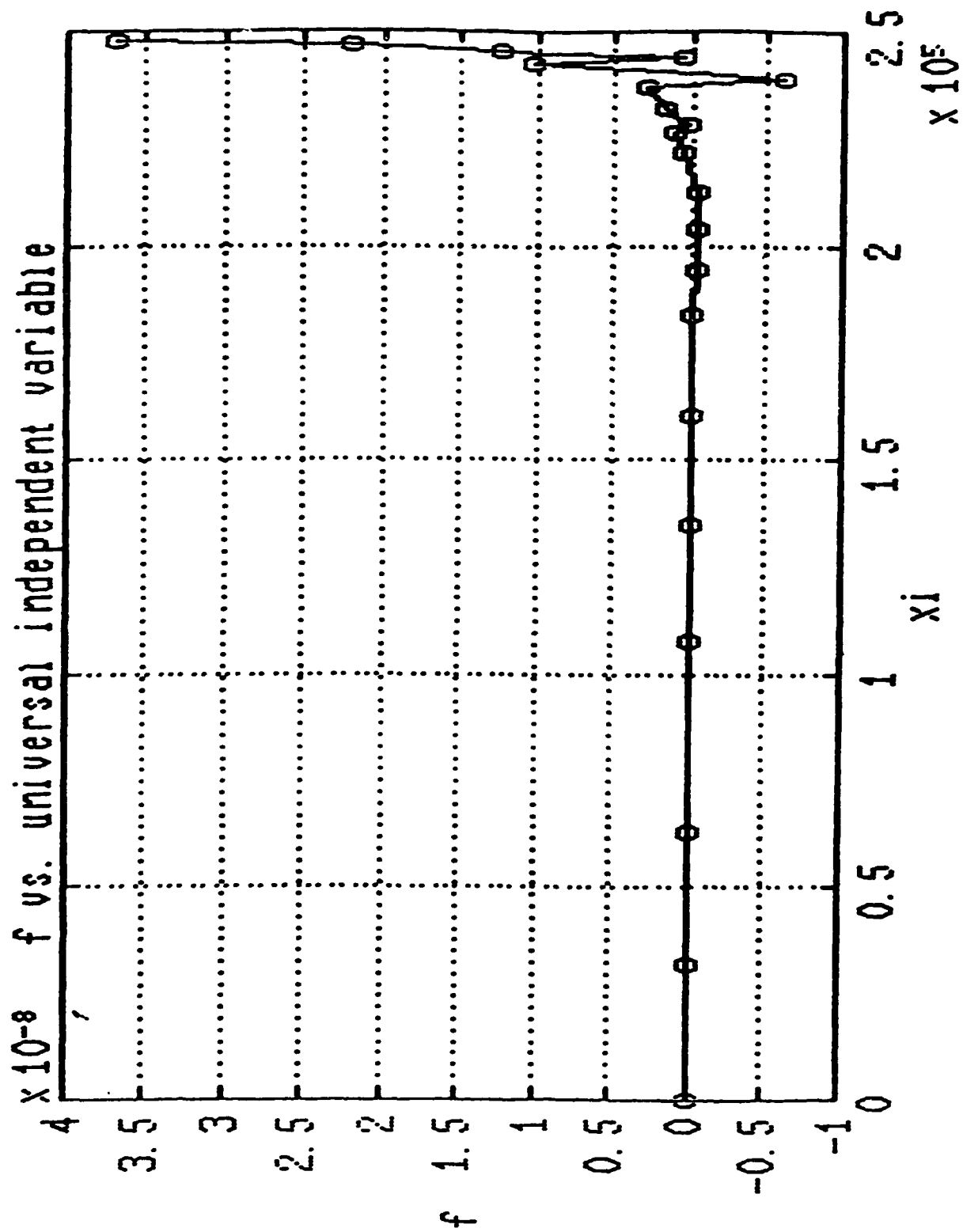


Fig. 21. Space Shuttle Re-entry.

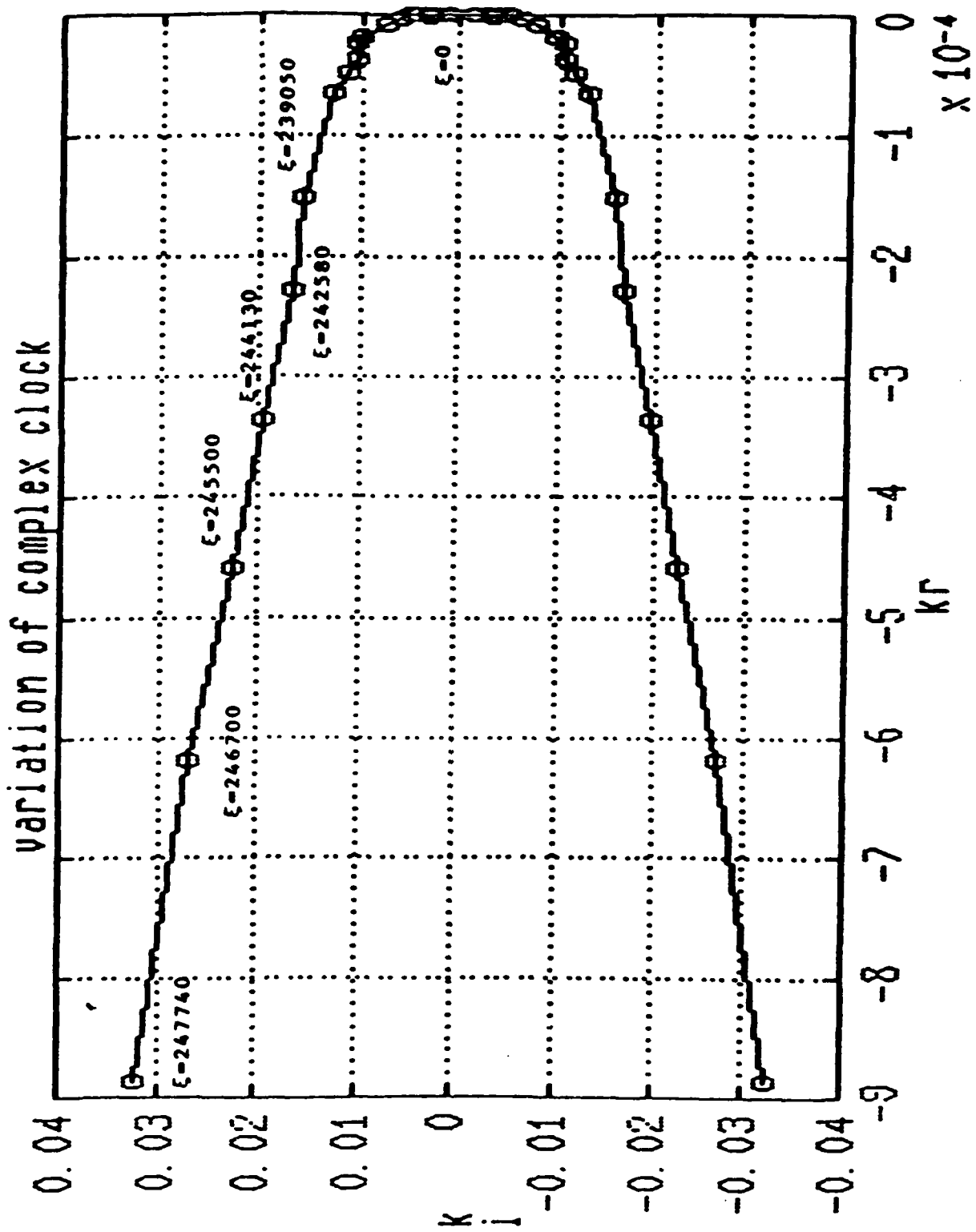


Fig. 22. Space Shuttle Re-entry.

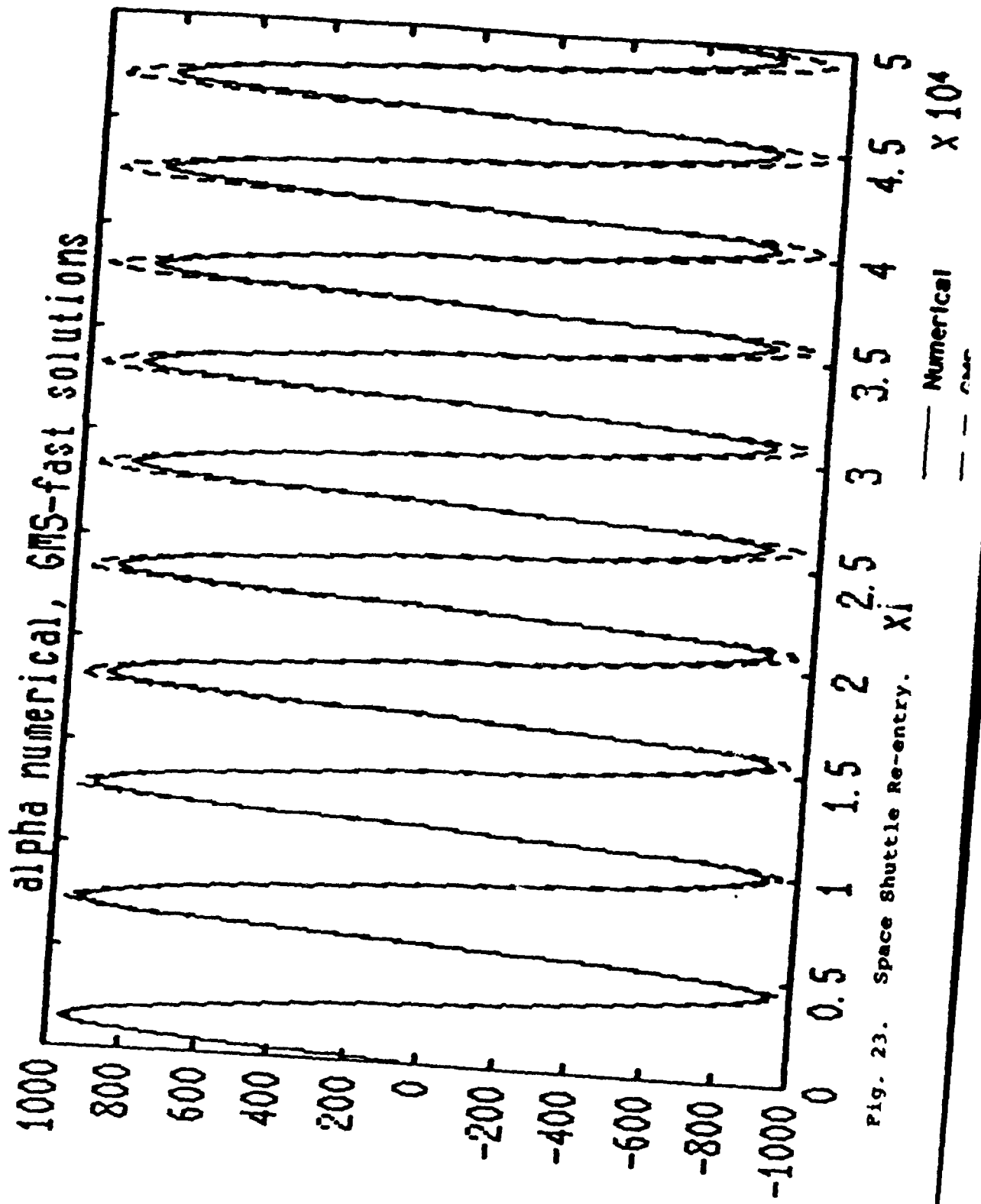
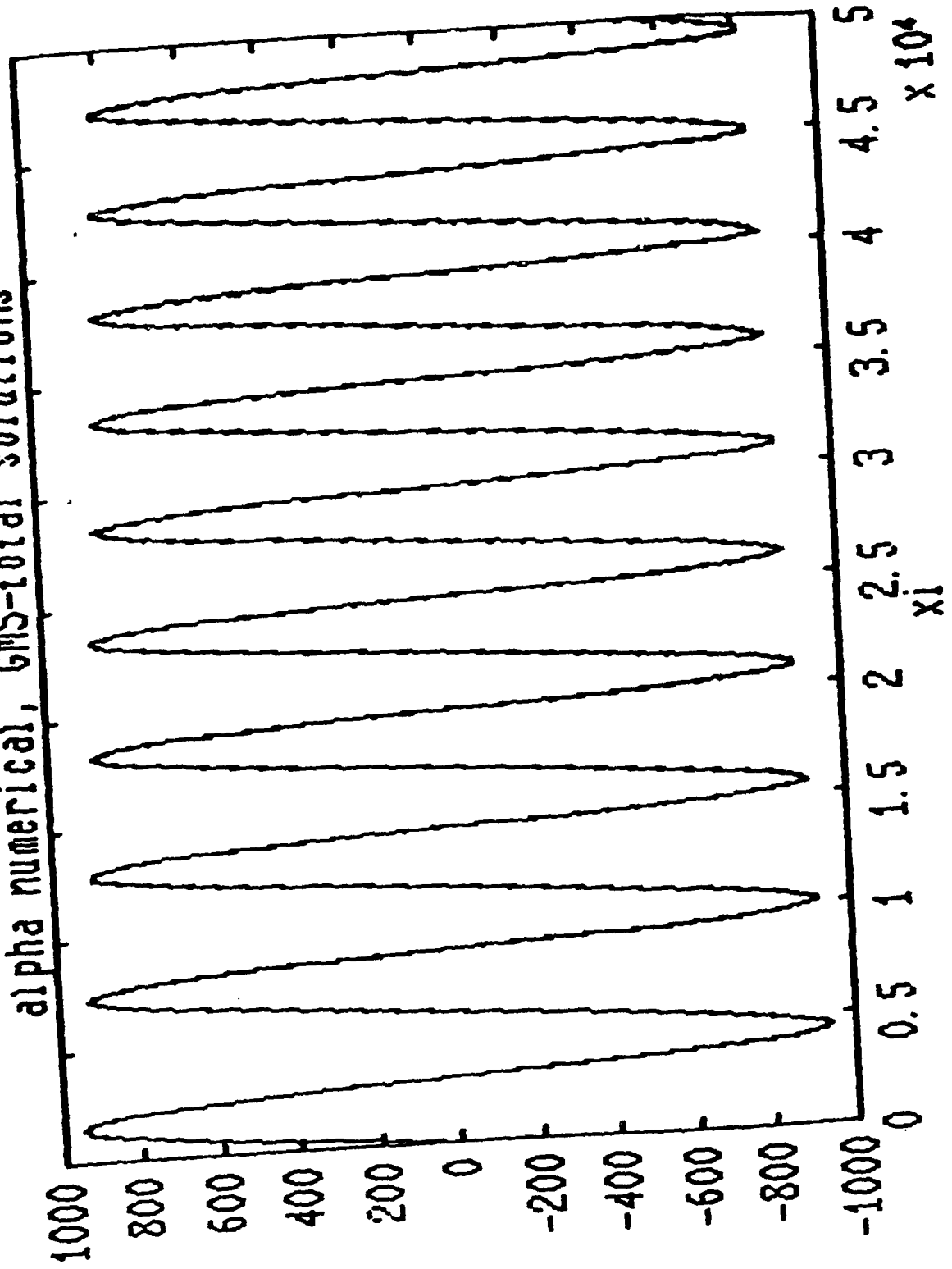
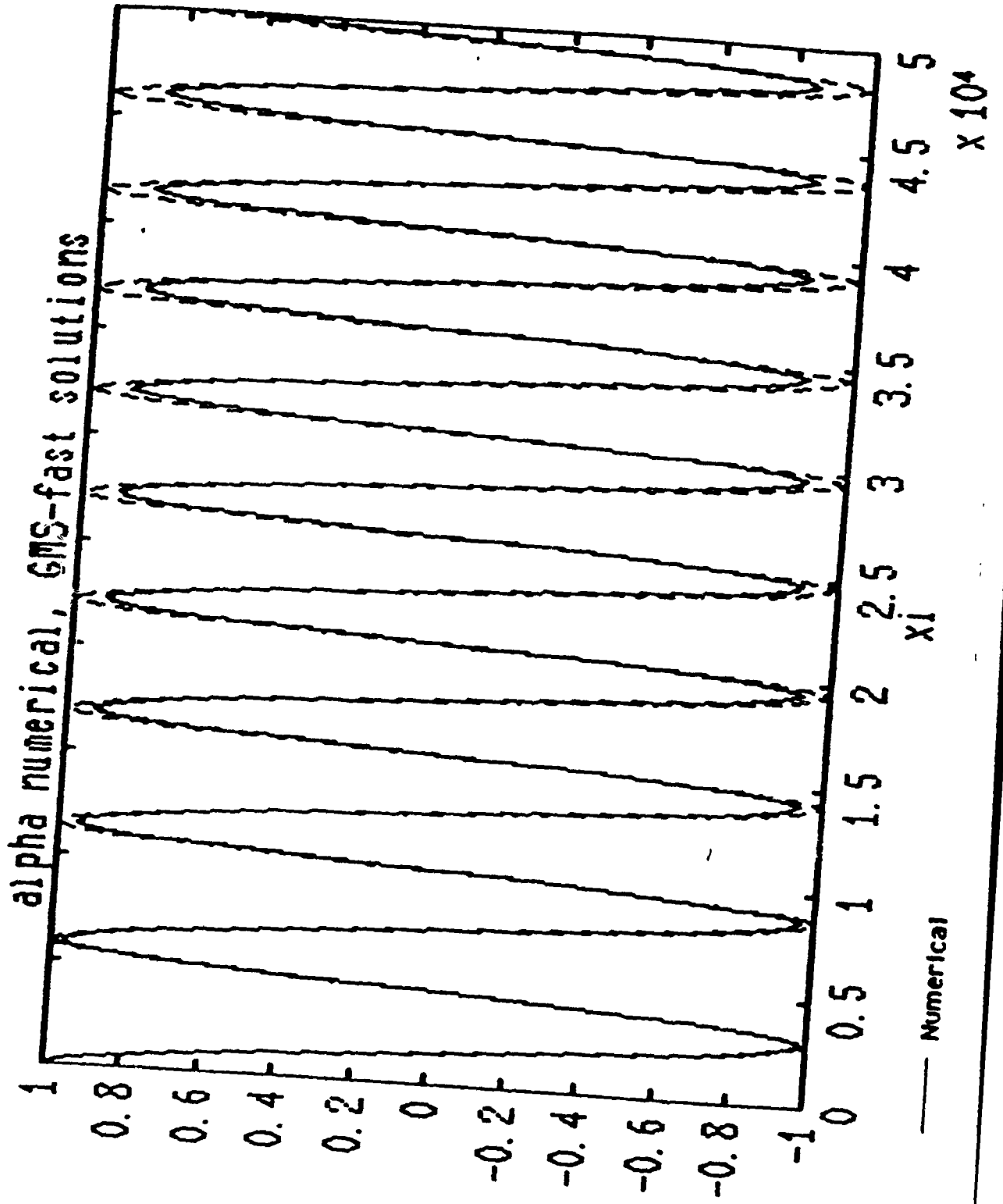


Fig. 23. Space Shuttle Re-entry.  $\alpha_i$

alpha numerical, GMS-total solutions



— Numerical  
- - - GMC



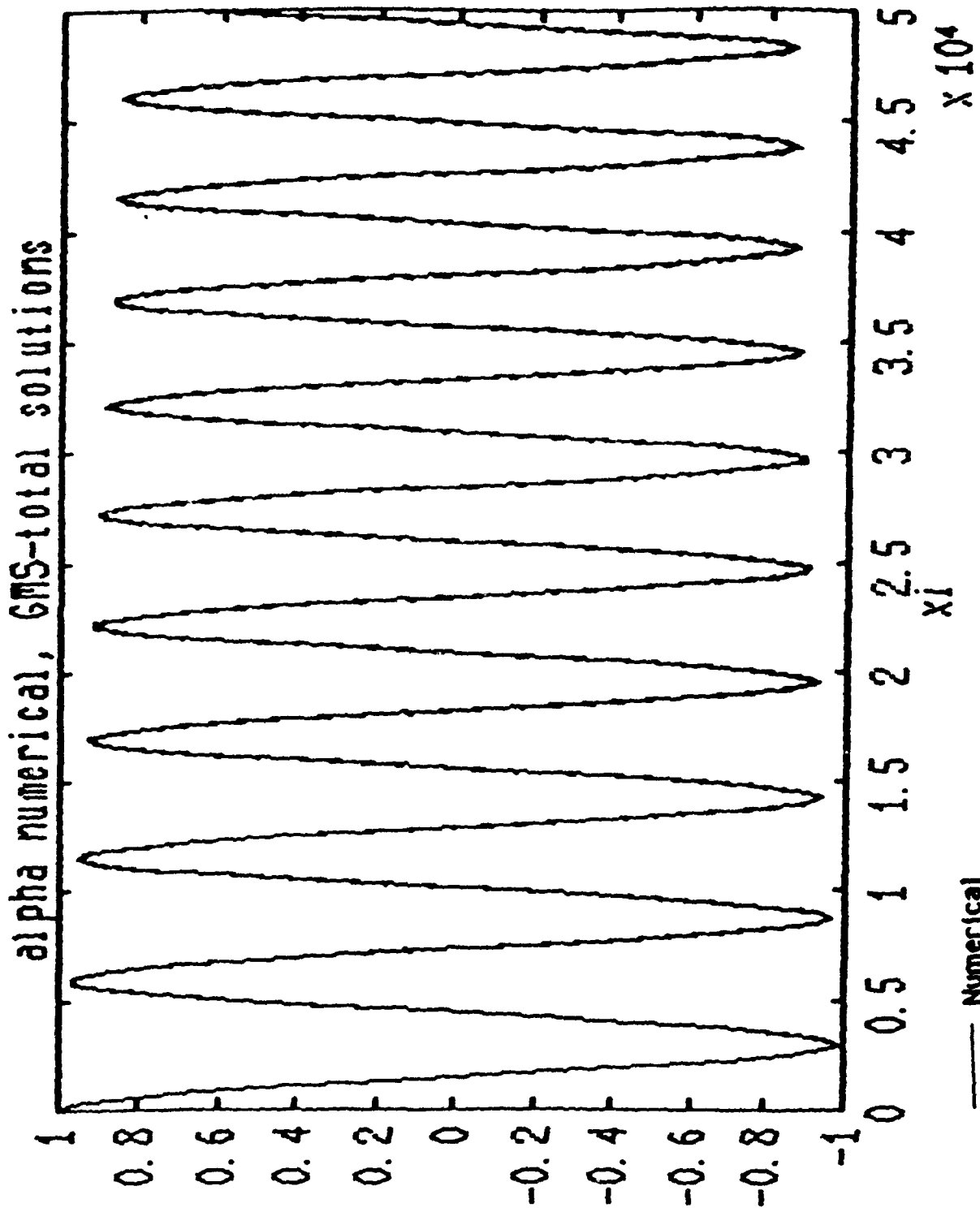
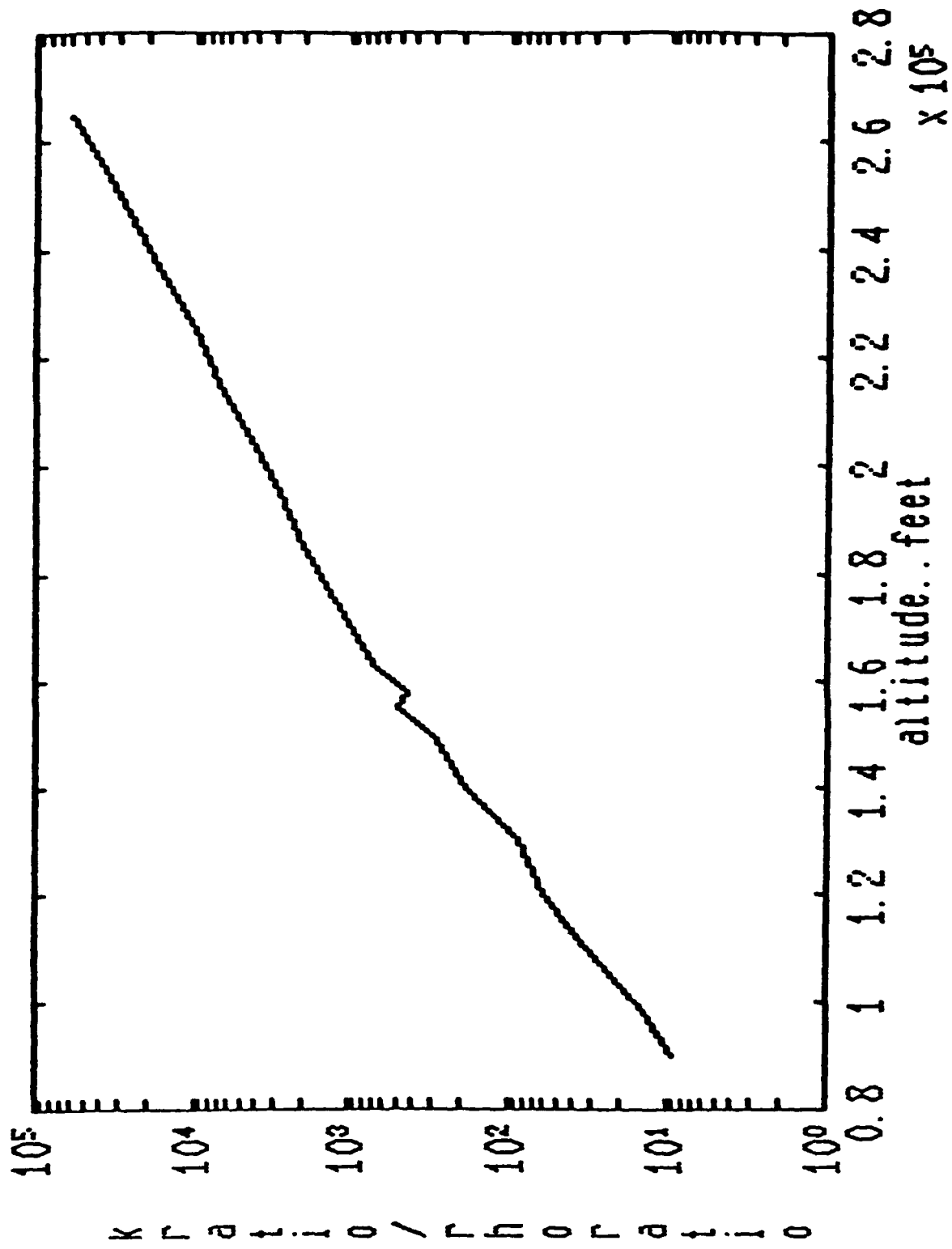
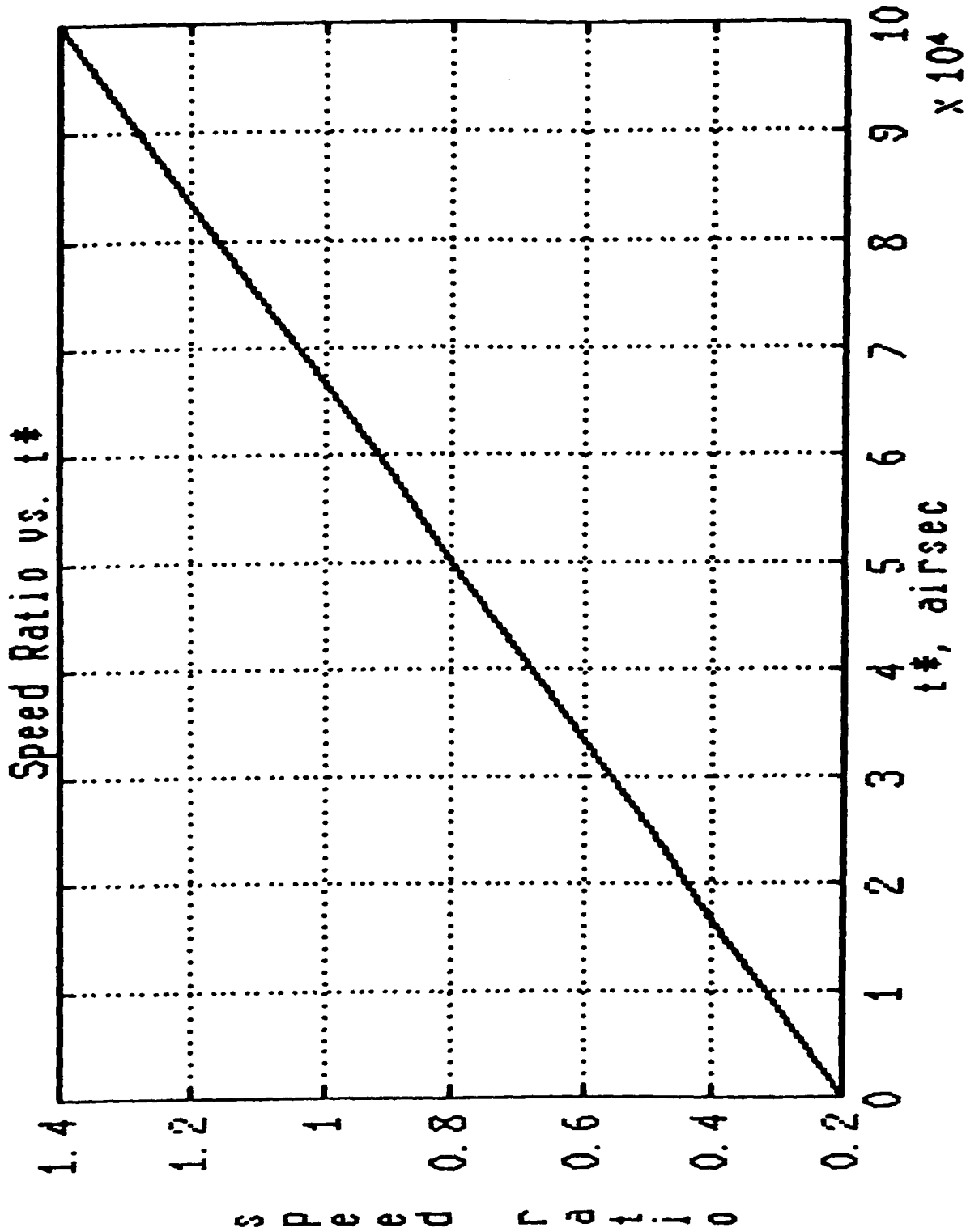


Fig. 26. Error Chisla Damentu





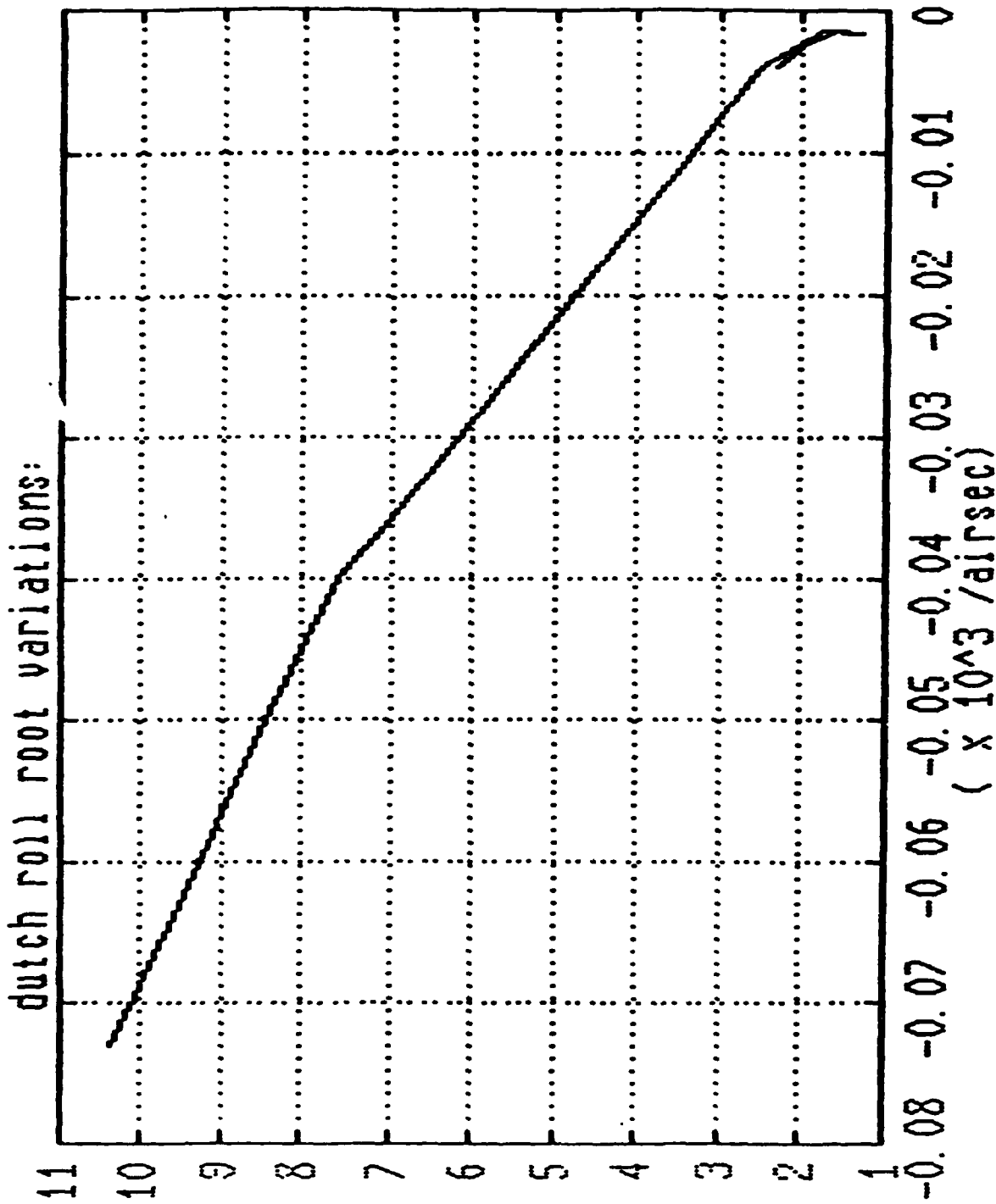
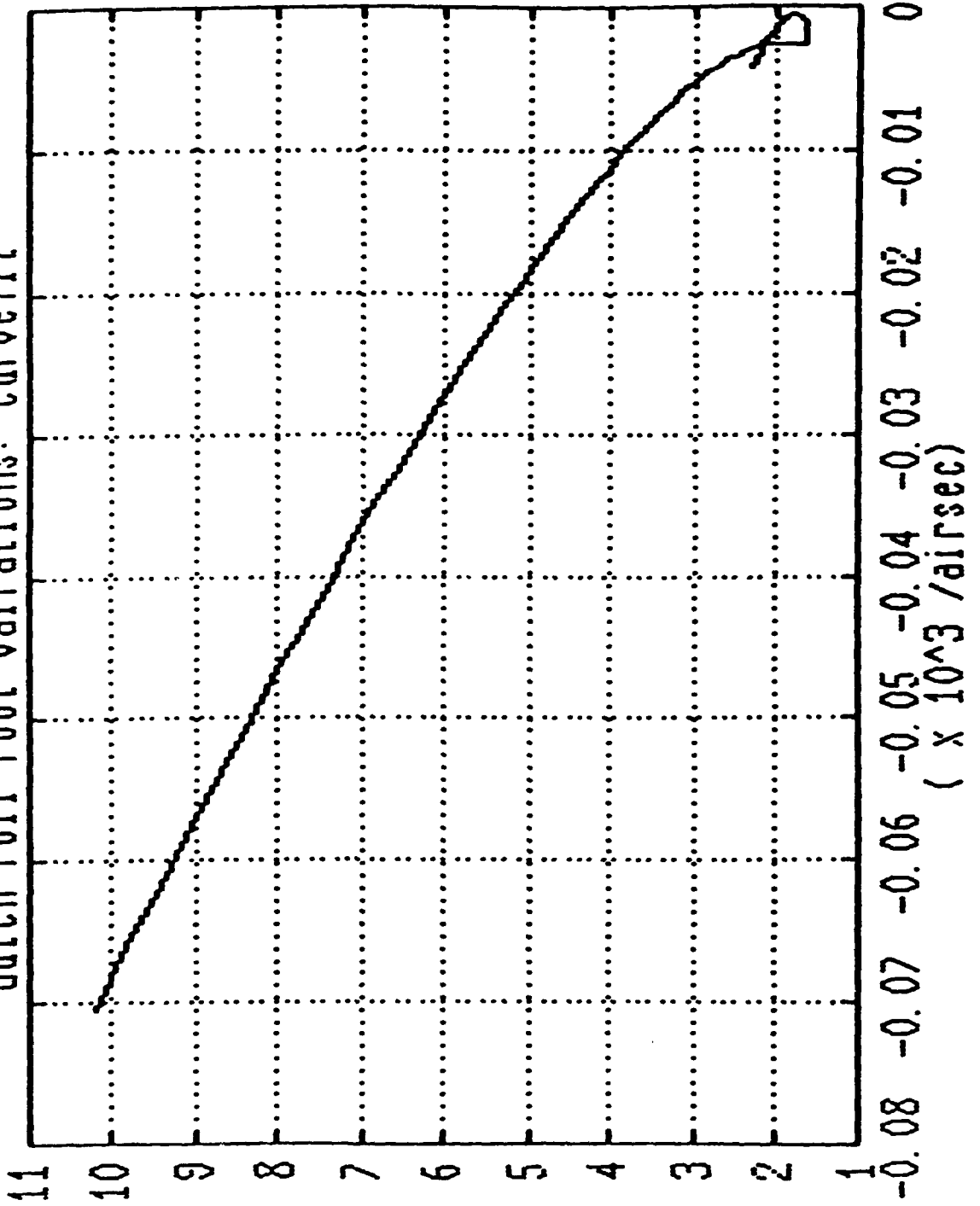
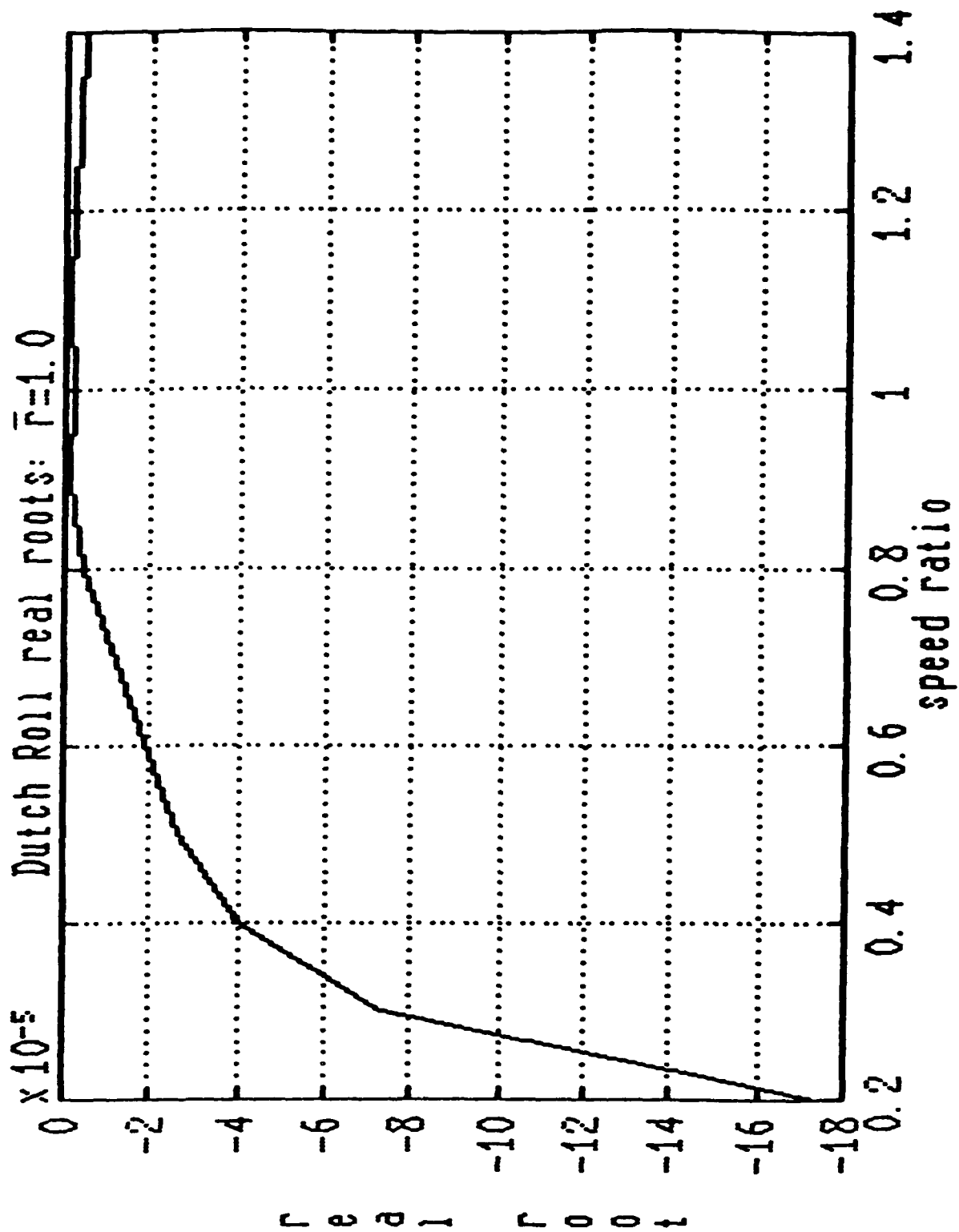


Fig. 29 - FLIGHT ON MINOR CIRCLES

dutch roll root variations: curvefit



CURTIS AND MERRILL, 1954



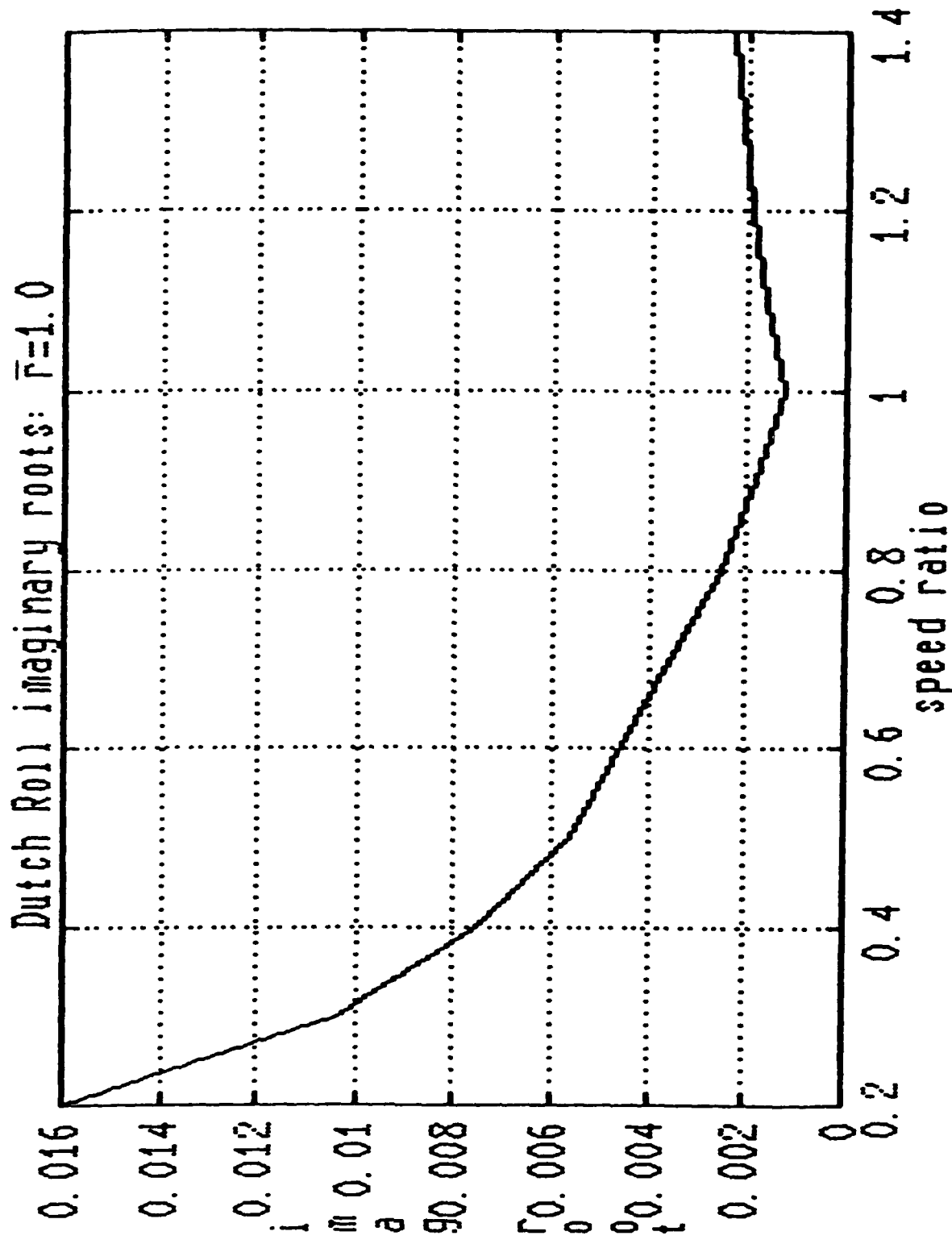


Fig. 32. - FLIGHT ON MINOR CIRCLES

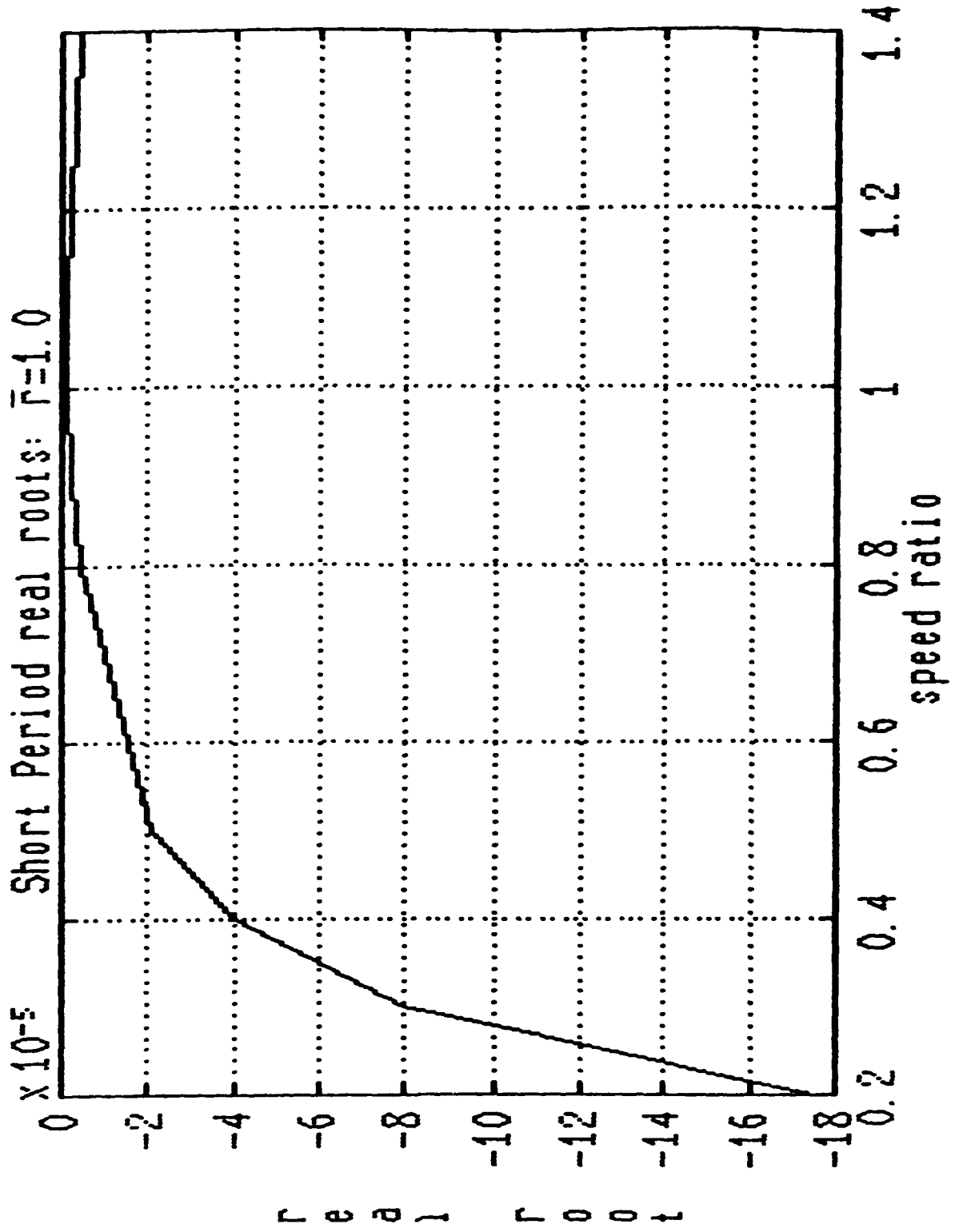


FIG. 33. : FLIGHT ON MINOR CIRCLES

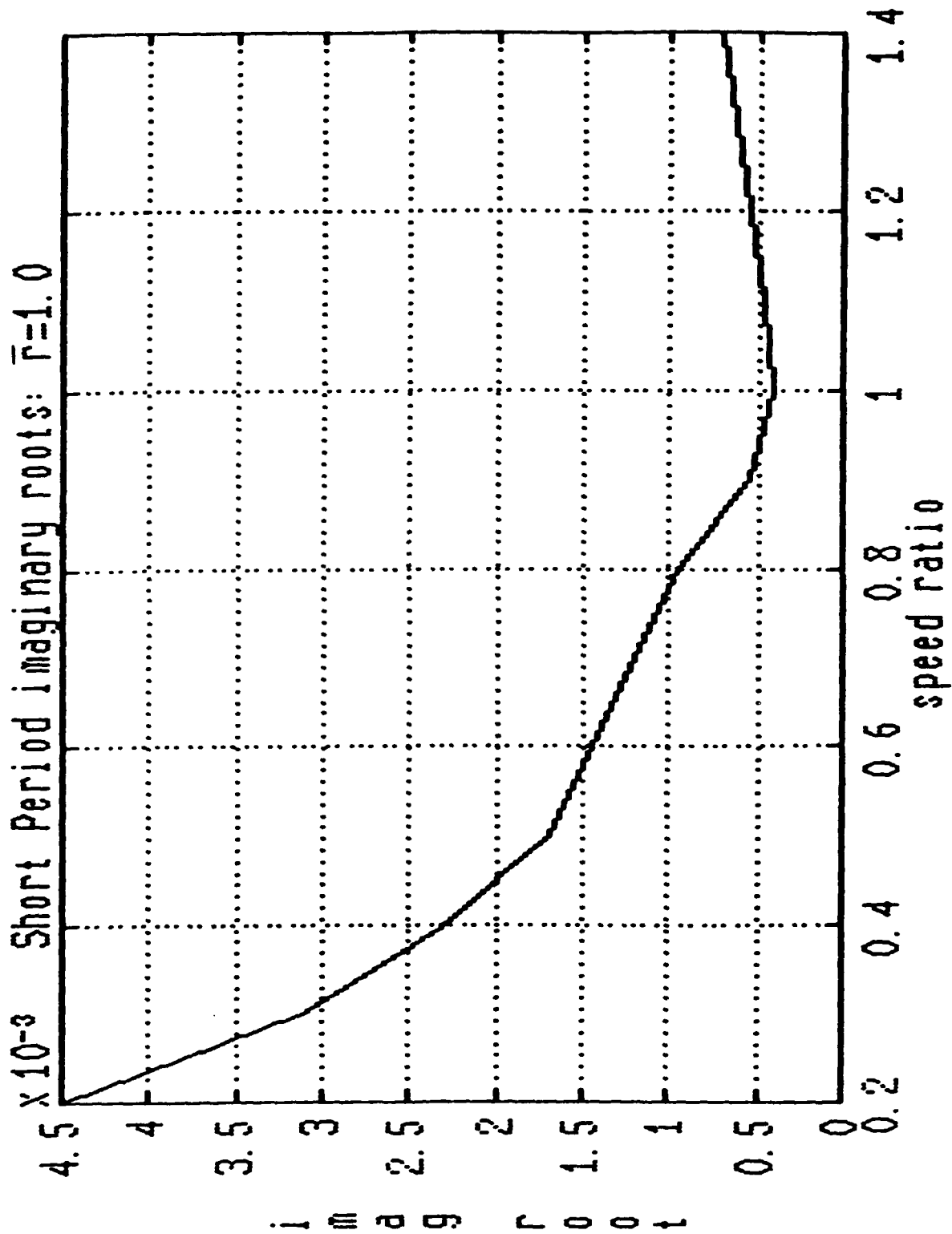


Fig. 34. - FLIGHT ON MINOR CIRCLES

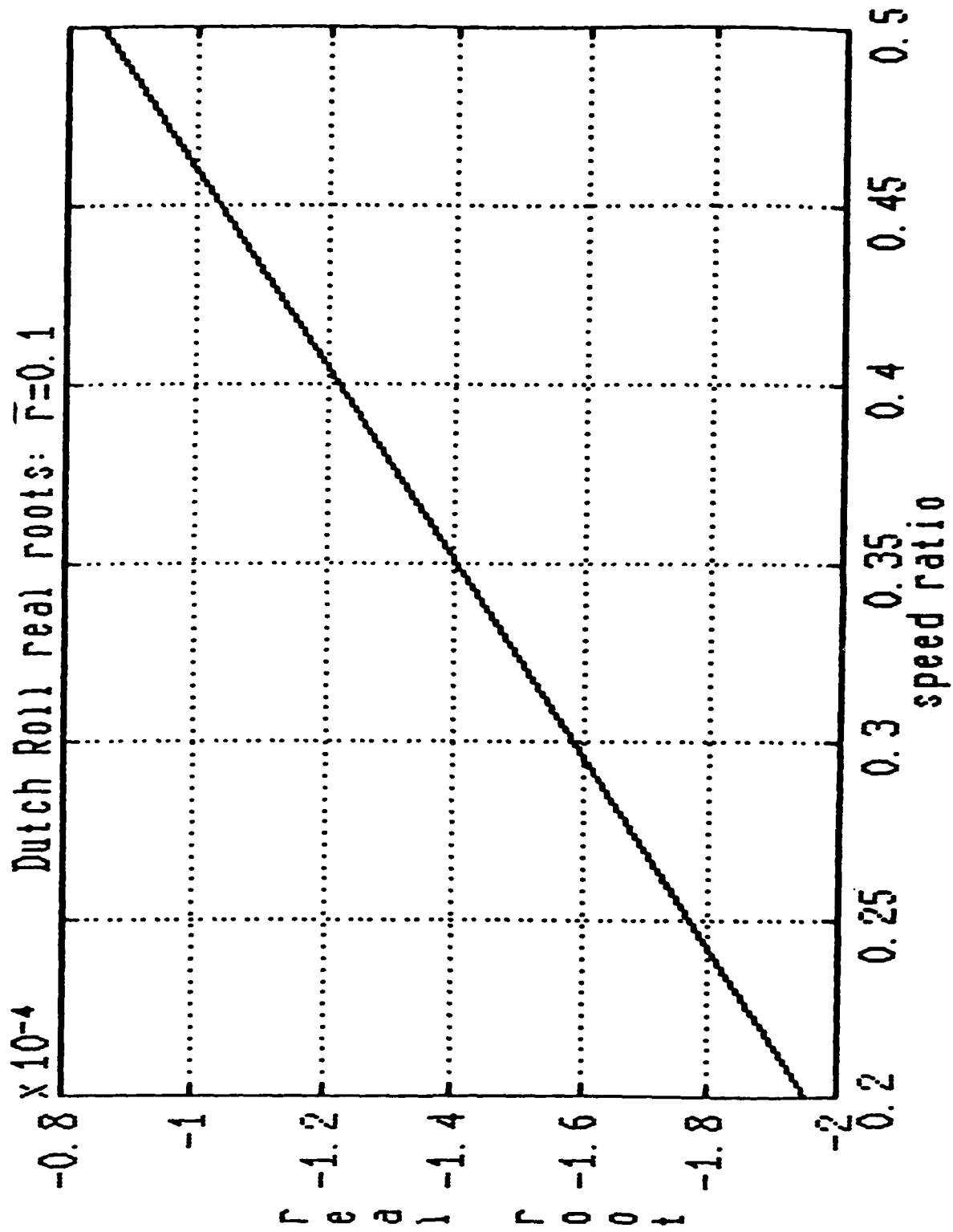


Fig. 35. - FLIGHT ON MINOR CIRCLES

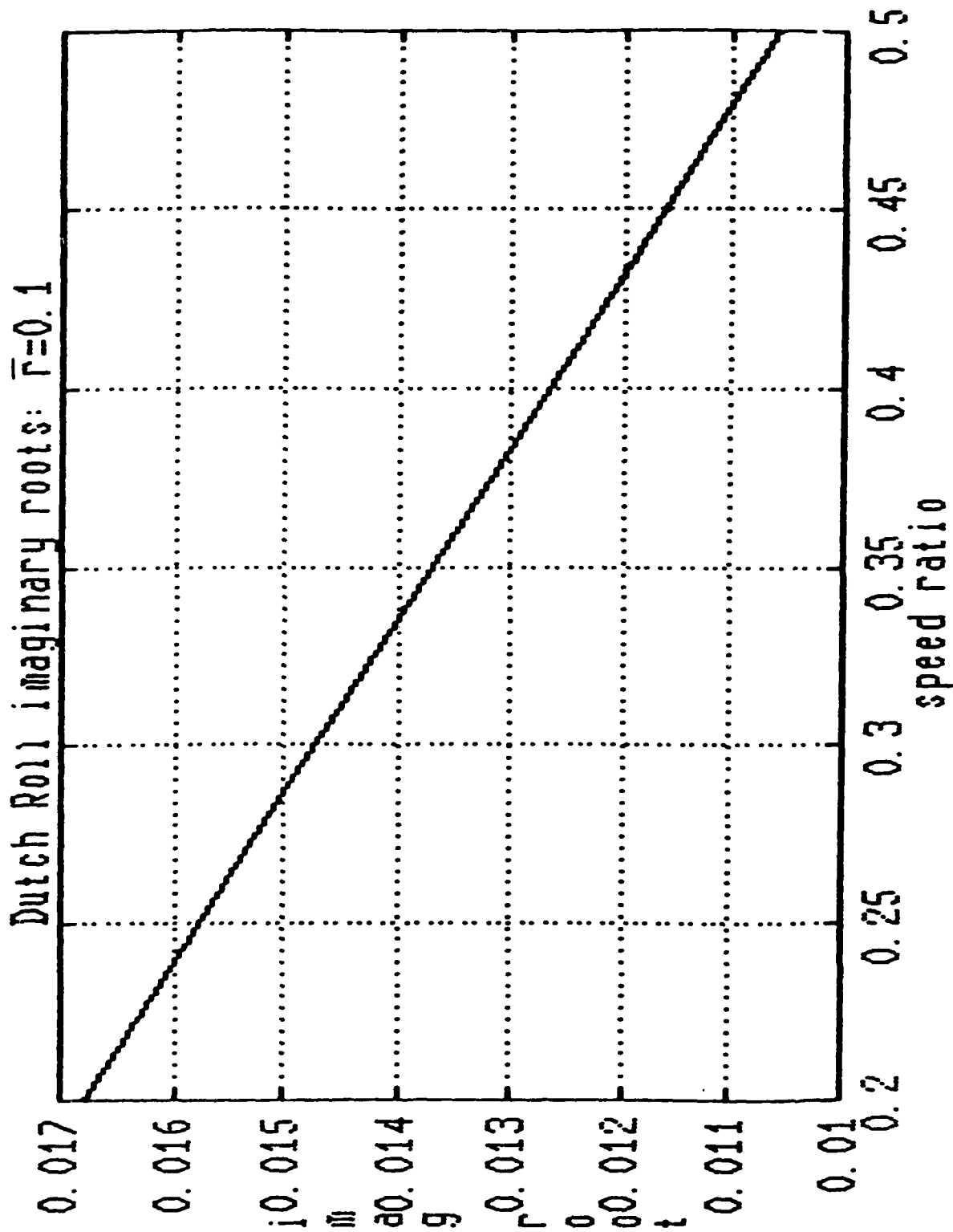


Fig. 36. - FLIGHT ON MINOR CIRCLES

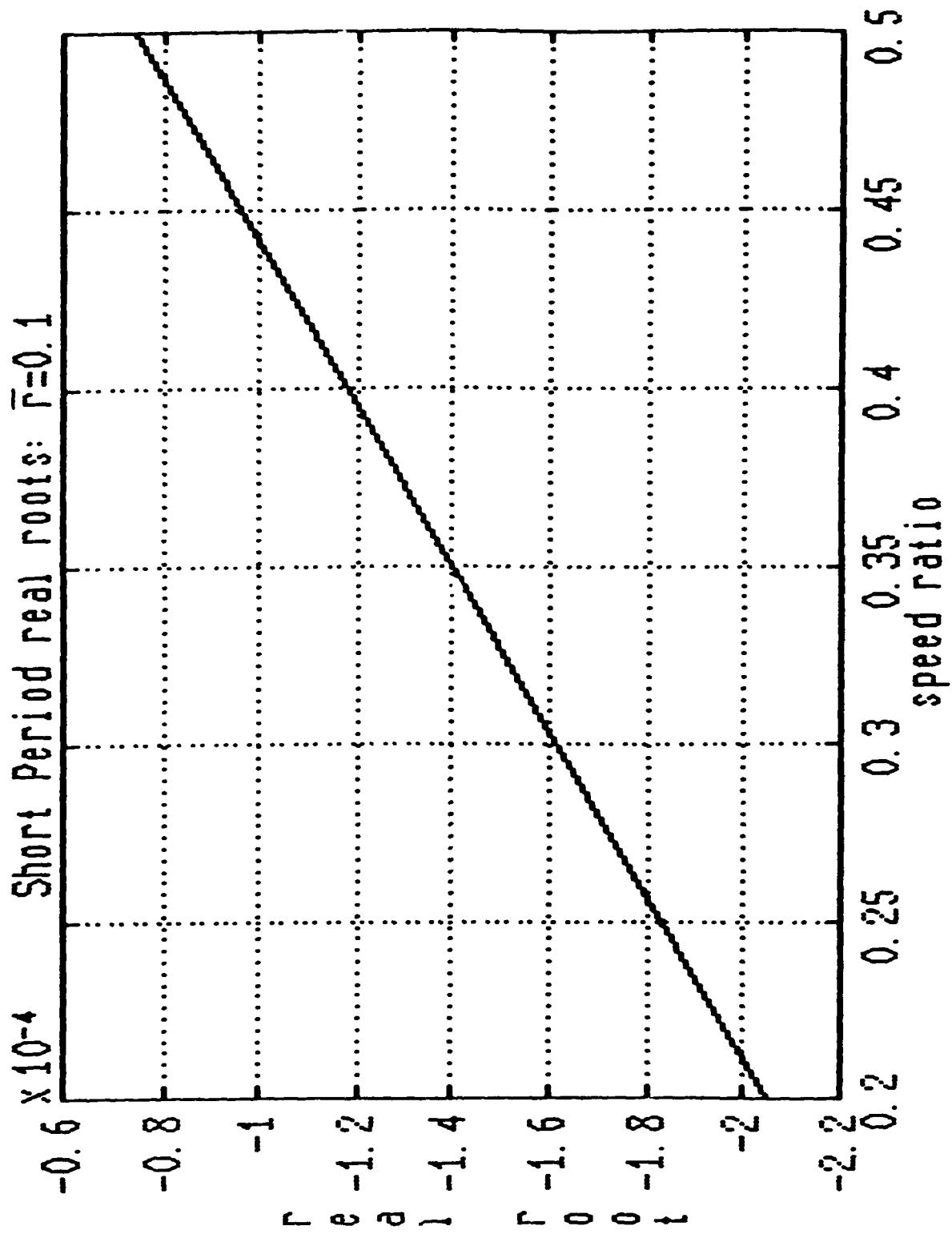


FIG. 37. - FLIGHT ON MINOR CIRCLES

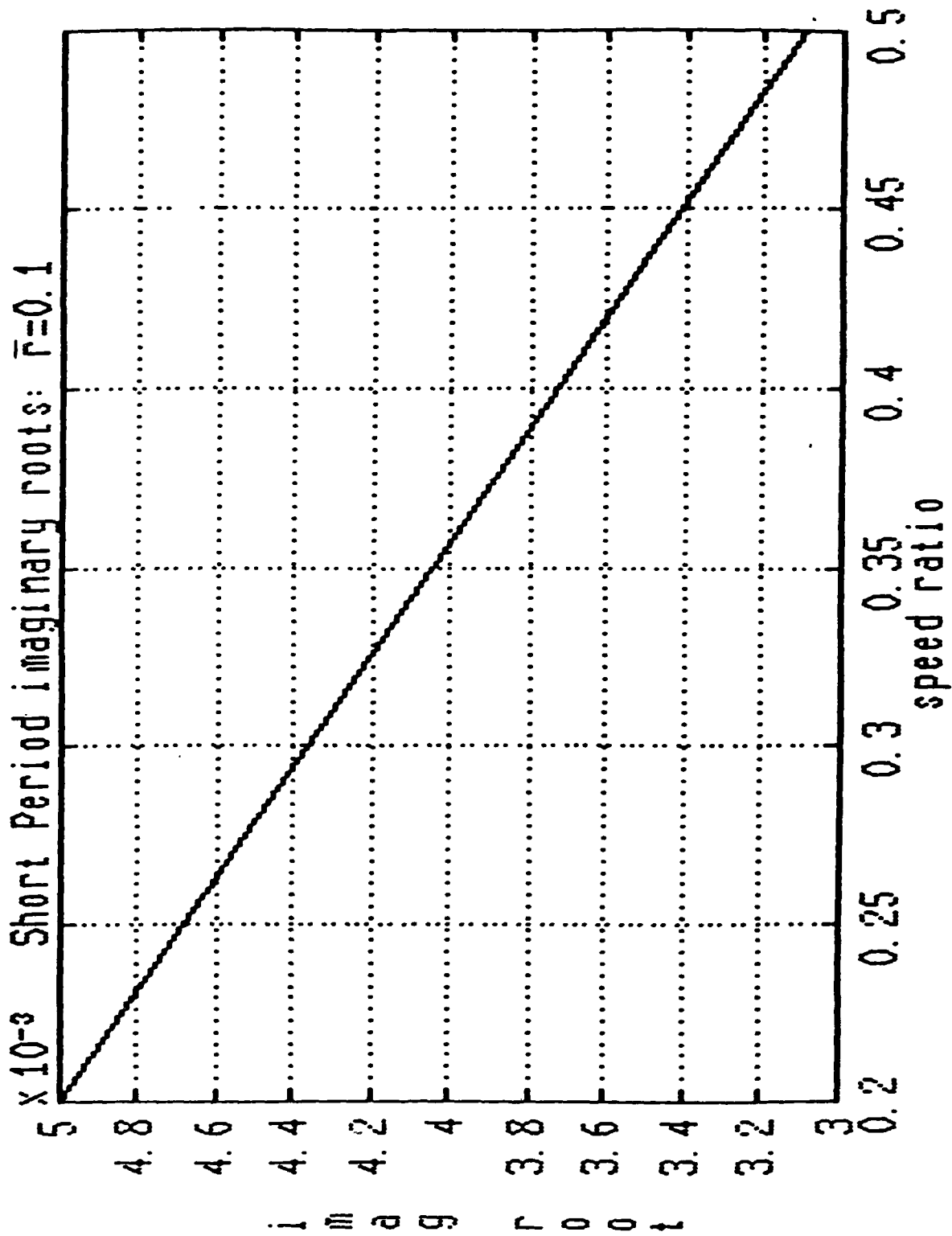
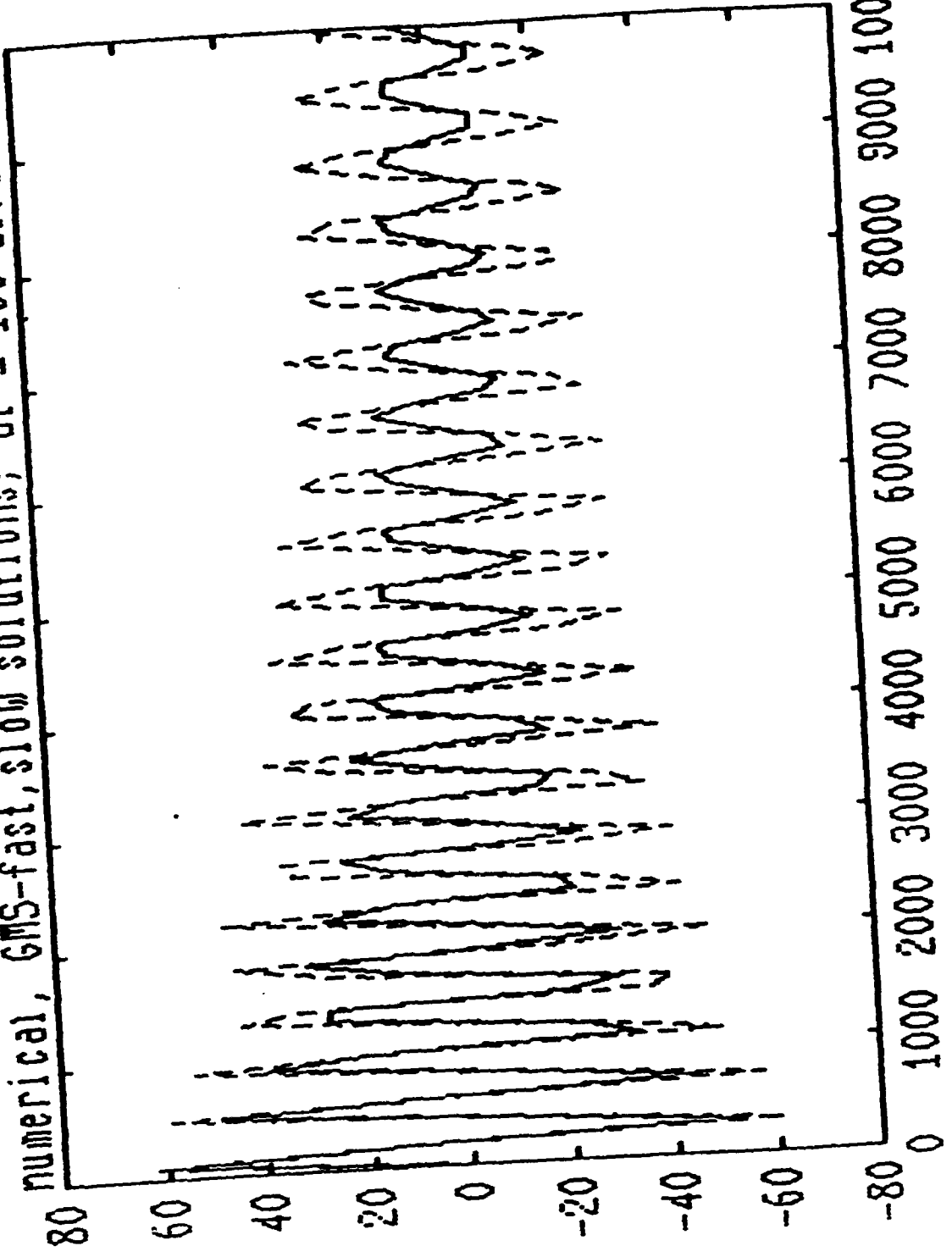


FIG. 20. CIRCUIT ON WING AIRFOIL

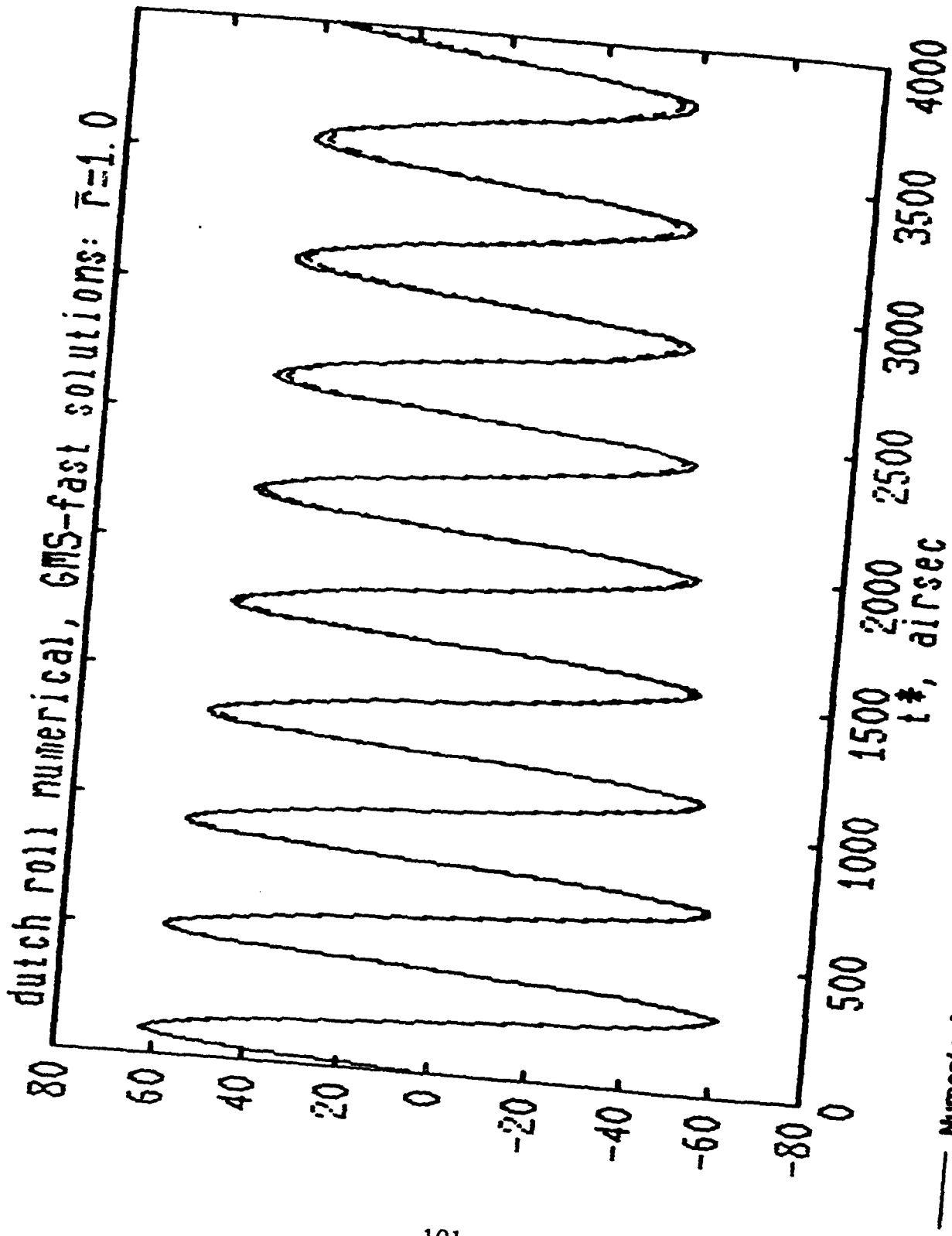
numerical, GMS-fast, slow solutions; dt = 100 airsec



100

— Numerical  
-- GMS

Fig. 39. - NUMERICAL INSTABILITY. NITOU CASE. CASE NO. 10000



P19. 40. - FLIGHT ON MINOR CIRCLES

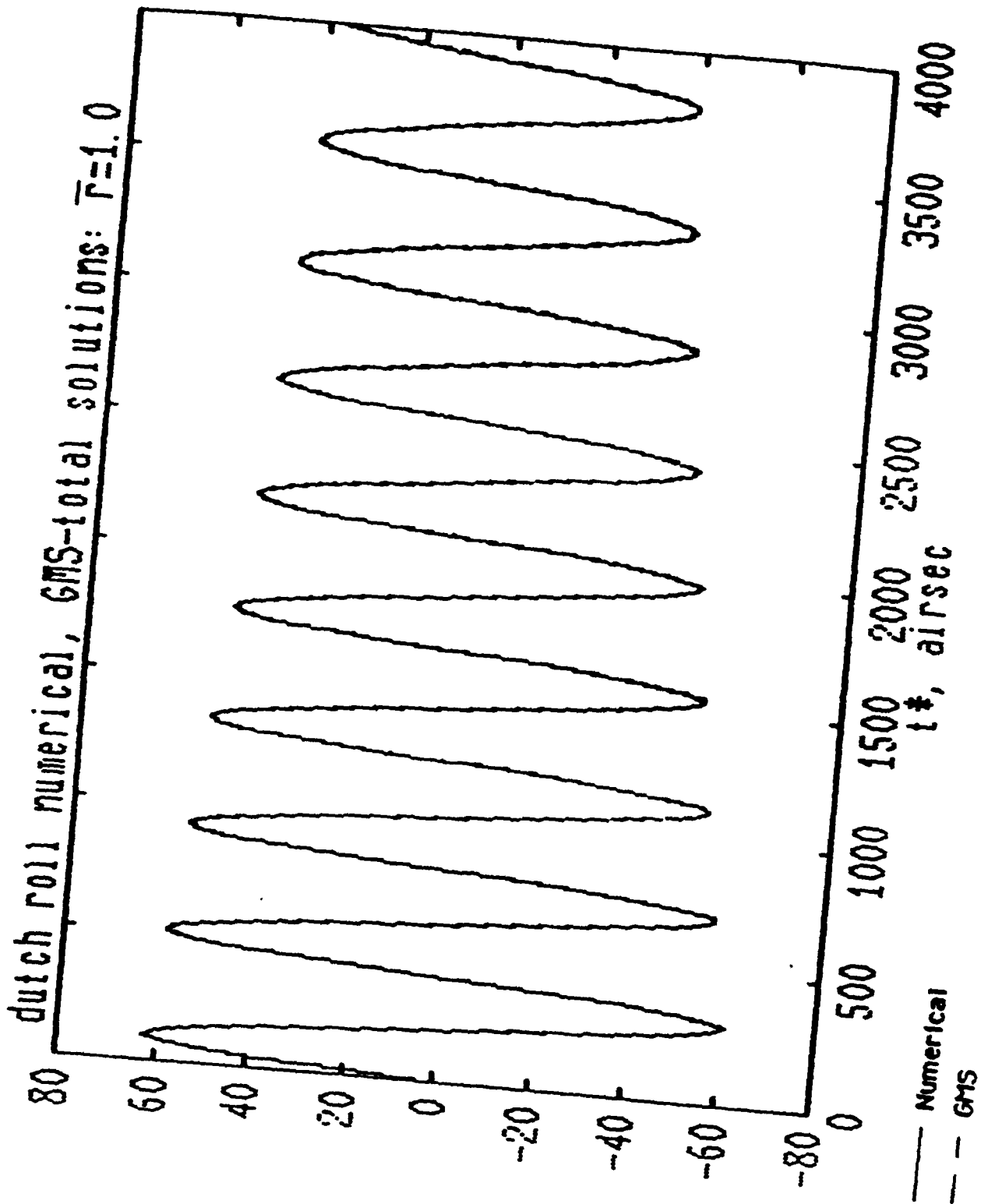


Fig. 41. - FLIGHT ON MINOR CIRCLES

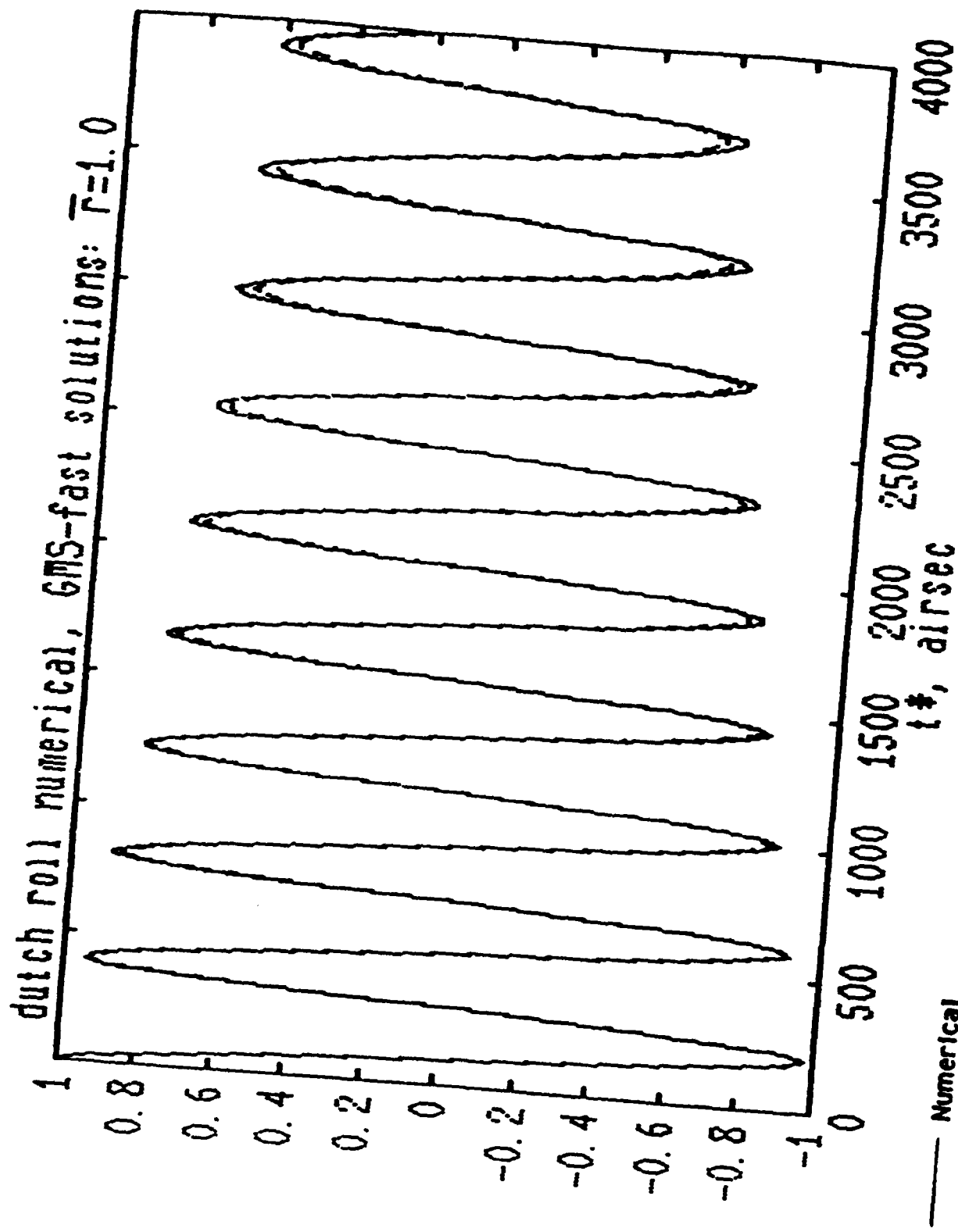


Fig. 42. - FLIGHT ON MINOR CIRCLES

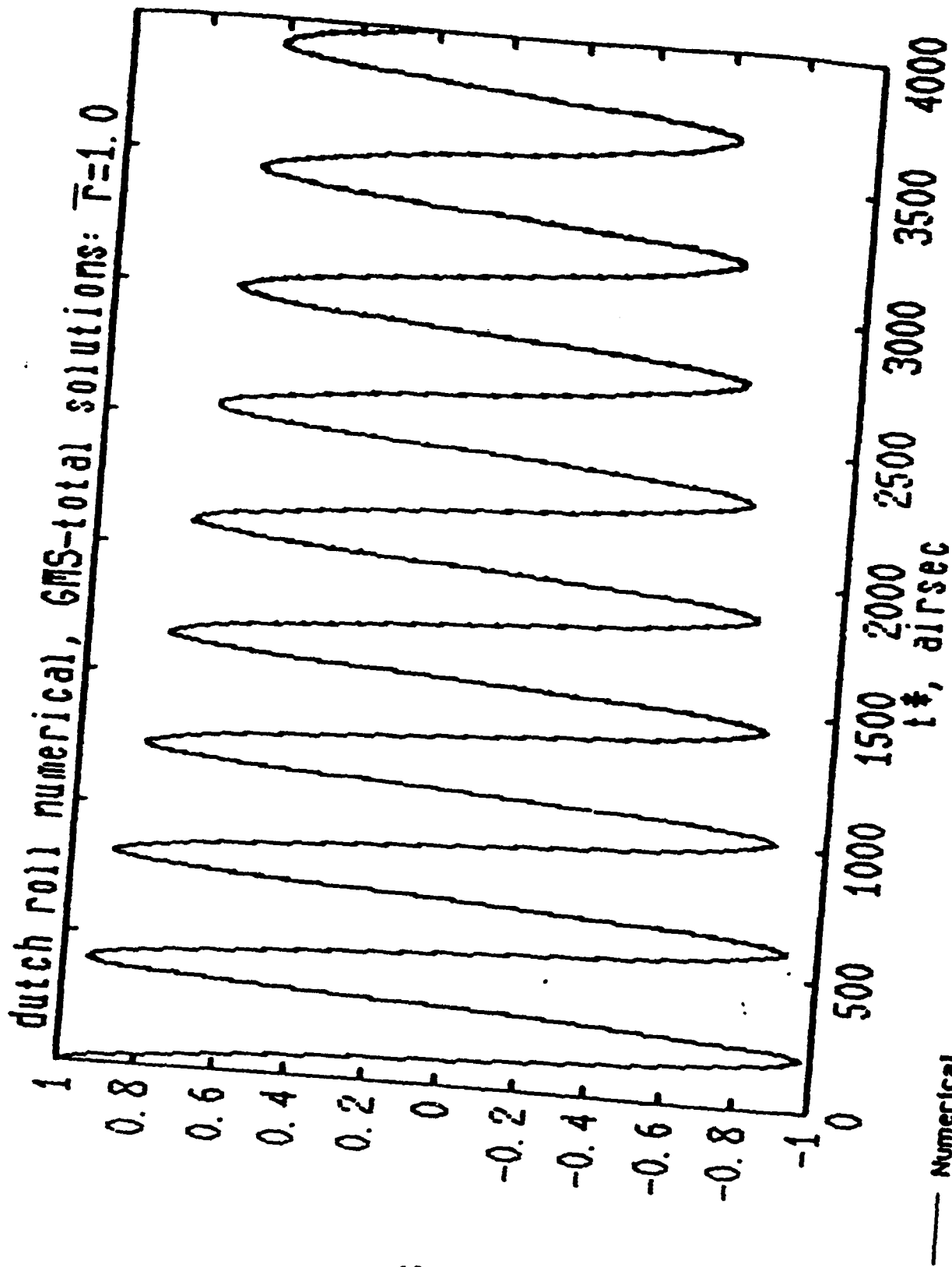


FIG. 43. - FLIGHT ON MINOR CIRCLES

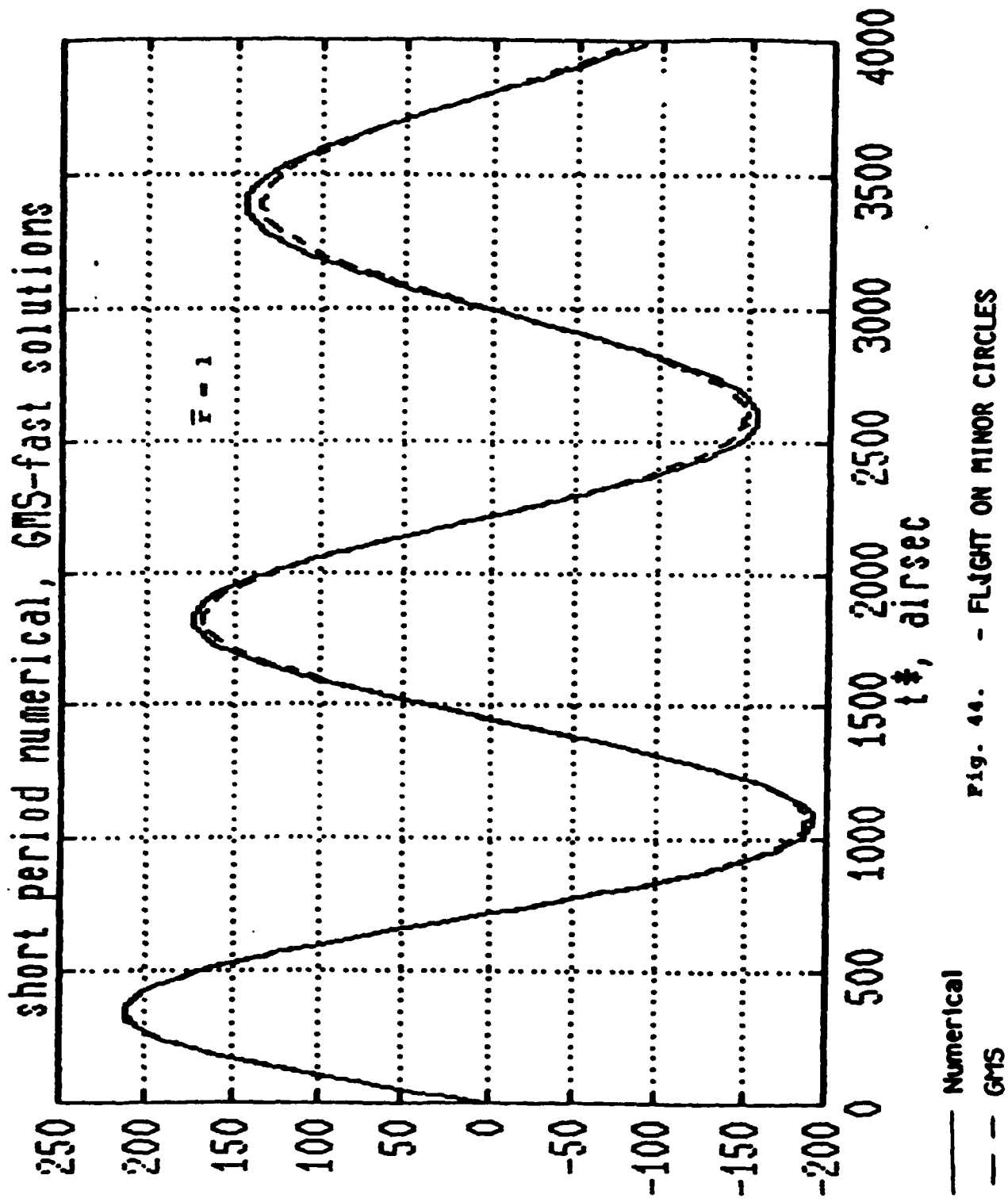


Fig. 44. - FLIGHT ON MINOR CIRCLES

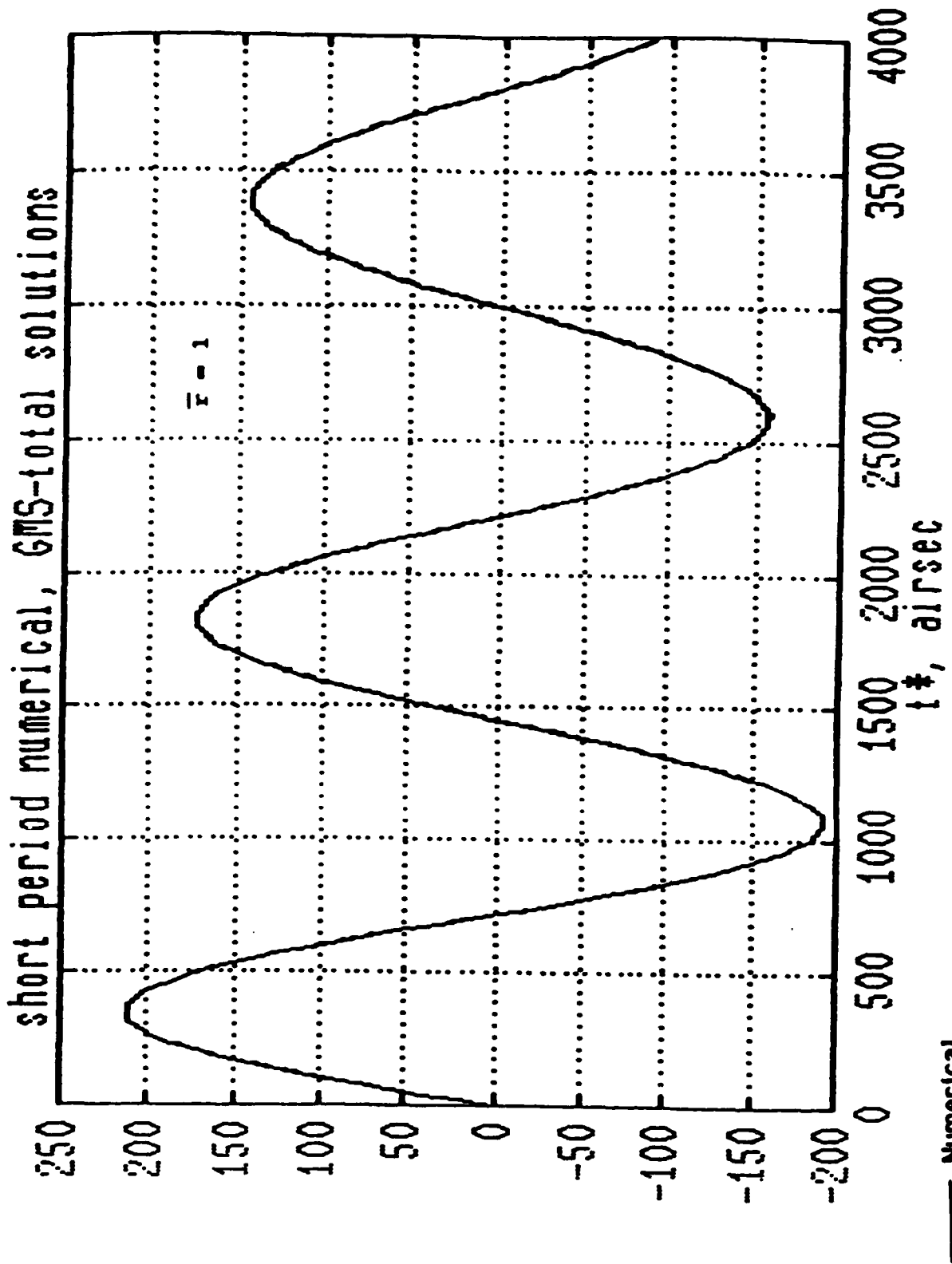


Fig. 45. - FLIGHT ON MINOR CIRCLES

dutch roll numerical, GMS-fast solutions:  $\bar{r}=0.1$

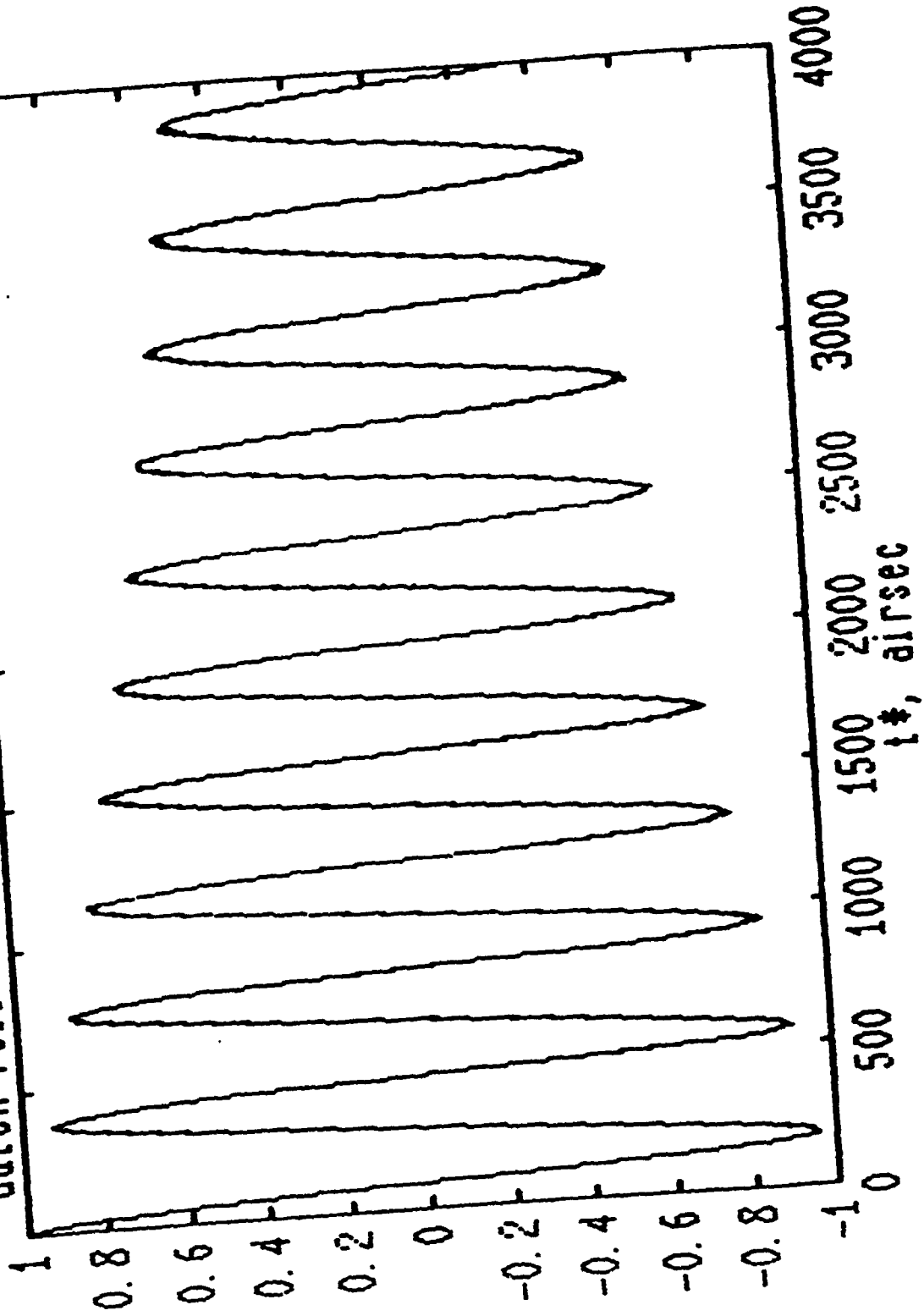


Fig. 46. - FLIGHT ON MINOR CIRCLES

— Numerical  
-- GMS

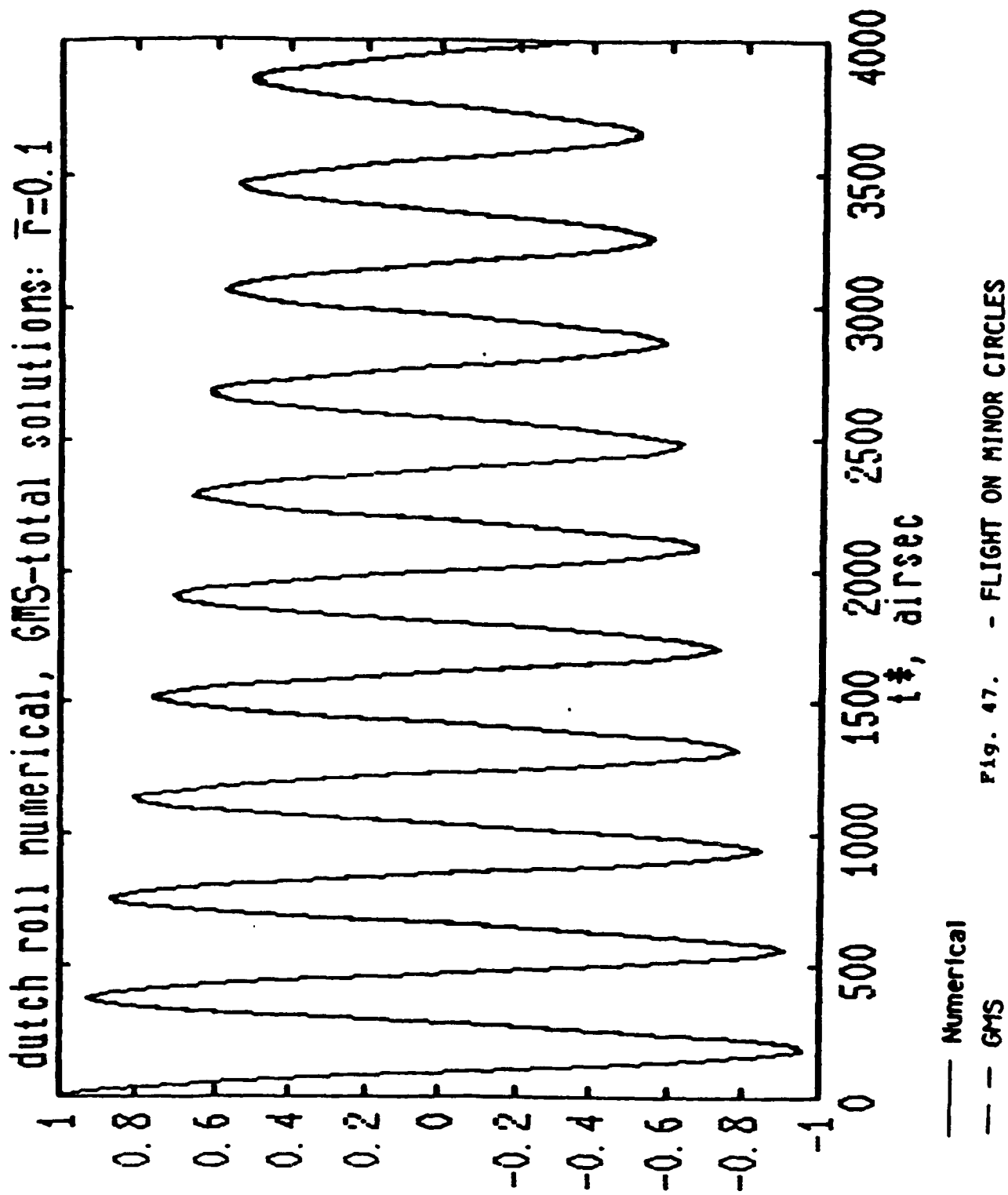


FIG. 47. - FLIGHT ON MINOR CIRCLES

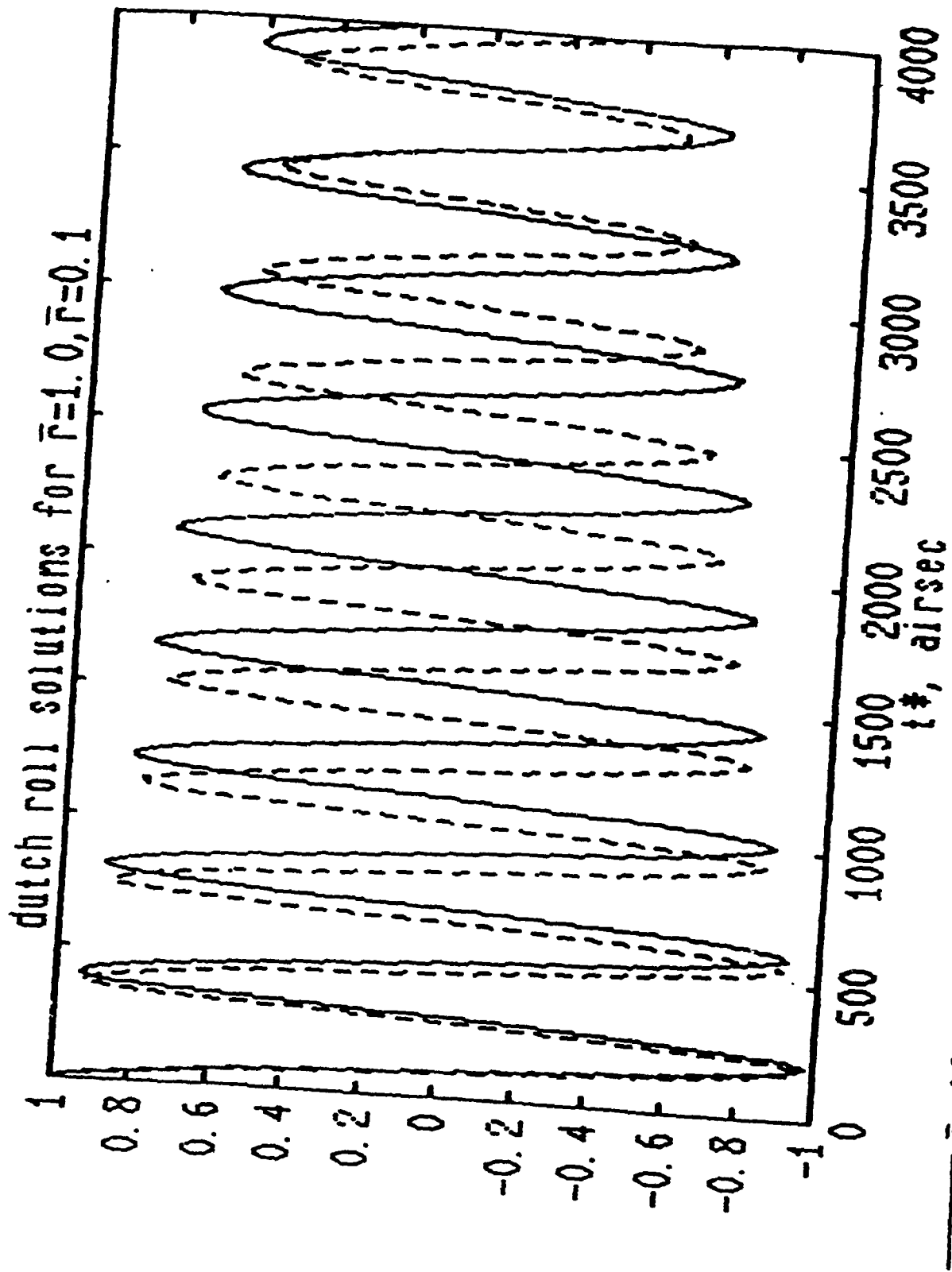


Fig. 48. - FLIGHT ON MINOR CIRCLES

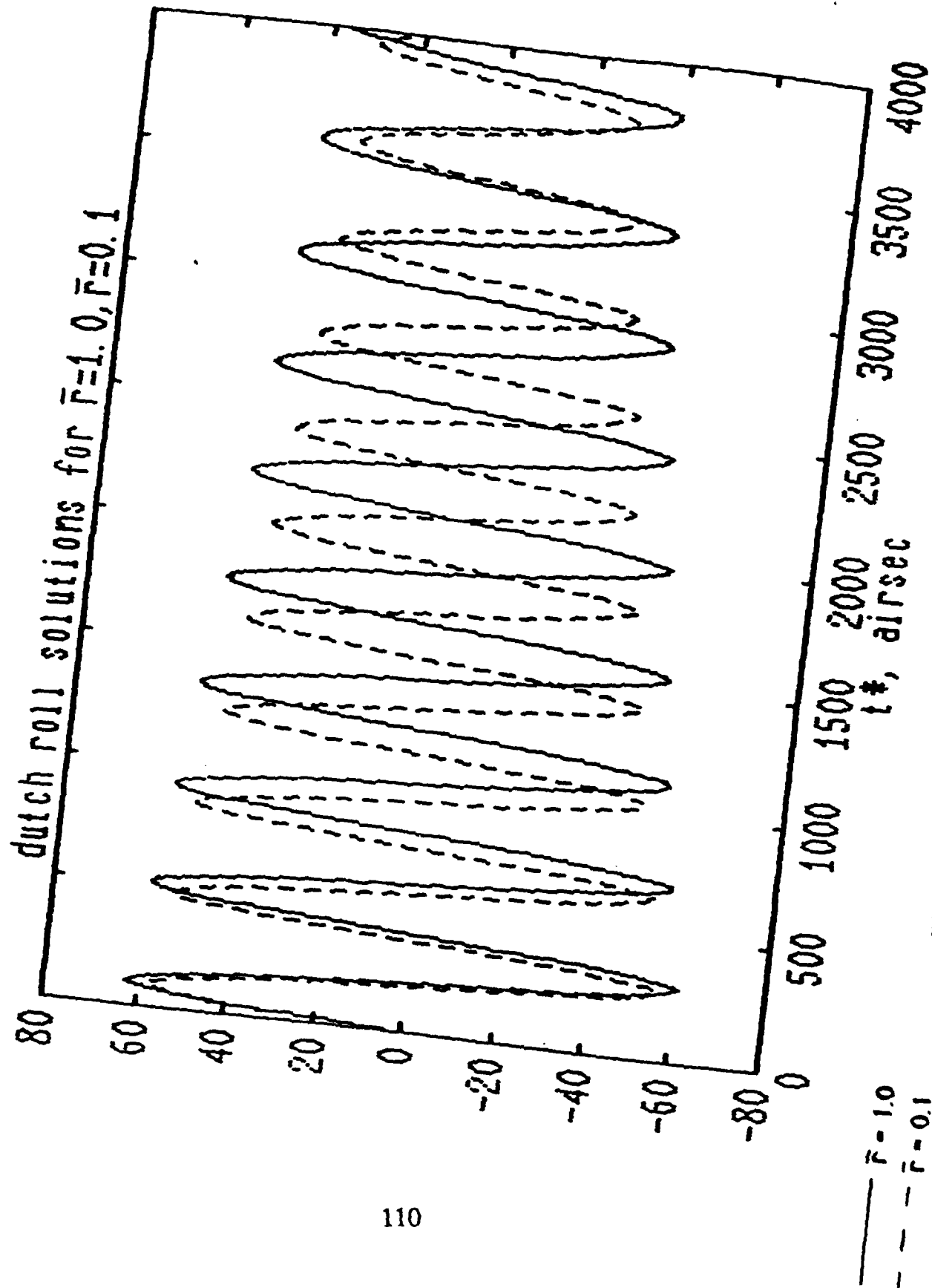


Fig. 49. - FLIGHT ON MINOR CIRCLES

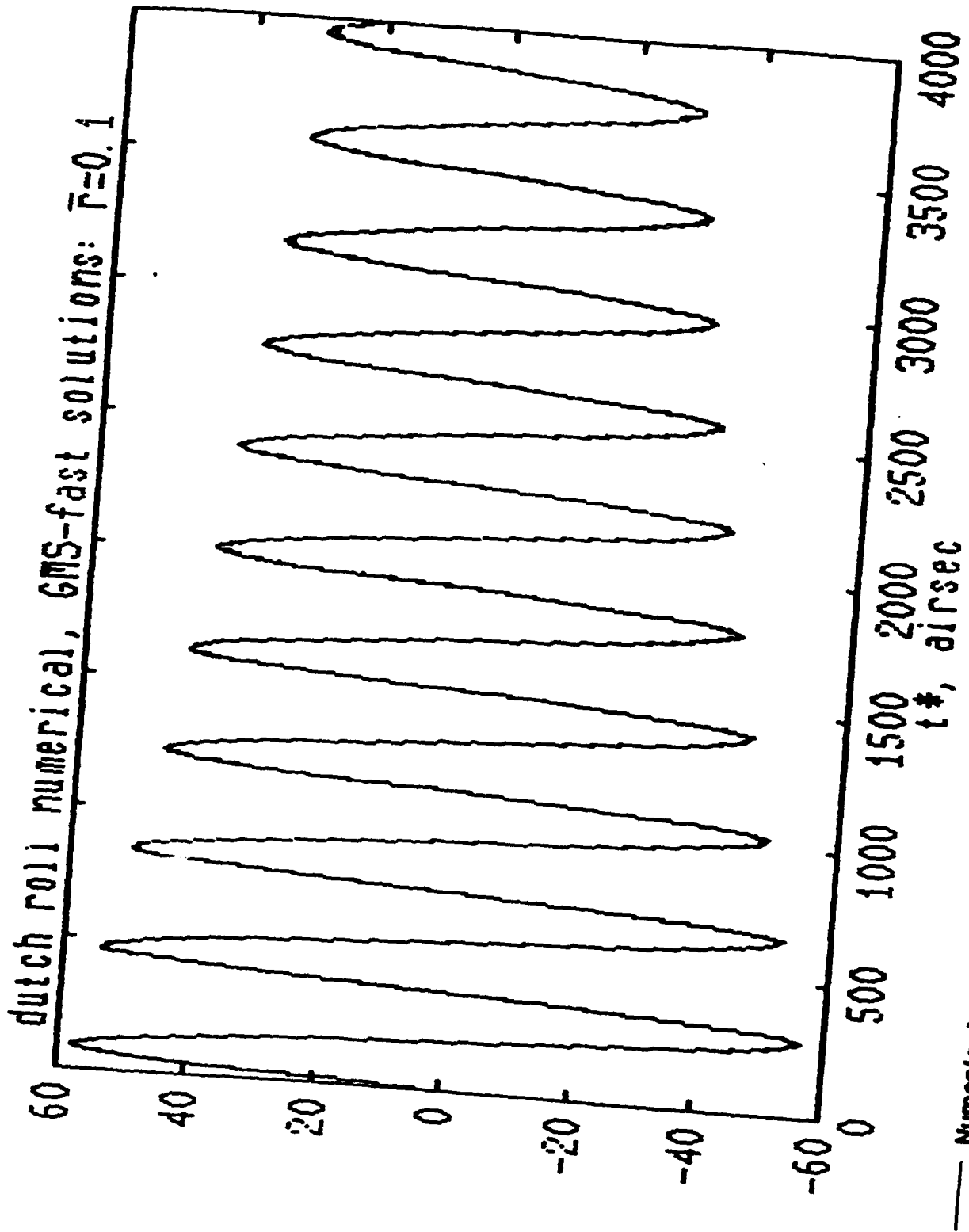
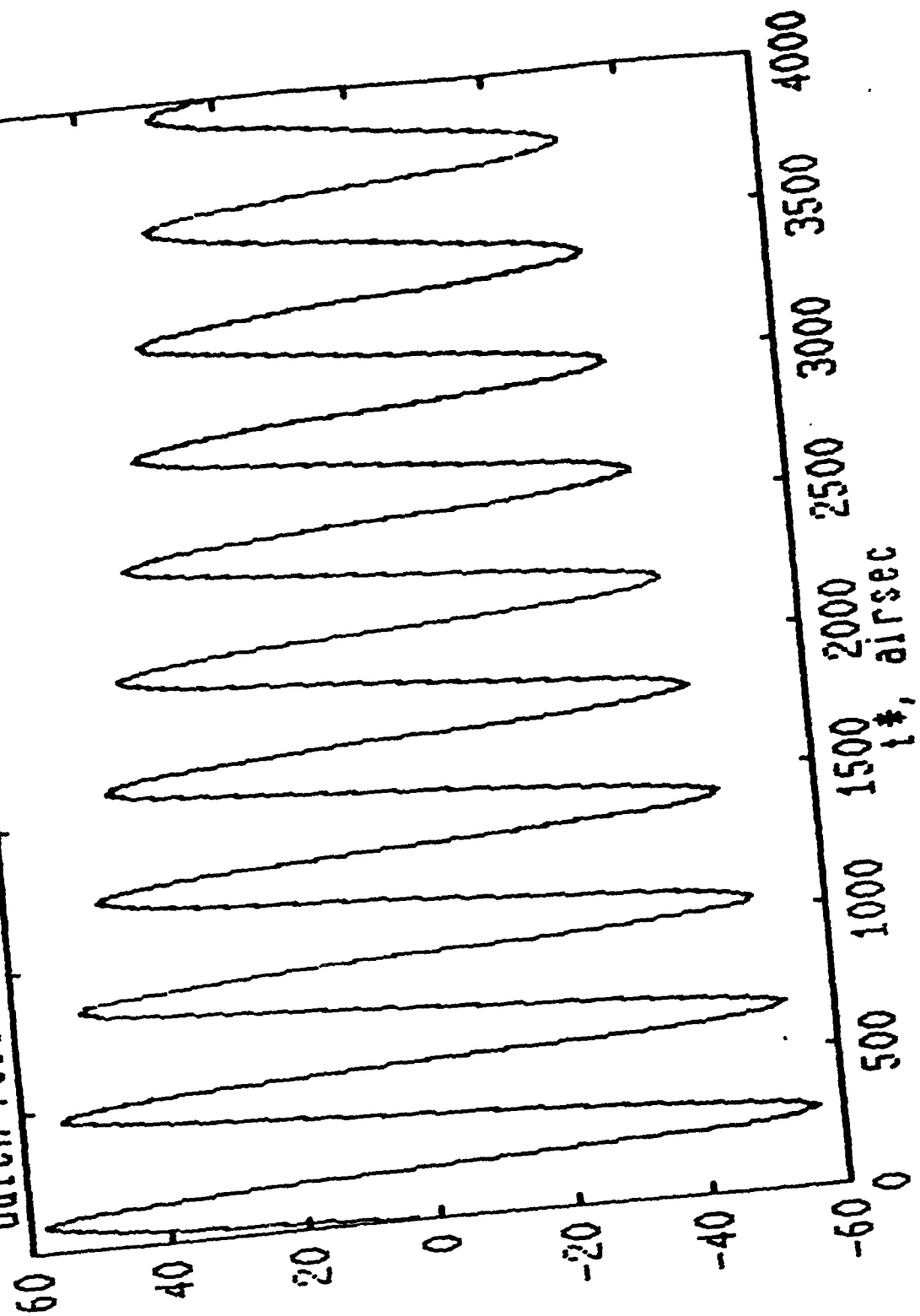


FIG. 10 - FLIGHT ON STRIP

dutch roll numerical, GMS-total solutions:  $\bar{r}=0.1$



— Numerical

- FLIGHT ON MINOR CIRCLES

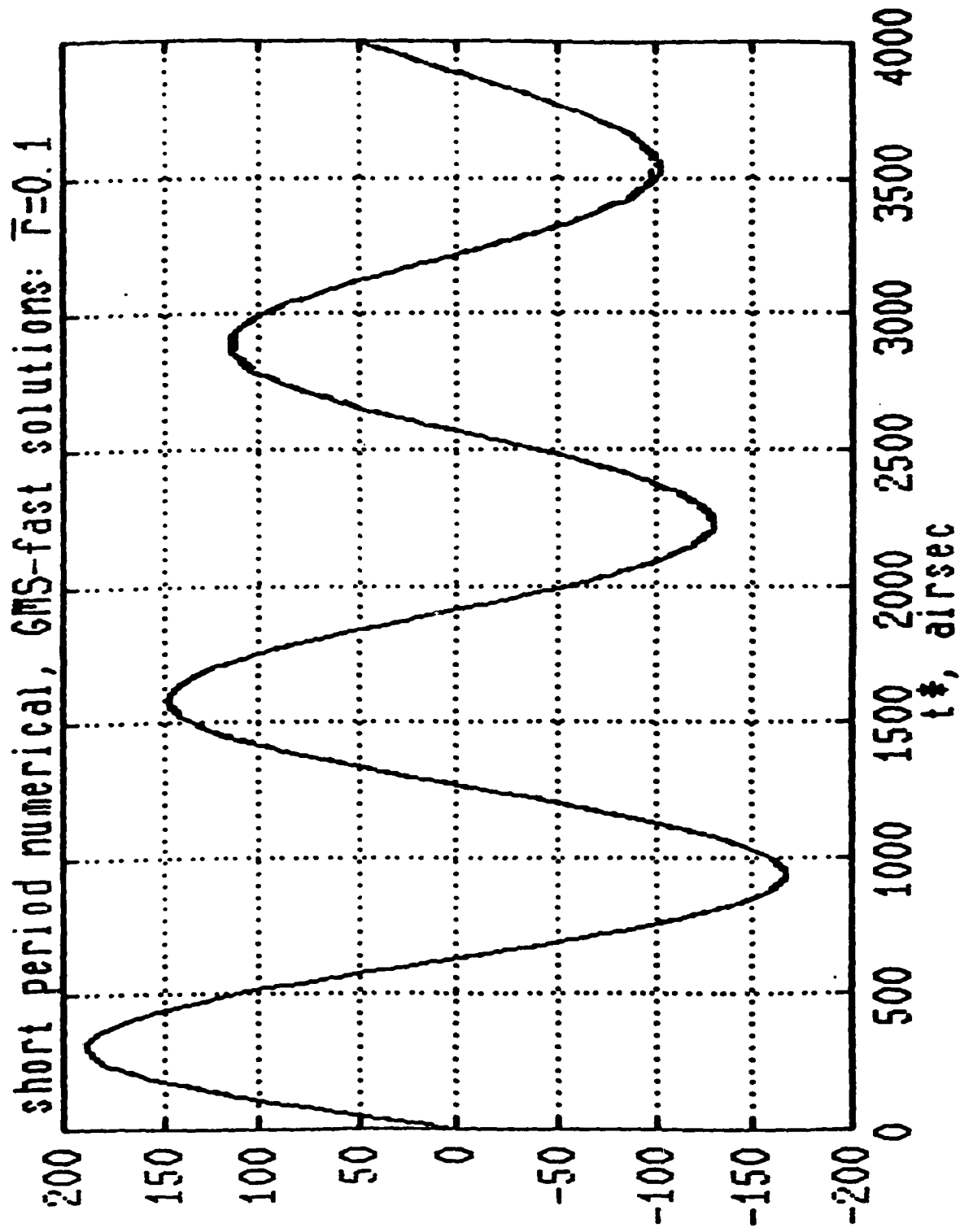


FIG. 52. - FLIGHT ON MINOR CIRCLES

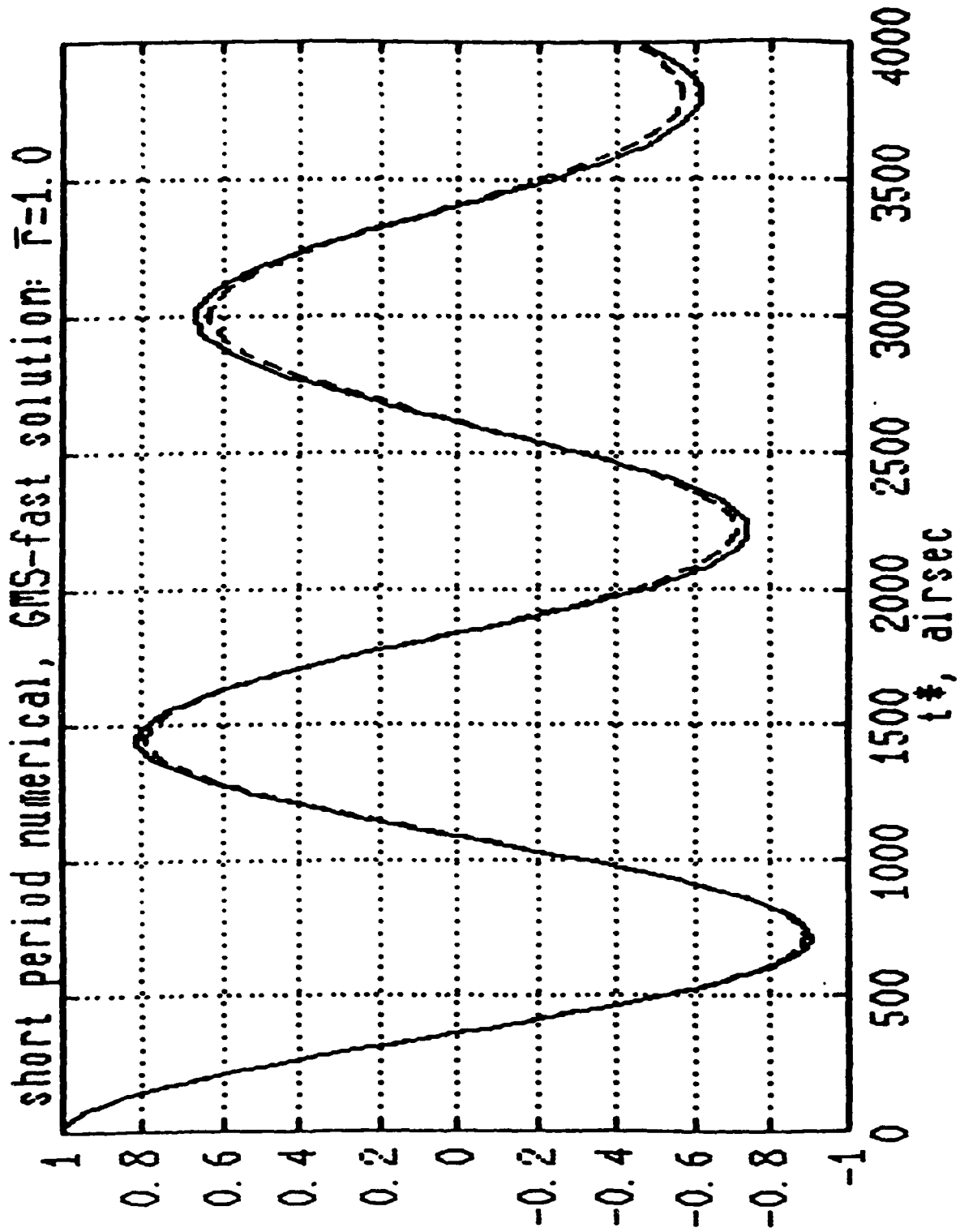


Fig. 53. - FLIGHT ON MINOR CIRCLES

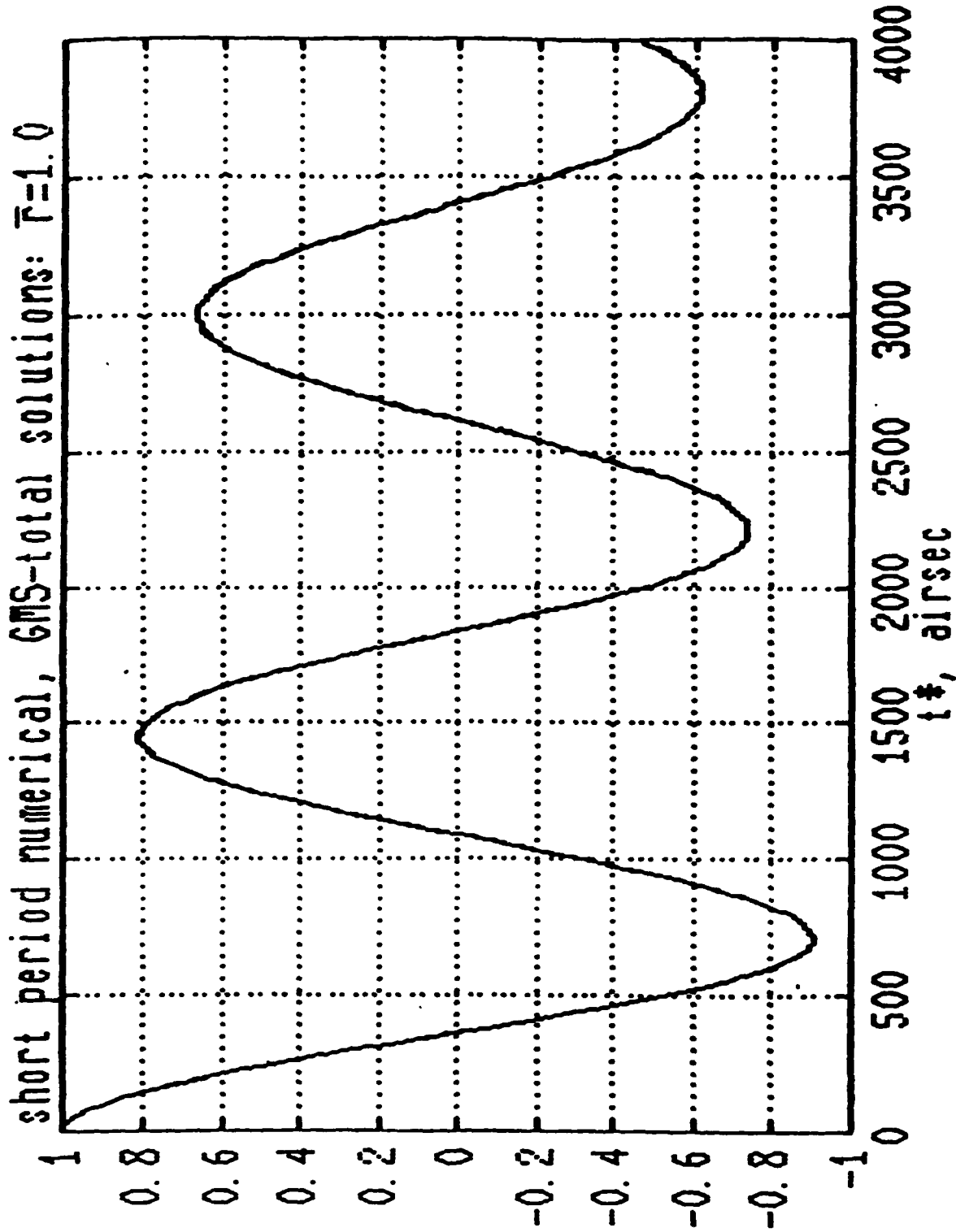


Fig. 54. - FLIGHT ON MINOR CIRCLES

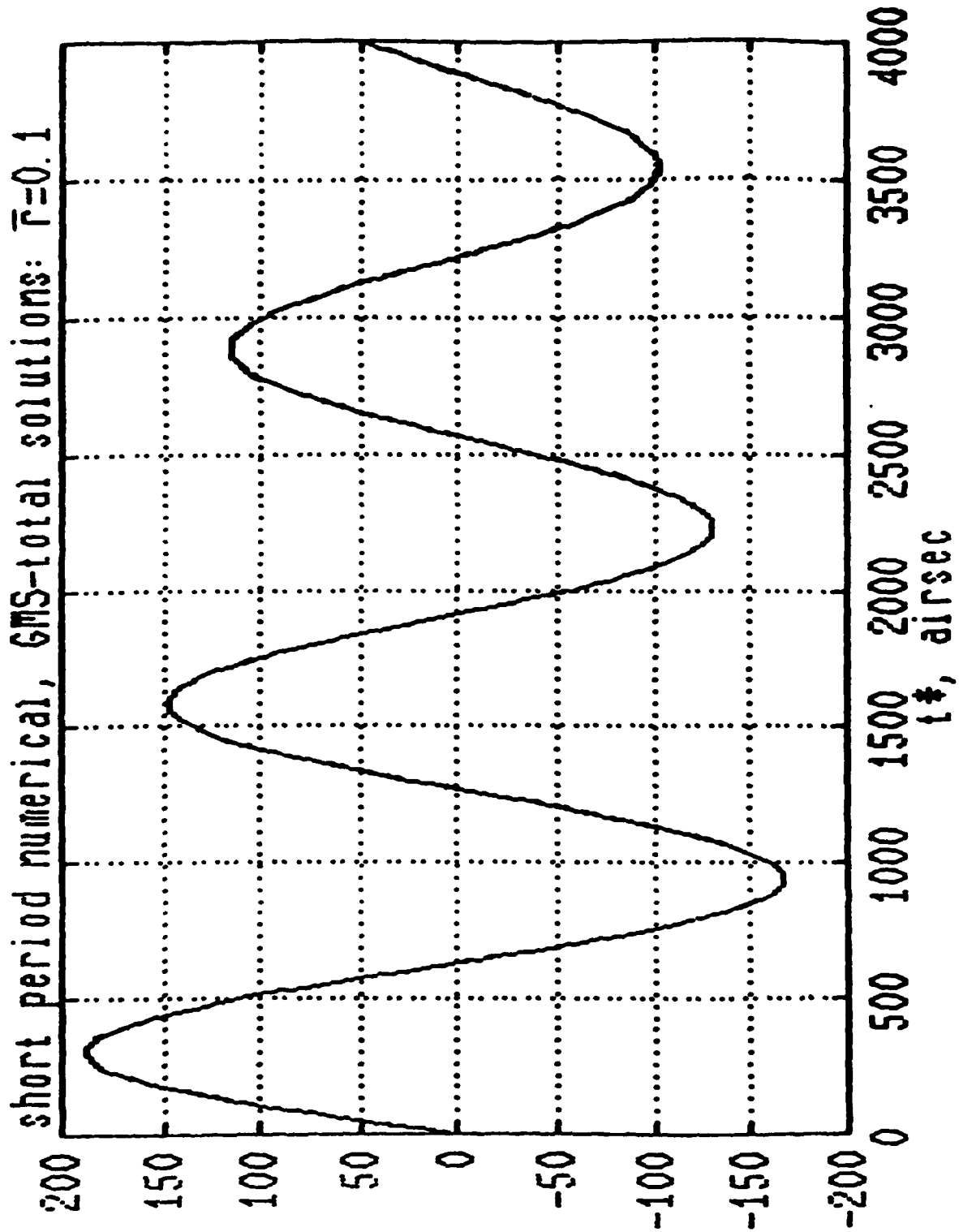


Fig. 55. - FLIGHT ON MINOR CIRCLES

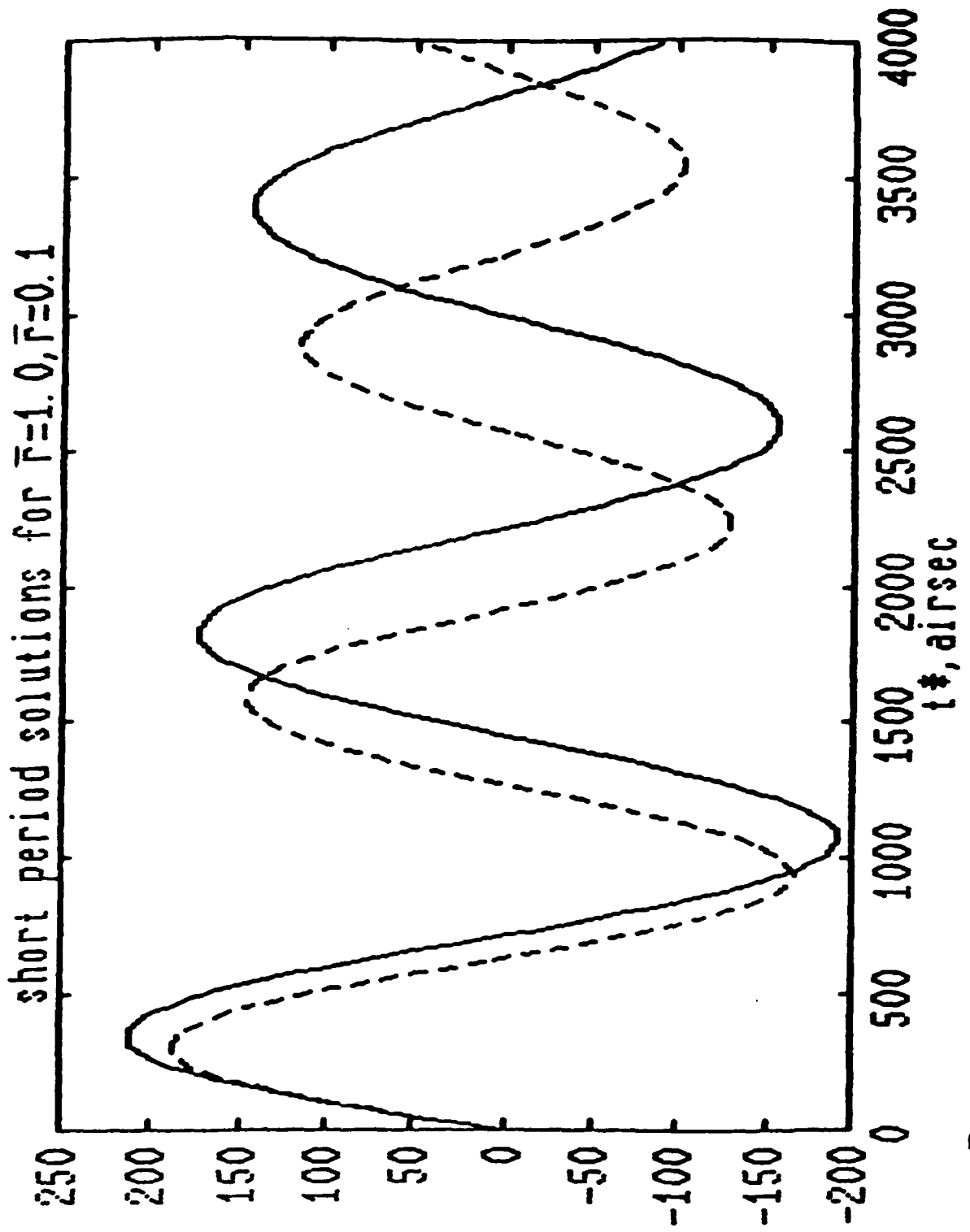
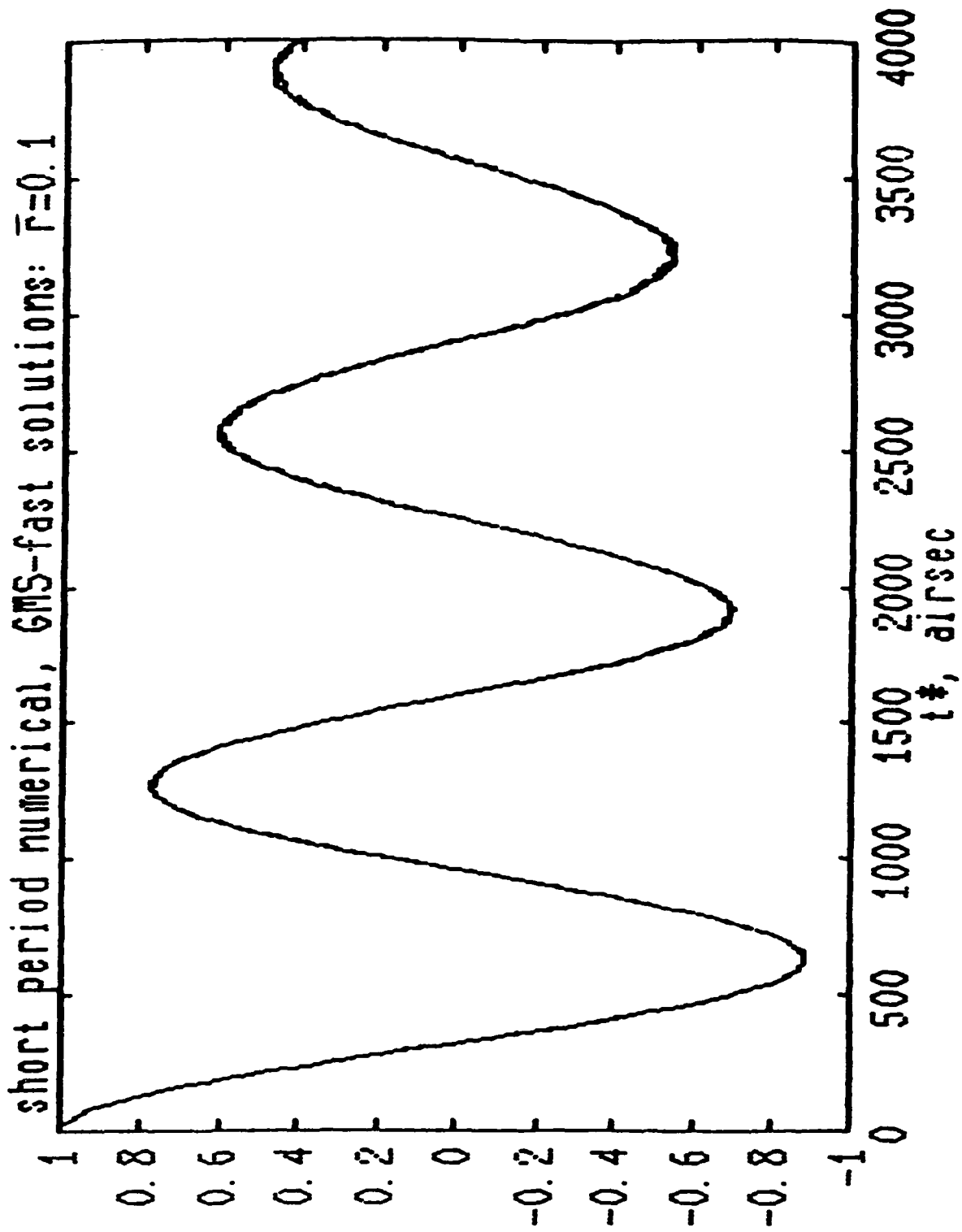


Fig. 56. - FLIGHT ON MINOR CIRCLES



— Numerical  
 - - GMS  
 Fig. 57. - FLIGHT ON MINOR CIRCLES

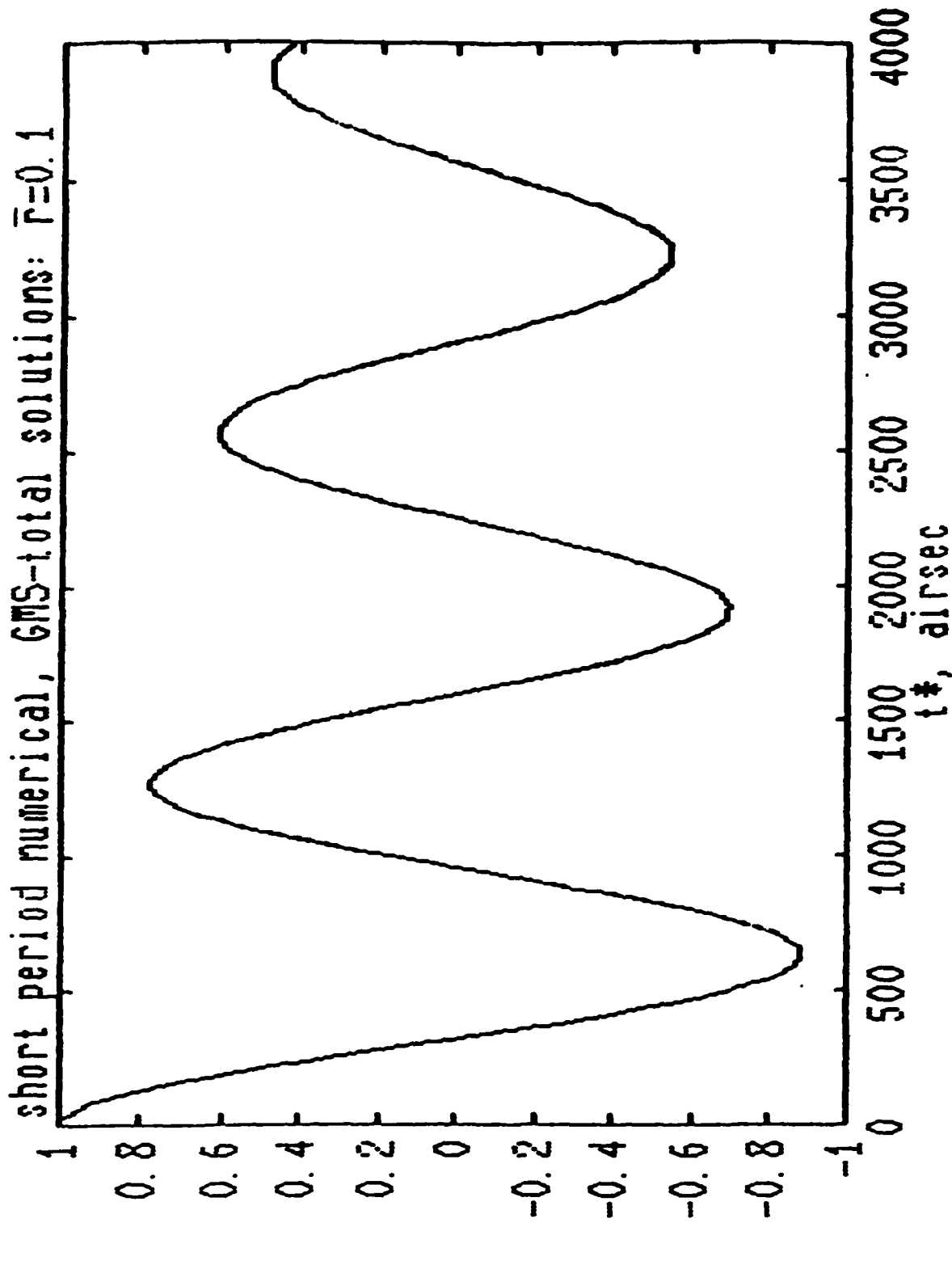
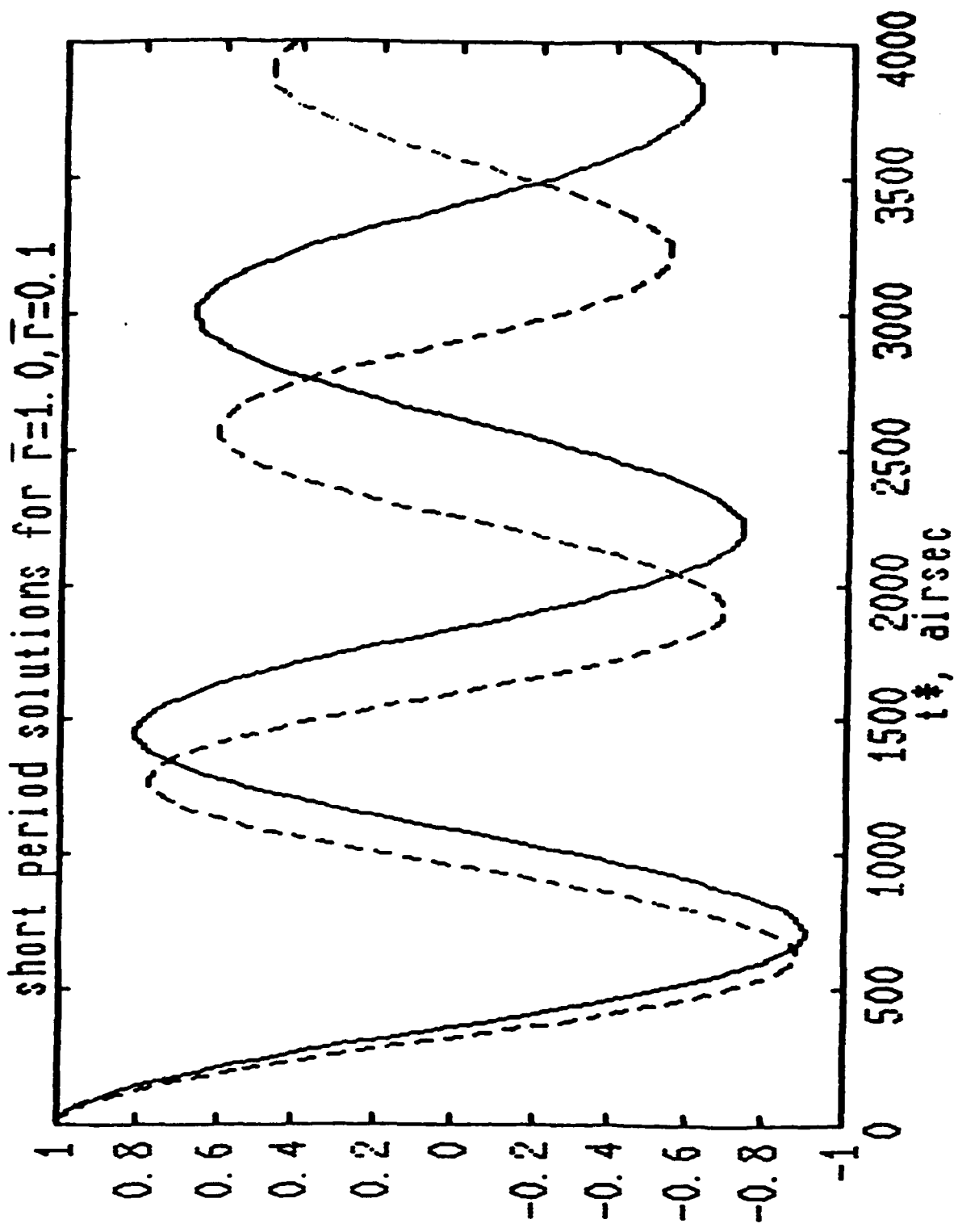


FIG. 58. - FLIGHT ON MINOR CIRCLES



—  $\bar{r} = 1.0$   
 - - -  $\bar{r} = 0.1$

Fig. 59. - FLIGHT ON MINOR CIRCLES

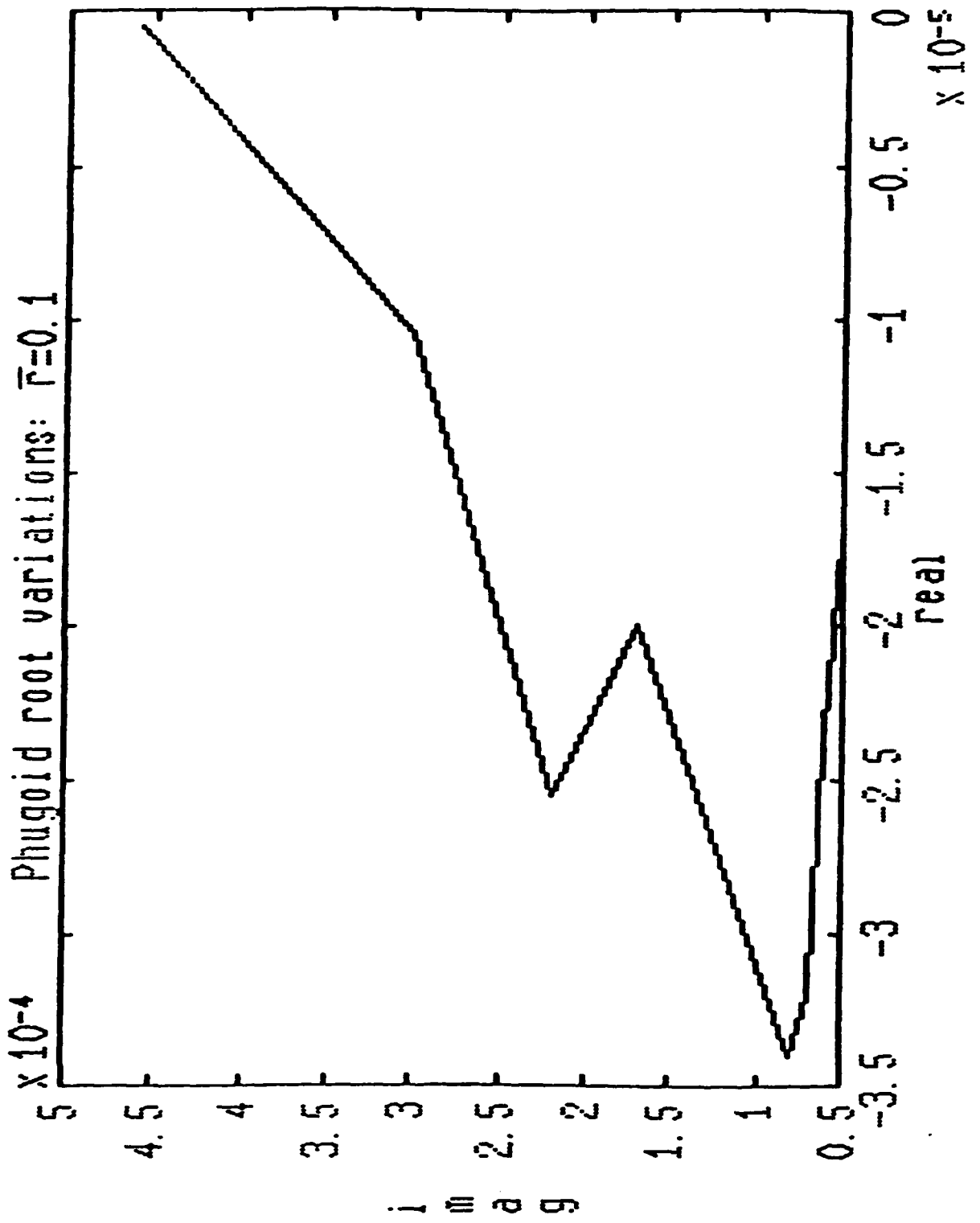


Fig. 60. - FLIGHT ON MINOR CIRCLES

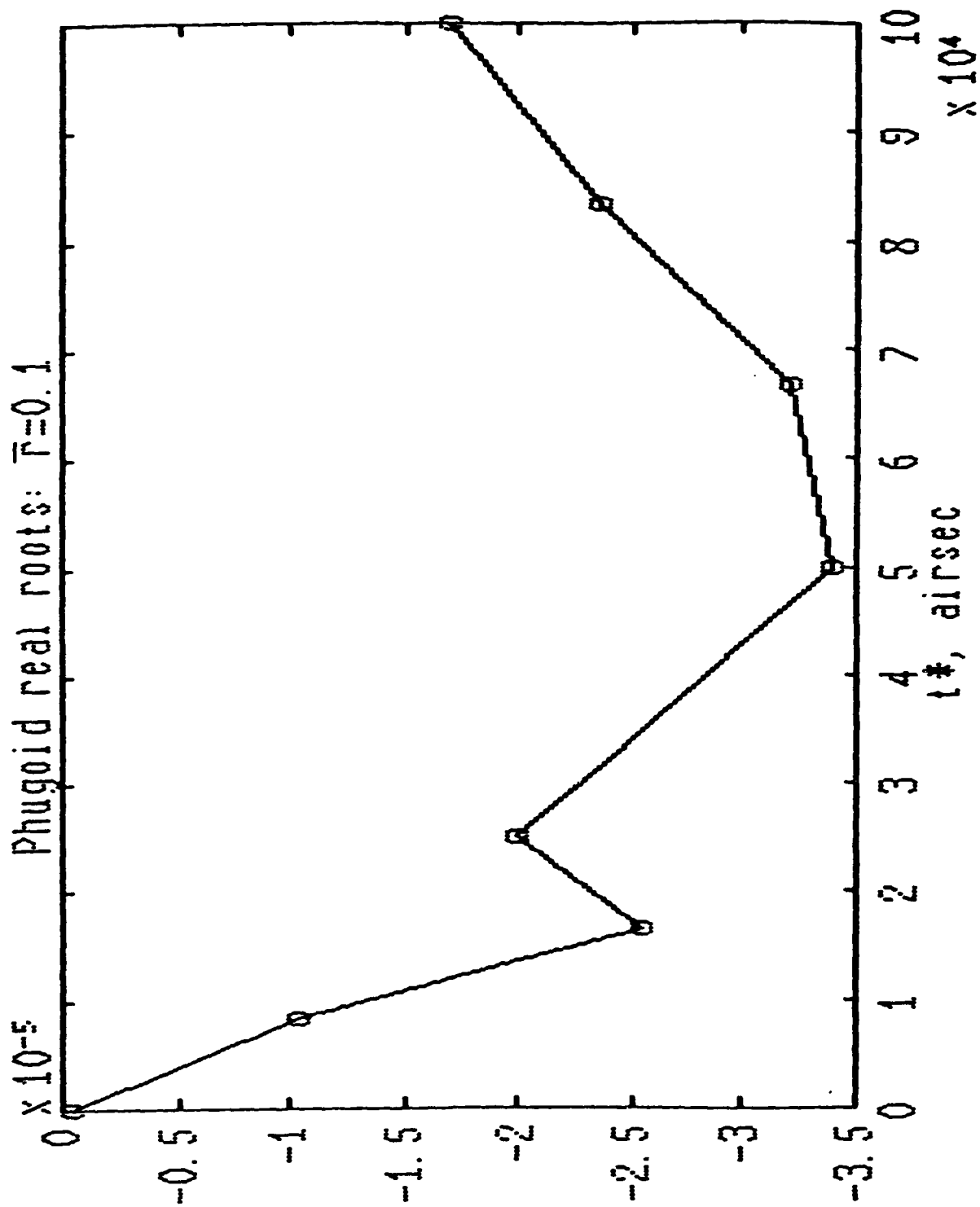


Fig. 61. - FLIGHT ON MINOR CIRCLES

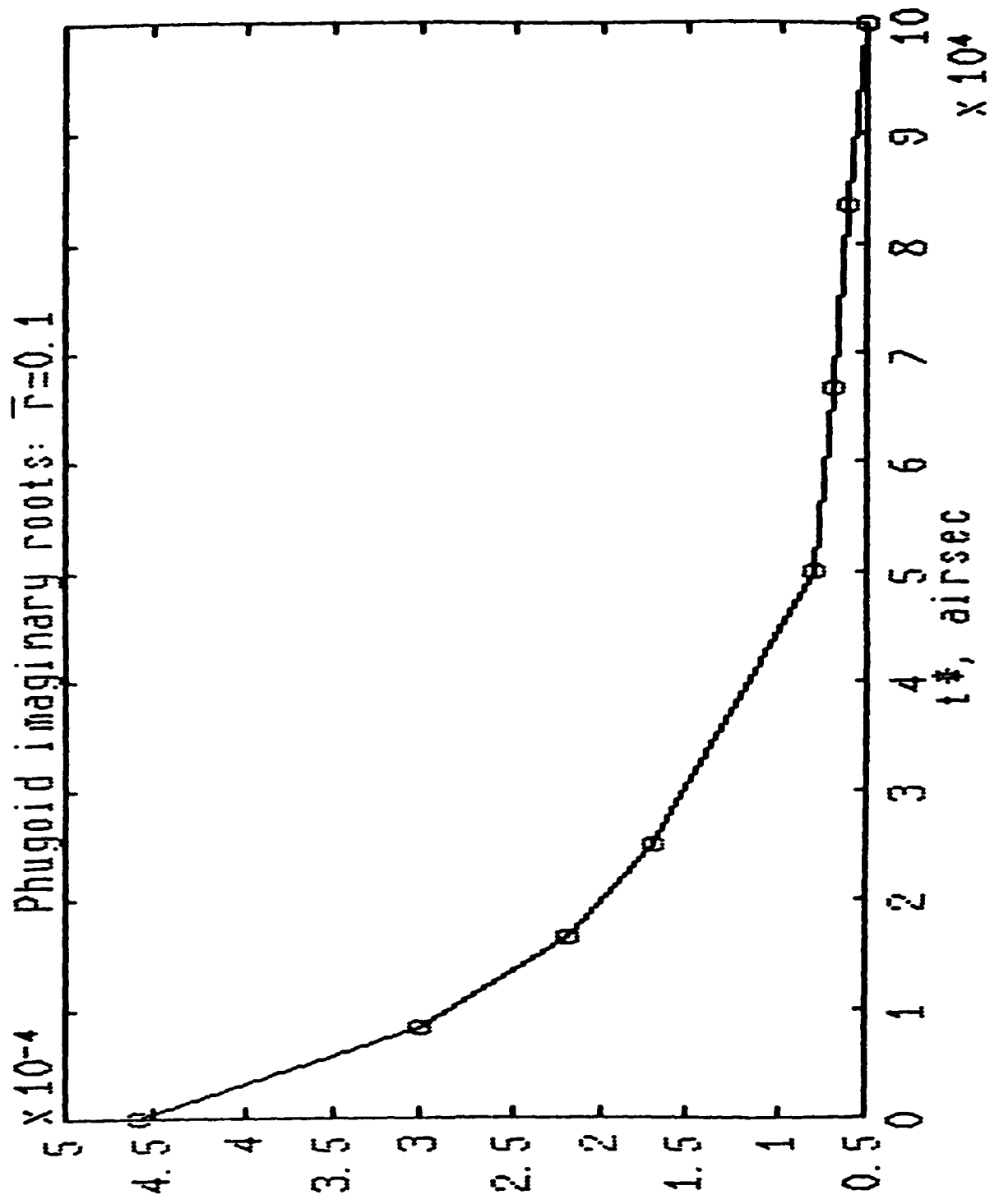


Fig. 62. - FLIGHT ON MINOR CIRCLES

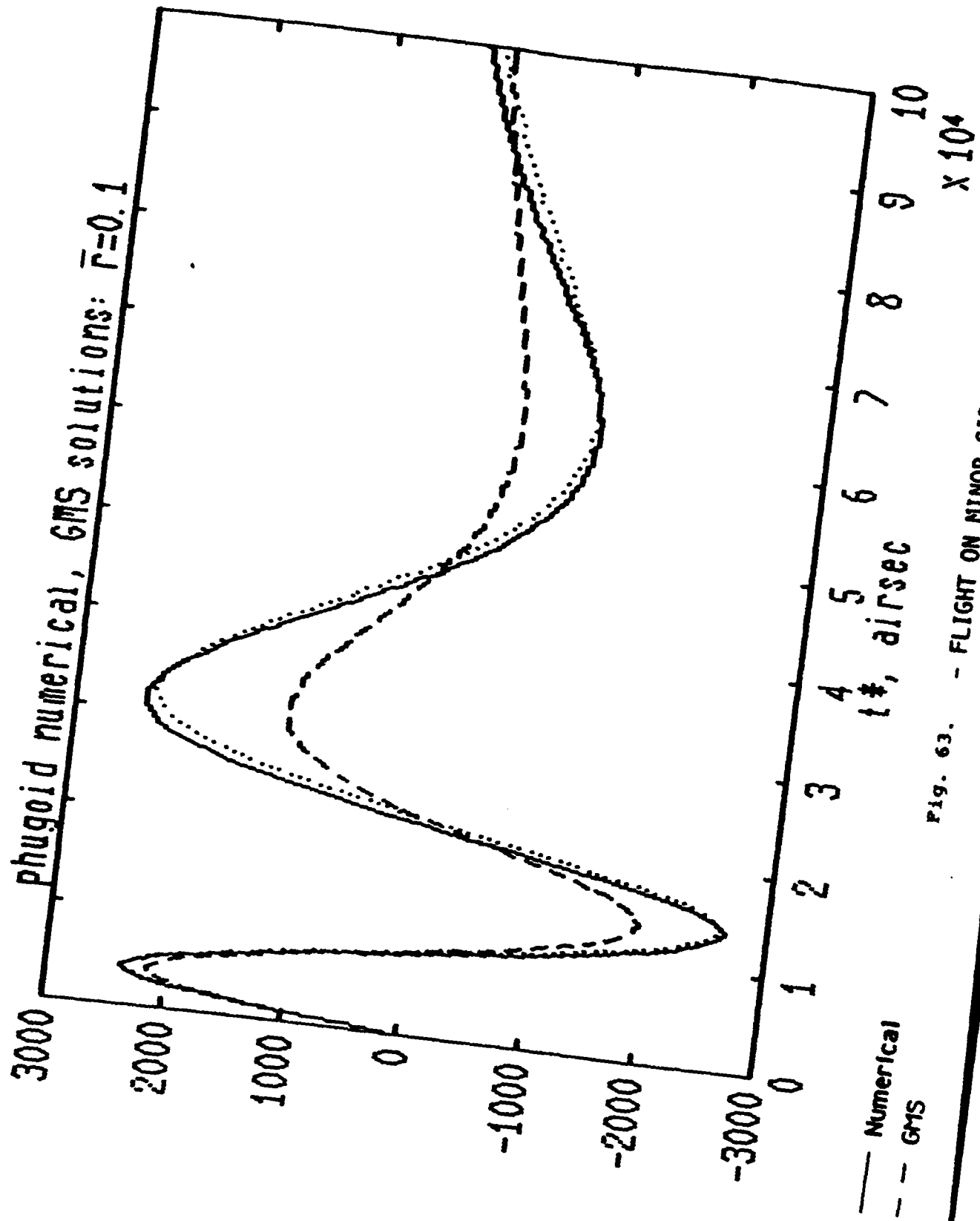


Fig. 63. - FLIGHT ON MINOR CIRCLES

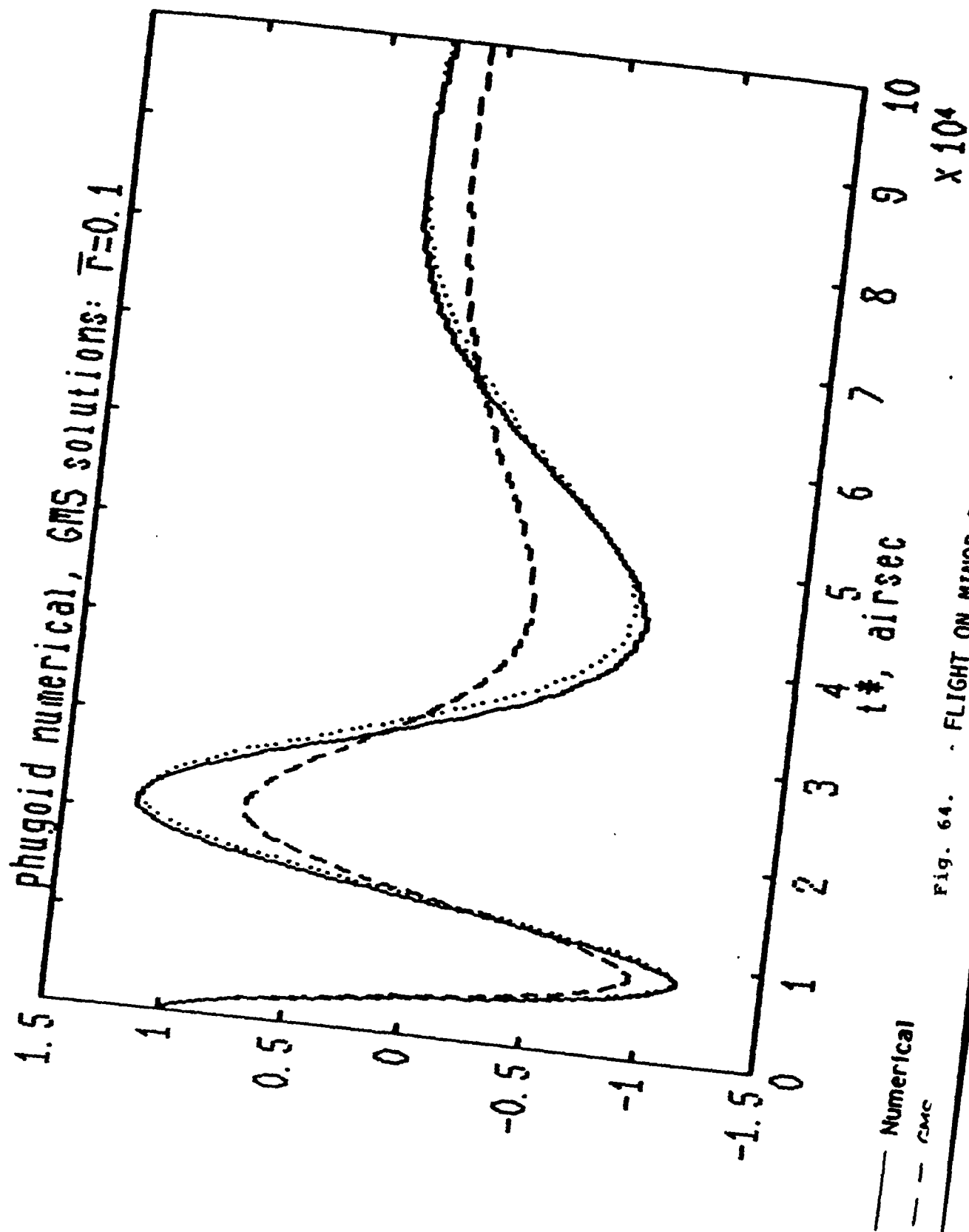


Fig. 64. FLIGHT ON MINOR CIRCLES

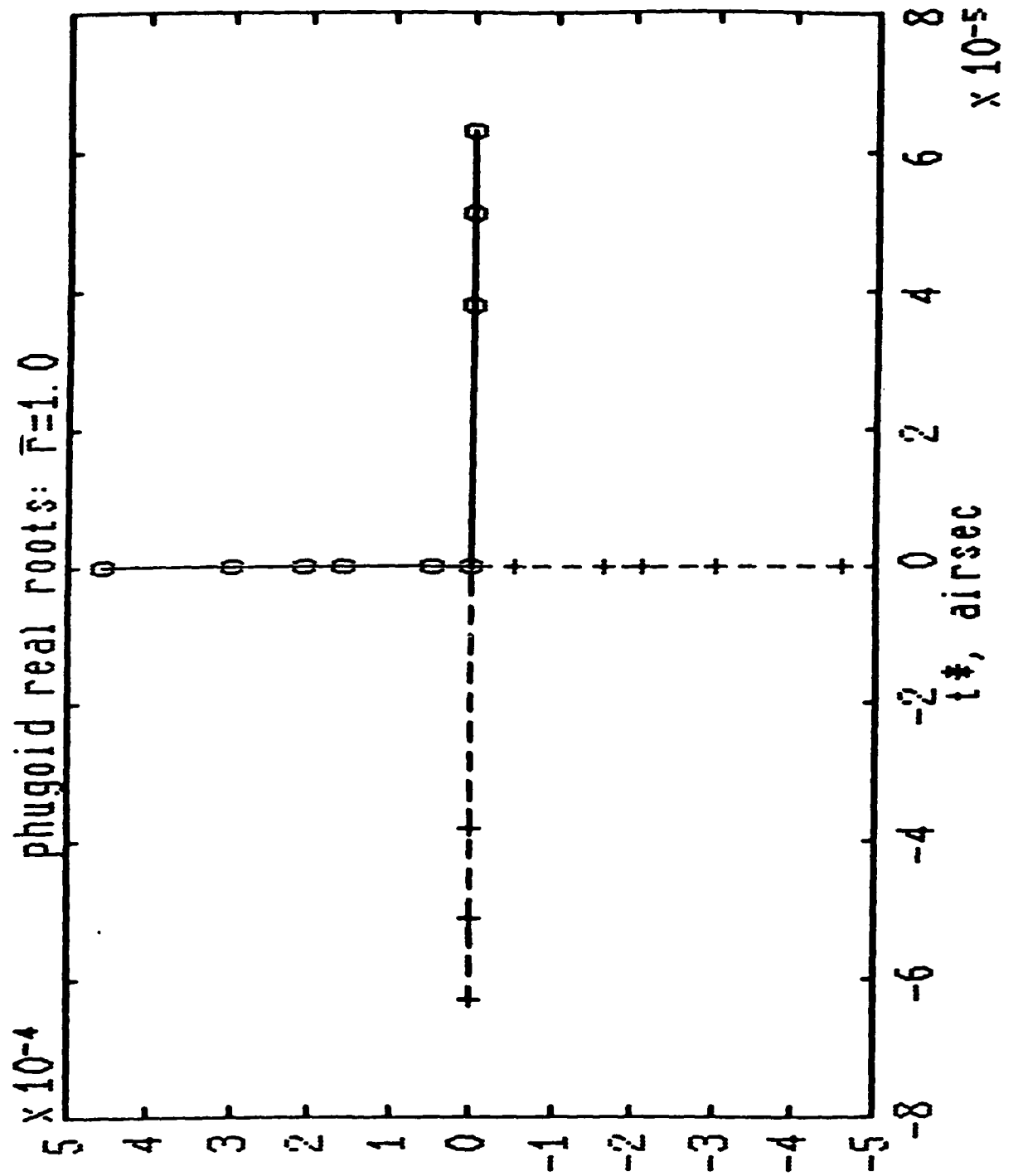


Fig. 65. - FLIGHT ON MINOR CIRCLES: TURNING POINT PROBLEM

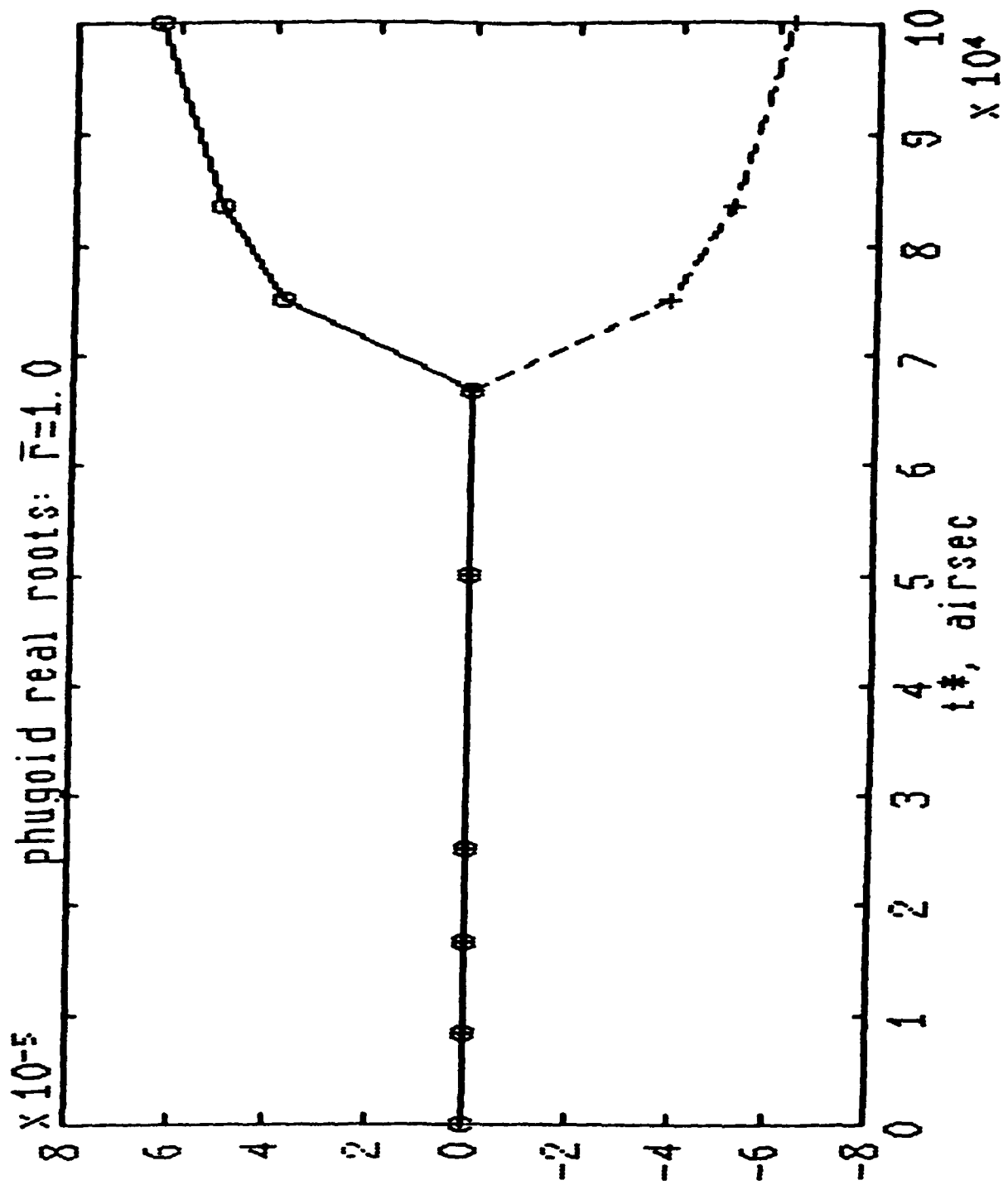


Fig. 66. - FLIGHT ON MINOR CIRCLES: TURNING POINT PROBLEM

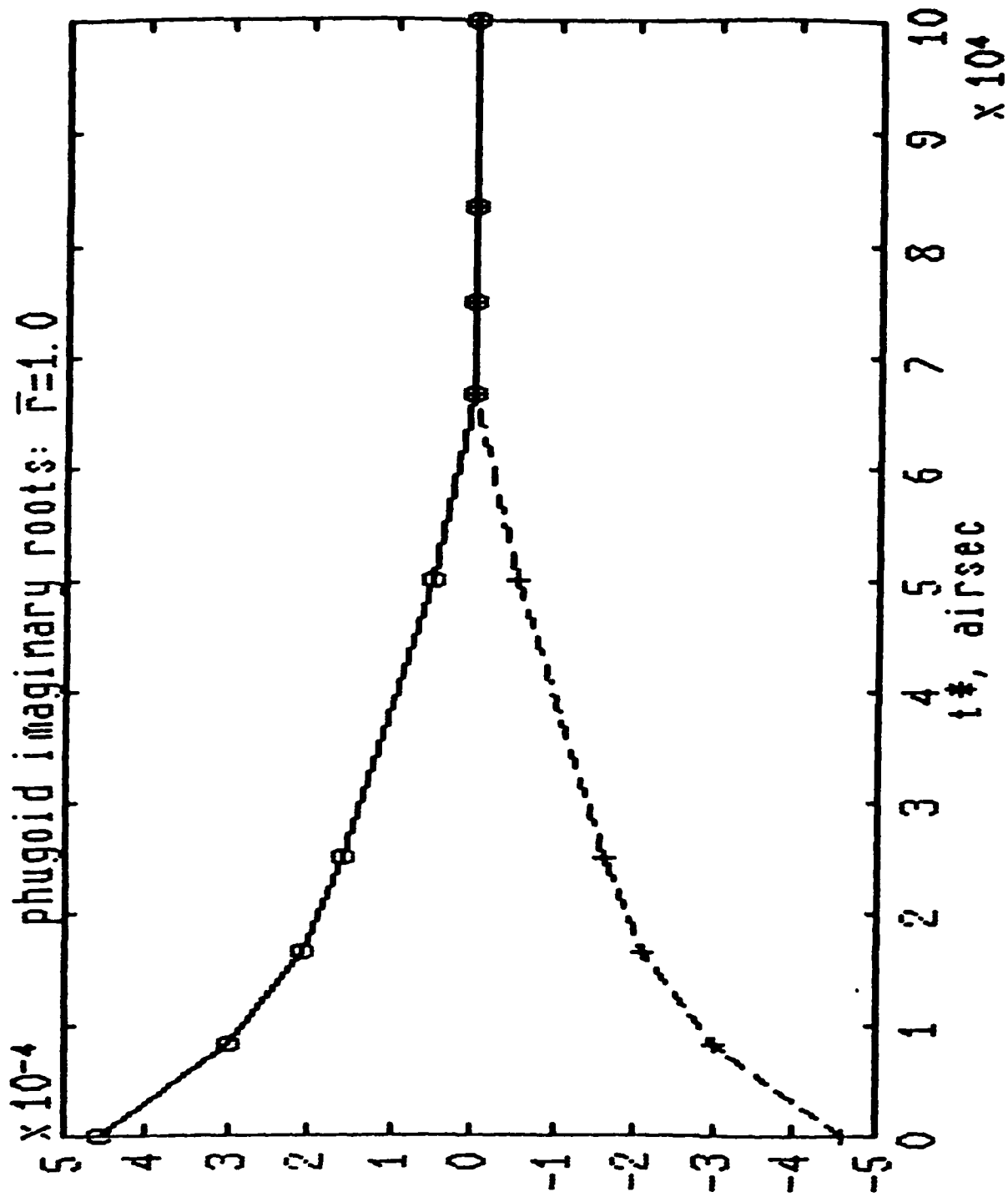
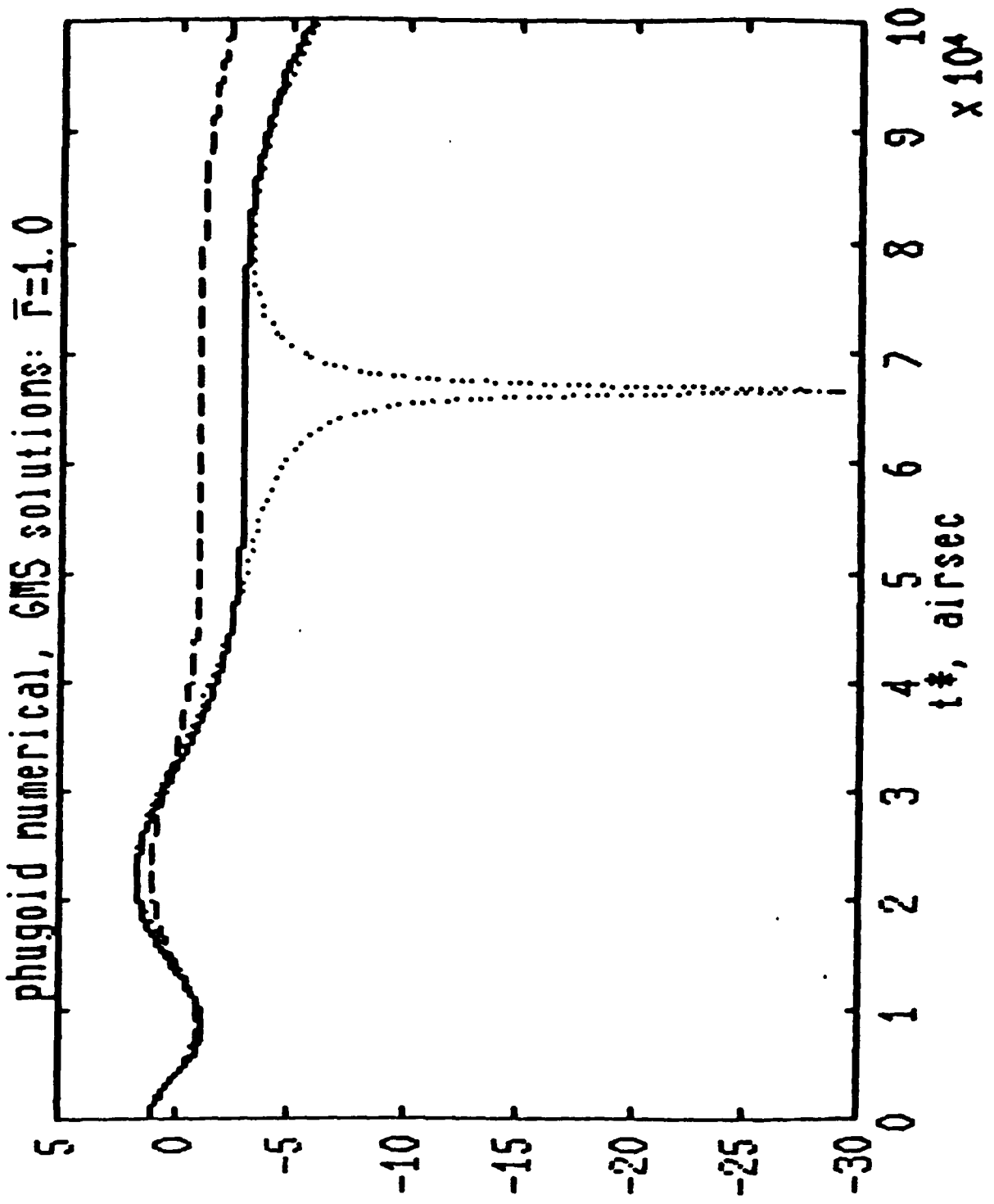


Fig. 67. - FLIGHT ON MINOR CIRCLES: TURNING POINT PRORI FM



— Numerical  
 - - GMS  
 Fig. 68. - FLIGHT ON MINOR CIRCLES: TURNING POINT PROBLEM

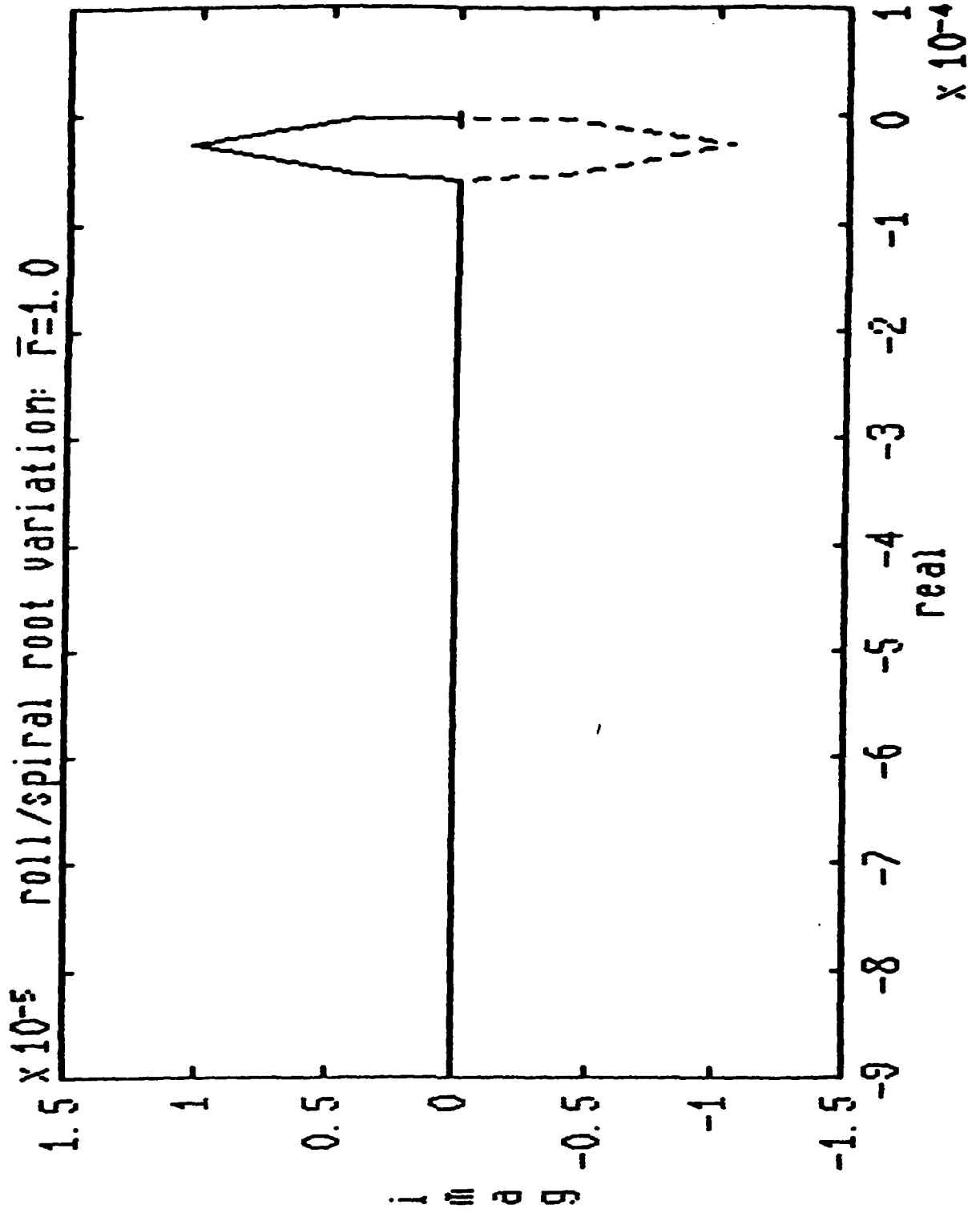


Fig. 69. - FLIGHT ON MINOR CIRCLES: TURNING POINT PROBLEM

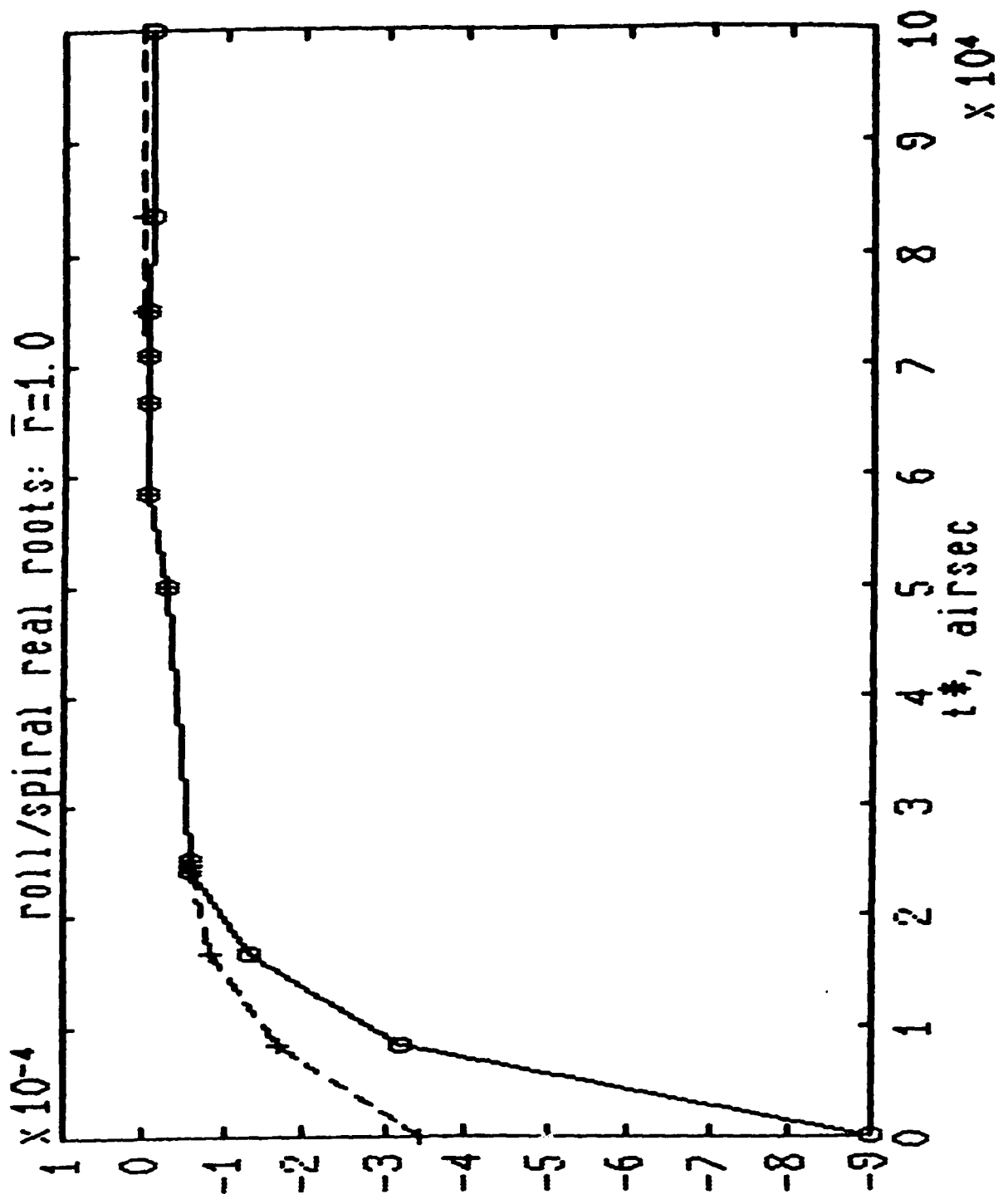
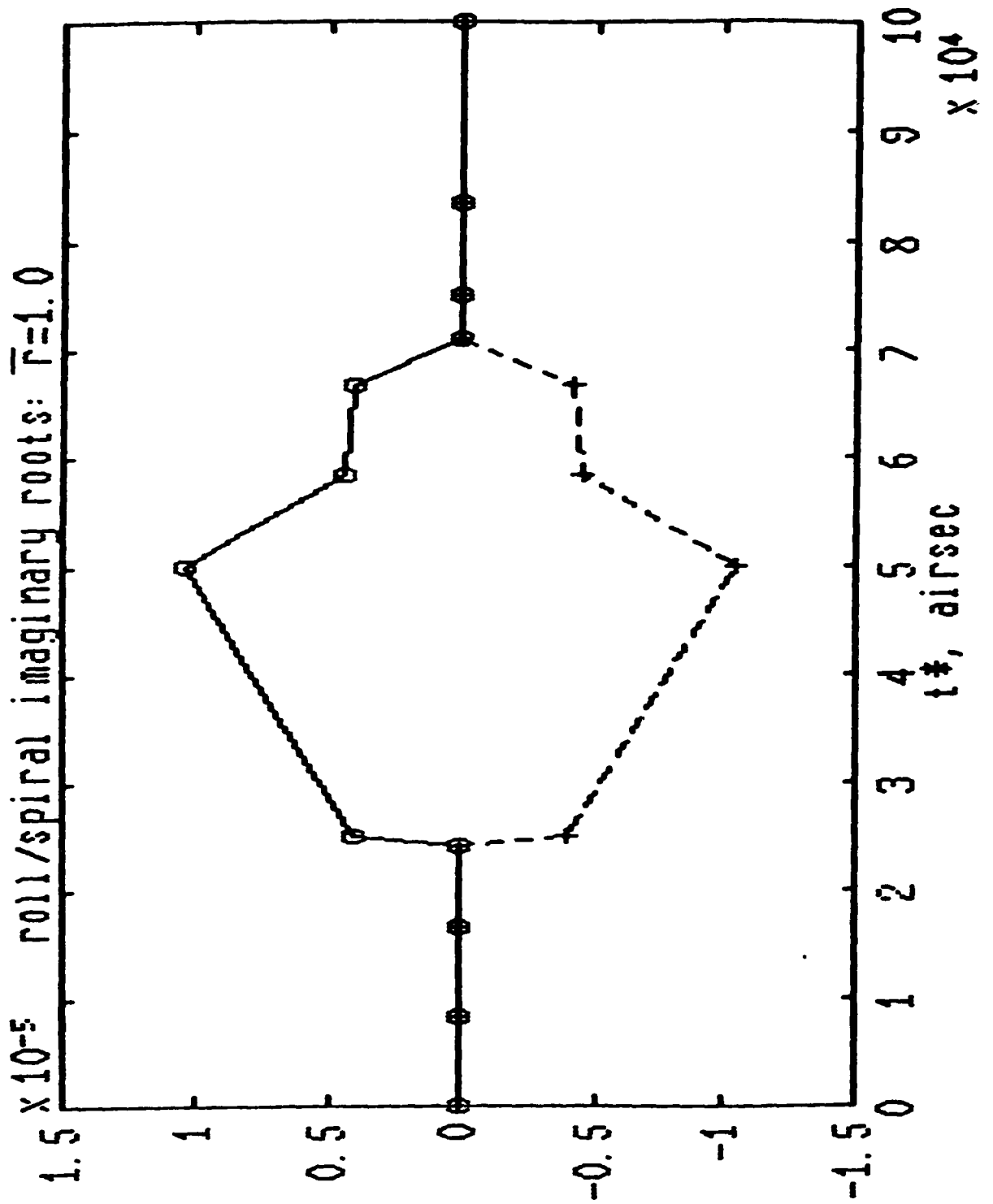


Fig. 70. - FLIGHT ON MINOR CIRCLES: TURNING POINT PROBLEM



P19. 71. - FLIGHT ON MINOR CIRCLES: TURNING POINT PROBLEM

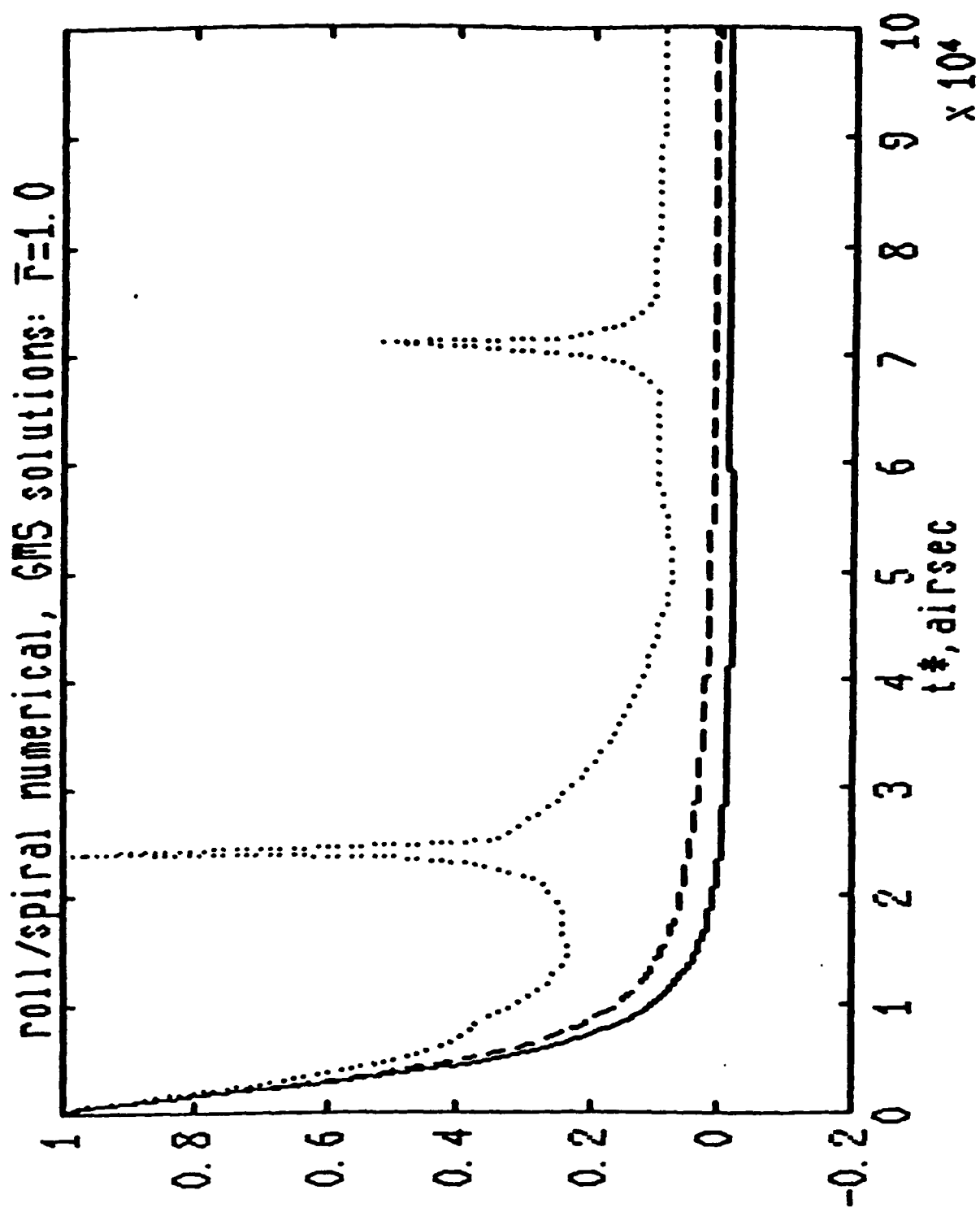


Fig. 72. — Numerical — — GMS · FLIGHT ON MINOR CIRCLES: TURNING POINT PROBLEM

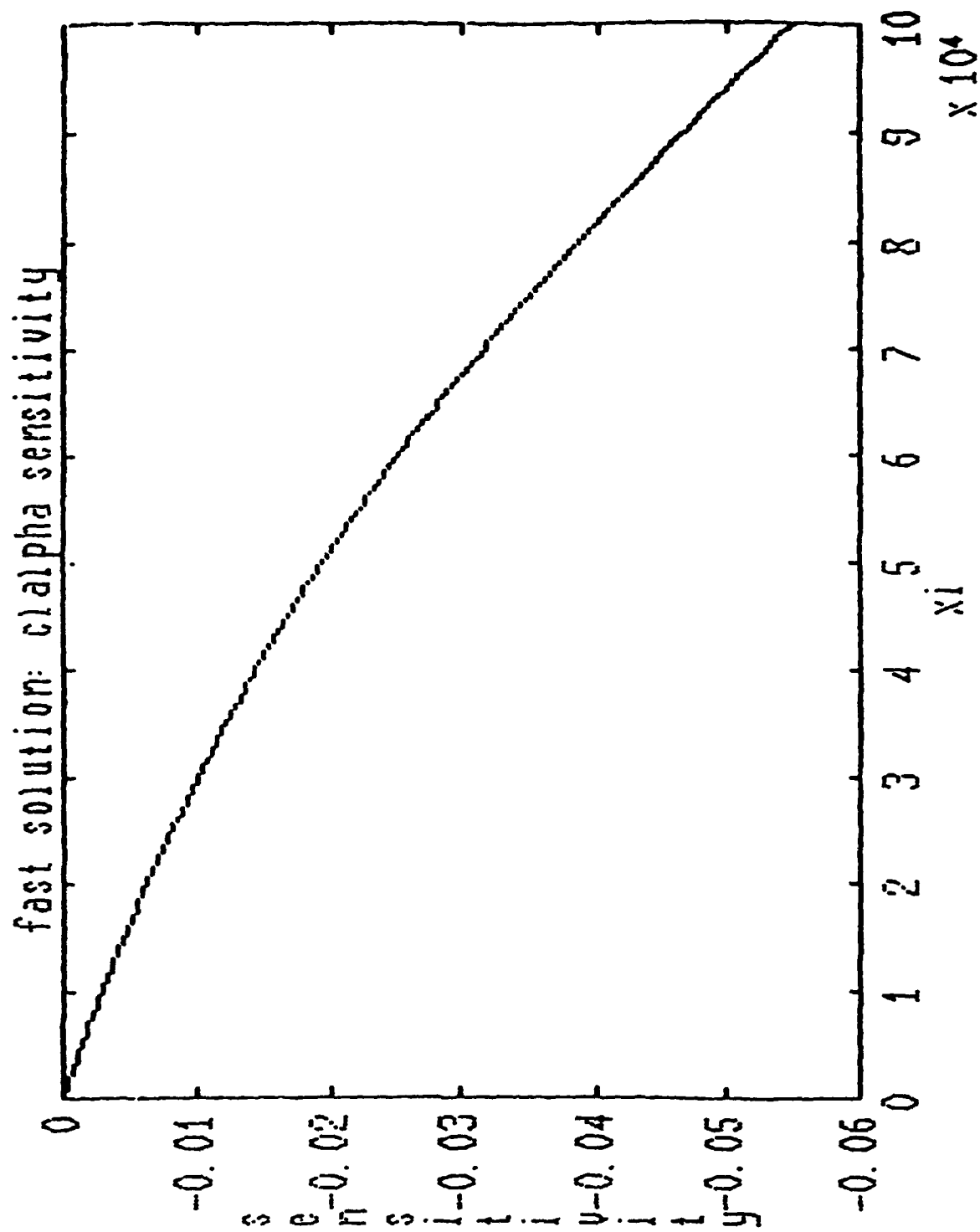


Fig. 73. - PARAMETER SENSITIVITY (RF-FNTRV)

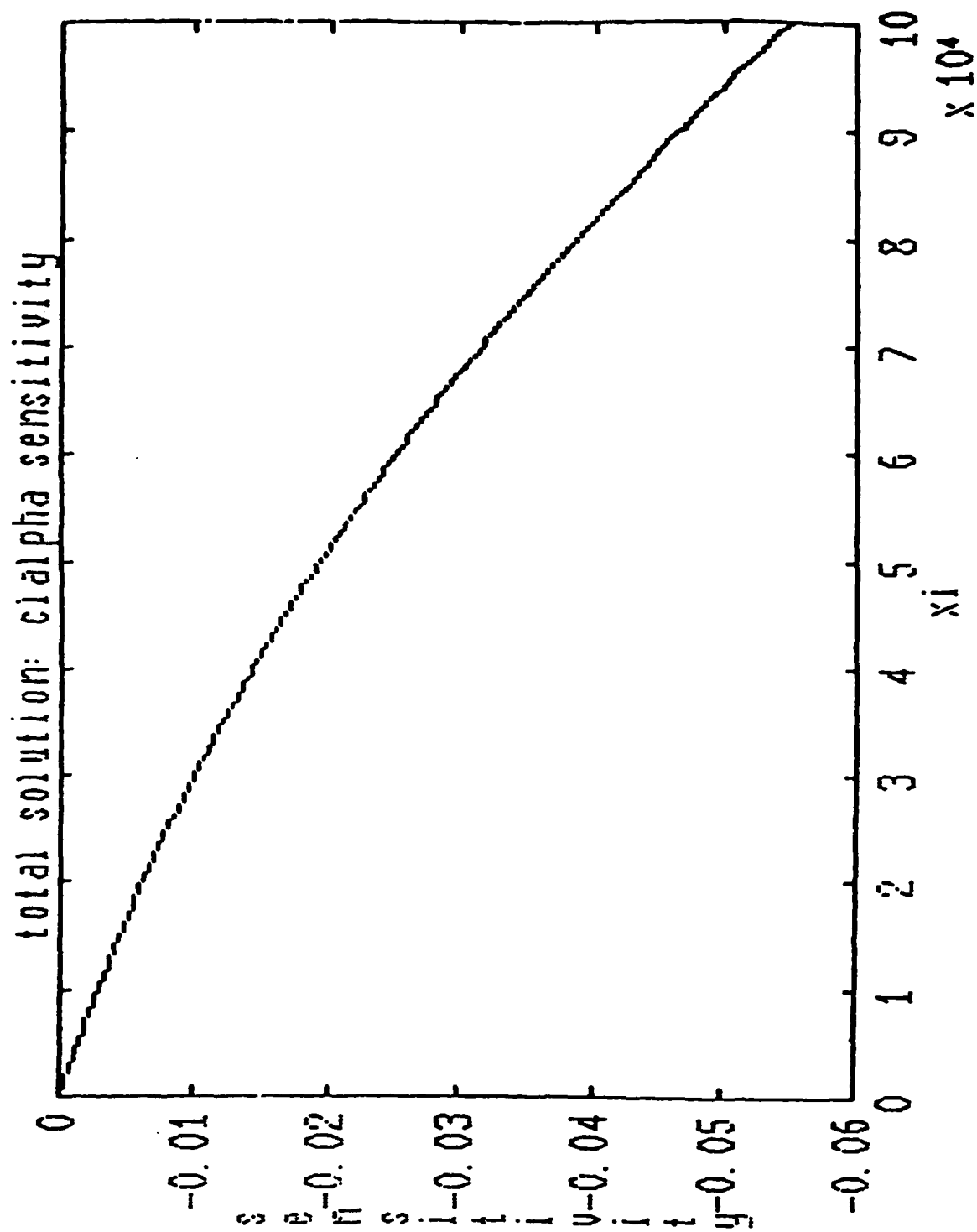


Fig. 74. - PARAMETER SENSITIVITY (RE-ENTRY)

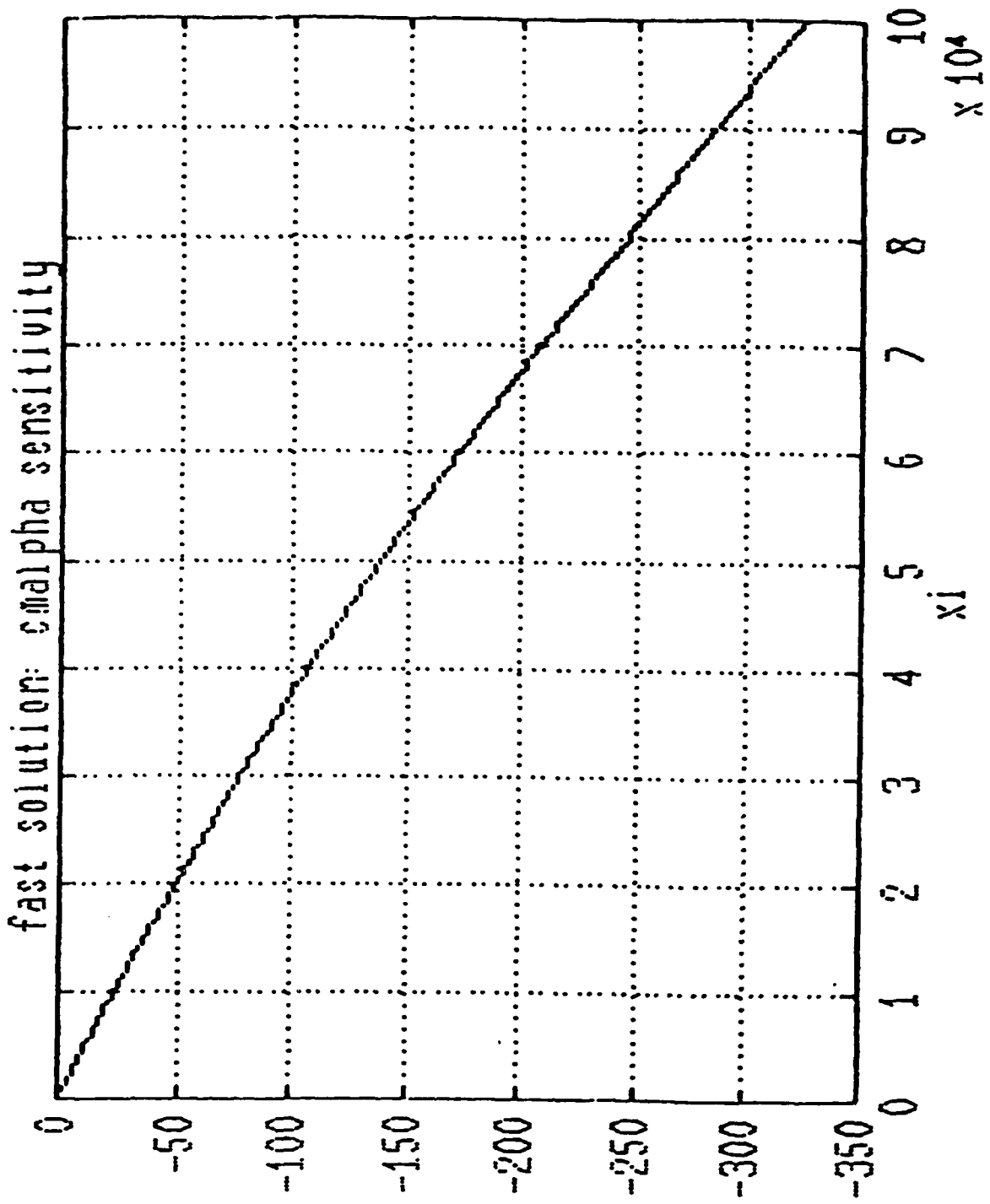


Fig. 75. - PARAMETER SENSITIVITY (RE-ENTRY)

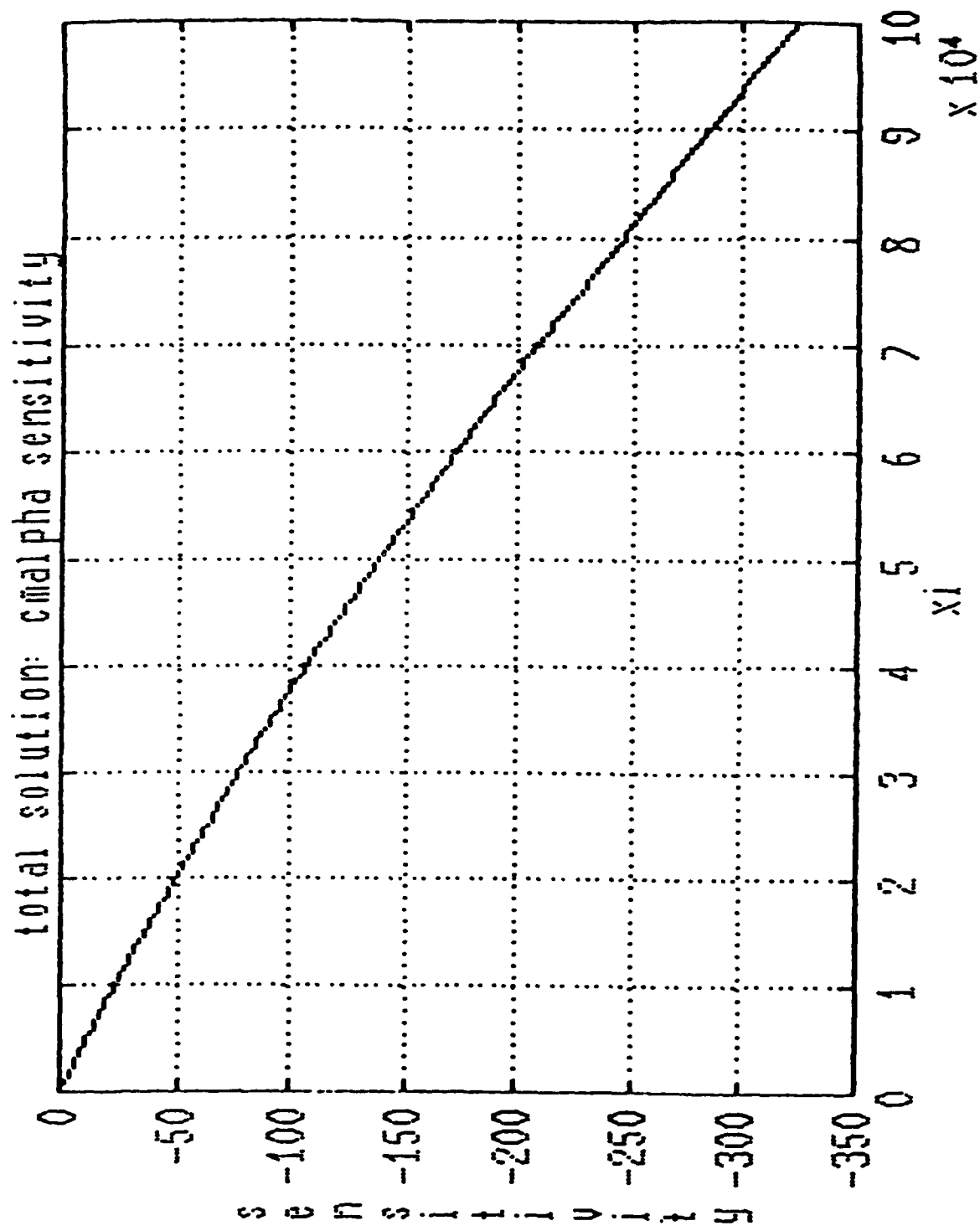


Fig. 76. - PARAMETER SENSITIVITY (RE-ENTRY)

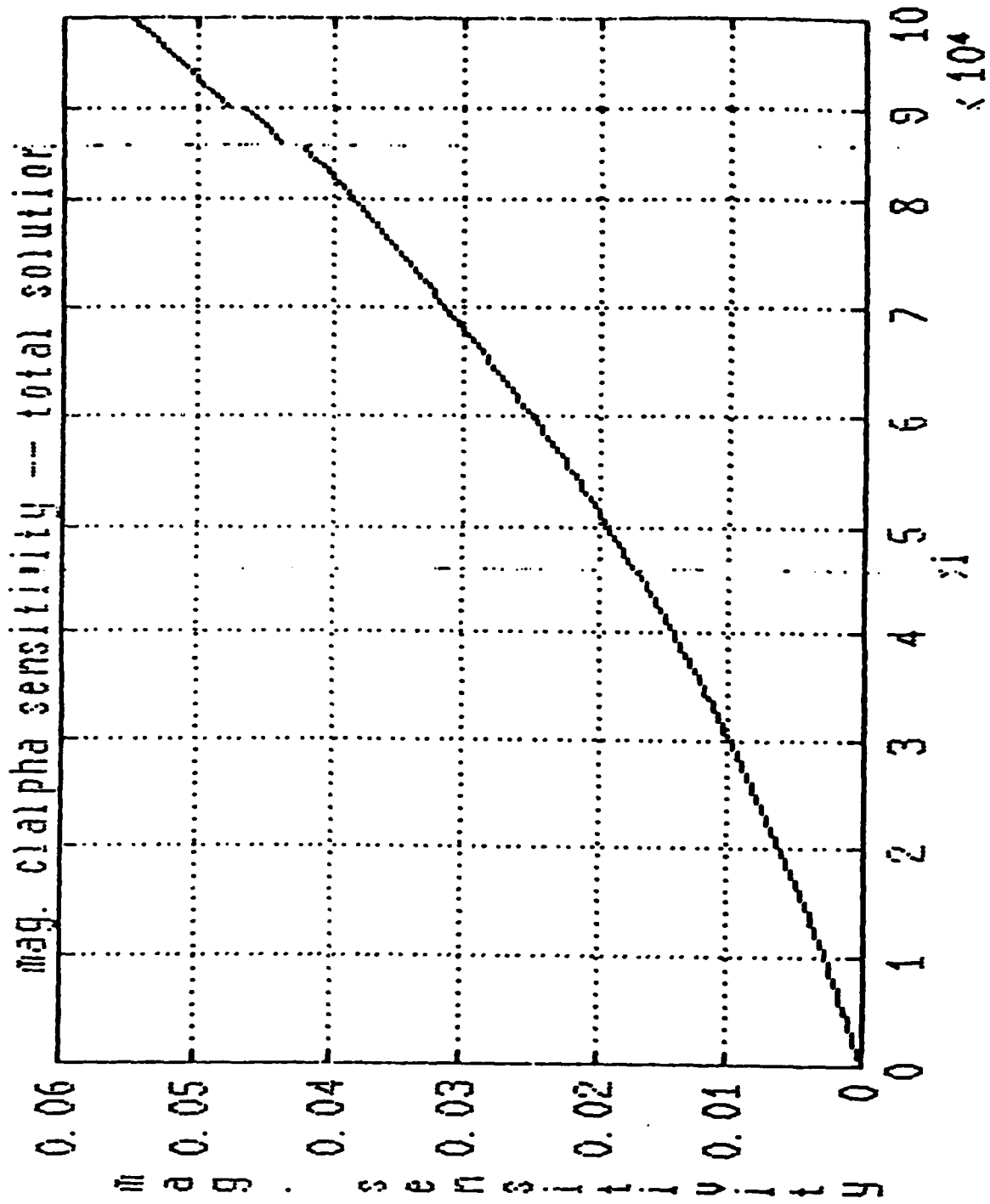


Fig. 77. - PARAMETER SENSITIVITY (RE-ENTRY)

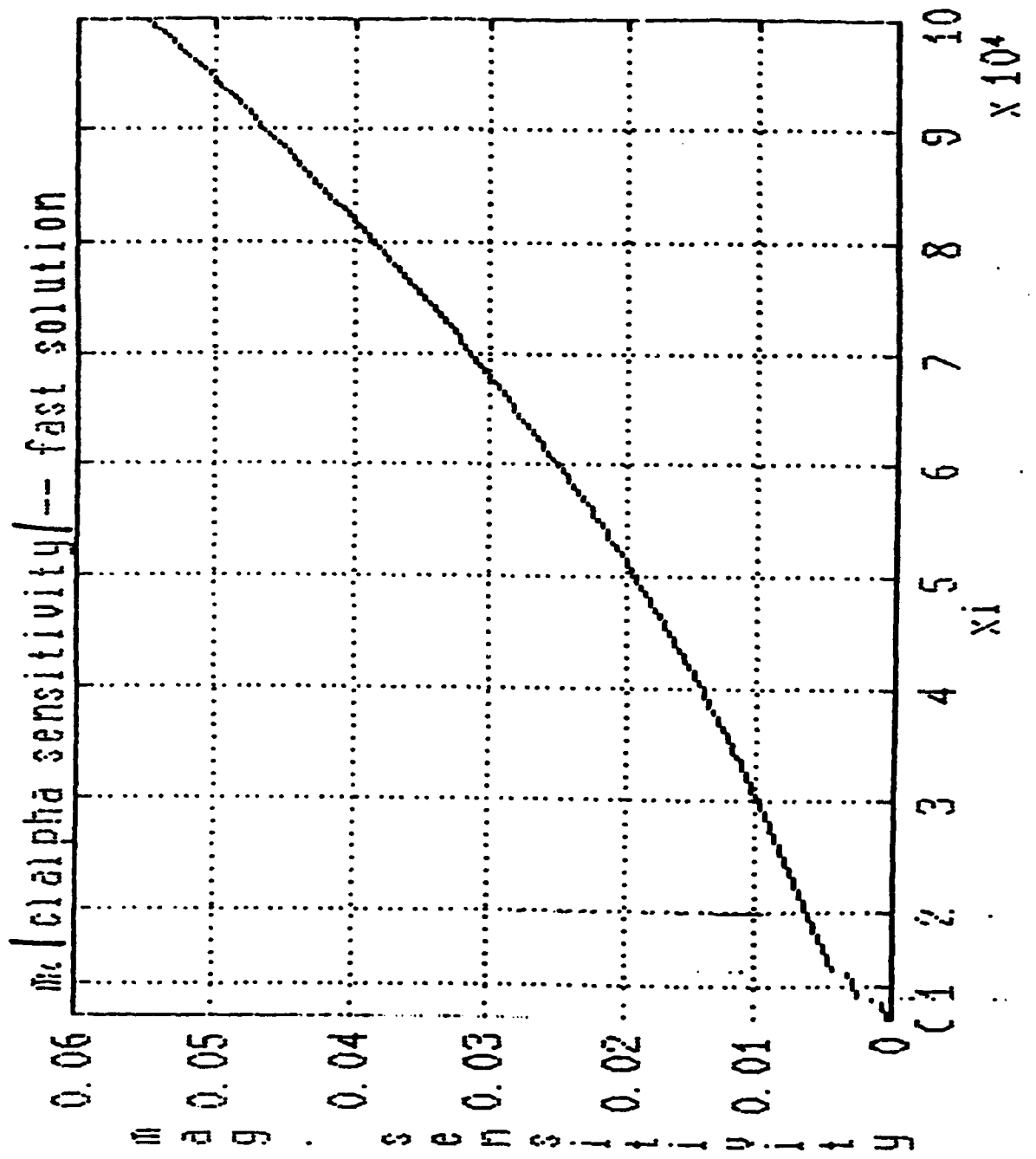


Fig. 78. . . PARAMETER SENSITIVITY (RE-ENTRY)

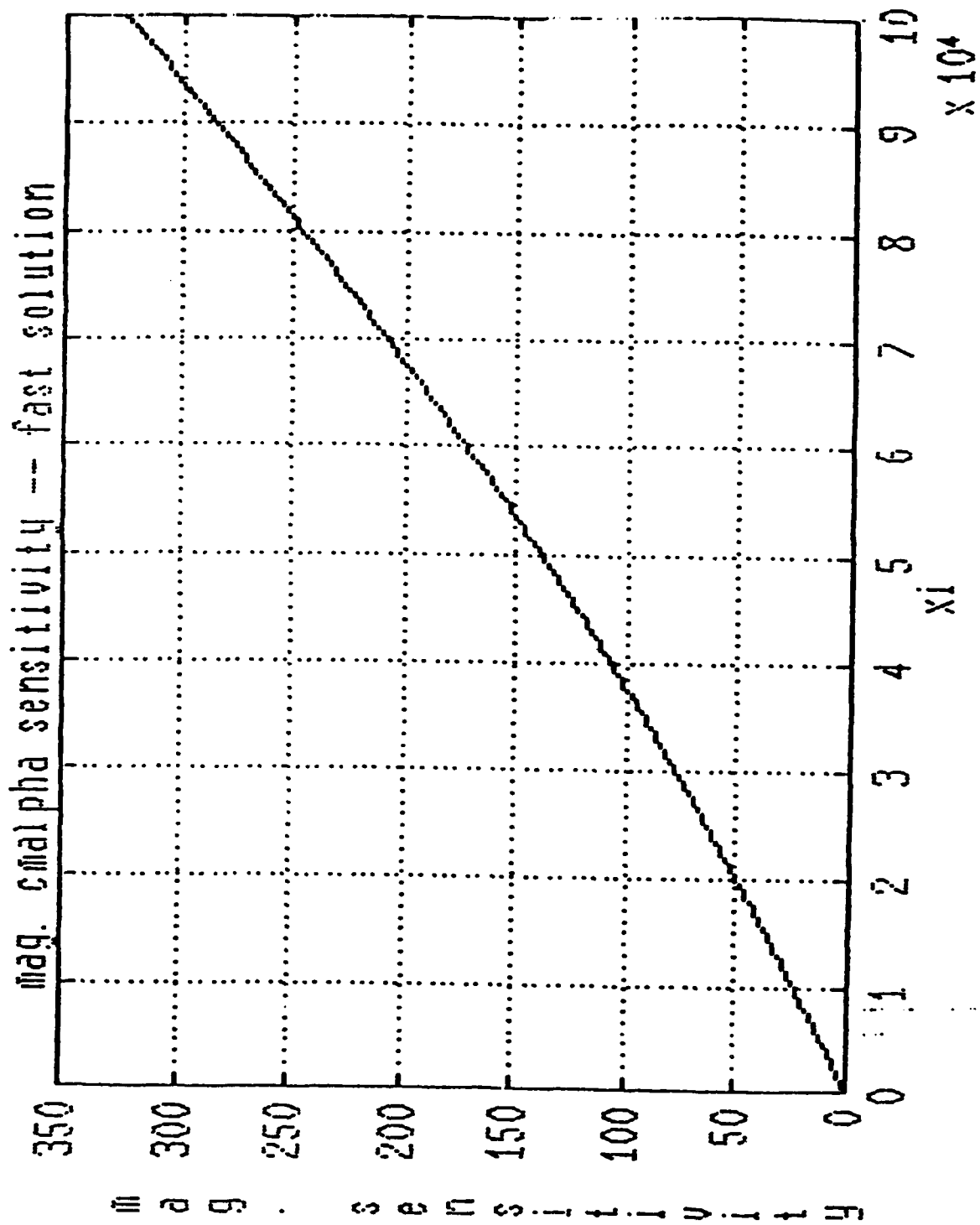


Fig. 79. - PARAMETER SENSITIVITY (RE-ENTRY)

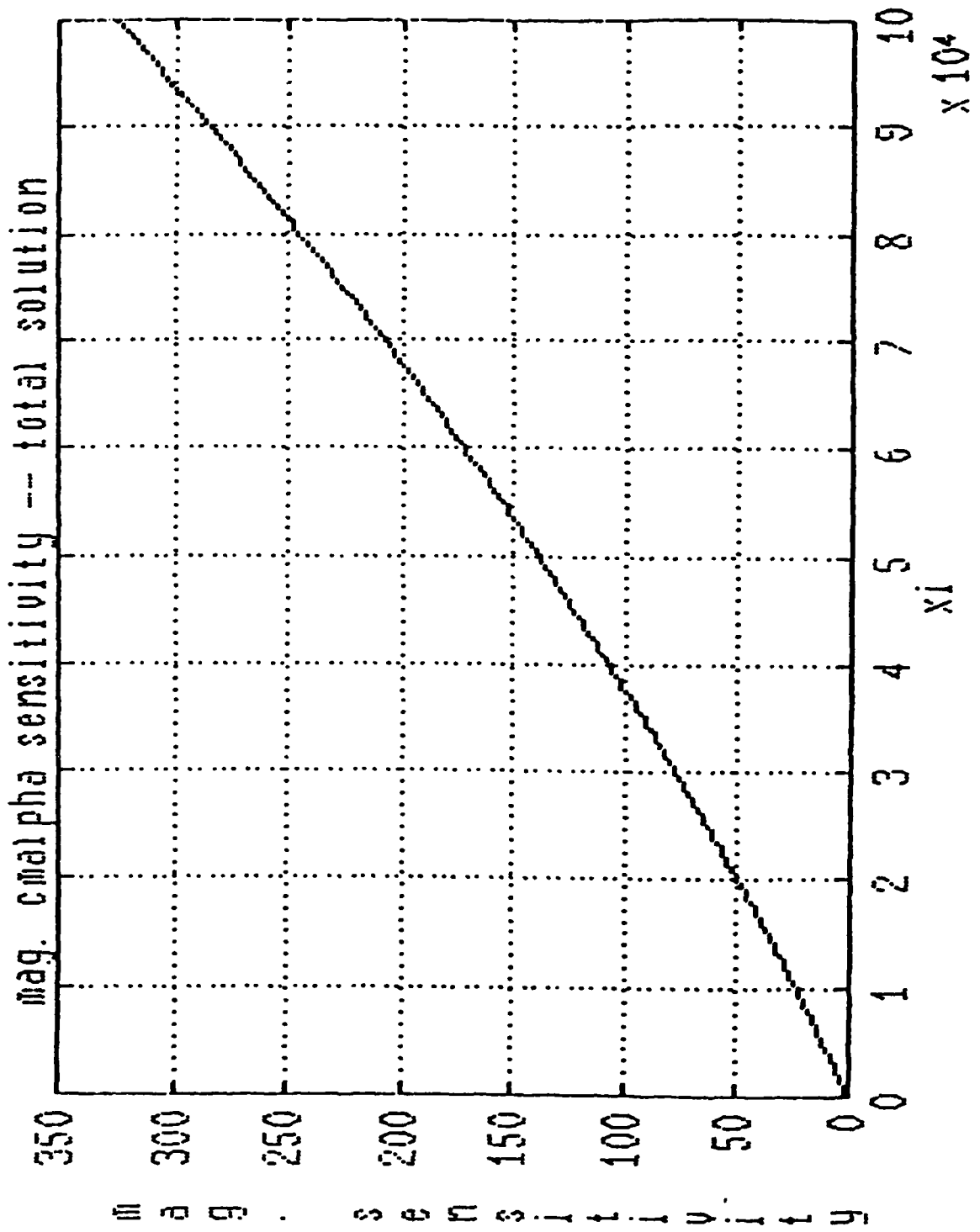


Fig. 80. - PARAMETER SENSITIVITY (RE-ENTRY)

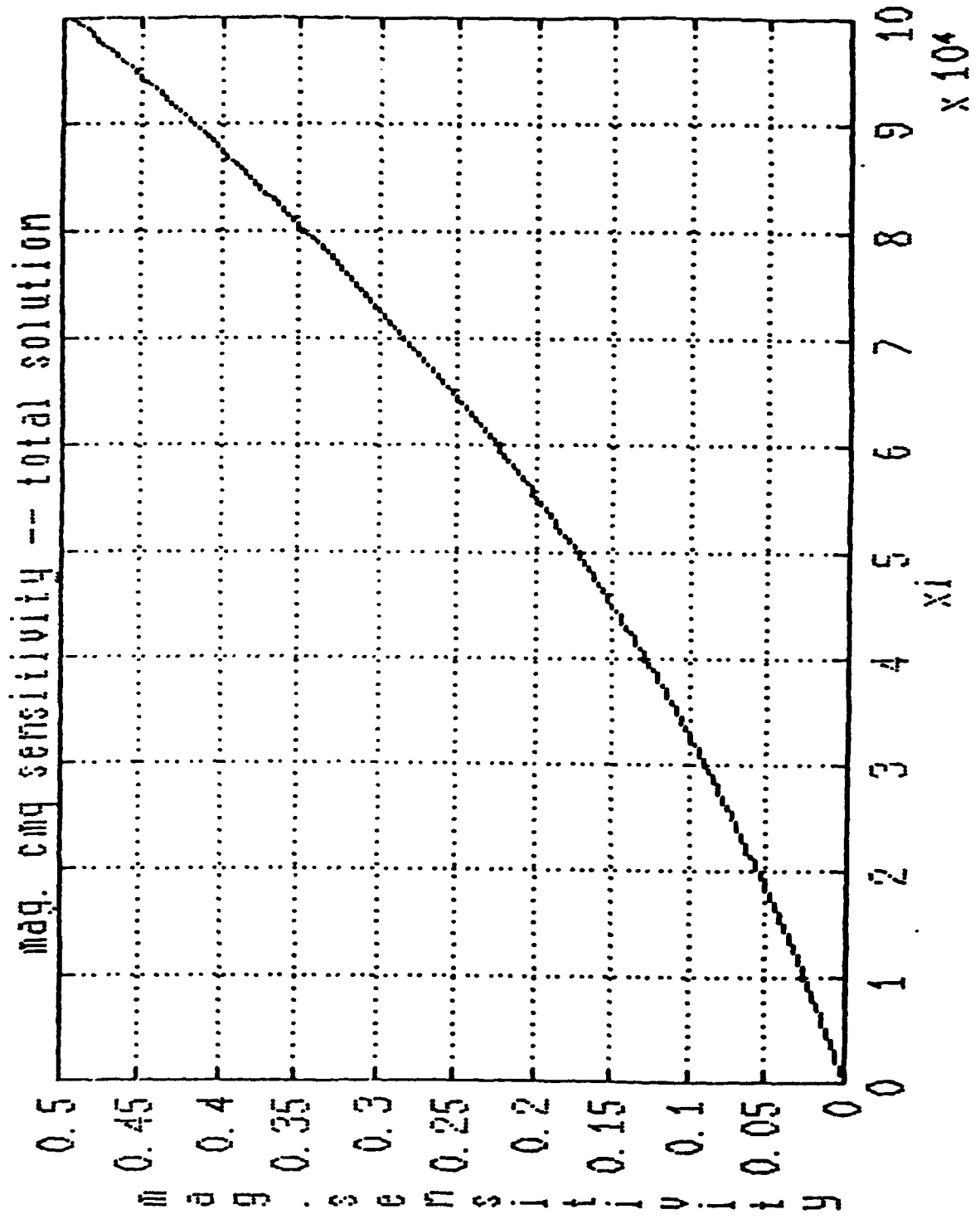
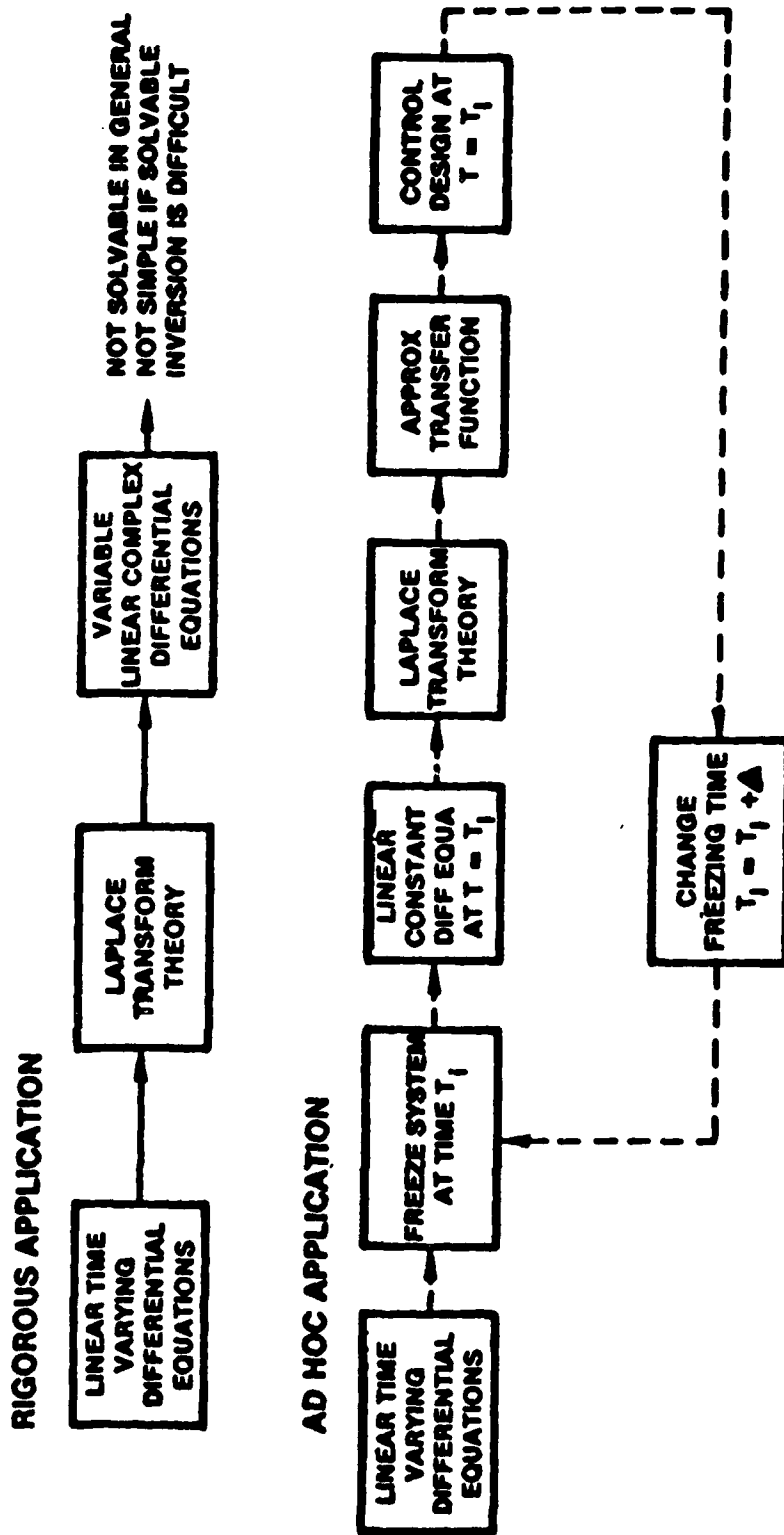


Fig. 81. - PARAMETER SENSITIVITY (RE-ENTRY)

# STANDARD APPROACH TIME VARYING LINEAR SYSTEM



+ SIMULATION

Fig. 82.

# MULTIPLE SCALES APPROACH (GMS) RIGOROUS APPLICATION

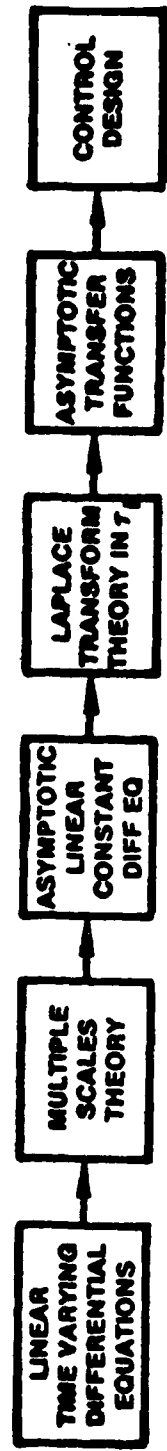


Fig. 83

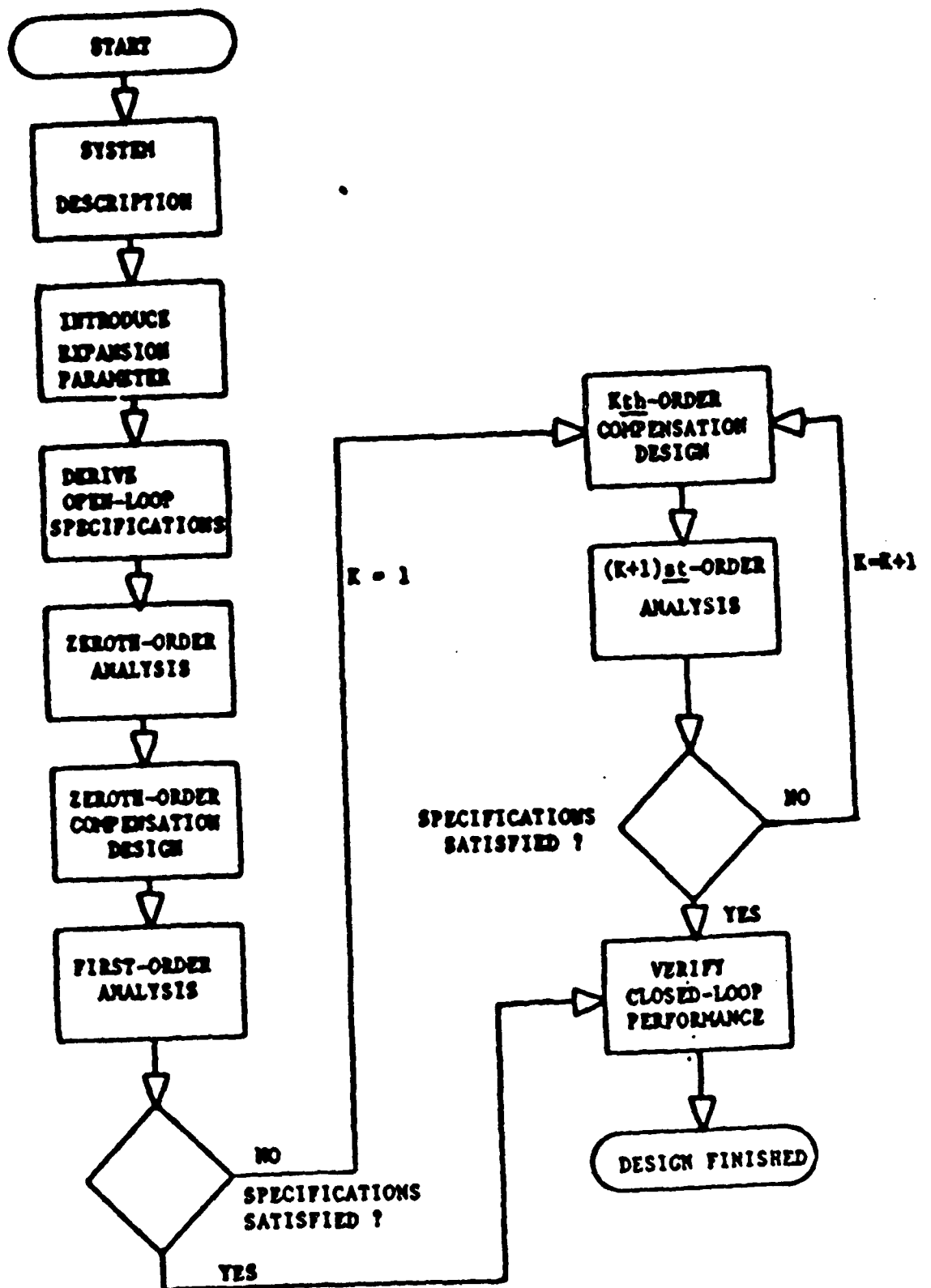


Figure 84 PROPOSED DESIGN PROCEDURE